

Study BEA

Piston engine induction system icing

Warning

This document and the photographs and technical information within it are subject to the distribution and confidentiality rules of European Regulation 996 of 20 October 2010.

The findings of this document were established following work conducted by the Bureau d'Enquêtes et d'Analyses (BEA) for civil aviation safety.

TABLE OF CONTENTS	ERREUR ! SIGNET NON DÉFINI.
1 - INTRODUCTION	6
2 - IMPORTANCE OF INDUCTION SYSTEM ICING IN ACCIDENTOLOGY	8
2.1. Bibliographic research	8
2.2. BEA statistics	10
2.3. Comments and analyses	12
3 - BIBLIOGRAPHIC RESEARCH	13
3.1. Types of icing	13
3.2. Carburettors studied	16
3.2.1. Types of carburettors	16
3.2.1.1 - <i>Float-type carburettors</i>	16
3.2.1.2 - <i>Pressure carburettors</i>	17
3.2.2. Description of float-type carburettors	18
3.2.2.1 - <i>Conventional carburettors</i>	18
3.2.2.2 - <i>Constant depression carburettors</i>	22
3.3. Certification, monitoring and continuing airworthiness authorities	24
3.3.1. Sources and method	24
3.3.2. EASA and FAA publications	24
3.3.2.1 - <i>EASA</i>	24
3.3.2.2 - <i>FAA</i>	31
3.3.3. National authority publications	34
3.3.4. Safety lessons	36
3.4. Investigation authorities	37
3.4.1. Investigation reports	37
3.4.1.1 - <i>Objective, sources and overview of results</i>	37
3.4.1.2 - <i>Results</i>	38
3.4.2. Feature Publications	42
3.5. Consultations with authorities	43
3.6. Federations, associations and expert websites	45
3.7. Pilot training in France	46
3.7.1. Private Pilot Licence (PPL)	46
3.7.2. Airline Transport Pilot Licence (ATPL)	46

3.8. Manufacturers	47
3.8.1. Aircraft manufacturers (excluding aircraft equipped with Rotax engines)	47
3.8.2. Engine manufacturers	49
3.8.3. Carburettor manufacturers	49
3.9. Scientific articles	50
3.9.1. Introduction	50
3.9.2. Publications between 1943 and 1950	52
3.9.3. Publications between 1950 and present day	70
3.10. Comparison of the different graphs	76
3.10.1. Reminder of the sources identified	76
3.10.2. Comparison of the graphs proposed by the different authorities	78
3.10.3. Comparison of the graphs proposed by the scientific articles	83
3.10.4. Comparison of the graph proposed by the EASA with those identified in the scientific articles	88
3.11. Overview of the bibliographic research	92
4 - POWERPLANT ICING TESTS	93
4.1. Test centre	93
4.2. Test objectives	93
4.3. Feasibility study	94
4.3.1. Phase one of the feasibility study	94
4.3.2. Phase two of the feasibility study	100
4.3.2.1 - <i>Presentation of the simulation tool</i>	100
4.3.2.2 - <i>Initial open field simulation</i>	111
4.3.2.3 - <i>Series of simulations considering different types of test section</i>	113
4.3.2.4 - <i>Series of simulations considering a new type of test section</i>	117
4.3.3. Detailed overview of the test setup	126
4.3.3.1 - <i>Assembly of the engine and its associated equipment</i>	126
4.3.3.2 - <i>Sensors installed on the engine</i>	128
4.3.3.3 - <i>Supply and extraction ducts</i>	131
4.4. Test results	133
4.4.1. Introduction	133
4.4.2. Test points completed	134

4.4.3.	Observed occurrences of icing.....	139
4.4.3.1	- 1st observed icing occurrence.....	139
4.4.3.2	- 2nd observed icing occurrence	151
4.4.3.3	- 3rd observed icing occurrence	153
4.4.3.4	- Another phenomenon.....	153
4.4.3.5	- Conclusion	154
4.4.4.	Identification of parameters contributing to the phenomenon of icing in the carburettor.....	155
4.4.4.1	- Temperature of the outer surface of the carburettor and temperature downstream of the butterfly.....	155
5 -	POWERPLANTS EQUIPPED WITH A ROTAX ENGINE.....	159
5.1.	Rotax engines considered	159
5.2.	Presentation of types of powerplants	165
5.3.	Presentation of the 912 and 914 Series carburettors	168
5.4.	Icing prevention systems	169
5.5.	Publications	170
5.5.1.	Aircraft manufacturer	170
5.5.2.	Rotax.....	174
5.5.3.	Articles, websites and forums	175
5.6.	Measurements on aircraft	180
5.6.1.	Objectives.....	180
5.6.2.	Measuring resources	182
5.6.3.	Measurements taken on aircraft.....	184
5.6.3.1	- First series of measurements	184
5.6.3.2	- Second series of measurements	196
5.6.4.	Measurements at the test stand.....	225
5.7.	Summary and comments	230
6 -	CONCLUSIONS.....	237
6.1.	Established facts	237
6.2.	Analysis and comments	239

1 - INTRODUCTION

The phenomenon of piston engine induction system icing crops up regularly in safety investigations as a cause of or a factor contributing to a decrease in power, in particular when no other hypothesis is susceptible.

During safety investigations, when engine data is not recorded and accidents are fatal, this phenomenon is essentially studied and analysed through weather conditions and how they relate to the graph shown below (**Figure 1**). Indeed, due to the nature of the phenomenon, its observation by the BEA investigators on the wreckage or the identification of any physical evidence are very unlikely.

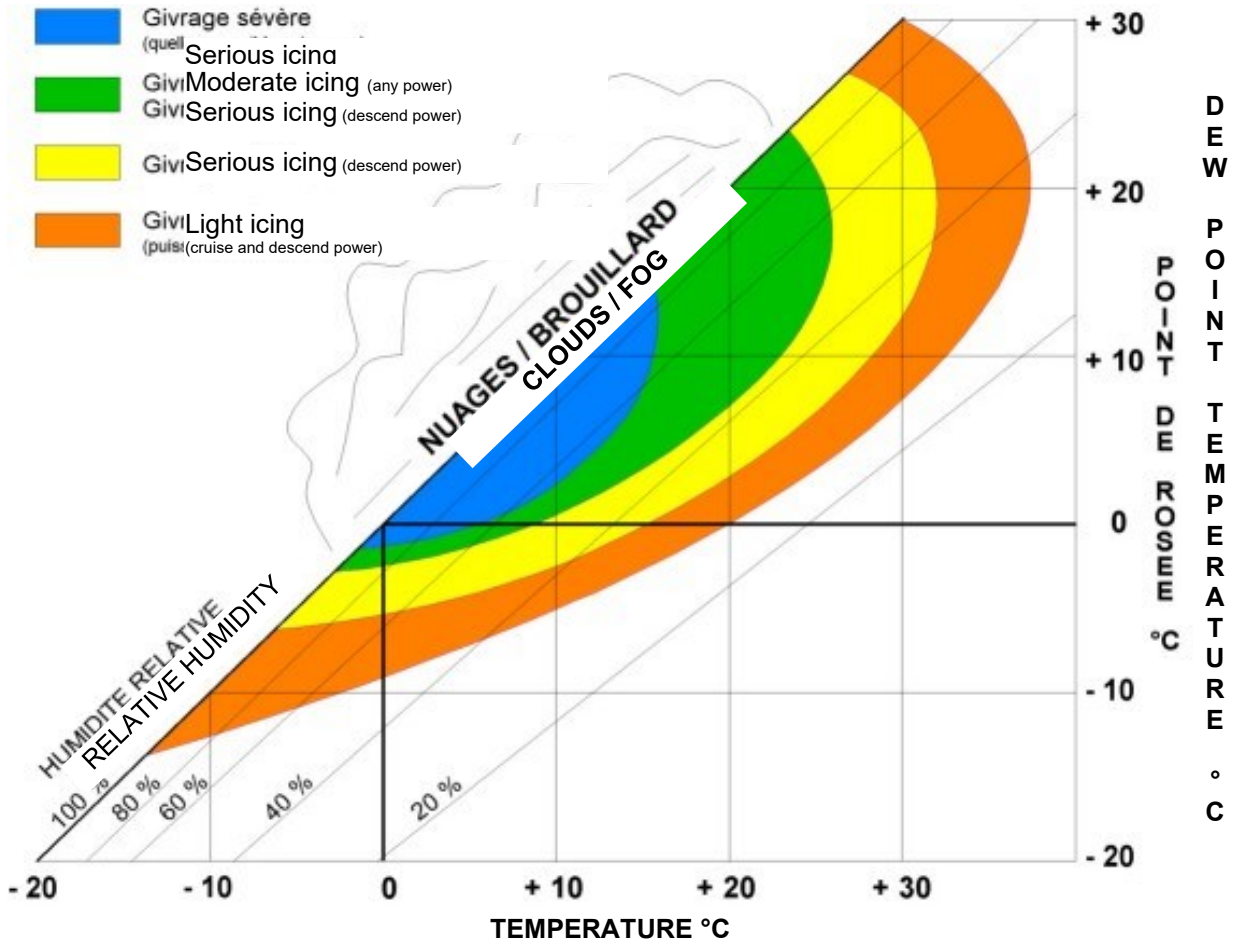


Figure 1: graph proposed by the EASA, published in the *Piston Engine Icing* document

Source: *Piston Engine Icing* _European General Aviation Safety Team _GA5

(link: <https://www.easa.europa.eu/document-library/general-publications/egast-leaflet-ga-5-piston-engine-icing>)

This graph used by investigators indicates, as a function of the air and dew point temperatures, the probability of icing and its severity. It is presented in an EASA publication on the phenomenon and cross-referenced in various pilot training documents.

In all of these publications, the origin of this graph and the data used to compile it are not specified. This presentation tends to view this graph as a “universal law” applicable to all existing powerplants.

In these conditions, the simple use of weather conditions and this graph do not appear to meet the requirements of a rigorous investigative approach that must be painstaking. Some investigators have questioned the relevance of this topic and its very frequent coverage, which does not match their own flying experience.

During a recent investigation, the BEA initiated work with an “icing” expert from the Ministry of Defence. This work consisted in attempting to study in more depth the probability of icing having occurred during the accident flight, taking into account the specificities of the given propulsion system.

This work demonstrated:

- the availability of several graphs, not necessarily identical and for which the data used to compile them remains unknown;
- the option of using modelling tools to define the probability of the occurrence of icing, considering the specific characteristics of the powerplant in question;
- the requirement for input parameters to use modelling tools, not always accessible;
- numerous American publications on the topic, in particular during the period between 1945 and 1950, on propulsion systems sometimes far removed from those studied today.

This preliminary work has led to a broader study aimed at consolidating the investigation approach with regards to icing phenomena that can initiate in piston engine induction systems.

This study comprises three parts:

- bibliographic research focusing on the information available from the various authorities, manufacturers and scientific sites;
- a test campaign on a powerplant equipped with a Lycoming engine;
- a series of measurements on aircraft equipped with Rotax engines, supplemented by measurements on an engine of the same type installed at a test stand.

2 - IMPORTANCE OF INDUCTION SYSTEM ICING IN ACCIDENTOLOGY

2.1. Bibliographic research

Several articles presenting the statistics of the number of accidents associated with the phenomenon of piston engine induction system icing were identified:

Article title	Study period	Geographic area	Information extracted
<i>A Review of Service Experience with Aircraft Powerplant Installations</i> Posner D.L. 1947	1930 to 1946	United States	Twenty-three percent of incident reports drafted by the civil administration (i.e. 1,094 reports out of the 4,833 reports published over the period in question) make reference to this phenomenon.
<i>A study of carburetor/induction system icing in general aviation accidents</i> L. Gardner, G. Moon, R.B. Whyte March 1971	1966 to 1967	Canada	Forty-four accidents were attributed to this phenomenon (<i>BEA comment: the total number of accidents for the period is not given</i>)
<i>Carburetor ice in general aviation</i> NTSB January 1972	1967 to 1971	United States	Three hundred and sixty accidents were attributed to this phenomenon (<i>BEA comment: the total number of accidents for the period is not given</i>) These accidents involved 636 people. They resulted in the fatal injury of 40 people and in the injury of 160 people.
<i>A study of carburetor/induction system icing in general aviation accidents</i> Richard W. Obermayer and William T. Roe (NASA) March 1975	1968 to 1973	United States	The data used is that of the NTSB. The phenomenon of icing causes approximately 10% of engine malfunctions/failures in general aviation, involving in particular pilots who have logged less than 1,000 flight hours. When conditions are conducive to icing, between 50 and 70% of engine malfunctions/failures would be caused by icing. Icing would be the cause of or a contributing factor in 65 to 90 accidents on average per year. Most icing problems involve float-type carburetors
<i>Aircraft Icing</i> NASA/FAA conference held in July 1978	1973 to 1977	United States	Over the given period, 311 accidents occurred in conditions conducive to induction system icing, representing 1.5% of all accidents. Most accidents involved single-engine aeroplanes, in VFR flight. In this case, this type of accident has a very high survival rate, with only approximately 0.8% being fatal. For multi-engine aeroplanes, the probability of an accident occurring due to induction system icing is relatively low, but the risk of this being a fatal accident is fairly high in relation to single-engine aeroplanes.

Article	Period	Geographic area	Information
<i>Light Airplane Piston Engine Carburetor Ice Detector/Warning</i> W. Cavage, J. Newcomb, K. Biehl June 1982	1976 to 1982	United States	329 occurrences were associated with this phenomenon (<i>BEA comment: the total number of accidents for the period is not given</i>) The main flight phases in which this phenomenon occurred were: <ul style="list-style-type: none"> • 20% of cases at take-off; • nearly 50% of cases in cruise flight; • nearly 20% of cases on approach. These occurrences concerned a very varied list of aircraft. Accidents/incidents to which icing was a contributing factor involved in particular pilots who had logged less than 150 flight hours. However, other categories of pilot were not excluded.
<i>UK General Aviation Accidents: Increasing Safety Through Improved Training</i> A. Taylor 2014	2005 to 2011	Great Britain	Of the 13 fatal accidents recorded as being caused by a technical problem, 10 were cited as failures caused by the engine or by carburettor icing. More than one third (34.9%) of the 149 engine failures were determined as likely to have been caused by carburettor icing.
Presentation to NCAR <i>In-flight Icing Users Technical Interchange Meeting (TIM)</i> February 2015	2000 to 2011	United States	The presentation indicates that 29% of accidents (around 435 accidents out of a total of 1,500) were weather-related. Of the weather-related accidents, 6% of cases were associated with induction system icing.
<i>Fatal weather-related general aviation accidents in the United States</i> Andrew J. Fultz & Walker S. Ashley July 2016	1982 to 2013	United States	During the period in question, 58,687 general aviation accidents occurred in the United States, of which 11,354 were fatal. The meteorological conditions were a cause or a contributing factor in 25% of cases or 15,439 general aviation accidents. 1,019 accidents, of which 79 were fatal (approximately 7.7%) were attributed to carburettor icing.

The American AOPA (*Aircraft Owners and Pilots Association*) website provides a database of accidents and incidents that occurred in the United States regarding general aviation aircraft, aeroplanes only. The data used is that of the NTSB.

Over the past 10 years, the database has included 11,804 occurrences, of which 110 (i.e. 0.9%) directly involved piston engine induction system icing.

Only five events resulted in fatal injury of the occupants.

Of these events, 105 occurred in VMC conditions.

2.2. BEA statistics

In April 2020, the BEA analyzed the occurrences in its database meeting the following criteria:

- occurring between January 1, 2010 and April 1, 2020;
- involving an airplane, microlight or helicopter weighing less than 2,250 kg, equipped with a piston engine;
- having been the subject of an investigation by the BEA¹ and this investigation having been completed.

A total of 941 occurrences met these criteria.

13 occurrences (i.e. 1.4%) pertained to the phenomenon of carburettor icing:

- in 11 cases, the hypothesis of icing during the event flight was evoked but not proven;
- in 2 cases, the occurrence of icing during the event flight was confirmed.

In these last two cases, the analysis was based:

- on weather conditions for one;
- on weather conditions at altitude modelled by Météo-France and data logged by on-board equipment.

The second of the two aforementioned cases was a confirmed case of icing (investigation following the accident to the aircraft registered D-EIOI):

The investigation report is available on the BEA website (link: <https://bea.aero/en/investigation-reports/notified-events/detail/accident-to-the-vans-rv7-registered-d-eioi-on-29-08-2018-at-bourg-saint-maurice/>).

This case concerns a Van's Aircraft RV7, equipped with a Lycoming YO-360-A1A engine and a constant speed propeller, with a MA.4-5 carburettor (this type of carburettor is described in para. 3.2.2). This carburettor was equipped with a temperature probe located just after the carburettor.

The carburettor was associated with a mixing unit allowing the pilot to select an alternate hot air source to the cold air directly coming from the air intake.

The engine data was recorded on a Dynon device.

The read-out of the parameters recorded during the flight show three icing phases of the induction system (shown as Icing 1, Icing 2 and Icing 3 on the reference graphs - Figure 2). For each phase, the parameter curves show that the hot air source was indeed selected to remedy this. The third and last phase shows a more sudden onset of the phenomenon occurred doubtlessly due to the more severe icing conditions. The return of engine power was identified around one minute 50 s after this action.

Comments:

The recording of engine parameters is a precious aid for investigators . The icing phenomenon is identified accurately here. Without this data, the hypothesis of an icing phenomenon could not have been consolidated.

¹ For microlights, the BEA's investigation policy changed during the chosen analysis period, from January 1, 2010 to April 1, 2020. Between 2010 and 2015, few investigations were carried out on this type of aircraft. From 2015, only fatal accidents were the subject of an investigation. As a result, the statistics proposed by the BEA for microlights are a priori minimized.

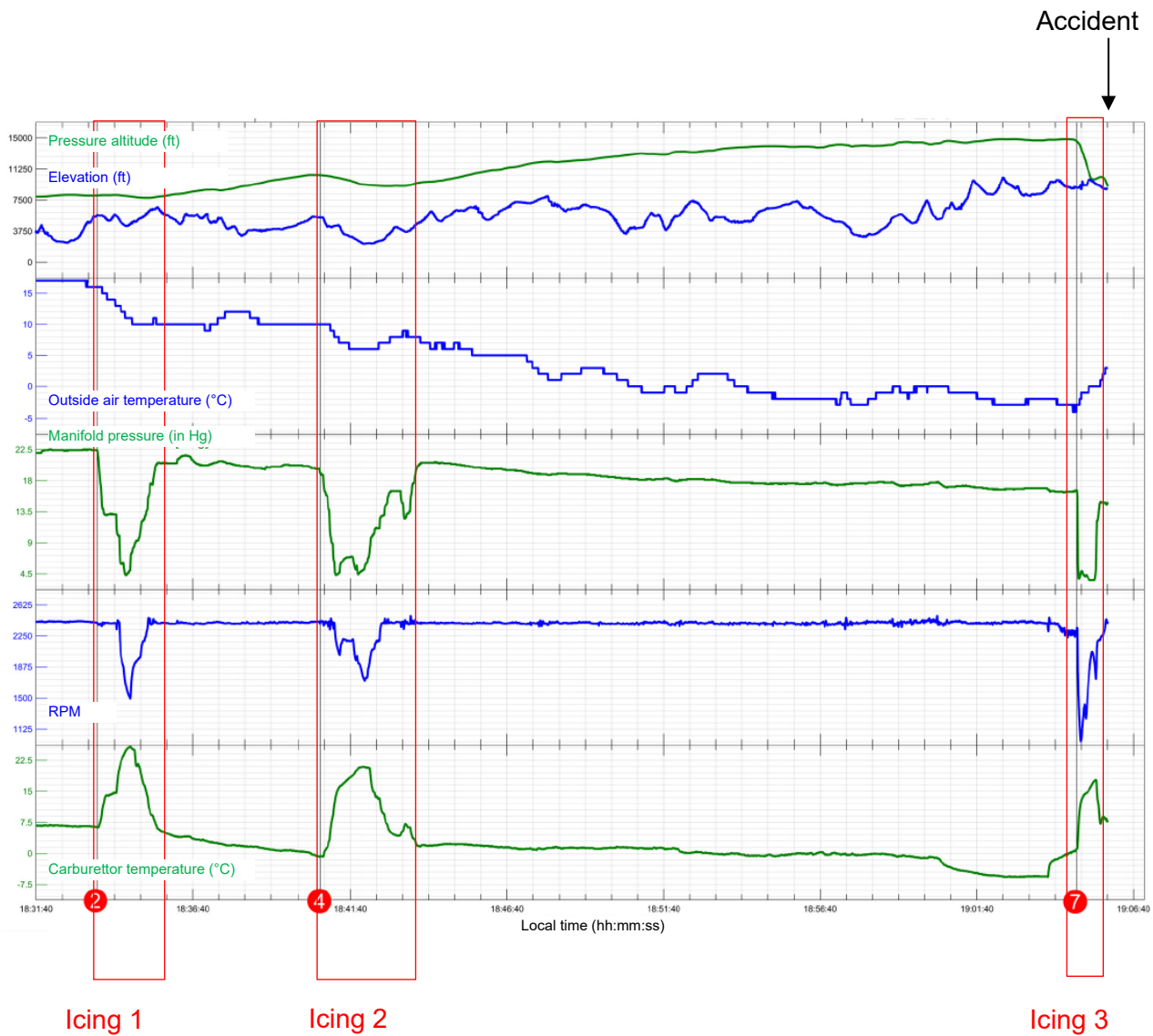


Figure 2: read-out of parameters recorded during the flight
Source: BEA

Of the 23 identified occurrences, 6 resulted in fatal injury of the occupants. Five of these occurrences involved microlights (with six microlights involved in total).

These occurrences can also be classified according to the flight phase during which the occurrences happened:

- four occurrences happened during approach;
- six occurrences happened in cruise flight;
- seven occurrences happened at take-off or in initial climb;
- for 6 occurrences, the phase of flight is unknown.

2.3. Comments and analyses

The most recent data shows that the percentage of events associated with the piston engine induction system icing is low, between 1 and 2.5%. This percentage is higher in the document concerning the UK.

Notably older data provides equivalent percentages.

Of these events, the percentage that resulted in the fatal injury of the occupants is also low for the United States. However, it is higher with the data issued by the BEA. This difference can be explained by the taking into account of events involving microlights.

3 - BIBLIOGRAPHIC RESEARCH

3.1. Types of icing

Three types of icing are associated with the induction system in piston engines equipping certified general aviation aircraft and microlights. The literature all concurs on this topic.

The three types of icing are as follows:

- Impact icing:

This type of icing occurs when supercooled water droplets, which can be present in the clouds or freezing rain, come into contact with a thermal wall. When the droplet strikes the surface, a small amount of the water instantly freezes and the latent heat that is released increases the temperature of the remaining water to 0°C. The transfer of heat to the surface and into the atmosphere freezes this water.

This type of icing can occur on the inlet lips, on filters and on all protruding parts (Figure 3 and Figure 4).



Figure 3: zone conducive to impact icing
Source: aopa.com

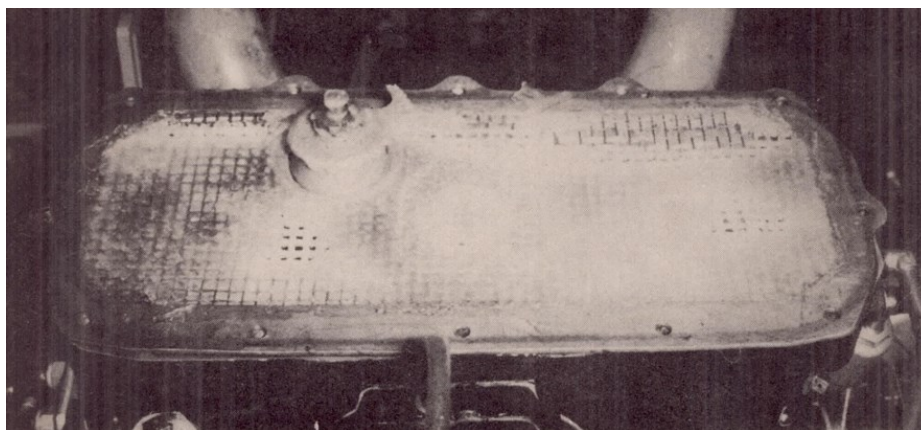


Figure 4: impact icing on a filter

Source: *Laboratory investigation of ice formation and elimination in the induction system of a large twin-engine cargo aircraft - Willard D. Coles - 1947*

- Carburettor or butterfly valve icing

This is the most common type of icing. This type of icing usually forms on the carburettor butterfly valve (or throttle valve) and in its direct vicinity (**Figure 5** and **Figure 6**).

This type of icing is associated with a sudden decrease in temperature due to two phenomena:

- the vaporization of fuel in the air (latent vaporization heat taken up by the fuel in the vicinity);
- the venturi effect that causes a drop in pressure and therefore a decrease in the environmental temperature (gas expansion).

If the decrease in temperature makes the air colder than its dew point, the water vapour in the air condenses. If the temperature of the mixture falls below zero, the condensed water will turn to ice on the surfaces of the carburettor.



Figure 5: icing of a constant depression carburettor

Source: *flygemair.com*

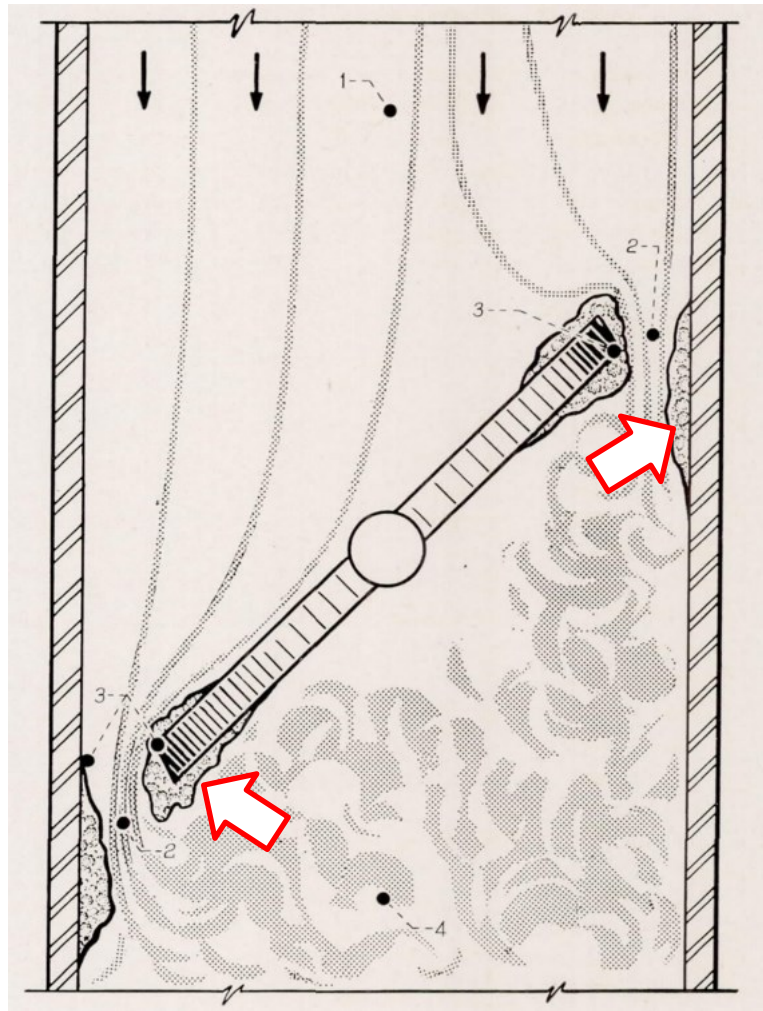


Figure 6: diagram illustrating carburettor icing

Source: excerpt from the article "Icing protection requirements for reciprocating-engine induction systems" - Willard D.Coles, Vern G.Rollin, Donald R.Mulholland - 1950

- Fuel icing:

This is the least common type of icing.

This phenomenon is caused by the presence of water held in suspension in the fuel that can precipitate and freeze on the walls when the temperature of the fuel is below zero.

3.2. Carburetors studied

3.2.1. Types of carburetors

Piston engines with carburetors that are currently installed on certified general aviation aircraft or microlights are essentially float-type carburetors.

There are two carburettor families:

- float-type carburetors;
- pressure carburetors.

3.2.1.1 - Float-type carburetors

Float-type carburetors are so-called due to the float that rests on the surface of the fuel in its bowl, or tank (this bowl constitutes a reserve of fuel between the aircraft tank and the fuel injection zone). A needle valve, attached to the float, opens and shuts off the supply of fuel from the carburettor bowl. When the level of fuel forces the float to rise, the needle valve closes the fuel opening and stops fuel flow to the carburettor. The needle valve reopens when the fuel level drops in the bowl.

The stream through which the air circulates is equipped with two devices:

- a venturi device;
- a butterfly valve (located downstream of the venturi).

The flow of the air-fuel mixture to the cylinders is regulated by the butterfly valve, which is directly associated with the throttle lever in the cockpit. The fuel is “sucked” from the bowl towards the air stream (in the form of small droplets) due to the drop in pressure occurring in the throat of the venturi device.

According to the literature, the main disadvantage of the float-type carburettor is its propensity to icing. Taking into account the “suction” of the fuel by depression, the fuel discharge nozzle is located in line with the throat of the venturi, upstream of the butterfly valve (**Figure 7**). This means that the decrease in temperature caused by the vaporization of the fuel occurred inside the venturi, in addition to the decrease in temperature associated with the venturi itself. This in turn facilitates the formation of ice in the venturi and on the butterfly valve.

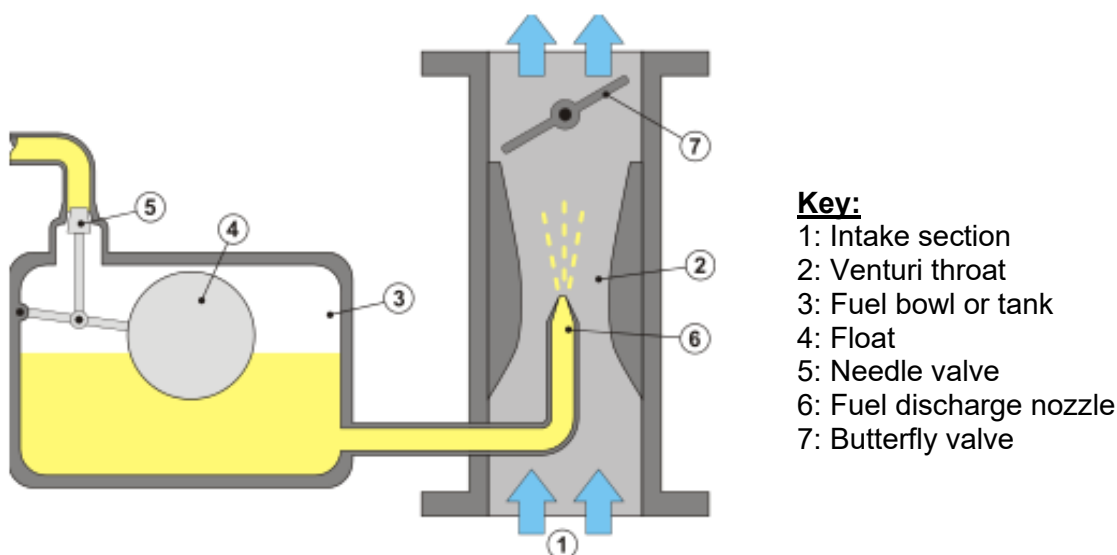


Figure 7: schematic diagram of a float-type carburettor

Source : <https://fr.wiktionary.org/wiki/flotteur>

3.2.1.2 - Pressure carburetors

A pressure carburettor discharges the fuel into the flow of air after the air has passed through the butterfly valve (**Figure 8**). This optimises vaporization.

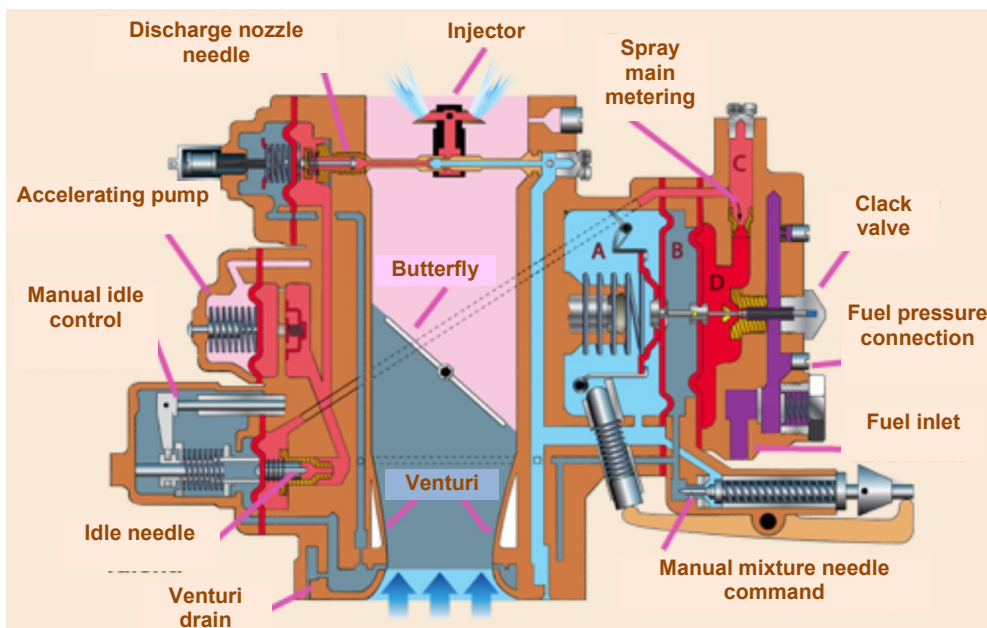


Figure 8: Stromberg PS carburettor (pressure carburettor)

Source : <https://www.lavionnaire.fr/PistonCarburation.php>

3.2.2. Description of float-type carburetors

There are two main types of float-type carburetors:

- conventional carburetors;
- constant depression carburetors.

3.2.2.1 - Conventional carburetors

Conventional carburetors used in general aviation are essentially made by the manufacturer Marvel-Schebler. The description of the operation of a carburettor of this type is demonstrated for the model MA.4-5 (link: <https://msacarbs.com/product-category/carburetors/ma-4-5/>).

In general aviation, this type of carburettor principally equips direct-drive, four- or six-cylinder, horizontally opposed, and air-cooled engines that are manufactured by Lycoming (link: <https://lycoming.com>) and Continental Aerospace Technologies (link: <https://www.continental.aero>). On these propulsion systems, the carburettor is positioned under the engine as shown in **Figure 9**.

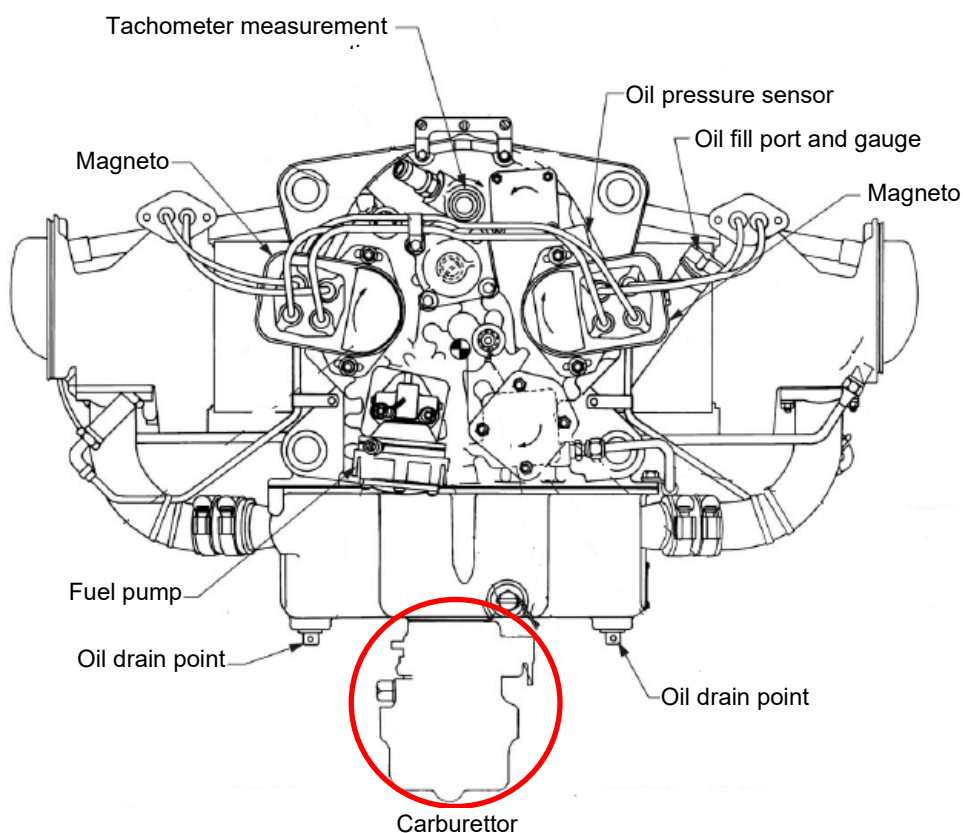


Figure 9: illustration of the position of the carburettor on a Lycoming 0-360-A1AD engine
Source: excerpt from the Lycoming operator's manual

Externally, this carburettor comprises (**Figure 10**):

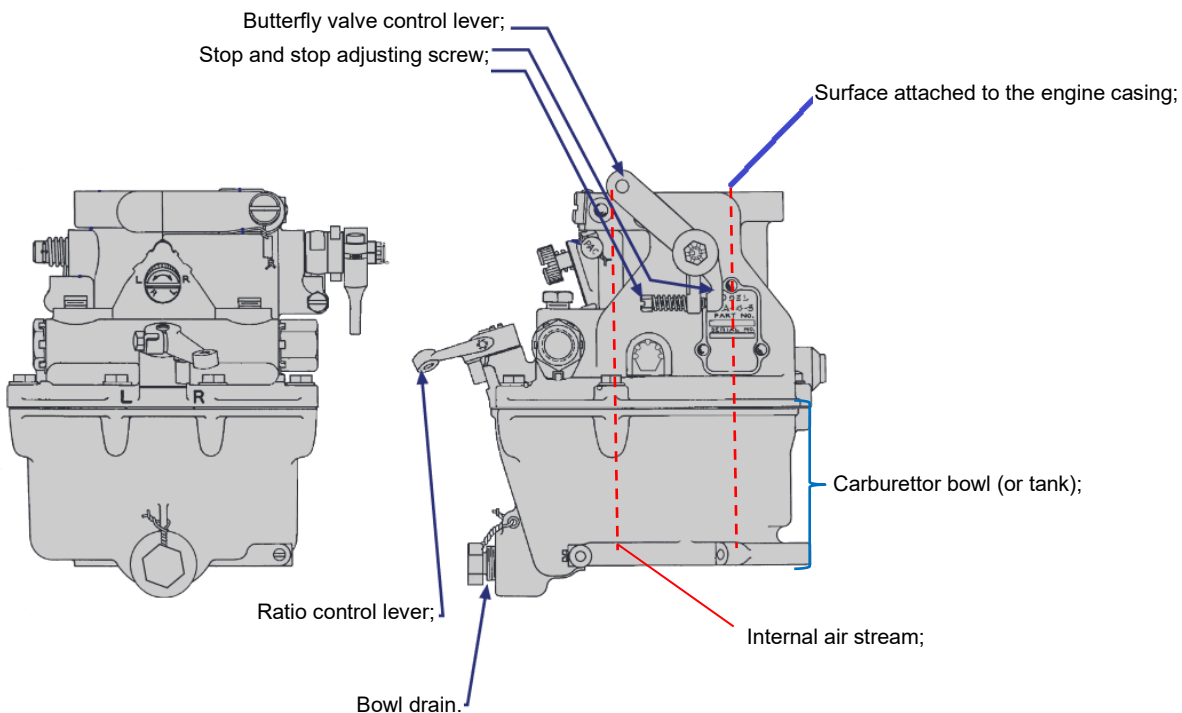


Figure 10: diagram of the outside of a carburettor
 Source: excerpt from the Precision Airmotive / Marvel Schebler manual, Revision 1, issued in 2002

This carburettor is equipped with two floats interconnected by a metallic part (**Figure 11**).



Figure 11: illustration of two floats interconnected by a metallic part
 Source: BEA



Figure 12: fuel bowl or tank
 Source: BEA

The stream through which the air circulates, followed by the air/fuel mixture, comprises a venturi and a butterfly valve downstream as shown in the diagram in **Figure 13**.

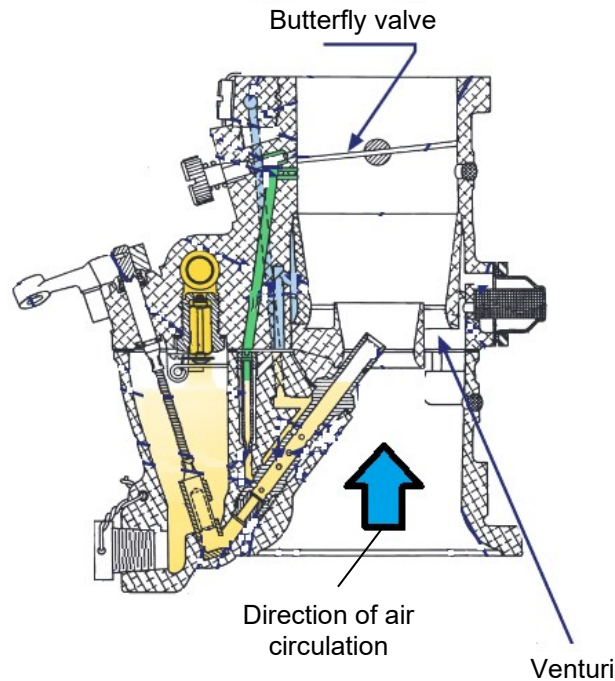


Figure 13: cutaway diagram of the carburettor

Source: excerpt from the Precision Airmotive / Marvel Schebler manual, Revision 1, issued in 2002

Two pressures are exerted to discharge the fuel contained in the carburettor bowl into the carburettor stream:

- atmospheric pressure prevailing over the fuel level in the bowl chamber and thus exerting a downward force on the fuel inside the bowl;
- a pressure below the atmospheric pressure in line with the venturi in the carburettor throat.

The resulting differential pressure creates a push/pull action on the fuel. The fuel is correctly metered by the strategic positioning of the discharge nozzle in the venturi tube. The venturi is positioned in the intake air flow at the average speed point immediately upstream of the throttle butterfly valve.

The arrival of air through the valve body serves to vaporise the fuel and to mix it with the air as it is directed towards the cylinder inlets. This fuel and air mixture in the carburettor throat helps to convert a significant quantity of the liquid fuel into a gaseous state. The speed, effectiveness and power of the engine are significantly influenced by the quantity and nature of this homogeneous mixture. Air flow quality has a direct influence on fuel metering.

The fuel system comprises two sections:

- the main circuit associated with the main discharge nozzle;
- the idle circuit.

At idle and up to low speeds, little or no fuel passes through the main injector. Indeed, the butterfly valve is almost closed and the air flow is low. At this stage, the fuel is sucked into the idle bleed tube in the bowl, then through the idle emulsion tube towards the idle injectors located in line with the butterfly valve. When this butterfly valve is open, suction that occurs upon the opening of the fuel supply at idle reduces and the main jet completely takes over. The various in-line idle injectors help with the smooth transition between idle and full power (**Figure 14**).

Any sudden opening of the butterfly valve causes an offset between the time when the idle circuit ceases to function and the main jet takes over. In effect, there is not enough air that flows in through the carburettor stream to take in the fuel from the main discharge nozzle in addition to the fuel sucked in the idle circuit. An accelerating pump is then used to offset this shortfall and to eliminate the temporarily lean mixtures. This accelerating pump is mechanically linked to the butterfly valve control and discharges the fuel through a tube adjacent to the main nozzle.

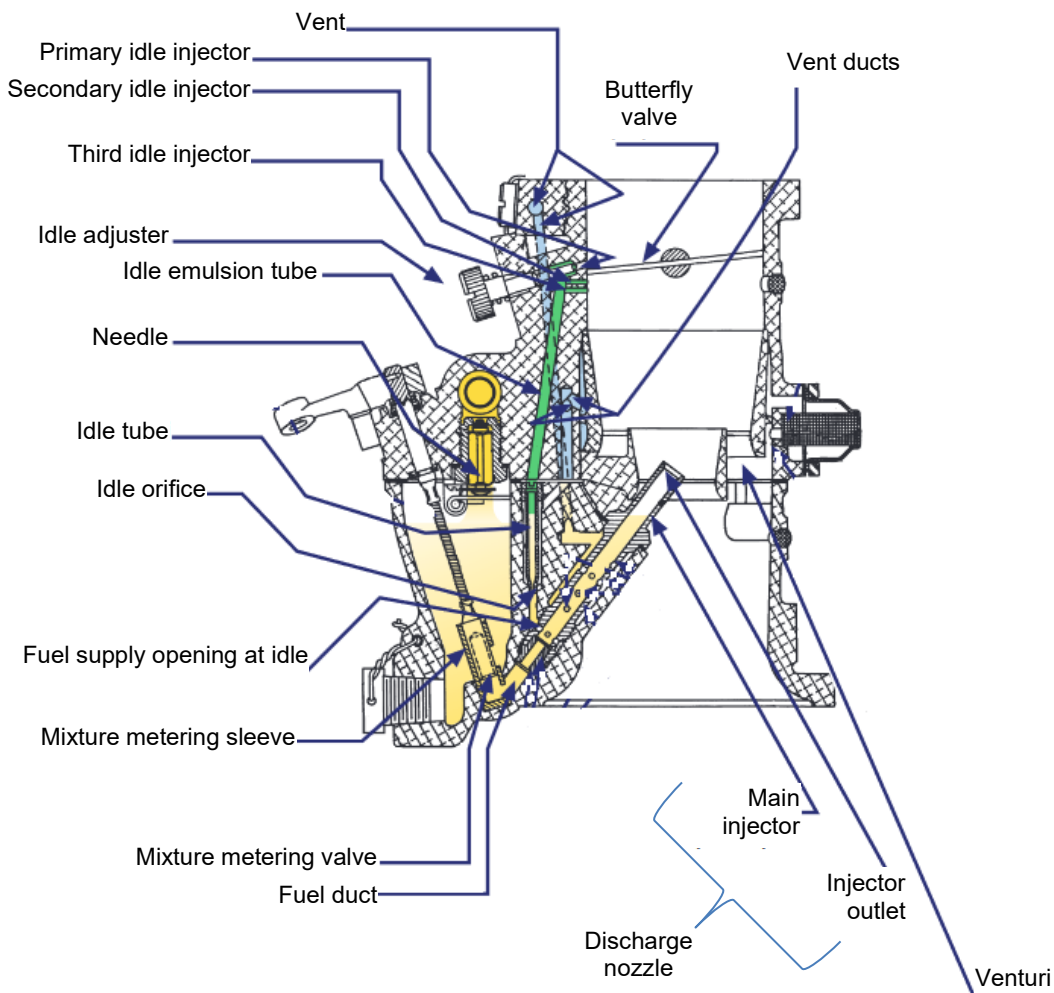


Figure 14: sectional view of the carburettor

Source: excerpt from the Precision Airmotive / Marvel Schebler manual, Revision 1, issued in 2002

3.2.2.2 - Constant depression carburetors

Constant depression carburetors used on certified general aviation aircraft or on microlights are essentially Bing models as shown in the schematic diagram below (**Figure 15**). The BEA mostly encounters this type of carburettor on Rotax engines (para. 5).

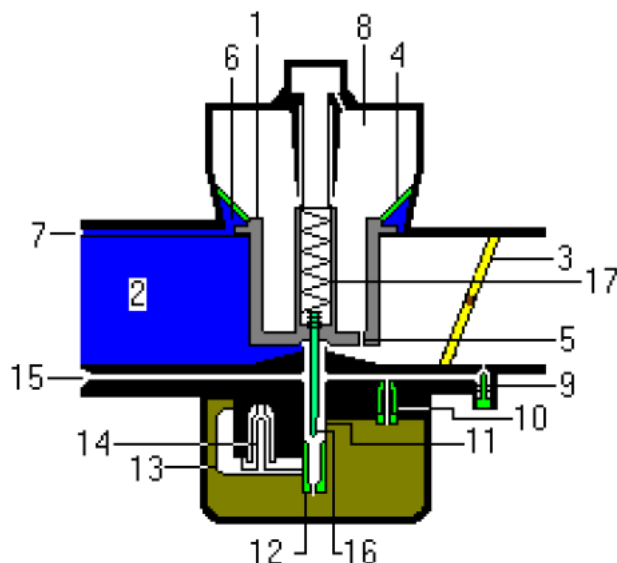
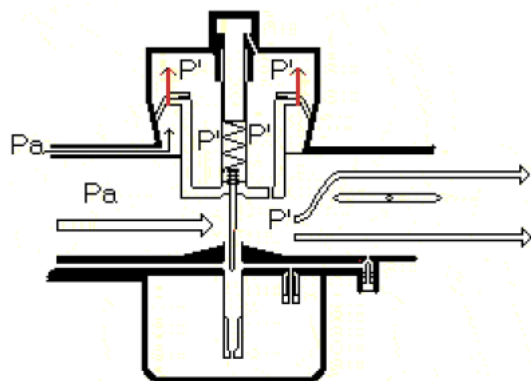


Figure 15: schematic diagram of a constant depression carburettor

Source: excerpt from the website www.aero-hesbaye.be

Key:

- 1: Throttle valve
- 2: Carburettor stream
- 3: Butterfly valve
- 4: Diaphragm
- 5: Duct carrying negative pressure air into the upper chamber
- 6: Lower chamber
- 7: Duct carrying atmospheric pressure air to the lower chamber
- 8: Upper chamber
- 9: Ratio adjuster
- 10: Idle jet
- 11: Needle jet
- 12: Main jet
- 13: Float
- 14: Needle valve
- 15: Main nozzle air duct
- 16: Needle
- 17: Return spring (tension spring)



This type of carburettor is equipped with a throttle valve that slides into a housing to fully or partially obstruct the air flow. The butterfly valve is used to adjust the opening of the throttle valve based on the extent of engine negative pressure. When the butterfly valve is slightly open, the throttle valve remains in the low position. When the butterfly valve is fully open, the throttle valve lifts up and is held in the up position by the return spring.

The throttle valve is associated with a diaphragm that creates a leaktight separation in the vacuum bell (upper chamber - item 8 in figure 15 and lower chamber - item 6 in figure 15) without preventing it from sliding up and down.

The induction vacuum is connected to the bell by a drillhole in the bottom of the throttle valve. The lower chamber of the diaphragm is vented. The vacuum, of varying degrees, adjusted by the position of the butterfly valve, communicates with the bell and thus lifts the throttle valve.

The carburettor therefore operates as a result of the differences in pressure: between the atmospheric pressure and the pressure prevailing in another zone. The level of pressure in this specific carburettor zone in relation to the atmospheric pressure determines the position of the throttle valve and an air/fuel ratio that must be constant. A wedge needle attached to the throttle valve drops into a diffuser called the needle well. This diffuser is equipped with a calibrated orifice called the needle jet. When the throttle valve is fully open, the needle is raised and the annular space between the calibrated orifice of the well and the needle is at its largest. The amount of fuel that then passes through the carburettor body is at its maximum (Figure 16). As the throttle valve descends, the needle sinks into the well, and as its section increases, the annular section decreases, and subsequently so does the fuel flow.

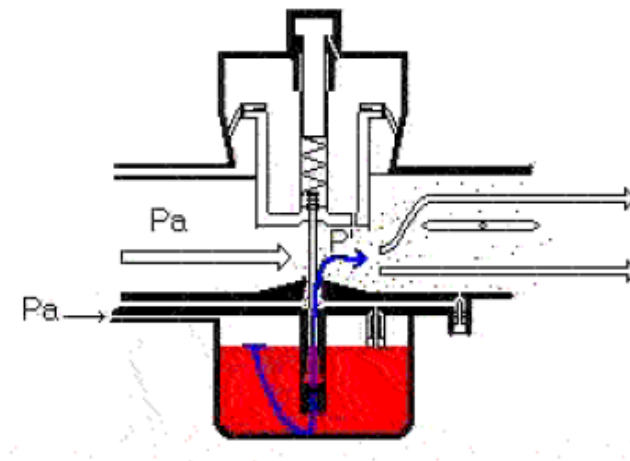


Figure 16: schematic diagram of fuel injection
Source: excerpt from the website www.aero-hesbaye.be

3.3. Certification, monitoring and continuing airworthiness authorities

3.3.1. Sources and method

Research was conducted on the following ministerial and authority websites focusing on public-access documents:

Authority	Country
EASA	Europe
DGAC	France
FAA	USA
Transport Canada	Canada
CASA	Australia
CAA	UK
CAA	New Zealand
CAA	South Africa
Luftfahrt-Bundesamt	Germany
Federal public service Mobility and Transport	Belgium
National Civil Aviation Agency (ANAC)	Brazil
CAA	Finland
Danish Meteorological Institute - Ministry of Transport	Denmark
Irish Aviation Authority	Ireland
CAA	Japan
CAA	Norway
CAA	Sweden
Federal Office of Civil Aviation	Switzerland

The review of the literature on these websites focused on the following two points:

- the contents of regulations pertaining to carburettor icing;
- publications specific to this phenomenon;

Keywords used:

- carburettor icing;
- induction icing.

3.3.2. EASA and FAA publications

3.3.2.1 - EASA

The certification documents used and information issued pertaining to the phenomenon of induction system icing in piston engines are summarised in the table below.

The following certification documents are used:

- CS 23: Normal, Utility, Aerobatic and Commuter Category Aeroplanes;
- CS 27: Small Rotorcraft;
- CS 22: Sailplanes and Powered Sailplanes;
- CS LSA: Light Sport Aeroplanes;
- CS VLR: Very Light Rotorcraft;
- CS VLA: Very Light Aeroplanes;
- CS E: Engines.

With regards to document CS 23, there has been a change in specification since the last amendment 5 published in March 2017. Since then, the specifications pertaining to the protection of the powerplant against icing refer to the ASTM standards (F3062, F3063 and F3066) of which the content remains identification to the previous version of the CS. It should be noted that document CS-VLA was combined with document CS 23 *Amendment 5*.

Prior to this amendment (period between the *Initial Issue* and *Amendment 4*), the specifications were specified in the CS document. These specifications pertain to the heating conditions of the induction system based on the type of carburettor concerned. The two types of carburettor described in chapter 3.1 were considered: float-type carburettor, designated the “Venturi Carburettor”, the pressure carburettor, designated the “Carburettor Tending to Prevent Icing”. They also mention injection devices that do not require a carburettor.

The specifications defined for document CS-LSA are identical to those defined for document CS 23. The document refers to the same ASTM standards.

The contents of documents CS 27 and CS-VLR are identical. The contents are similar to those of the previous version of document CS 23.

The contents of document CS 22 are very similar to the contents of documents CS 27 and CS VLR. We note that only float-type carburettors are dealt with.

In all these documents, the requirements concern only the means to prevent and eliminate icing. Specific temperature rises are required by the heater under defined conditions. These requirements are specified in the tables below.

Document	Version	Date of publication	Information																																		
CS-23 Normal, Utility, Aerobatic and Commuter Category Aeroplanes	Initial issue Amendment 4	November 2003 June 2018	<p>No changes were made to this document between the issue of its first version in November 2003, and the version issued in June 2018.</p> <p>Information pertaining to this phenomenon is specified in the following chapters:</p> <ul style="list-style-type: none"> - CS 23.1093: Induction System Icing Protection - Flight Test Guide / Chapter 4 Powerplant / Section 6 Induction system <p>Firstly, it is specified that the induction system must have means to prevent and eliminate icing.</p> <p>The conditions listed below must be fulfilled, taking into consideration air free of visible moisture at a temperature of -1°C:</p> <table border="1"> <thead> <tr> <th>Powerplant</th> <th>Power</th> <th>Altitude or sea level</th> <th>Specifications</th> </tr> </thead> <tbody> <tr> <td>Engine equipped with a conventional (float-type) venturi carburettor</td> <td>75% of the maximum power</td> <td>Sea level</td> <td>Heat system required Required temperature increase of 50°C</td> </tr> <tr> <td>Engine equipped with a conventional (float-type) venturi carburettor</td> <td>75% of the maximum power</td> <td>Altitude</td> <td>Heat system required Required temperature increase of 67°C</td> </tr> <tr> <td>Engine equipped with a pressure carburettor</td> <td>60% of the maximum power</td> <td>Altitude</td> <td>Heat system required Required temperature increase of 56°C or 22°C if a fluid de-icing device is used</td> </tr> <tr> <td>Single-engine aeroplane</td> <td>/</td> <td>Sea level</td> <td>Heat system required Temperature supplied greater than or equal to the engine cooling temperature</td> </tr> <tr> <td>Twin-engine aeroplane Engine equipped with a pressure carburettor</td> <td>75% of the maximum power</td> <td>Sea level</td> <td>Heat system required Required temperature increase of 50°C</td> </tr> <tr> <td>Engine with a fuel injector Fuel injected downstream of any obstacle on which ice can form</td> <td>75% of the maximum power</td> <td>Sea level or altitude</td> <td>Heat system required Required temperature increase of 16°C</td> </tr> </tbody> </table> <p><i>Notes: for engines equipped with a supercharger, the increase in temperature inherent to this device can be used to reach the previous conditions.</i></p> <p>The demonstration conditions of the previous specifications are as follows:</p> <table border="1"> <tr> <td>The temperature must be measured at several points of the induction system.</td> </tr> <tr> <td>The in-flight test procedure considers three altitudes (low: below 1,500 ft, intermediate: between 1,500 and 8,000 ft and high: over 8,000 ft). For each altitude, and for three different airspeeds (full throttle, 90% max. speed, 80% max. speed), the temperature is measured with the heat system inactive, then active.</td> </tr> </table> <p>The specifications associated with the fluid heat system are as follows:</p> <table border="1"> <tr> <td>The fluid must be introduced into the induction system, in the vicinity of and upstream of the carburettor; distributed throughout the induction system air flow area.</td> </tr> <tr> <td>The system must be able to supply fluid at the specified flow rate for a duration equal to 3% of the aeroplane's maximum endurance or 20 minutes, without exceeding the quantity required for two hours.</td> </tr> </table> <p>The specifications associated with the air heat system are as follows:</p> <table border="1"> <tr> <td>the system surrounding the exhaust muffler must be ventilated when the system is not activated;</td> </tr> <tr> <td>the muffler and system components must be able to be inspected.</td> </tr> </table>	Powerplant	Power	Altitude or sea level	Specifications	Engine equipped with a conventional (float-type) venturi carburettor	75% of the maximum power	Sea level	Heat system required Required temperature increase of 50°C	Engine equipped with a conventional (float-type) venturi carburettor	75% of the maximum power	Altitude	Heat system required Required temperature increase of 67°C	Engine equipped with a pressure carburettor	60% of the maximum power	Altitude	Heat system required Required temperature increase of 56°C or 22°C if a fluid de-icing device is used	Single-engine aeroplane	/	Sea level	Heat system required Temperature supplied greater than or equal to the engine cooling temperature	Twin-engine aeroplane Engine equipped with a pressure carburettor	75% of the maximum power	Sea level	Heat system required Required temperature increase of 50°C	Engine with a fuel injector Fuel injected downstream of any obstacle on which ice can form	75% of the maximum power	Sea level or altitude	Heat system required Required temperature increase of 16°C	The temperature must be measured at several points of the induction system.	The in-flight test procedure considers three altitudes (low: below 1,500 ft, intermediate: between 1,500 and 8,000 ft and high: over 8,000 ft). For each altitude, and for three different airspeeds (full throttle, 90% max. speed, 80% max. speed), the temperature is measured with the heat system inactive, then active.	The fluid must be introduced into the induction system, in the vicinity of and upstream of the carburettor; distributed throughout the induction system air flow area.	The system must be able to supply fluid at the specified flow rate for a duration equal to 3% of the aeroplane's maximum endurance or 20 minutes, without exceeding the quantity required for two hours.	the system surrounding the exhaust muffler must be ventilated when the system is not activated;	the muffler and system components must be able to be inspected.
			Powerplant	Power	Altitude or sea level	Specifications																															
			Engine equipped with a conventional (float-type) venturi carburettor	75% of the maximum power	Sea level	Heat system required Required temperature increase of 50°C																															
			Engine equipped with a conventional (float-type) venturi carburettor	75% of the maximum power	Altitude	Heat system required Required temperature increase of 67°C																															
			Engine equipped with a pressure carburettor	60% of the maximum power	Altitude	Heat system required Required temperature increase of 56°C or 22°C if a fluid de-icing device is used																															
			Single-engine aeroplane	/	Sea level	Heat system required Temperature supplied greater than or equal to the engine cooling temperature																															
			Twin-engine aeroplane Engine equipped with a pressure carburettor	75% of the maximum power	Sea level	Heat system required Required temperature increase of 50°C																															
			Engine with a fuel injector Fuel injected downstream of any obstacle on which ice can form	75% of the maximum power	Sea level or altitude	Heat system required Required temperature increase of 16°C																															
			The temperature must be measured at several points of the induction system.																																		
			The in-flight test procedure considers three altitudes (low: below 1,500 ft, intermediate: between 1,500 and 8,000 ft and high: over 8,000 ft). For each altitude, and for three different airspeeds (full throttle, 90% max. speed, 80% max. speed), the temperature is measured with the heat system inactive, then active.																																		
The fluid must be introduced into the induction system, in the vicinity of and upstream of the carburettor; distributed throughout the induction system air flow area.																																					
The system must be able to supply fluid at the specified flow rate for a duration equal to 3% of the aeroplane's maximum endurance or 20 minutes, without exceeding the quantity required for two hours.																																					
the system surrounding the exhaust muffler must be ventilated when the system is not activated;																																					
the muffler and system components must be able to be inspected.																																					

Document	Version	Date of publication	Information																												
CS-23 Normal, Utility, Aerobatic and Commuter Category Aeroplanes (CS-VLA)	Amendment 5	March 2017	<p>The CS document simply specifies that any build-up or forecast ice or snow fall that could be detrimental to the operation of the engine must be avoided.</p> <p>The AMC document refers to the following ASTM standards:</p> <ul style="list-style-type: none"> • F3062/F3062M-16 Standard Specification for Installation of Powerplant Systems • F3063/F3063M-16a Standard Specification for Design and Integration of Fuel/Energy Storage and Delivery System Installations for Aeroplanes • F3066/F3066M-15 Standard Specification for Powerplant Systems Specific Hazard Mitigation <p>The specifications pertaining to induction system icing are presented in standard F3066. The details are specified in the table below.</p>																												
ASTM Standard F3066	Latest version published	21 May 2018	<p>The specifications are similar to those described in the aforementioned amendment 4.</p> <p>The conditions listed below must be fulfilled, taking into consideration air free of visible moisture at a temperature of -1°C:</p> <table border="1"> <tbody> <tr> <td>Engine equipped with a conventional (float-type) venturi carburettor</td> <td>75% of the maximum power</td> <td>Sea level</td> <td>Heat system required Required temperature increase of 50°C</td> </tr> <tr> <td>Engine equipped with a conventional (float-type) venturi carburettor</td> <td>75% of the maximum power</td> <td>Altitude</td> <td>Heat system required Required temperature increase of 67°C</td> </tr> <tr> <td>Engine equipped with a carburettor tending to prevent icing</td> <td>60% of the maximum power</td> <td>Altitude</td> <td>Heat system required Required temperature increase of 56°C or 22°C if a fluid de-icing device is used</td> </tr> <tr> <td>Engine with a fuel injector with measuring components on which impact ice can accumulate</td> <td>75% of the maximum power</td> <td>Sea level or altitude</td> <td>Heat system required Required temperature increase of 24°C</td> </tr> <tr> <td>Engine using a fuel metering system tending to prevent icing</td> <td>75% of the maximum power</td> <td>Sea level</td> <td>Heat system required Required temperature increase of 16°C</td> </tr> <tr> <td>Twin-engine aeroplane Engine equipped with a pressure carburettor</td> <td>75% of the maximum power</td> <td>Sea level</td> <td>Heat system required Required temperature of 50°C</td> </tr> <tr> <td>Engine with a fuel injector Fuel injected downstream of any obstacle on which ice can form</td> <td>75% of the maximum power</td> <td>Sea level or altitude</td> <td>Heat system required Required temperature increase of 16°C</td> </tr> </tbody> </table>	Engine equipped with a conventional (float-type) venturi carburettor	75% of the maximum power	Sea level	Heat system required Required temperature increase of 50°C	Engine equipped with a conventional (float-type) venturi carburettor	75% of the maximum power	Altitude	Heat system required Required temperature increase of 67°C	Engine equipped with a carburettor tending to prevent icing	60% of the maximum power	Altitude	Heat system required Required temperature increase of 56°C or 22°C if a fluid de-icing device is used	Engine with a fuel injector with measuring components on which impact ice can accumulate	75% of the maximum power	Sea level or altitude	Heat system required Required temperature increase of 24°C	Engine using a fuel metering system tending to prevent icing	75% of the maximum power	Sea level	Heat system required Required temperature increase of 16°C	Twin-engine aeroplane Engine equipped with a pressure carburettor	75% of the maximum power	Sea level	Heat system required Required temperature of 50°C	Engine with a fuel injector Fuel injected downstream of any obstacle on which ice can form	75% of the maximum power	Sea level or altitude	Heat system required Required temperature increase of 16°C
Engine equipped with a conventional (float-type) venturi carburettor	75% of the maximum power	Sea level	Heat system required Required temperature increase of 50°C																												
Engine equipped with a conventional (float-type) venturi carburettor	75% of the maximum power	Altitude	Heat system required Required temperature increase of 67°C																												
Engine equipped with a carburettor tending to prevent icing	60% of the maximum power	Altitude	Heat system required Required temperature increase of 56°C or 22°C if a fluid de-icing device is used																												
Engine with a fuel injector with measuring components on which impact ice can accumulate	75% of the maximum power	Sea level or altitude	Heat system required Required temperature increase of 24°C																												
Engine using a fuel metering system tending to prevent icing	75% of the maximum power	Sea level	Heat system required Required temperature increase of 16°C																												
Twin-engine aeroplane Engine equipped with a pressure carburettor	75% of the maximum power	Sea level	Heat system required Required temperature of 50°C																												
Engine with a fuel injector Fuel injected downstream of any obstacle on which ice can form	75% of the maximum power	Sea level or altitude	Heat system required Required temperature increase of 16°C																												

Document	Version	Date of publication	Information															
CS 27 Small Rotorcraft	Initial issue Amendment 8	November 2003 June 2021	<p>No changes were made to these documents between the issue of their first versions in November 2003, and their latest versions. Information pertaining to this phenomenon is specified in the following chapter:</p> <ul style="list-style-type: none"> - CS 23.1093: Induction System Icing Protection <p>Firstly, it is specified that the induction system must have means to prevent and eliminate icing. The conditions listed below must be fulfilled, taking into consideration air free of visible moisture at a temperature of -1°C and a power of 75%:</p> <table border="1"> <thead> <tr> <th>Powerplant</th> <th>Altitude or sea level</th> <th>Specifications</th> </tr> </thead> <tbody> <tr> <td>Engine equipped with a conventional (float-type) venturi carburettor</td> <td>Sea level</td> <td>Heat system required Required temperature increase of 50°C</td> </tr> <tr> <td>Engine equipped with a conventional (float-type) venturi carburettor</td> <td>Altitude</td> <td>Heat system required Required temperature increase of 67°C</td> </tr> <tr> <td>Engine equipped with a pressure carburettor</td> <td>Sea level</td> <td>Heat system required Temperature supplied greater than or equal to the engine cooling temperature</td> </tr> <tr> <td>Engine equipped with a pressure carburettor</td> <td>Altitude</td> <td>Heat system required Required temperature increase of 56°C or 22°C if a fluid de-icing device is used</td> </tr> </tbody> </table> <p><i>Notes: for engines equipped with a supercharger, the increase in temperature inherent to this device can be used to reach the previous conditions.</i></p>	Powerplant	Altitude or sea level	Specifications	Engine equipped with a conventional (float-type) venturi carburettor	Sea level	Heat system required Required temperature increase of 50°C	Engine equipped with a conventional (float-type) venturi carburettor	Altitude	Heat system required Required temperature increase of 67°C	Engine equipped with a pressure carburettor	Sea level	Heat system required Temperature supplied greater than or equal to the engine cooling temperature	Engine equipped with a pressure carburettor	Altitude	Heat system required Required temperature increase of 56°C or 22°C if a fluid de-icing device is used
Powerplant	Altitude or sea level	Specifications																
Engine equipped with a conventional (float-type) venturi carburettor	Sea level	Heat system required Required temperature increase of 50°C																
Engine equipped with a conventional (float-type) venturi carburettor	Altitude	Heat system required Required temperature increase of 67°C																
Engine equipped with a pressure carburettor	Sea level	Heat system required Temperature supplied greater than or equal to the engine cooling temperature																
Engine equipped with a pressure carburettor	Altitude	Heat system required Required temperature increase of 56°C or 22°C if a fluid de-icing device is used																
CS 22 Sailplanes and Powered Sailplanes	Initial issue Amendment 3	November 2003 September 2021	<p>No changes were made to this document between the issue of its first version in November 2003, and the version issued in September 2021. Information pertaining to this phenomenon is specified in the following chapter:</p> <ul style="list-style-type: none"> - CS 22.1093: Induction System Icing Protection <p>The conditions listed below must be met:</p> <table border="1"> <tr> <td>For aircraft with an engine that is equipped with a conventional (float-type) venturi carburettor, an intake air heat system is required. When the air is free from visible moisture at a temperature of -1°C and a power of 75%, the required temperature increase is 50°C.</td> </tr> <tr> <td>When the air intake is continuously heated, the aforementioned heat system is not required.</td> </tr> </table>	For aircraft with an engine that is equipped with a conventional (float-type) venturi carburettor, an intake air heat system is required. When the air is free from visible moisture at a temperature of -1°C and a power of 75%, the required temperature increase is 50°C.	When the air intake is continuously heated, the aforementioned heat system is not required.													
For aircraft with an engine that is equipped with a conventional (float-type) venturi carburettor, an intake air heat system is required. When the air is free from visible moisture at a temperature of -1°C and a power of 75%, the required temperature increase is 50°C.																		
When the air intake is continuously heated, the aforementioned heat system is not required.																		
CS E Engines	Initial issue Amendment 6	October 2003 June 2020	<p>No changes were made to the contents of this document pertaining to the phenomenon between the issue of its first version in October 2003, and the version issued in June 2020. Information pertaining to this phenomenon is specified in the following chapter:</p> <ul style="list-style-type: none"> - CS-E 230: De-Icing and Anti-Icing Precautions - CS-E 470: Contaminated Fuel <p>Chapter one specifies that the induction system must minimise the risk of ice formation that can affect engine operation. If necessary, this chapter must include provisions for the use of a prevention means. In this case, an indicator that can define the presence of ice must be installed.</p> <p>Chapter two specifies that the complete fuel system must be able to operate without engine malfunction with probable quantities of solid contaminant, water and ice present in the fuel.</p>															

In addition, the EASA published several documents pertaining to the icing of carburetors in general aviation:

- a document presented as a cartoon strip in the Sunny Swift series:
 - latest version published in April 2018;
 - available at: <https://www.easa.europa.eu/newsroom-and-events/news/sunny-swift-carburettor-icing>;
 - its contents are presented below;
- a publication entitled “Piston Engine Icing”:
 - published in June 2013;
 - available at: <https://www.easa.europa.eu/document-library/general-publications/egast-leaflet-ga-5-piston-engine-icing> ;
 - its contents are presented below;
- the EASA Safety Information Bulletin No. 2010-03:
 - published in October 2010;
 - available at: <https://ad.easa.europa.eu/ad/2010-03>;
 - this document incorporates the *Special Airworthiness Information Bulletin (SAIB) CE-09-35*, published by the FAA on 30 June 2009, described in para. 3.3.2.3.

The contents of the first two documents are similar. The detailed contents of the publication “Piston Engine Icing” are as follows:

- The publication “Piston Engine Icing” is presented as a safety promotion leaflet to assist pilots of piston engined aircraft operating below 10,000 ft.
 - The first information emphasised is that the phenomenon is not solely linked to temperature, but also to relative humidity. It can therefore occur on warm days if the relative humidity is high.
- To define the probability of icing and its severity as a function of the temperature and the dew point temperature, a graph is proposed (Figure 17).

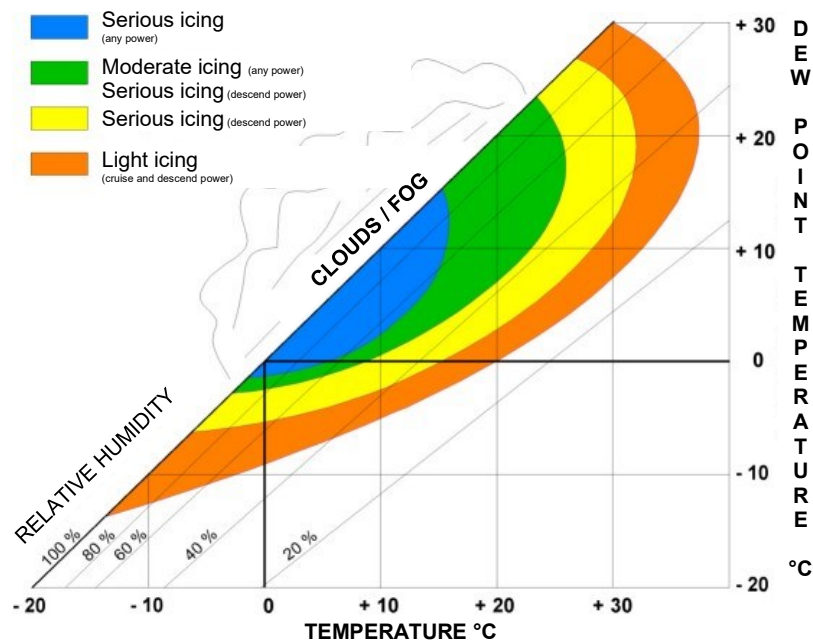


Figure 17: graph proposed by the EASA
 Source: *Piston Engine Icing European General Aviation Safety Team GA5*

- The phenomenon is solely presented as a factor contributing to the accident or the incident.
- The phenomenon especially occurs at low power and is more likely with some powerplants (**BEA comment: no specific explanation**) and when MOGAS is used (**BEA comment: unsubstantiated**).
- The three types of icing are described.
- The document specifies that pilots must be constantly on the alert for this type of phenomenon and to detect the risk of icing, using the weather forecasts available and by analysing their flight environment (e.g. very high relative humidity combined with clouds or fog). Pilots must always refer to the information in the flight manual.
- For aircraft equipped with a fixed pitch propeller, it specifies that the phenomenon results in a decrease in engine speed and aircraft performance (speed and/or altitude).
- For aircraft equipped with a constant speed propeller, it specifies that the phenomenon results in a decrease in manifold pressure. It also specifies that a slight decrease in exhaust gas temperature may be detected before the decline in engine performance.
- It specifies that the carburettor heat system must normally be used in the ON/OFF position; partial use should only be considered if specifically recommended in the Flight Manual. The publication recommends the use of carburettor heating in the following conditions:
 - ⇒ periodic use when the conditions are conducive to icing (per phase lasting around at least 15 seconds) (**BEA comment: unsubstantiated**);
 - ⇒ when the phenomenon occurs and the signs are identified by the pilot, by ensuring that the heating is stopped when the ice has completely melted;
 - ⇒ systematically when conditions are favourable to this phenomenon.
 This heat system must be regularly tested to check efficiency. The system must only be used during take-off if permitted by the Flight Manual.
- To conclude, the publication “Piston Engine Icing” provides pilots with the information they need to prevent, detect, and if necessary, manage icing. No literature source is specified. The data used to compile the icing probability graph is not specified.

3.3.2.2 - FAA

The following certification documents are used:

- Part 23 _ Airworthiness Standards: Normal Category Airplanes
- Part 27 _ Airworthiness Standards: Normal Category Rotorcraft
- Part 33 _ Airworthiness Standards: Aircraft Engines
- Advisory Circular 20-73A _ Aircraft Ice Protection _ Version published on 16 August 2006
- Advisory Circular 23-16A _ Powerplant Guide For Certification Of Part 23 Airplanes And Airships _ Version published on 23 February 2004.

The contents of Part 23 are identical to those of document CS 23.

The contents of Part 27 are identical to those of document CS 27.

The contents of Part 33 are identical to those of document CS E.

Advisory Circular 20-73A:

This circular is not mandatory and does not constitute a regulation. It states how to comply with the icing protection requirements specified by the FAA.

This circular does not provide any supplementary information of use for the study conducted by the BEA.

Advisory Circular 23-16A:

This circular provides information and guidance about the means of compliance with the requirements of Part 23, subpart E. This circular is neither mandatory nor regulatory in nature and does not constitute a regulation.

This circular contains a specific chapter “23.1093 Induction system icing protection”. We note the following contents in this chapter:

Excerpt 1:

“Compliance with § 23.1093 can be shown using an appropriate combination of the methods listed and described below.

- 1. Compliance with part 33 icing requirements;*
- 2. Similarity and service experience;*
- 3. Analysis;*
- 4. Ground testing;*
- 5. Flight testing with an airborne icing tanker;*
- 6. Flight testing in natural icing conditions.”*

Excerpt 2:

“Engine certification to part 33 does not fully address all the part 23 engine installation requirements. ”

Excerpt 3:

“It is the responsibility of the airplane applicant and not the engine manufacturer to show compliance with the part 23 induction system ice protection requirements. ”

Excerpt 4:

“The engine manufacturer should be able to identify critical points, conditions, and operational requirements that may need to be addressed when showing compliance with the installation requirements. ”

Excerpt 5:

“Even if previous experience and data are used, each intake/engine installation and the associated operating characteristics can be different and should be considered individually. ”

Excerpt 6:

“Airplanes being certified for flight into icing conditions according to § 23.1419 will require flight test into natural icing conditions. The results of this testing can be used to show compliance with § 23.1093. ”

BEA comments:

- This chapter focuses on the importance of integrating the propulsion system in the aircraft and the associated specificities.
- The consideration of icing in the induction system is a collaborative work between the aircraft manufacturer and the engine manufacturer.

This type of comment was not identified in the EASA texts.

According to this guidance and these recommendations, we can expect each aircraft manufacturer to have an in-depth knowledge of the phenomenon, along with the specificities of each aircraft.

In addition, the FAA published several documents or articles pertaining to carburettor icing:

- Advisory Circular 20-113:
 - published on 22 October 1981;
 - available at: https://www.faa.gov/regulations_policies/advisory_circulars/index.cfm/go/document.information/documentID/22120;
 - the contents and the philosophy of the Advisory Circular are similar to those of the EASA publication “Piston Engine Icing”. The Advisory Circular is distinguished by a bibliography.
- Special Airworthiness Information Bulletin (SAIB) CE-09-35:
 - published on 30 June 2009;
 - available at: <http://www.tdatacorp.com/saib/CE-09-35.htm>;
 - The FAA specifies that, under the regulations, carburettor icing is not considered an unsafe condition.
The FAA indicated that there were 212 accidents attributed to carburettor icing between 1998 and 2007. Of these accidents, 13 resulted in fatalities.
The document then shows a graph that can be used to determine the probability of carburettor icing and its severity (Figure 18). The data used to compile this graph is not specified.

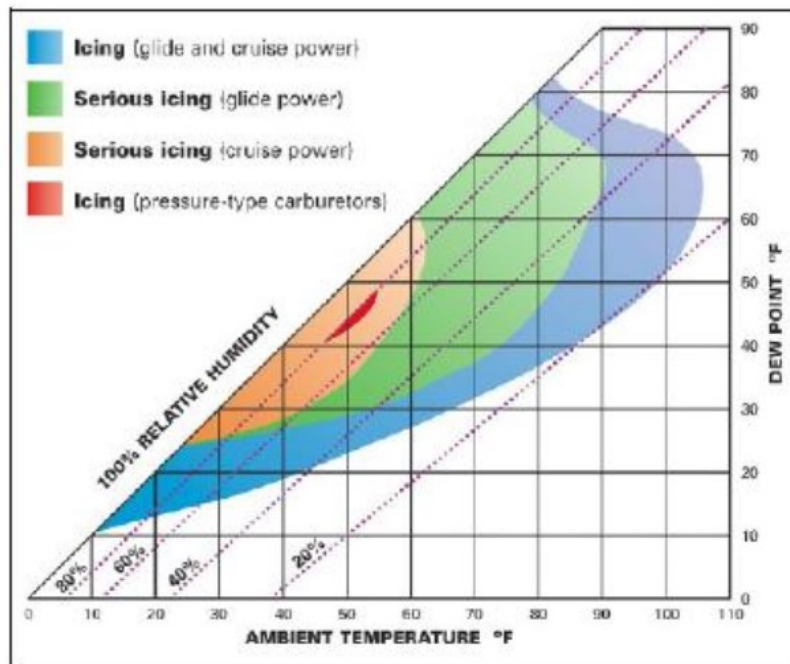


Figure 18: graph proposed by the FAA
 Source: *Special Airworthiness Information Bulletin (SAIB) CE-09-35*

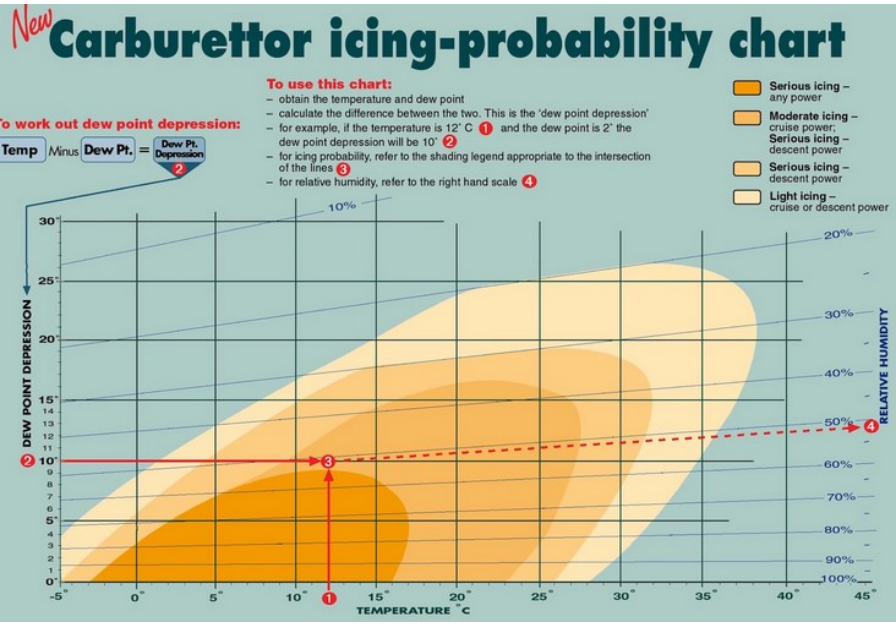
The document then gives information from the EASA publication.

- Articles in *FAA Aviation News*:
 - January-February 2010 issue in which the phenomenon is summarised;
 - January-February 2017 issue in which the phenomenon is also summarised, and in which emphasis is placed on the importance of using a heat system.
- Several publications:
 - *Aviation Maintenance Technician Handbook-Powerplant Volume 1*;
 - *Aviation Maintenance Technician Handbook-Airframe Volume 2*;
 - *Aviation weather*;

The information in these publications is identical to that presented in the other publications.

3.3.3. National authority publications

The publications identified and a summary of their contents are presented in the table below.

Authority	Publication	Date of publication	Contents
	Symposium	October 2008	Topic addressed very briefly with a reminder of the graph proposed by the EASA.
DGAC (France)	DSAC Safety Bulletin No. 16	January 2013	<p>Presentation of feedback (case of a Cessna 150)</p> <p>The consensus was that this graph has its limits and only gives a vague estimation of the risk, which is largely determined by the aeroplane. The question arose about how, by entering the meteorological parameters T° and Td°, it is possible to determine the risk of carburettor icing. In fact, these risk zones were established after nearly 5,400 cases of carburettor icing with temperature conditions observed on the ground. Not all cases are therefore covered and caution is therefore advised.</p> <p>BEA comment: The BEA's bibliographic research did not therefore enable the information specified in the above comment to be confirmed or disproved.</p>
CAA UK	Safety Sense Leaflet - Piston Engine Icing - 14 _version b	January 2013	The contents of this document are strictly identical to the EASA publication entitled "Piston Engine Icing".
	Article disponible sur le site : https://shop.casa.gov.au/products/carburettor-icing-probability-chart	Publication in force	Refers to the graph mentioned hereinafter.
ATSB (Australia)	The authority published a specific graph to define the probability and severity of icing.	Publication in force	<p>The latest version of the graph is the following:</p>  <p>New Carburettor icing-probability chart</p> <p>To use this chart:</p> <ul style="list-style-type: none"> – obtain the temperature and dew point – calculate the difference between the two. This is the 'dew point depression' – for example, if the temperature is 12° C (1) and the dew point is 2° the dew point depression will be 10° (2) – for icing probability, refer to the shading legend appropriate to the intersection of the lines (3) – for relative humidity, refer to the right hand scale (4) <p>Legend:</p> <ul style="list-style-type: none"> Serious icing – any power Moderate icing – cruise power; Serious icing – descent power Serious icing – descent power Light icing – cruise or descent power <p>Figure 19: Graph proposed by the Australian authorities</p> <p>Source: https://www.google.com/url?sa=t&rct=j&q=&esrc=s&source=web&cd=&ved=2ahUKEwin7_un84j2AhWK4IUKHehzDBwQFnoECAgQAQ&url=https%3A%2F%2Fwww.atsb.gov.au%2Fmedia%2F47763%2Fcarb_icing.pdf&usq=AOvVaw2YdHq7rNGCrzkxZU6rXWXP</p>

Authority	Publication	Date of publication	Contents
Transport Canada	"Carburetor icing" within the series of documents "Take Five for safety".	2014	<p>This document specifies that carburetor icing is a common cause of accidents. It also states that in most of these accidents, the pilot had not fully understood the process of ice formation or the workings of the heat system.</p> <p>The document then shows the following graph that can be used to determine the probability of carburetor icing and its severity:</p> <p>Figure 20: graph proposed by the Canadian authorities</p> <p>Source: Take five for safety, https://tc.canada.ca/en/aviation/publications/take-five-for-safety-tp-2228/take-five-carburetor-icing-tp-2228e-38</p> <p>The data used to compile this graph is not specified.</p> <p>It shall be stated that this graph does not apply to a carburetor operating on automotive gasoline (MOGAS) due to its higher volatility and greater susceptibility to icing.</p>
CAA New Zealand	Aircraft Icing Handbook	June 2000	The document includes a chapter specific to the induction system. The information published is similar to that published in the EASA document.
	Article in Vector Magazine	November / December 2002	Subject briefly addressed with the most common information.
	Safety Message "No Ice, Thanks"	2015	Refers to the graph proposed by the Australian authorities.

Authority	Publication	Date of publication	Contents
Denmark - Transport Ministry / Meteorological service	Carburetor Icing-Probability	2004	<p>This technical report was written at the request of the <i>Danish Accident Investigation Board</i>.</p> <p>The study consisted in generating carburetor icing probability statistics, in Denmark, for each month of the year and for seven distinct heights: 124, 1,250, 2,500, 3,750, 5,000, 6,250 and 7,500 ft.</p> <p>These statistics were generated from radiosonde data, measuring the temperature and the dew point temperature, twice daily for 24 years. For each measuring point, the probability of icing and its severity are defined based on the graph published by the Australian authorities, for the temperature and the dew point temperature.</p> <p>The report specifies that no information pertaining to the compilation of the graph proposed by the Australian authorities is available, and its origin remains unknown.</p> <p>It also specifies that the effect of the altitude, and more precisely its influence on the decrease in relative pressure as a consequence of the venturi phenomenon, was not studied.</p> <p>This study concludes that:</p> <ul style="list-style-type: none"> • the risk of serious/moderate icing was present at all of the heights studied, year-round; • the probability of serious or moderate icing decreases with height, with significant seasonal variations; • at ground level, the probability of serious or moderate icing has only minor seasonal variations; • seasonal variation is more pronounced from the height of 2,500 ft, with icing more likely to occur in the summer months.

3.3.4. Safety lessons

These publications do not provide the BEA with additional information to take into account and to analyse in its investigations the phenomenon of piston engine induction system icing.

The certification requirements focus essentially on the heat system. One FAA publication also specifies that it is the aeroplane manufacturer's responsibility to integrate the engine and to ensure conformity to the icing protection requirements. In these conditions, we should expect the aeroplane manufacturer to be very knowledgeable about propulsion system performance in icing conditions.

3.4. Investigation authorities

3.4.1. Investigation reports

3.4.1.1 - Objective, sources and overview of results

The aim was to identify how the phenomenon of piston engine induction system icing is dealt with in investigation reports.

The table on the next page lists the investigation reports used, specifying the country that published the report, the type of aircraft and the reference material used. These reports were found on the websites of the authorities concerned. The BEA decided to narrow this research down to reports published since 2000.

The different investigation reports reviewed present the phenomenon of induction system icing in a similar way. The phenomenon is generally presented as a hypothetical loss of power that resulted in or was a factor contributing to an accident or incident.

The investigation authorities process this information by considering the ground weather conditions on the day, and by recording these conditions on one of the aforementioned graphs. The presentation made in these reports is therefore similar to that made by the BEA.

With the exception of one document, none of the reports conducted the analysis with focus on the powerplant.

3.4.1.2 - Results

Year Report reference	Aircraft	Engine	Conditions	Comments	Type of icing defined (refer to chapter 5.8)
United States					
2018 CEN18LA385	Zenair ZENITH CH 750	General Motors Corvair model	Temperature: 21°C Dew point temperature: 19°C	In initial climb Refers to Special Airworthiness Information Bulletin CE-09-35 published by the FAA	Serious in glide power
2018 CEN18TA233	Cessna 150F	Continental O-200A	Temperature: 26°C Dew point temperature: 23°C	In cruise flight Refers to Special Airworthiness Information Bulletin CE-09-35 published by the FAA	Serious in glide power
2018 CEN18LA152	Grumman G 164A	Pratt&Whitney R-1340-AN1	Temperature: 25°C Dew point temperature: 9°C	Immediately after take-off Refers to Special Airworthiness Information Bulletin CE-09-35 published by the FAA	Serious in glide power
2018 CEN18LA138	Piper PA 24	Lycoming O-360 SER	Temperature: 29°C Dew point temperature: 18°C	On final Refers to Special Airworthiness Information Bulletin CE-09-35 published by the FAA	Serious in glide power
2018 CEN18LA131	Cessna 180	Continental O 470J	Temperature: 12°C Dew point temperature: 5°C	Refers to Special Airworthiness Information Bulletin CE-09-35 published by the FAA	Serious at any power
2018 ERA18LA059	Cessna 172	/	Temperature: 10°C Dew point temperature: 5°C	Refers to Special Airworthiness Information Bulletin CE-09-35 published by the FAA	Serious at cruise power
2018 GAA18CA038	Piper PA 28-140	Lycoming O-320-E2A	Temperature: 20°C Dew point temperature: 17°C	On approach Refers to Special Airworthiness Information Bulletin CE-09-35 published by the FAA	Serious in glide power
2017 CEN17LA376	Cessna 182M	Continental O-470-R	Temperature: 26°C Dew point temperature: 18°C	Refers to Special Airworthiness Information Bulletin CE-09-35 published by the FAA	Moderate cruise/ Serious descent
Canada					
2000 A00P0094	Stits Playmate SA-11A	Lycoming O-320-B1A	Temperature: 12°C Dew point temperature: 7°C	In cruise flight Refers to the AIR section (Aeronautical discipline 2.3 of the Aeronautical Information Publication (AIP Canada) The investigation authority considered icing to be the most likely explanation for the engine's performance. The report also focused on the use of automotive gasoline, which is even more susceptible to icing.	Serious at any power
2003 A03O0285	Cessna 172N	Lycoming O-320-H2AD	Temperature: 23°C Dew point temperature: 14°C	In cruise flight Refers to the graph presented in the publication "Take Five for safety"	Moderate
2011 A11O0222	Robinson R22	Lycoming O-320-B2C	Temperature: 4°C Dew point temperature: 1°C	At take-off Refers to the graph presented in the publication "Take Five for safety" Refers to the Safety Notice SN 25 published by the manufacturer Robinson The investigation authority introduced the specific nature of the use of the engine on a helicopter with possible consequences on the risks of icing at take-off.	Serious at any power

Year Report reference	Aircraft	Engine	Conditions	Comments	Type of icing defined (refer to chapter 5.8)
Australia					
2009 ao2009031	Robinson R22	Lycoming O-360-J2A	Temperature: 13°C Dew point temperature: 13°C	Refers to the conventional graph published by the Australian authorities Icing was presented as a hypothesis.	Serious at any power
2011 ao2011098	Cessna 177	Lycoming O-360-A1F6D	Temperature: 18°C Dew point temperature: 10°C	Refers to the conventional graph published by the Australian authorities Icing was presented as a hypothesis.	Moderate cruise/ Serious descent
2012 ao2012078	Robinson R44	Lycoming	Temperature: 13°C Dew point temperature: -4°C	Refers to the conventional graph published by the Australian authorities	Serious in glide power
2013 ao2013119	Bell 47G2A		Temperature: 13.5°C Dew point temperature: 9.1°C	Refers to the conventional graph published by the Australian authorities	Serious at any power
2014 ao2014149	Van's Aircraft RV-6	Lycoming O-360	Temperature: 17°C Dew point temperature: 11°C	Refers to the conventional graph published by the Australian authorities Icing was presented as a contributing factor.	Moderate cruise/ Serious descent
2016 ao2016059	Piper PA-28-161	Lycoming O-320	Temperature: 10,9°C Dew point temperature: 6,5°C	Refers to the conventional graph published by the Australian authorities	Serious at any power
2016 ao2016153	Ryan STA-SPL	Menasco	Temperature: 14°C Dew point temperature: 10°C	Refers to the conventional graph published by the Australian authorities	Serious at any power
2017 ao2017110	Robinson R44	Lycoming		Refers to the conventional graph published by the Australian authorities	Serious in descent
UK					
2006 EW/G2006/05/19	Cessna F172M	Lycoming O-320-E2D	Temperature: 8°C Dew point temperature: 6°C	In climb Carburettor icing has been indicated as a contributing factor in 14 fatal accidents and more than 250 incidents since 1976.	Serious at any power
2006 EW/G2006/08/18	Cessna F172N	Lycoming O-320-H2AD	Temperature: 18°C Dew point temperature: 13°C (on the ground)	In cruise flight Refers to Safety Sense Leaflet 14	Moderate - cruise power
2006 EW/G2006/12/02	Pitts S-1S	Lycoming O-360-A4A	Temperature: 9.5°C Dew point temperature: 5°C	During an aerobatic manoeuvre Refers to Safety Sense Leaflet 14	Serious at any power
2007 EW/G2007/09/16	Piper PA-28-140	Lycoming O-320-E2A	Temperature: 15°C Dew point temperature: 11°C	In descent Refers to Safety Sense Leaflet 14	Cruise and descent
2007 EG/G2007/11/04	Cessna F172	Lycoming O-235-L2C	Temperature: 12°C Dew point temperature: 11°C	Refers to Safety Sense Leaflet 14	Serious at any power
2009 EW/G2009/06/23	Jodel D117	Continental C90-14F	Temperature: 24°C Dew point temperature: 17°C	/	Moderate cruise / Serious descent

UK

2009 EW/G2009/10/01	Piper J3C-65	Continental C85-12F	Temperature: 4°C Dew point temperature: 2°C	Refers to Safety Sense Leaflet 14	Serious at any power
2011 EW/G2011/01/02	DR400-180	Lycoming O-360-A3A	Temperature: 7°C Dew point temperature: 2°C	In climb Refers to Safety Sense Leaflet 14	Serious at any power
2013 EW/G2013/05/01	Piper PA-28-140	Lycoming O-320-E3D	Temperature: 13°C Dew point temperature: 7°C	On approach Refers to Safety Sense Leaflet 14	Serious at any power
2014 EW/G2014/10/07	Piper PA-28-161	Lycoming O-320-D3G	Temperature: 15°C Dew point temperature: 14°C	In descent Refers to Safety Sense Leaflet 14	Serious at any power
2016 EW/G2016/06/20	Piper PA-28-161	Lycoming O-320-D3G	Temperature: 20°C Dew point temperature: 13°C	On final approach Refers to Safety Sense Leaflet 14	Moderate cruise / Serious descent
2017 EW/G2017/04/09	Piper PA-28-151	Lycoming O-320-E3D	Temperature: 11°C Dew point temperature: 4°C	In descent Refers to Safety Sense Leaflet 14	Serious at any power

Year Report reference	Aircraft	Engine	Conditions	Comments	Type of icing defined (refer to chapter 5.8)
Ireland					
2014 2014-012	Cessna F172M	Lycoming O-320-E2D	Temperature: 23°C Dew point temperature: 17°C	Refers to the Safety Sense Leaflet 14, as well as to the EASA publication "Piston Engine Icing"	Moderate cruise / Serious descent
Iceland					
2006 M-03506/AIG- 19	Cessna 180M	Texas Skyways O-470-U/TS	Temperature: 10°C Dew point temperature: 6°C	Refers to Safety Sense Leaflet 14	Serious at any power
Belgium					
2012 AAIU-2012-07	Socata MS880B	Continental O-200A	Temperature: 9°C Dew point temperature: 3°C	Refers to the graph proposed by the Canadian authorities	Serious at any power
Norway					
2017 SL2017/01	Robinson R22	Lycoming O-320-B2C	Temperature: 12- 13°C Dew point temperature: 0-3°C	Refers to the graph proposed in the SAIB CE-09-35 published by the FAA Also refers to the Safety Notice SN 25 published by the aircraft manufacturer and to the SIB 2010-13 "Carburetor icing prevention" published by the EASA	Serious at glide power
Sweden					
2009 RL 2009: 21e	Robinson R44	Lycoming O-540-F1B5	Temperature: 5°C Dew point temperature: 3°C	The report refers to two Safety Notices published by the helicopter manufacturer: <ul style="list-style-type: none"> • SN 25: Carburetor Ice • SN 31: Governor can mask carb ice Refers to the graph proposed by the Canadian authorities	Serious at any power
Switzerland					
2009 No.2143	Piper PA- 28-161	Lycoming O-320-D3G	Temperature: 0°C Dew point temperature: -7°C Approximation of altitude data in relation to ground data	In climb Refers to the graph proposed by the Canadian authorities, referred to in issue 21 of the "Safer flying" magazine published by the Swiss Flying Federation in November 2015	Light icing
Japan					
2017 AI2017-5	Scheibe SF25C Falke	Limbach L1700EA1	Temperature: 0°C Dew point temperature: -4°C	Refers to the document published by the New Zealand authority in 2005	Serious at glide power
South Africa					
2019 CA18/3/2/1241	Cessna Textron, C182N	/	Temperature: 32°C Dew point temperature: 18°C	Refers to the graph proposed by the Australian authorities The hypothesis of icing was not selected.	Light icing

3.4.2. Feature Publications

The NTSB and the ATSB published feature publications on this phenomenon. The content of these documents is similar to that of the EASA publication “Piston Engine Icing”.

The NTSB published Safety Alert SA-029, of which the latest version was issued in December 2015. In this publication, the NTSB specifies that from 2000 to 2011, carburettor icing was a cause or factor in around 250 accidents.

We are reminded that this phenomenon does not only occur when the OAT is very low. The NTSB advises operators to refer to the flight manual for their aircraft to effectively use the carb heat system.

The ATSB published an article pertaining to carburettor icing belonging to the “Melting Moments” series of articles. This article describes the phenomenon and issues a reminder of the signs used to recognise it. The ATSB specifies that carburettor icing is evoked when the engine is not damaged or on which no observation is made, fuel is present in the system and the flight control linkages are as they should be.

3.5. Consultations with authorities

To better understand the origin of the graphs proposed by the EASA, the FAA, Transport Canada and the Australian authorities, these authorities were consulted. The responses submitted to the BEA were as follows:

Authority	Information submitted to the BEA
EASA	No response received.
United States / NTSB / FAA	<p>Within the context of the investigation into the accident to the Cessna 172G Skyhawk registered N4379L on 27 August 2018, at Rushville, the NTSB specified to the BEA that a discussion had been held on the phenomenon of icing with the FAA. This discussion addressed the following points:</p> <ul style="list-style-type: none"> • Point 1: In these various publications, the FAA proposed three different graphs. One further graph was proposed by the TSB. The NTSB questioned which graph to use. The FAA specified that the information to be considered is the information contained in the following two documents: <ul style="list-style-type: none"> - Advisory Circular 20-113; - Special Airworthiness Information Bulletin (SAIB) CE-09-35. The FAA also specified that specific information that may be provided in the flight manuals must also be considered. In addition, the FAA specified that <ul style="list-style-type: none"> - the graphs proposed are intended to inform pilots of the extent of the atmospheric conditions in which carburettor icing can occur rather than the specific moment at which it will occur; - the phenomenon depends on a number of factors, including not only atmospheric conditions, but also the operating configuration and condition of the aeroplane and the engine; - pilots must use the instruments available to identify the symptoms of icing and to implement practices to prevent a build-up of ice. • Point 2: Can the graphs proposed be used as a tool during an investigation? The FAA specified that these graphs can serve as a guide to identify that icing can occur if an aircraft flies in the environment defined in one of these graphs. However, the FAA specified the importance of not supposing that the phenomenon actually occurred simply because an aircraft flew in an environment conducive to icing identified in these graphs. • Point 3: How should these graphs be used? The FAA specified that these graphs are presented to highlight that icing can occur throughout most of the operating envelope, and includes areas inside this envelope in which a more serious build-up of ice can occur depending on the type of carburettor. This information is not supplied to inform pilots when to activate the carb heat system. The FAA indicated that these graphs are the result of laboratory tests conducted in the 1940s, without providing any further explanation.

Authority	Information submitted to the BEA
Transport Canada	No response received.
Australia / ATSB	<p>According to the information submitted by the ATSB investigator who worked on the latest graph proposed by the Australian authorities, the graph proposed by the Australian authorities was firstly copied from a document published by Asia Pacific Air Safety in 1999, itself taken from the book written by Wood and Sweginnis entitled "Aircraft Accident Investigation" (2nd edition). The graph created by Wood and Sweginnis would be based on an older ICAO document that was based on an even older document published by the TSB Canada, but of which the ATSB was unable to provide a copy. No specific information was therefore provided on this data used to compile the graph.</p> <p>The ATSB investigator who worked on the last graph proposed by the Australian authorities also specified that it was important to consider that some engine/airframe configurations were more subject to loss of power due to carburettor icing than others. Old C175 / 172 aeroplanes equipped with a Continental O-300 engine were known for their sudden shut-downs without warning.</p> <p>Moreover, the temperature/humidity conditions were only available at ground level. It was thought that loss of power associated with carburettor icing occurred during prolonged descents at low power (but there was not enough data to accurately evaluate the risk) and that icing could easily occur when still at altitude. The article available on the ATSB website was written to provide a major indication of the risk, as carburettor icing is not an "ON/OFF" phenomenon that suddenly appears in predetermined and predictable conditions. Carburettor icing may occur in hot and humid conditions and gradually worsen, and the graph was intended to provide an indication of the severity of the risk.</p> <p>The investigator stated that it would have been unhelpful and misleading to advise pilots to use the carb heat system only when the OAT falls below a defined value, while the pilot did not know the humidity, which is why the article on the ATSB's website only indicated compliance with SOPs. The investigator said that he would not recommend using the graph out of context. He added that the graph was a useful tool for operating pilots to make an approximate evaluation.</p>

3.6. Federations, associations and expert websites

The phenomenon is addressed in a number of safety bulletins, or equivalent publications, by multiple federations or associations. Some examples are given below:

Country	Federation or Association	Article or other	Contents
France	Fédération Française Aéronautique (French Aeronautical Federation)	Flight Safety Bulletin No. 14 Available at https://www.securitedesvols.aero/initiatives/ffa	Reminder of the graph proposed by the EASA and reminder of the use of the carb heat system
France	FFPLUM / French Microlight Federation	Microlight pilot safety memo, 5 th edition Available at https://ffplum.fr/securite/memo-securite	One chapter is dedicated to the phenomenon. This chapter reminds us: <ul style="list-style-type: none"> • of the graph proposed by the EASA; • that the phenomenon can occur on all carburettors, including on 2-stroke engines; • that the risk is greater between -5 et 15°C, in the presence of humidity and at low speeds; • of the importance of descending if possible, of applying full throttle and of using the carb heat system when the symptoms of icing are identified (engine spluttering and/or loss of speed).
		Flight safety bulletin No. 42 issued in November 2017 Available at https://ffplum.fr/securite/lettre-securite?idU=4	Very clear reminder of the conditions most likely to produce this phenomenon and the actions to be taken if the symptoms are identified.
Switzerland	Swiss Flying Federation	Article in Safety Bulletin No. 21 issued in November 2015 Available at https://svm.ch/index.php/information/safer-flying	Refers to the graph proposed by the Canadian authorities. The document specifies the conditions in which the phenomenon is most likely to occur (presence of humidity and temperature between -5 et 20°C) and reminds pilots of the conditions of use of the heat system based on the icing conditions (no icing, light icing, serious icing).
Great Britain	Light Aircraft Association	Safety Spot issued in December 2016 Available at: http://www.lightaircraftassociation.co.uk/2016/Magazine/Dec/issue_dec.html	Reference to Safety Sense Leaflet - Piston Engine Icing - 14 _ version b and its contents. Presentation of an event.
Aircraft Owners and Pilots Association (AOPA)	United States	https://www.aopa.org/training-and-safety/students/presolo/skills/carburetor-icing	Reminder of the phenomenon, the conditions conducive to icing and the use of the carb heat system
		Safety Brief No. 9 (issued in 2009) Safety Brief No. 9 issued in 2009 Available at: https://www.aopa.org/media/Files/AOPA/Home/Pilot-Resources/ASI/Safety-Briefs/SB09.pdf	

This information is also available on other expert websites. Some examples are given below:

- <https://www.boldmethod.com/learn-to-fly/aircraft-systems/dont-let-carb-ice-happen-to-you/>
- <https://www.flightliteracy.com/powerplants-induction-and-carburetor-systems-part-one-2/>
- https://www.skybrary.aero/index.php/Piston_Engine_Induction_Icing

These publications do not provide the BEA with additional information to take into account and to analyse in its investigations the phenomenon of piston engine induction system icing.

3.7. Pilot training in France

3.7.1. Private Pilot Licence (PPL)

The contents of the following manuals were used.

Aeroplane Pilot's Manual / published by CEPADUES	12 th edition / 2008
	17 th edition / 2015
	18 th edition / 2018

In each manual, one dedicated chapter was identified.

The contents of this chapter are the same in the three versions used.

This chapter contains:

- a description of the operating principle of the float-type carburettor;
- a description of the carb icing phenomenon (the most common type of icing), the other types of icing are not explained;
- a presentation of the conditions in which this phenomenon is most likely to occur, along with the temperature and relative humidity criteria, based on the graph proposed by the EASA;
- a list of symptoms that can indicate the occurrence of the phenomenon, making a clear distinction between engines equipped with a variable-pitch propeller and those equipped with a fixed-pitch propeller;
- a description of the heat system operating procedure.

The information published is more or less the same as that presented in the EASA document on carburettor icing.

3.7.2. Airline Transport Pilot Licence (ATPL)

The document used was the latest version of the Mermoz training manual (chapter on piston engines).

This document presents the phenomenon of carburettor icing very succinctly. It provides the following information:

- Overview of the most common symptoms:
 - ⇒ decrease in speed for an engine equipped with a fixed-pitch propeller;
 - ⇒ decrease in manifold pressure for an engine equipped with a variable-pitch propeller.
- Overview of the two main phenomena causing a decrease in temperature in the carburettor:
 - ⇒ decrease in temperature caused by the venturi;
 - ⇒ decrease in temperature caused by fuel evaporation.
- Reminder that the phenomenon can occur at temperatures of around 10 to 20°C.

3.8. Manufacturers

3.8.1. Aircraft manufacturers (excluding aircraft equipped with Rotax engines)

This research consisted in identifying information pertaining to the phenomenon of induction system icing provided by aircraft manufacturers in their flight manuals.

The list of flight manuals used is given in the following table.

No flight manual refers to a document published by an authority.

Generally, the flight manuals contain very little information about piston engine induction system icing.

- The most common symptoms are specified: decrease in power and occurrence of vibrations.
- The information provided essentially concerns use of the carb heat system, and in particular specifies that this system is an all-or-nothing type system and that the mixture needs to be adjusted when it is activated.

The manufacturer Robinson published a Safety Notice SN 25 and SN 31 specific to this phenomenon.

Manufacturer	Aircraft	Engine	Version of the manuals used
Robin	DR400-120	Lycoming O-235-L2A	September 1992, May 1998 and March 2018
Robin	DR400-140	Lycoming O-320-D Lycoming O-320-D2A	1975 and March 2005
Robin	DR400-160	Lycoming O-320-D2A	November 1993
Robin	DR400-180	Lycoming O-360-A3A	February 1980
Jodel	D112	Continental A65	1975 and November 2014
Jodel	D119	Continental C90	January 2014
Jodel	DR1050M	Continental O200	December 2016
Piper	PA28-140	Lycoming O-320-E3D	January 1973
Piper	PA28-180	Lycoming O-360-A3A Lycoming O-360-A4M	1972 and February 1980
Piper	PA44-180	Lycoming O-360-E1A6D	1978 and October 2011
Morane-Saulnier / Socata	Rallye 110ST	Lycoming O-235-L2A	1978
Morane-Saulnier / Socata	Rallye 150ST	Lycoming O-320-E2A	1975
Cessna	150	Continental O200A	1977
Cessna	172N	Lycoming O-320-H2AD	1978
Cessna	182	Continental O470U	1978
Beechcraft	Skipper 77	Lycoming O-235-L2C	January 1982
Beechcraft	Sport 150	Lycoming O-320-E2B	July 1994
Socata	TB10	Lycoming O-360-A1AD	September 1989
Robinson	R22	Lycoming O-320 or O-360	Latest version available on the manufacturer's website
Robinson	R44	Lycoming O-540-F1B5	Latest version available on the manufacturer's website

No information was identified that would enable to determine with more accuracy the induction system icing risk for an aircraft.

3.8.2.Engine manufacturers

Research was only conducted on Lycoming (<https://www.lycoming.com/>) and Continental (<http://www.continental.aero/home/>) engines. The results of the research relating to Rotax engines are given in para. 5.

- **Lycoming:**

Lycoming has published Service Instruction No1148C (<https://www.lycoming.com/content/service-instruction-no-1148c>).

In this document, the manufacturer recalls the main characteristics of icing. The mode of use of the heating device is then indicated according to the flight phase. This information is also included in the manuals for engines equipped with carburetors.

- On the ground: the device must be used a minimum, just to check its operation;
- Take-off: the aircraft must not be used. It is specified that the phenomenon of icing is unlikely at full speed. - Ascent: the use of the device must be avoided. If its use is chosen, the mixture should be slightly leaned.
- Cruise: In the event of an uncontrolled drop in intake pressure or rotation speed, use the heater and bring the engine to full speed.
- Landing approach: if icing conditions are suspected, the heater should be used. In the event that full power is needed, turn the carburetor heat back to "Full Cold".

Lycoming also cites the icing phenomenon in Service Instruction No1070AB (<https://www.lycoming.com/service-instruction-no-1070-AB>), "Specific Fuels for Spark-Ignited Gasoline Aircraft Engine Models", published on 8 April 2020.

In this document, it is specified: " Isopropyl alcohol in amounts not to exceed 1% by volume can be added only to aviation fuel (not automotive fuel) to prevent ice formation in fuel lines and tanks. Although approved for use in Lycoming engines, do not use isopropyl alcohol in the aircraft fuel systems unless approved by the aircraft manufacturer. »

- **Continental Aerospace Technologies:**

The phenomenon of carburettor icing is mentioned in the instructions for use of engines fitted with carburettors.

The O-200 engine operating manual specifies, for example:

- The phenomenon can occur on the ground when the engine is idling. In this case, it is recommended to activate the heating device.
- The heating device must be used when the phenomenon is detected (rough engine or during loss of speed).

3.8.3.Carburettor manufacturers

The main manufacturer is Marvel Schelber (<https://msacarbs.com/>). The results of the research relating to carburettors equipping Rotax engines are given in para. 5.

No information relating to induction system icing was identified.

3.9. Scientific articles

3.9.1. Introduction

The bibliographic research focused on public-access documents.

The first article identified, which was published in March 1938, deals with tests that were conducted to study the phenomenon of carburettor icing: Carburetor Icing / R.Sanders (<https://www.sae.org/publications/technical-papers/content/380067/?PC=DL2BUY>).

This article focuses on tests conducted in flight, on a Douglas DC-2 aeroplane equipped with Wright Cyclone engines² (Figure 21).

The article states that on this engine type, the vaporization of fuel in the carburettor causes a decrease in temperature of 20 to 30°C.



Figure 21: Douglas DC-2 aeroplane
Source: *Carburetor Icing* / R.Sanders / March 1938

² The Wright Cyclone R-1820 engine family is a nine-cylinder air-cooled radial engine. This engine was equipped with a pressure carburettor and an associated compressor. This induction system was very different from the systems dealt with by the BEA today.

The document incorporates a graph (Figure 22) which enables pilots to determine if, based on these conditions, a risk of icing is possible.

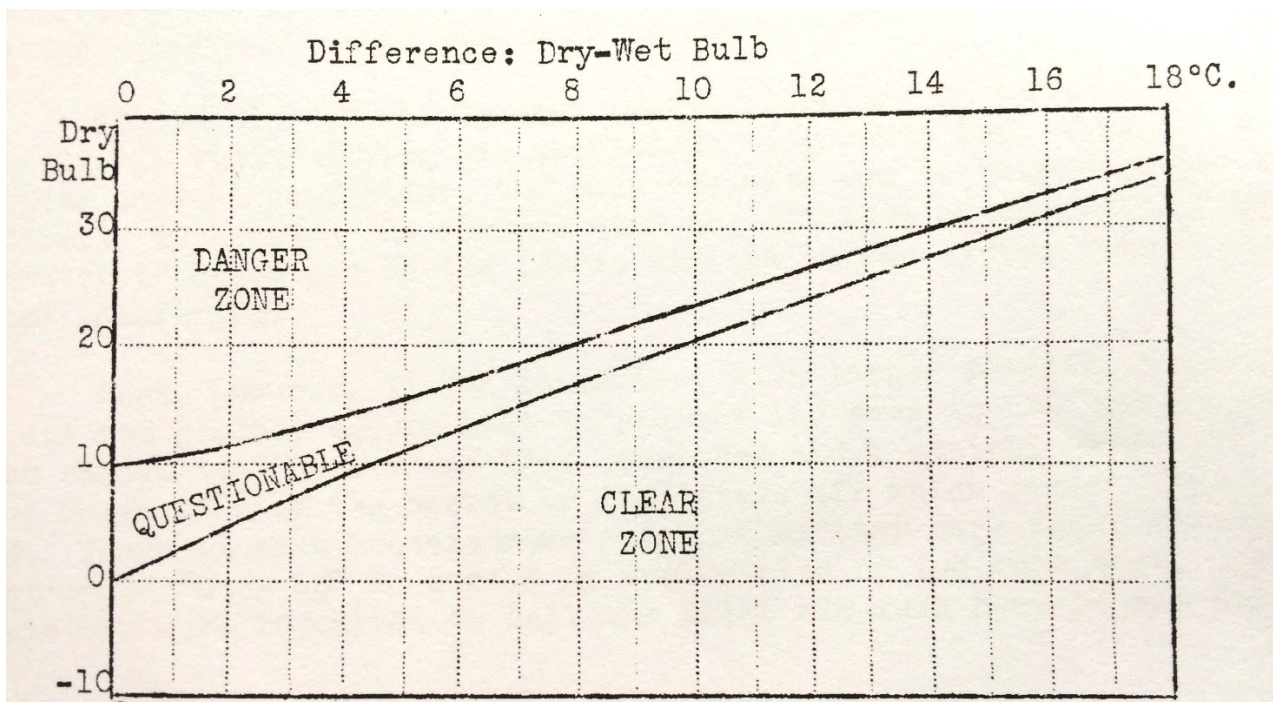


Figure 22: graph incorporated in the publication
Source: *Carburetor Icing* / R. Sanders / March 1938

Definition of temperatures read:

- Dry bulb: OAT, measurement protected from direct sunlight;
- Dry-wet bulb: temperature of the sprayed air-water mixture.

The first detailed and usable articles were identified in the 1940s (refer to para. 3.9.2). At this time, the increase in air operations in complex meteorological conditions led the Air Transport Association of America to recognise the need to improve understanding of the causes, effects and solutions concerning piston engine induction system icing. The NACA (*National Advisory Committee for Aeronautics*), whose activities were taken over by NASA in 1958, was asked to conduct a study programme.

The aim of this research programme was to determine the characteristics of icing and to define the requirements of de-icing using hot air and fluids for the different types of carburetors (float-type, pressure and injection), by associating representative manifolds and compressors with them. This work was conducted for the most part in a laboratory, in a wind tunnel for impact icing and sometimes on complete powerplants.

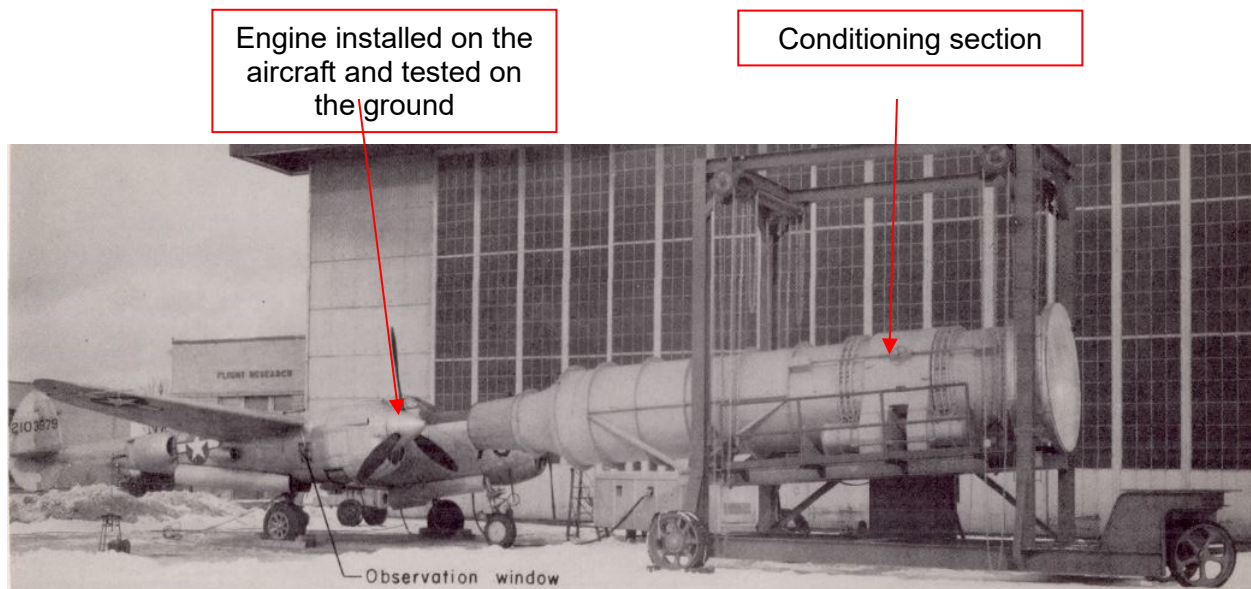


Figure 23: illustration of a test setup on a complete powerplant

Source: Investigation of ice formation in the induction system of an aircraft engine _ I-Ground tests _ Henry A. Essex, Edward D. Zlotowski and Carl Ellisman _ March 1946

3.9.2. Publications between 1943 and 1950

NACA's study programme gave rise to a number of publications. Those used for this report are listed in the table below.

Article title	Author	Date of publication
Icing Tests of Aircraft-Engine Induction systems.	Léo B.Kimball	01/1943
Laboratory investigation of icing in the carburetor and supercharger inlet elbow of an aircraft engine / I - Description of setup and testing technique https://ntrs.nasa.gov/citations/19930093100	Donald R. Mulholland, Vern G. Rollin, Herman B. Galvin	12/1945
Laboratory investigation of icing in the carburetor and supercharger inlet elbow of an aircraft engine / II - Determination of the limiting-icing conditions https://ntrs.nasa.gov/citations/19930093068	Henry A. Essex, Wayne C. Keith, Donald R. Mulholland	12/1945
Laboratory investigation of icing in the carburetor and supercharger inlet elbow of an aircraft engine / III - Heated air as a means of de-icing https://ntrs.nasa.gov/citations/19930093069	Richard E. Lyons, Willard D. Coles	12/1945
Laboratory investigation of icing in the carburetor and supercharger inlet elbow of an aircraft engine / IV - Effect of throttle design and method of throttle operation on induction-system icing characteristics https://ntrs.nasa.gov/citations/19930093070	G.E. Chapman, E.D. Zlotowski	01/1946
Laboratory investigation of icing in the carburetor and supercharger inlet elbow of an aircraft engine / V - Effect of injection of water-fuel mixtures and water-ethanol-fuel mixtures on the icing characteristics https://ntrs.nasa.gov/citations/19930093061	Clark E. Renner	12/1945
Laboratory investigation of icing in the carburetor and supercharger inlet elbow of an aircraft engine / VI - Effect of modifications to fuel-spray nozzle on icing characteristics https://ntrs.nasa.gov/citations/19930093062	Donald R. Mulholland, Gilbert E. Chapman	01/1946
Investigation of ice formation in the induction system of an aircraft engine _ I-Ground tests https://ntrs.nasa.gov/citations/19930093063	Henry A. Essex, Edward D. Zlotowski and Carl Ellisman	03/1946
A Preliminary investigation of the Icing Characteristic of a Large Rectangular-Throat Pressure-Type Carburetor https://ntrs.nasa.gov/citations/19930093067	Gilbert E. Chapman	07/1946
An investigation of the icing and heated-air de-icing characteristics of the R-2600-13 induction system https://ntrs.nasa.gov/citations/20090026508	Gilbert E. Chapman	12/1946
Effects of Induction-System Icing on Aircraft-Engine Operating Characteristics https://ntrs.nasa.gov/citations/20050080796	Stevens, Howard C., Jr.	01/1947
Carburetor icing	E. E. Dean	06/1947
Laboratory investigation of ice formation and elimination in the induction system of a large twin-engine cargo aircraft https://ntrs.nasa.gov/citations/19930082173	Willard D. Coles	09/1947
Investigation of icing characteristics of typical light-airplane engine induction systems https://ntrs.nasa.gov/citations/19810068626	Willard D. Coles	02/1947
Icing protection requirements for reciprocating-engine induction systems https://ntrs.nasa.gov/citations/19930092043	Willard D.Coles, Vern G.Rollin, Donald R.Mulholland	03/1950

As previously indicated, most of the work was laboratory-based. The standard setup used is presented on the next page. The detailed test conditions are not always specified. However, the following conditions were common to all of the tests:

	AN-F-22 (or AVGAS 115/145, fuel with a high octane rating, developed at the time to reduce the effects of knocking) or AN-F-28		
	Properties of AN-F-22 compared with those of today's AVGAS 100 LL (LL: Low Lead, fuel containing a low amount of tetraethyl lead developed to reduce the knocking phenomenon):		
Fuels		AN-F-22 or AVGAS 115/145	AVGAS 100LL
	Aviation Lean Rating	115 Min	100 Min
	Performance Number	145 Min	130 Min
	Specific energy (MJ/kg)	44 Min	43.5 Min
	Freezing Point (°C)	-60°C Max	-58°C Max
	Sulphur content (m/m)	0.05% Max	0.05% Max
	Lead content (gPb/L)	1.28 Max	0.56 Max
	Reid vapour pressure (kPa)	38.5-49	38-49
	Distillation		
	10% recovered at	75 Max	75 Max
40% recovered at	75 Min	75 Min	
50% recovered at	105 Max	105 Max	
90% recovered at	135 Max	135 Max	
Final Boiling Point	170 Max	170 Max	
Residue	1.5 Max	1.5 Max	
Loss	1.5 Max	1.5 Max	
Fuel temperature	Generally 40°F (4.4°C)		
Water temperature	Generally 40°F (4.4°C)		

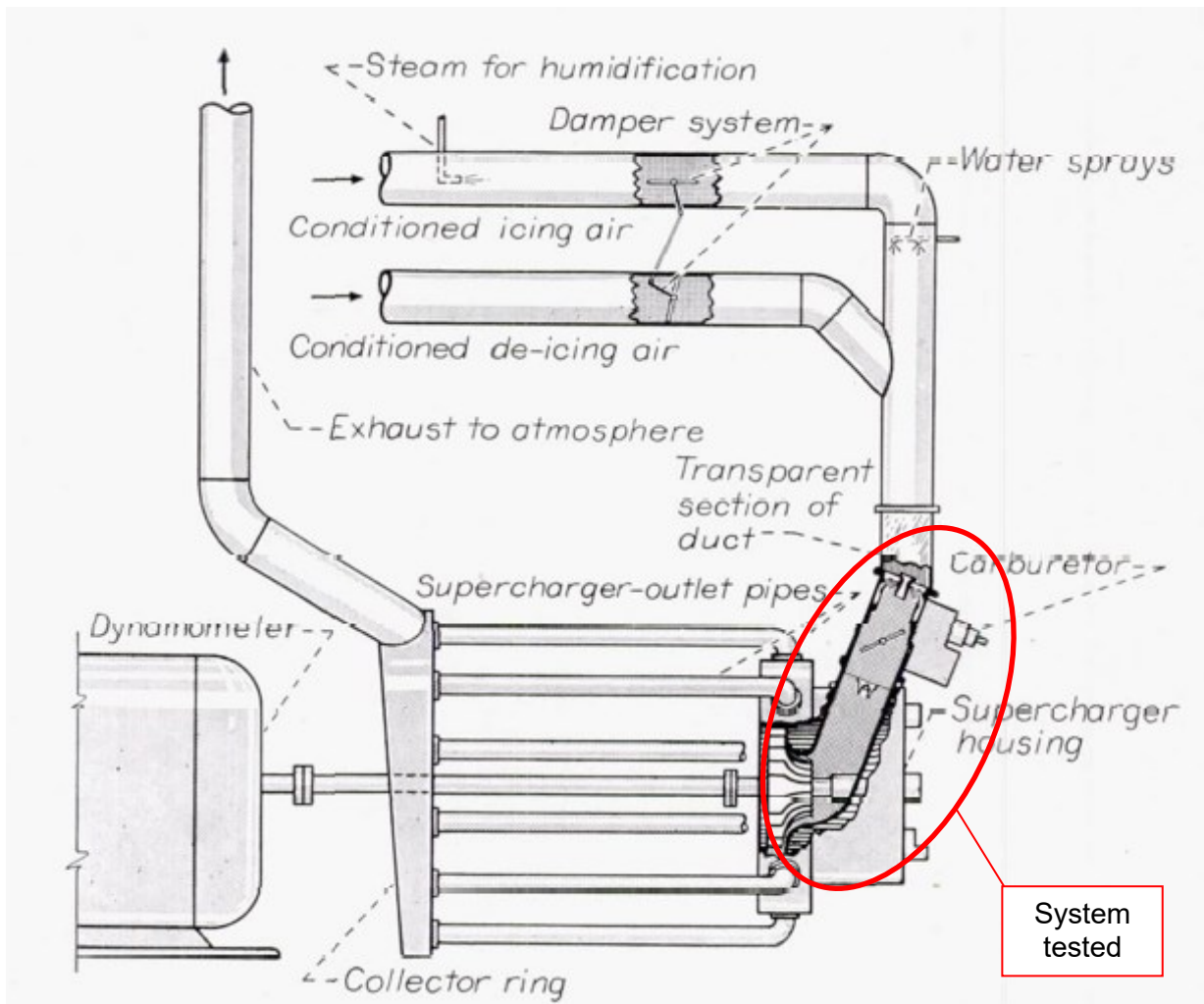


Figure 24: laboratory-implemented setup

Source: *Icing protection requirements for reciprocating-engine induction systems* - Willard D. Coles, Vern G. Rollin, Donald R. Mulholland - 1950

A review of the various publications revealed that the majority of the work was conducted with a pressure carburettor associated with a compressor, with various configurations as shown in **Figure 27**. These configurations seem very different from the induction systems dealt with by the BEA today. In addition, the influence of the engine is not taken into account, and in particular the associated thermal environment.

All these tests showed that ice tended to form on the butterfly valves and the downstream manifold (**Figure 25** and **Figure 26**).

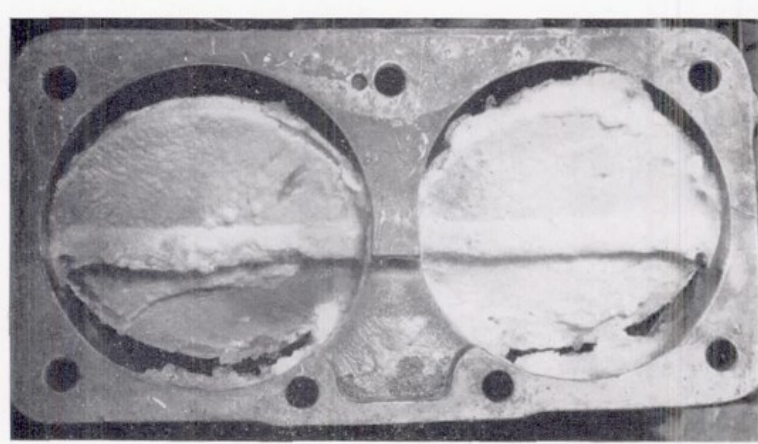


Figure 25: ice formed on butterfly valves

Source: *Icing protection requirements for reciprocating-engine induction systems* - Willard D.Coles, Vern G.Rollin, Donald R.Mulholland - 1950

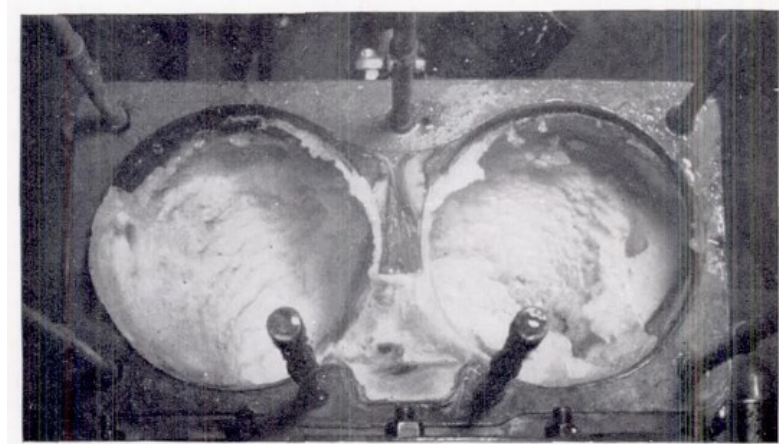


Figure 26: ice formed on manifolds downstream of butterfly valves

Source: *Icing protection requirements for reciprocating-engine induction systems* - Willard D.Coles, Vern G.Rollin, Donald R.Mulholland - 1950

These publications also specify the influence of various factors as detailed in the table below:

Factor	Influence
Type of butterfly valve	The studies showed the higher susceptibility to icing of some setups (of type E, as shown in Figure 27) in relation to others (of type B) (Figure 30). It is indicated that conventional butterfly valves (type E) create turbulence that is conducive to this phenomenon.
System size	Influence not significant.
Mixture ratio	Influence not significant.
Location of the fuel injector	Influence identified on the maximum temperature at which icing was observed.
Fuel volatility	Significant influence. The more volatile the fuel, the more serious the icing.
Fuel temperature	Influence not significant.

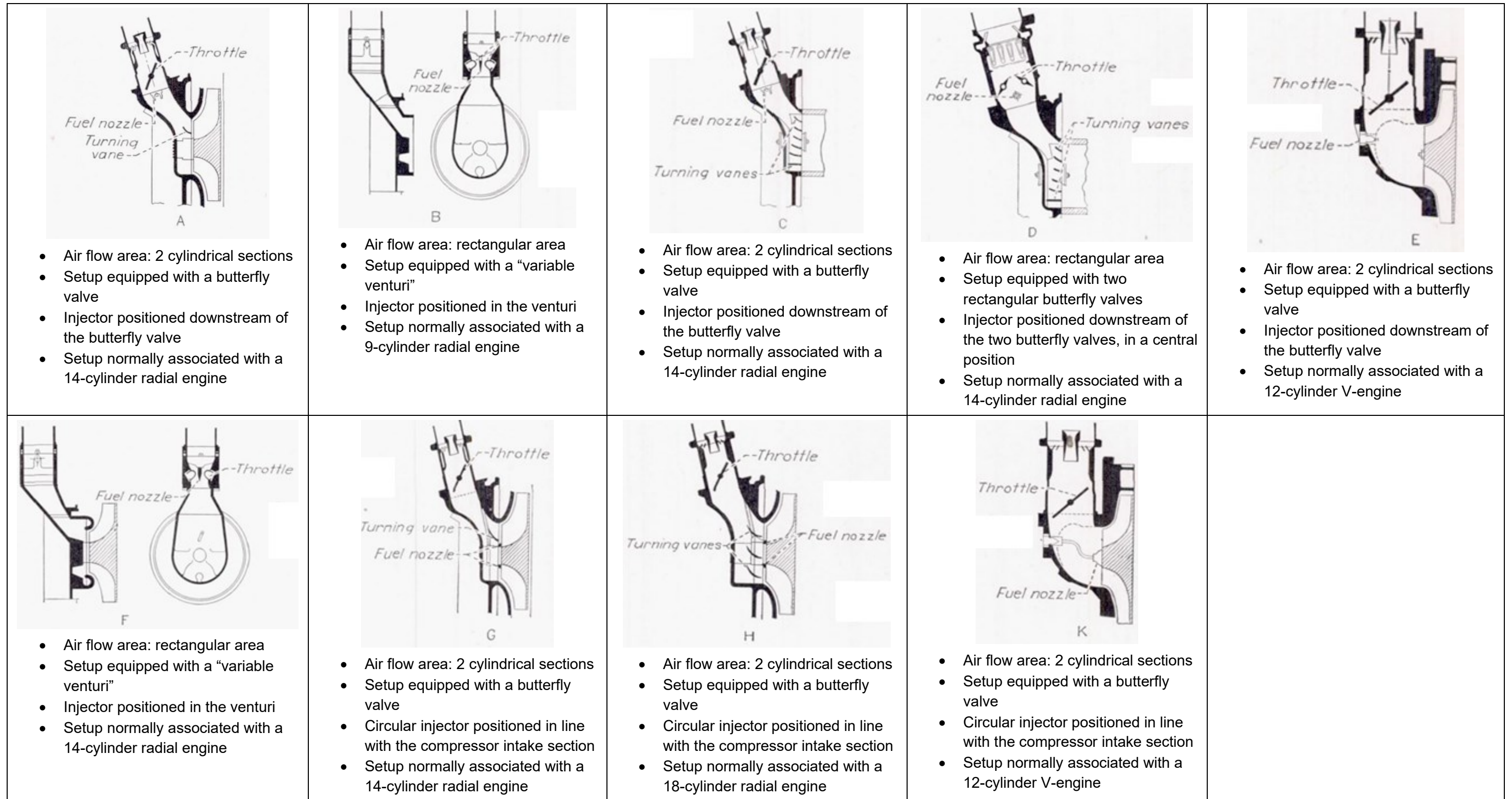


Figure 27: Various configurations studied, systematically comprising a pressure carburettor and a compressor
Source: *Icing protection requirements for reciprocating-engine induction systems* - Willard D.Coles, Vern G.Rollin, Donald R.Mulholland - 1950

Several publications propose graphs specifying icing zone limits. The limits on the graphs proposed on the next pages vary according to the setup in question (refer to Figure 27). The setup is specified for each graph.

Some of these graphs were reconstructed by the BEA following the same references as the graphs currently proposed by the different authorities (Temperature / Dew point temperature).

The different zones considered are defined on these graphs as follows:

serious icing	when the air flow drops by 2% in up to 15 minutes
visible icing	visible icing (visual observation of walls ³) without a significant decrease in air flow
non-visible icing	

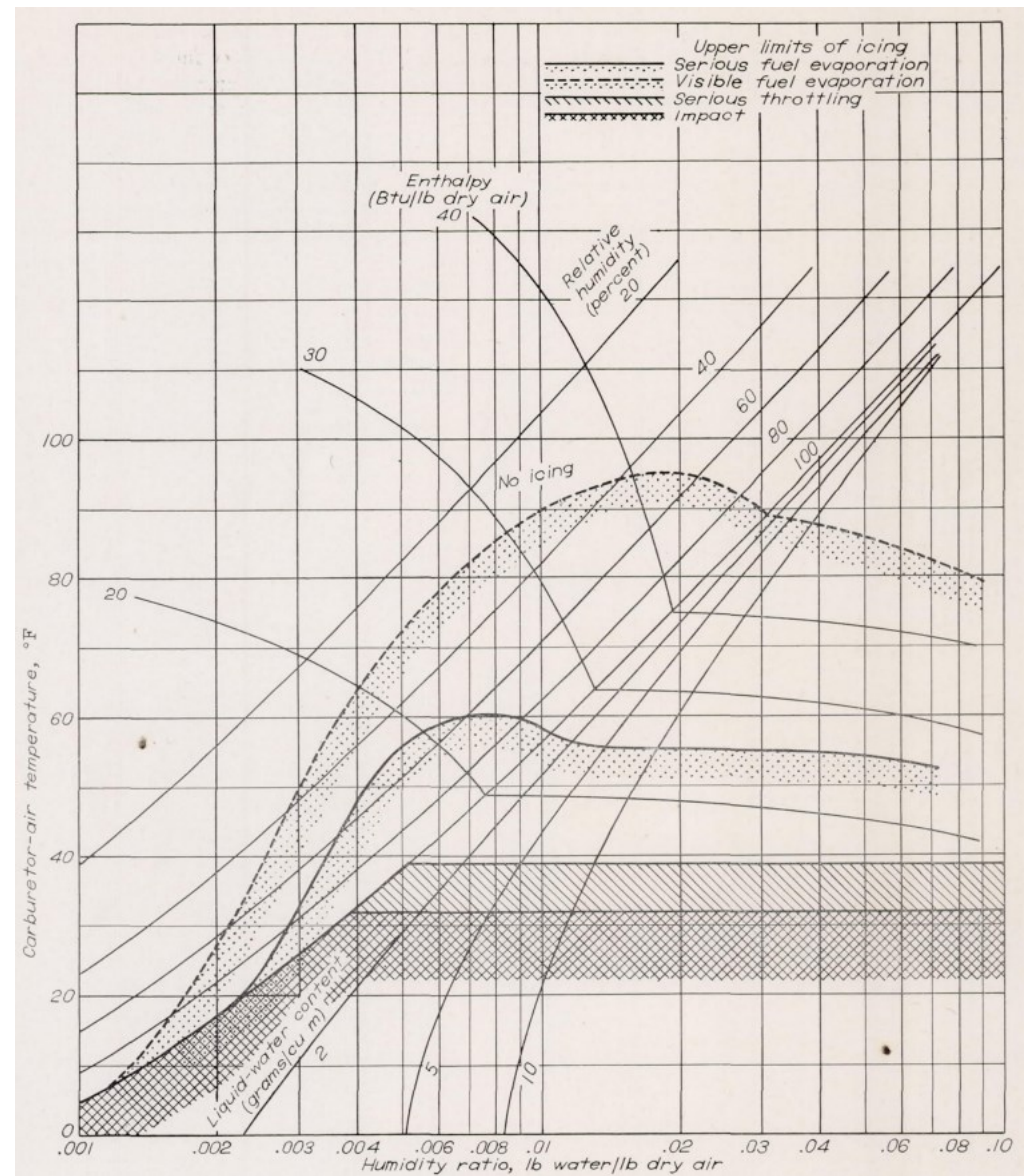
In these publications, five speeds were considered, each corresponding to a ratio between the pressure in line with the butterfly valve and the manifold pressure:

Glide	Ratio of approximately 0.53
Low Cruise	Ratio of approximately 0.6
High Cruise	Ratio of approximately 0.7
Normal Rated	Ratio of approximately 0.8
Take-off	Ratio of approximately 0.95

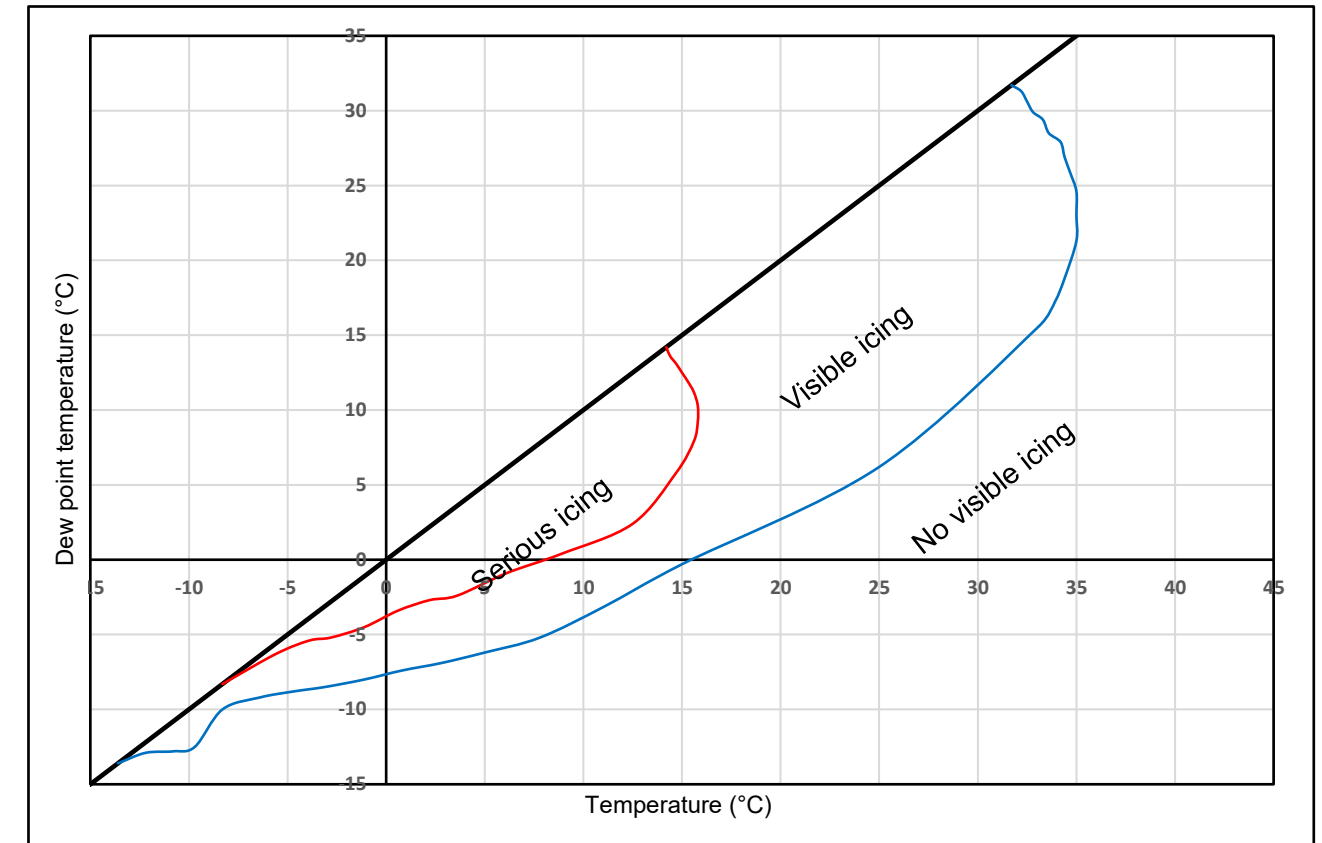
³ As the work presented was conducted at the same research centre, it would be reasonable to assume that the visual criteria were similar.

In the document published in March 1950, *Icing protection requirements for reciprocating-engine induction systems*, a graph defining the upper limits of the icing zones is proposed (Figure 28) for the type of icing associated with evaporation of the fuel and considering the configurations studied (refer to Figure 27). This graph was reconstructed based on current references (Temperature / Dew point temperature).

Graph taken from the publication “Icing protection requirements for reciprocating-engine induction systems”



Graph reconstructed based on current references



	Limit between the serious icing zone and the visible icing zone
	Limit between the visible icing zone and the no visible icing zone

Figure 28: graph defining the upper limits of the icing zones, for the type of icing associated with fuel evaporation and considering the configurations studied
 Source: *Icing protection requirements for reciprocating-engine induction systems* - Willard D.Coles, Vern G.Rollin, Donald R.Mulholland - 1950

The graphs in **Figure 29** define the limit of the serious icing envelope for four different types of powerplant, for the same power setting (*Low Cruise*). Note that this limit differs according to the type of powerplant.

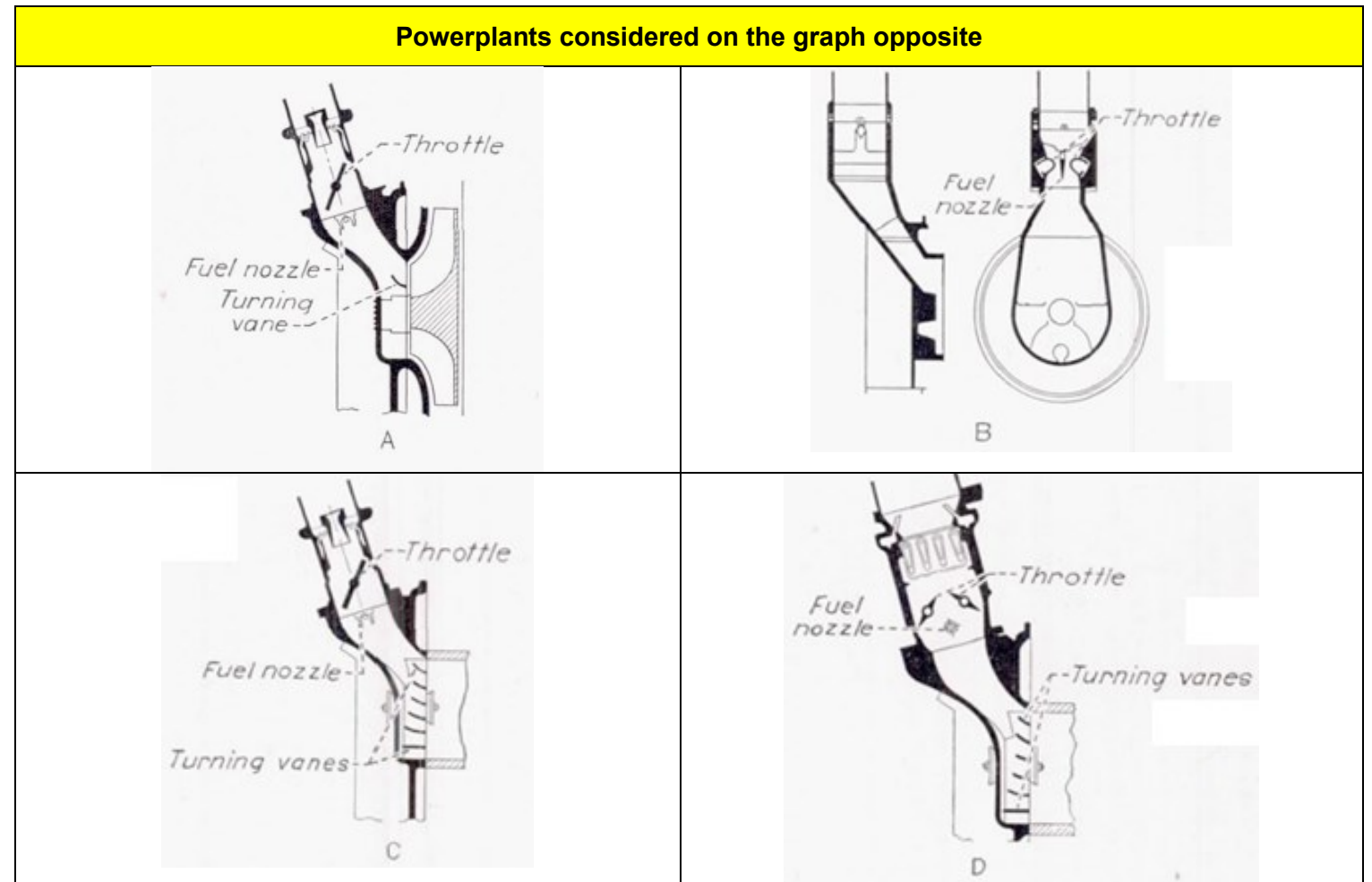
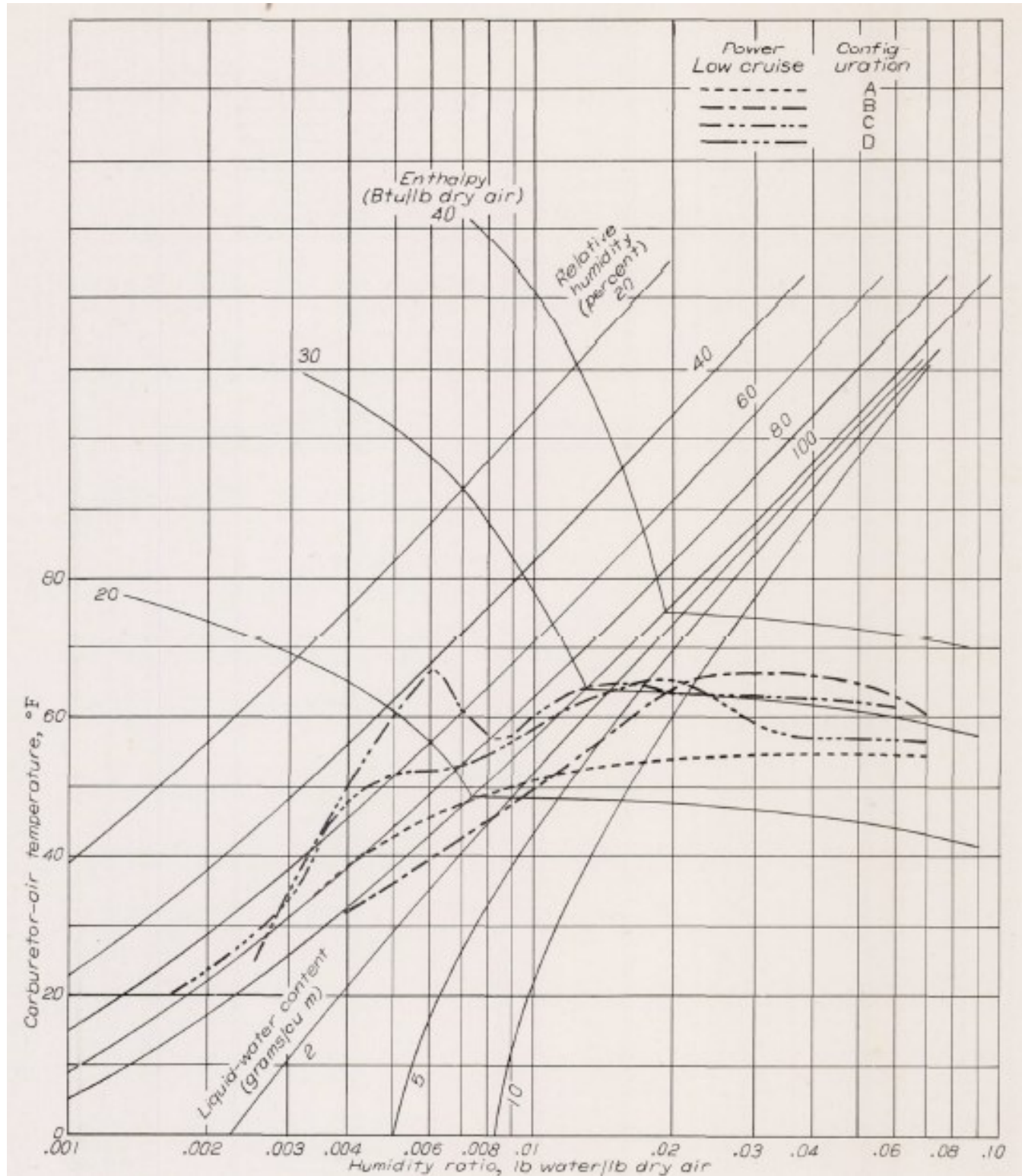


Figure 29: graphs defining the limit of the serious icing zone for four types of powerplant
 Source: *Icing protection requirements for reciprocating-engine induction systems* - Willard D.Coles, Vern G.Rollin, Donald R.Mulholland - 1950

The graphs in Figure 30 define the limit of the serious icing envelope for three types of powerplant with different types of butterfly valve but the same power setting (*Low Cruise*). Note that this limit differs according to the type of powerplant.

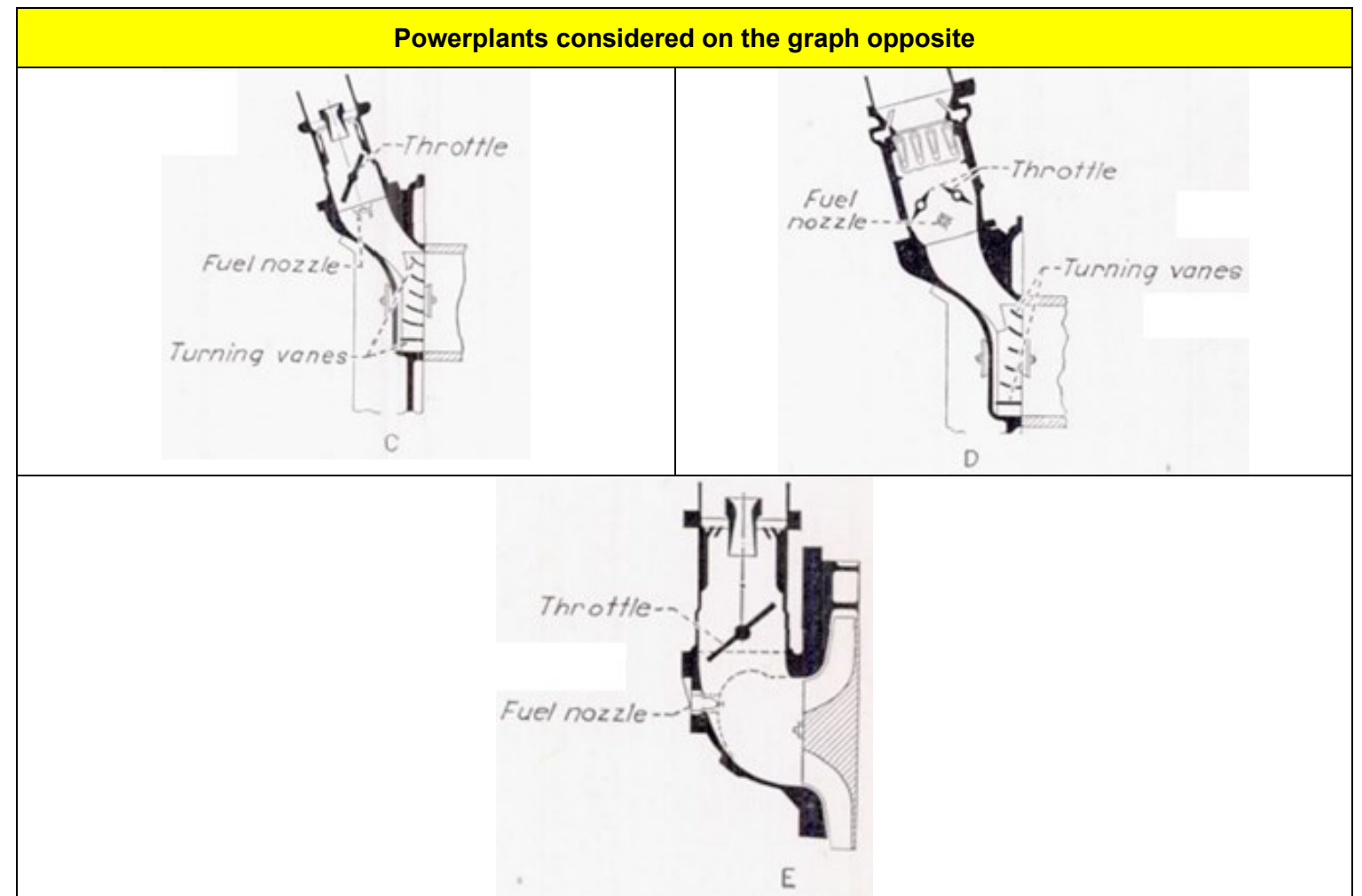
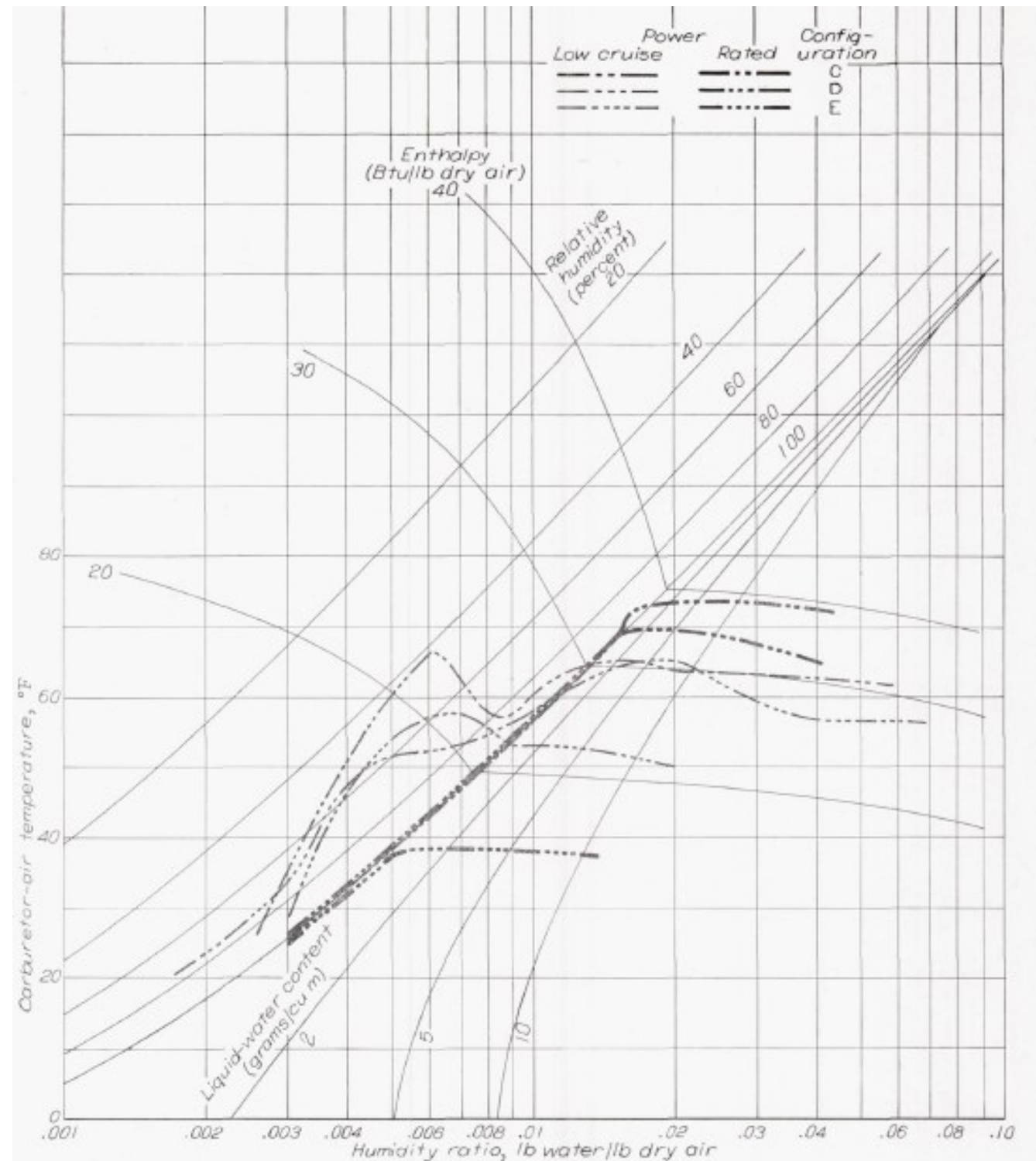


Figure 30: graphs defining the limit of the serious icing envelope for three different types of powerplant illustrating the butterfly type effect
 Source: *Icing protection requirements for reciprocating-engine induction systems* - Willard D.Coles, Vern G.Rollin, Donald R.Mulholland - 1950

Figure 31 shows the type of powerplant for which the graph in **Figure 32** was obtained. This graph shows the associated icing envelope in the conditions listed below and was established based on actual criteria (Temperature / Dew point temperature):

- tests conducted in a laboratory;
- pressure altitude at carburettor inlet: approx. 5,000 ft;
- speed: 2,000 rpm corresponding to the Low Cruise Power speed (60%);
- mixture = 0.079.

In these conditions, serious icing only occurs when the relative humidity is 100% with the addition of liquid water.

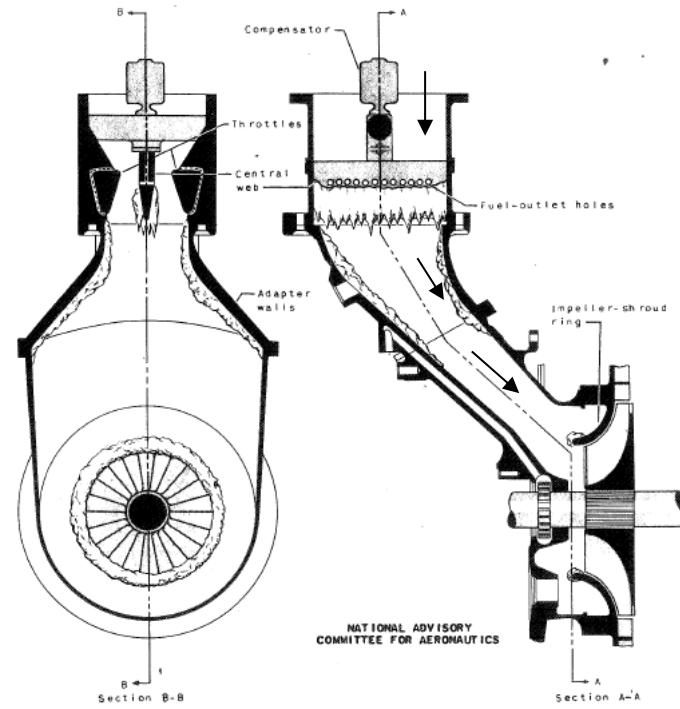


Figure 31: powerplant tested

Source: *An investigation of the icing and heated-air de-icing characteristics of the R-2600-13⁴ induction system* - Gilbert E. Chapman - 12/1946

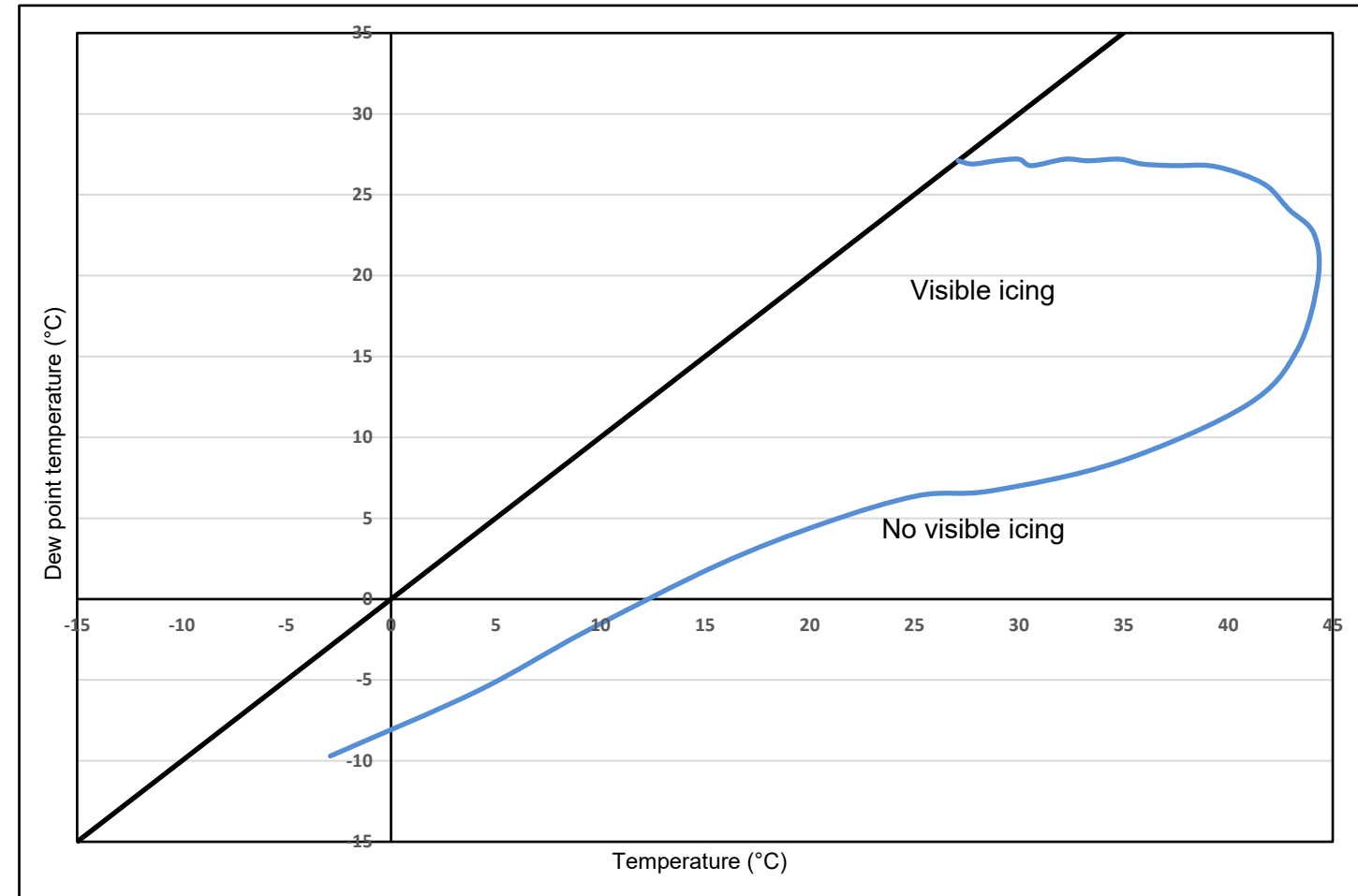


Figure 32: graph defining the limit between the visible icing zone and the no visible icing zone

⁴ The Wright Cyclone R-2600 engine was a 14-cylinder air-cooled radial engine equipped with a pressure carburettor and an associated compressor. Several aeroplanes equipped with this engine type: Boeing 314, Curtiss SB2C, Douglas B-23, Douglas A-20.

Figure 33 shows the type of powerplant for which the graph in Figure 34 was obtained. This graph shows the associated icing envelope in the conditions listed below and was established based on current criteria (temperature vs dew point temperature) (Figure 35):

- tests conducted in a laboratory;
- pressure altitude at carburettor inlet: approx. 4,200 ft;
- mixture = 0.082.

In these conditions, serious icing only occurs when the relative humidity is 100% with the addition of liquid water.

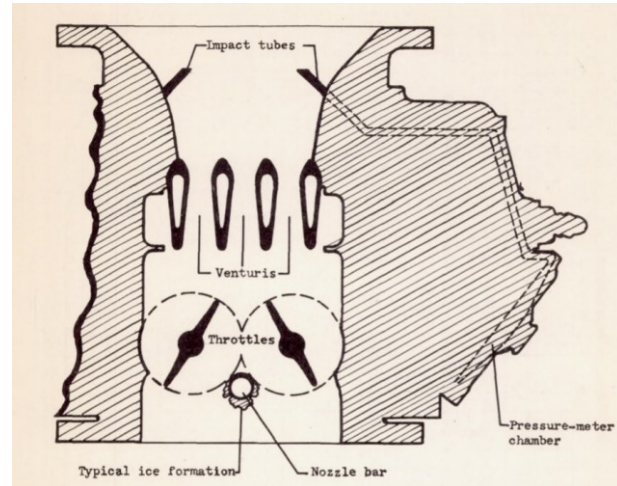


Figure 33: powerplant tested

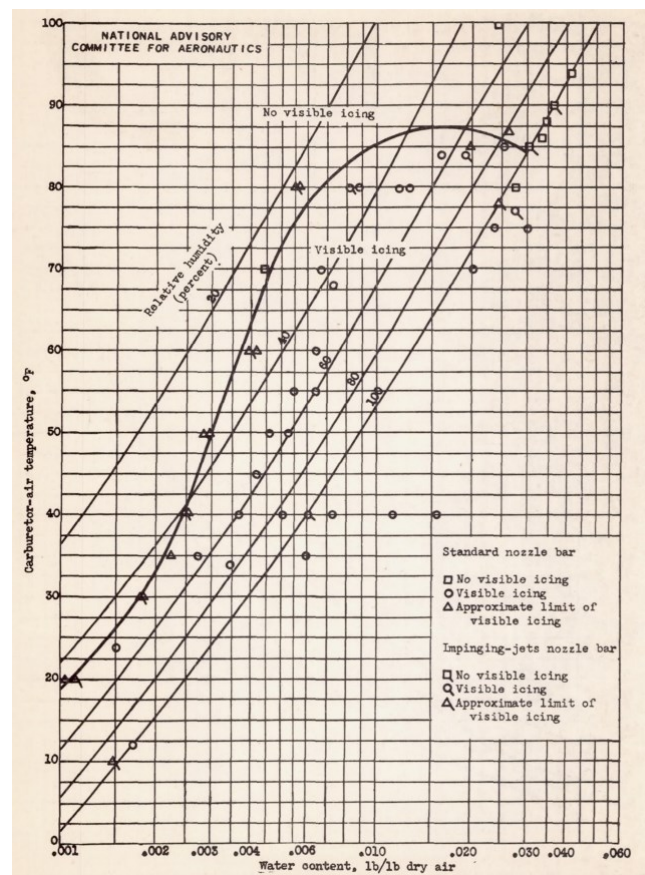


Figure 34: graph taken from the publication *A Preliminary investigation of the Icing Characteristic of a Large Rectangular-Throat Pressure-Type Carburetor* - Gilbert E. Chapman - 1946

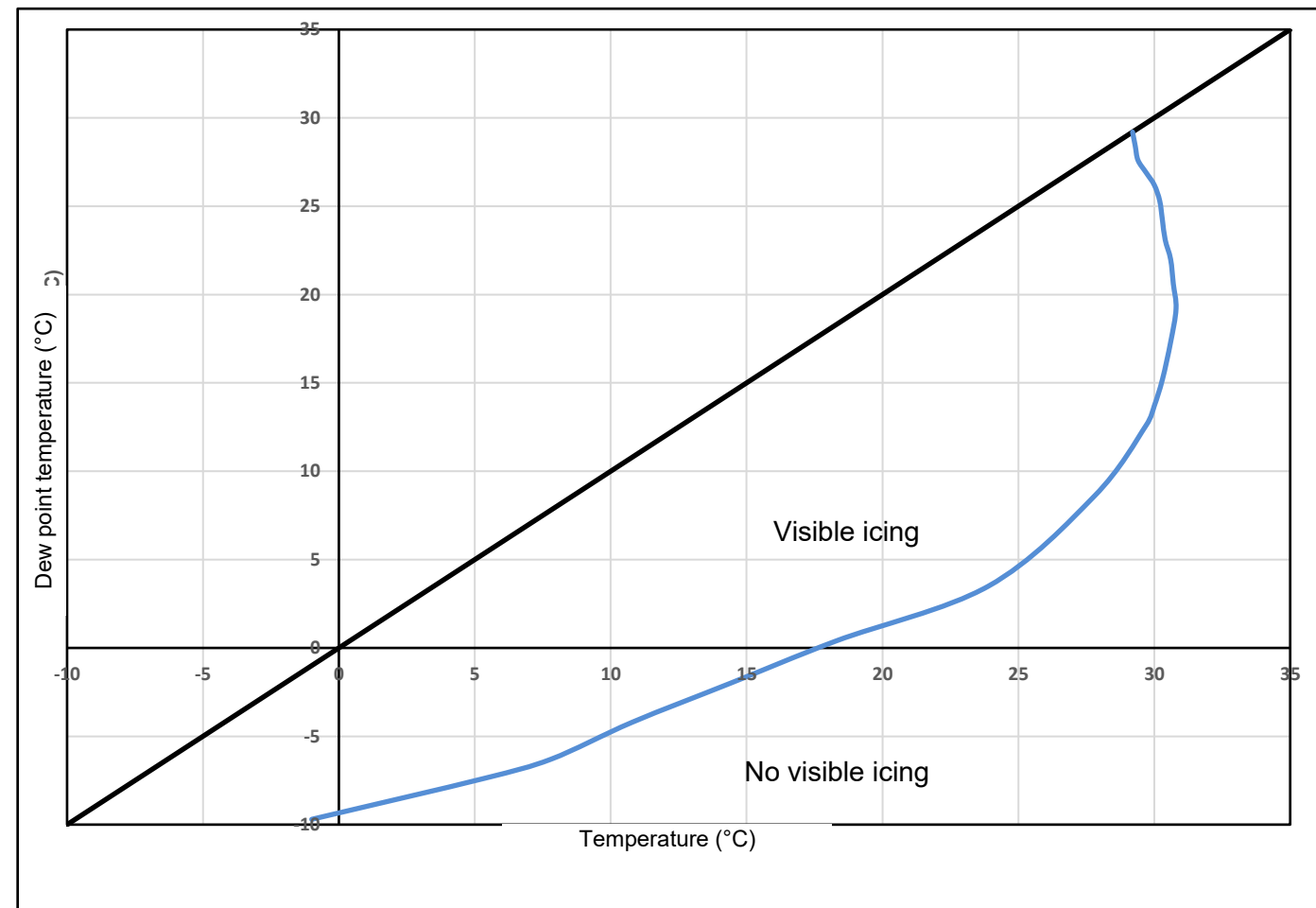


Figure 35: graph defining the limit between the visible icing zone and the no visible icing zone

The graph in **Figure 37** was reconstructed in accordance with current criteria (Temperature / Dew point temperature) based on data taken from the publication *Laboratory investigation of icing in the carburetor and supercharger inlet elbow of an aircraft engine / II - Determination of the limiting-icing conditions* - Henry A. Essex, Wayne C. Keith, Donald R. Mulholland - 12/1945.

Figure 36 presents the test setup used. The carburetor studied was a carburetor with two butterfly valves respectively positioned in a cylindrical duct. These tests were conducted in a laboratory. The pressure altitude at the carburetor inlet was set to around 4,200 ft, with a mixture of 0.080.

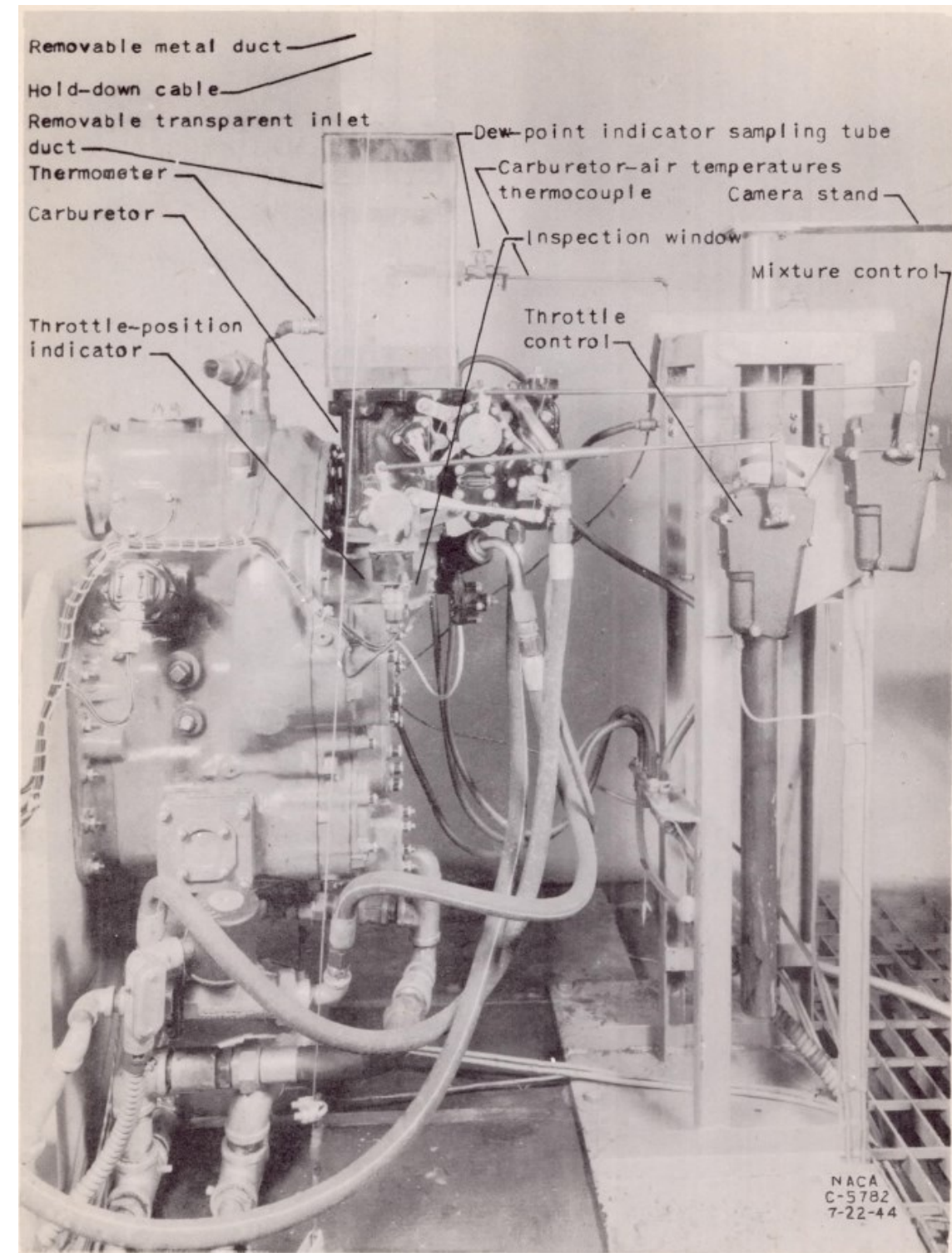
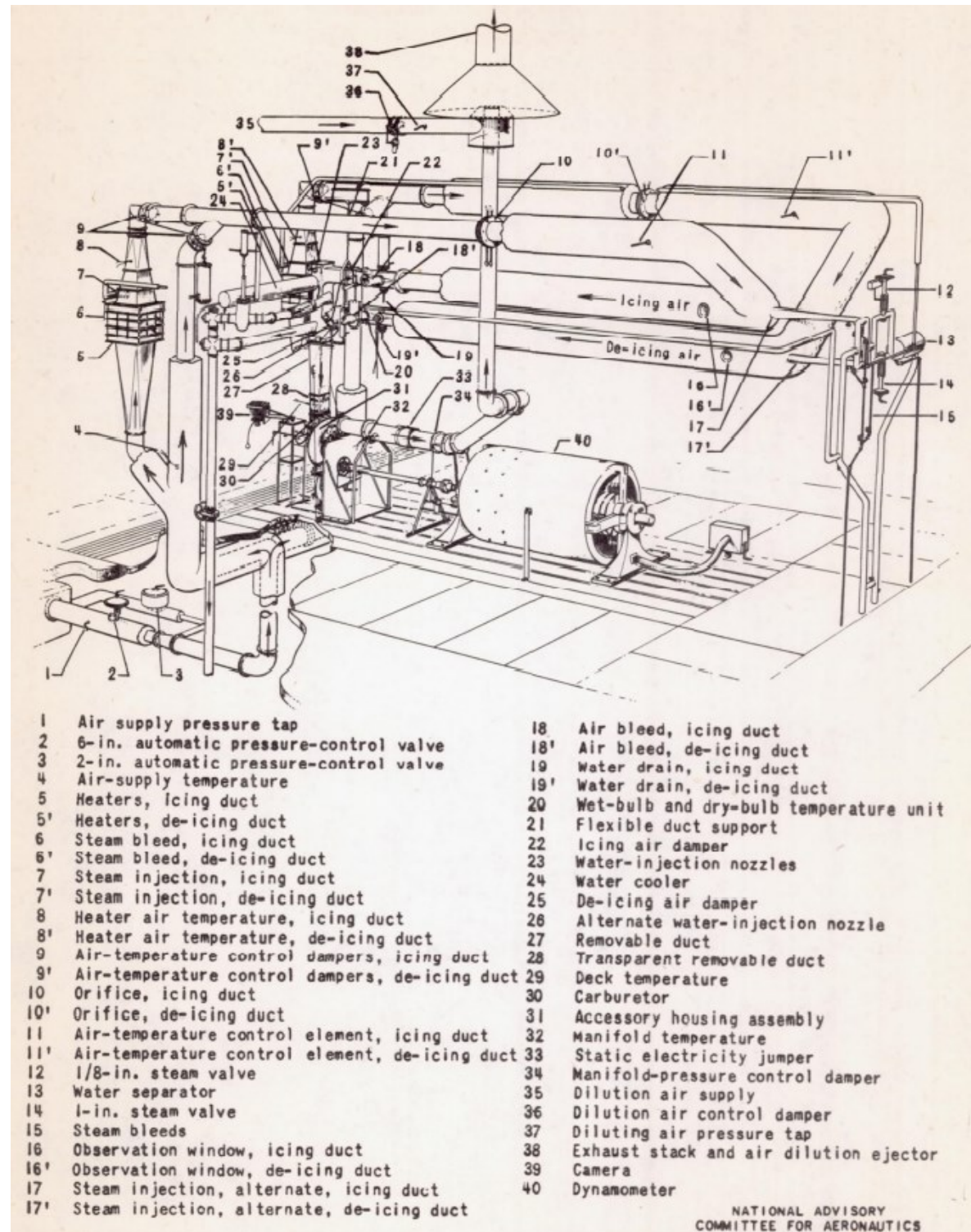


Figure 36: test setup

Source: *Laboratory investigation of icing in the carburetor and supercharger inlet elbow of an aircraft engine / I - Description of setup and testing technique* - Henry A. Essex, Wayne C. Keith, Donald R. Mulholland - 12/1945

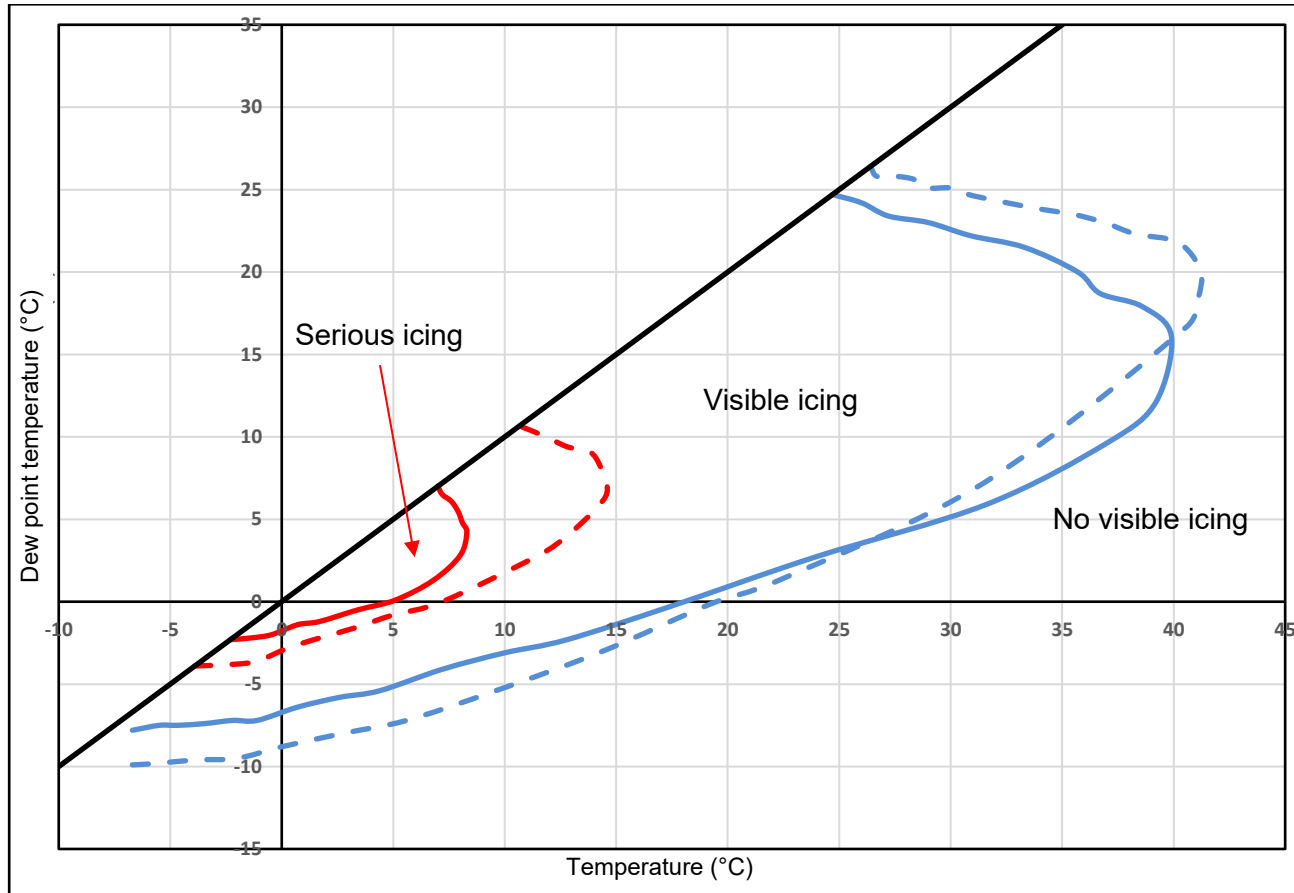


Figure 37: graph reconstructed based on data taken from the publication *Laboratory investigation of icing in the carburetor and supercharger inlet elbow of an aircraft engine / II - Determination of the limiting-icing conditions* - Henry A. Essex, Wayne C. Keith, Donald R. Mulholland - 12/1945

These reviewed publications particularly include the studies published by Willard D. Coles in February 1947, which were conducted in a laboratory, in identical conditions, on two types of carburetors:

- a float-type carburetor equipping a piston engine delivering between 65 and 85 hp **(BEA comment: the exact carburetor model was not specified)**;
- a pressure carburetor equipping a piston engine delivering between 165 and 185 hp.

The study of the former carburetor was particularly interesting due to it being the type that is closest to the modern-day carburetors with which the BEA is familiar.

The publication specified the following test conditions:

Air pressure	Standard pressure at sea level (considered to be conservative)
Fuel temperature	Less than 10°F above the air temperature
Engine power levels	Three configurations: <ul style="list-style-type: none">• glide;• low cruise;• high cruise.

Figure 38 below shows the test setup. Once again, we see that the carburetors are not associated with propulsion systems. The influence of the engine is therefore not taken into account, and in particular the associated thermal environment.

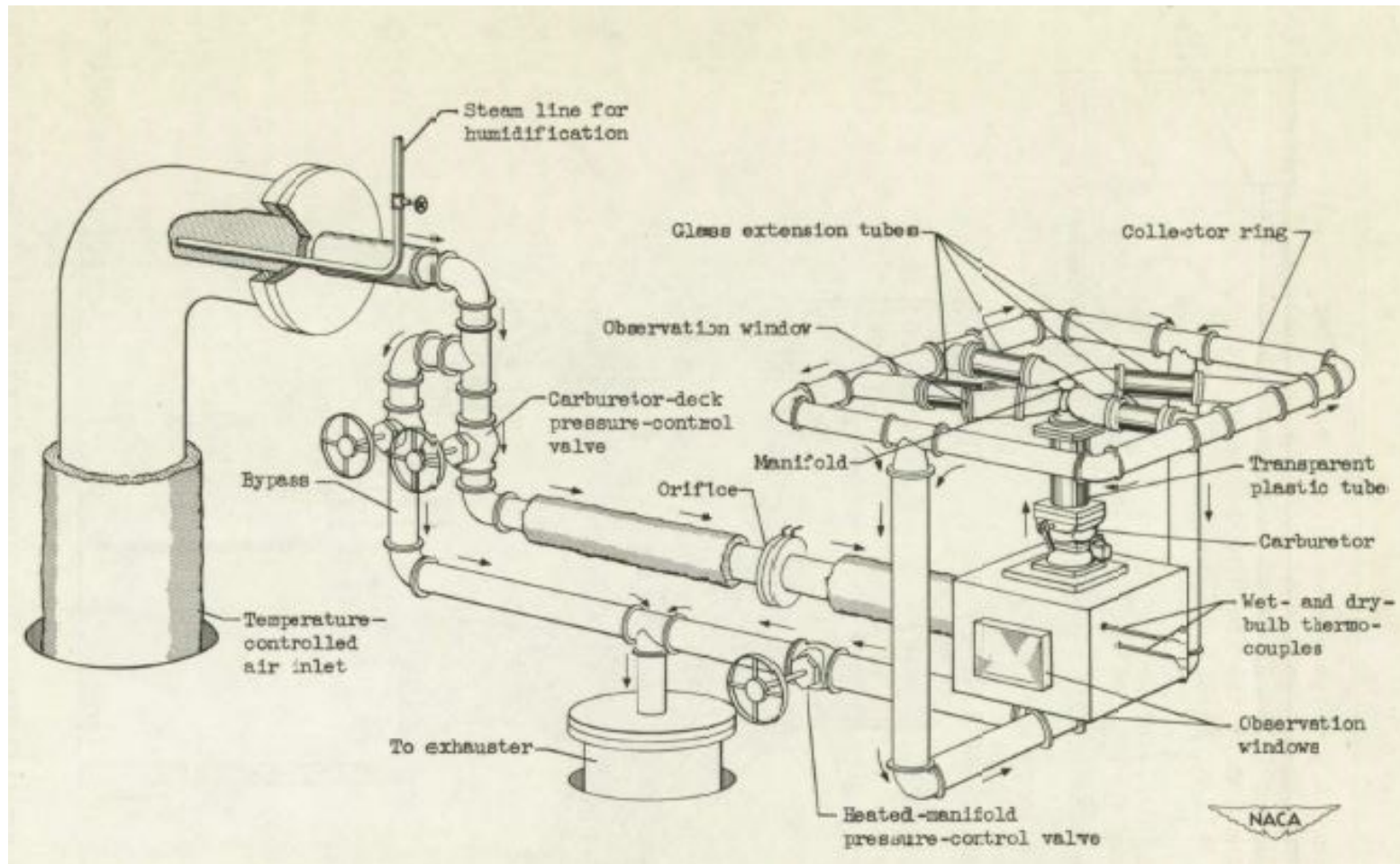


Figure 38: test setup

Source: *Investigation of icing characteristics of typical light-airplane engine induction systems* _ Willard D. Coles _ February 1947

A graph defining the limits of the icing zones is proposed for each carburettor. These graphs were reconstructed based on the same references as the graphs currently proposed by the different authorities (Temperature / Dew point temperature).

We note that the graphs differ markedly, clearly demonstrating that carburettor type is a criterion for defining icing zones.

Float-type carburettor

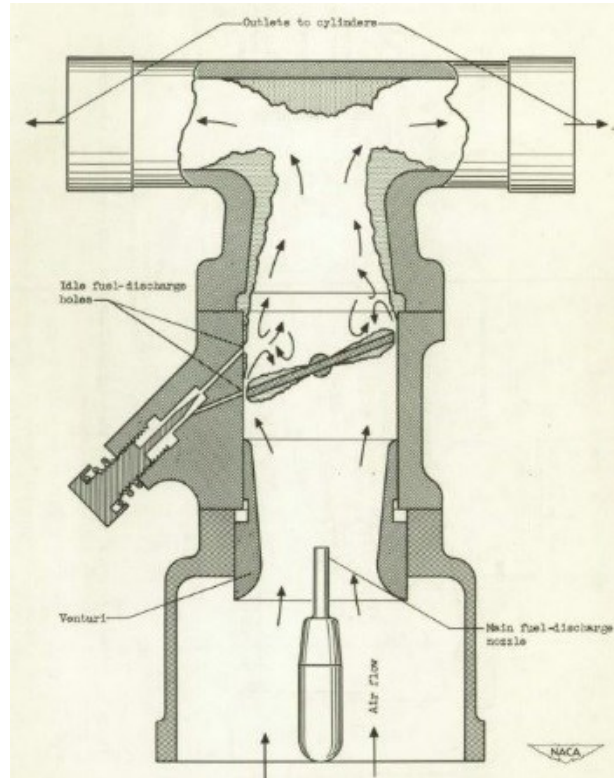


Figure 39: carburettor

Source: Investigation of icing characteristics of typical light-airplane engine induction systems _ Willard D. Coles _ February 1947

Figure 40: graphs obtained for "Glide Power"

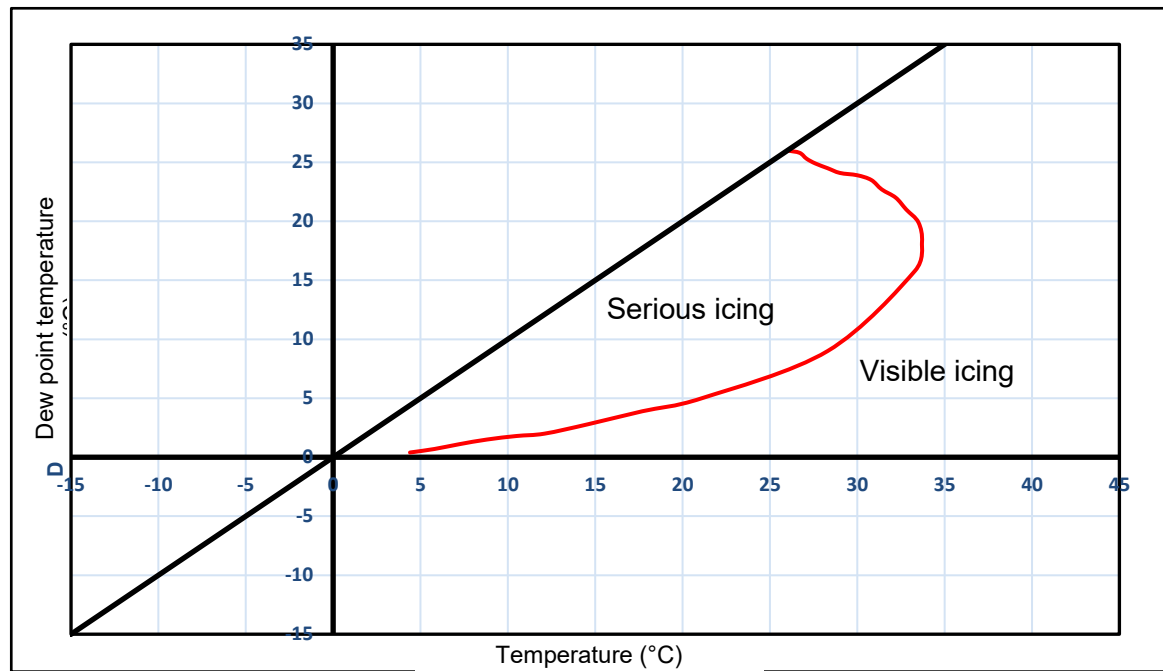
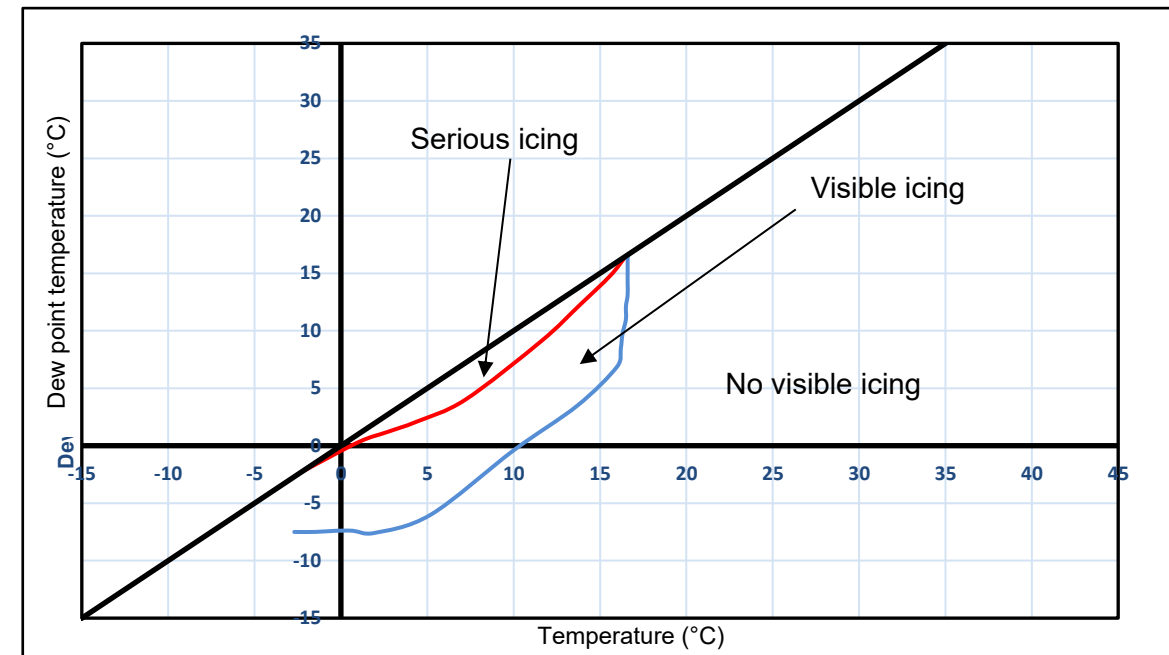
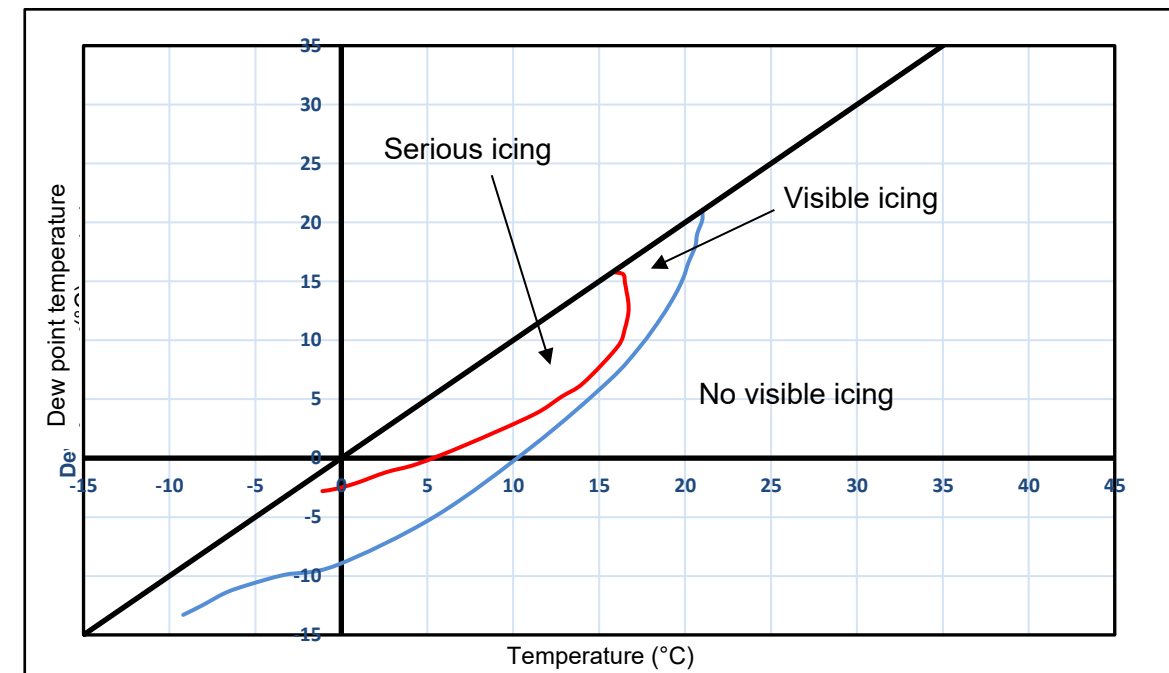


Figure 41: graphs obtained for "High Cruise Power"



—	Limit between the serious icing zone and the visible icing zone
—	Limit between the visible icing zone and the no visible icing zone

Figure 42: graphs obtained for "Low Cruise Power"



Pressure carburettor

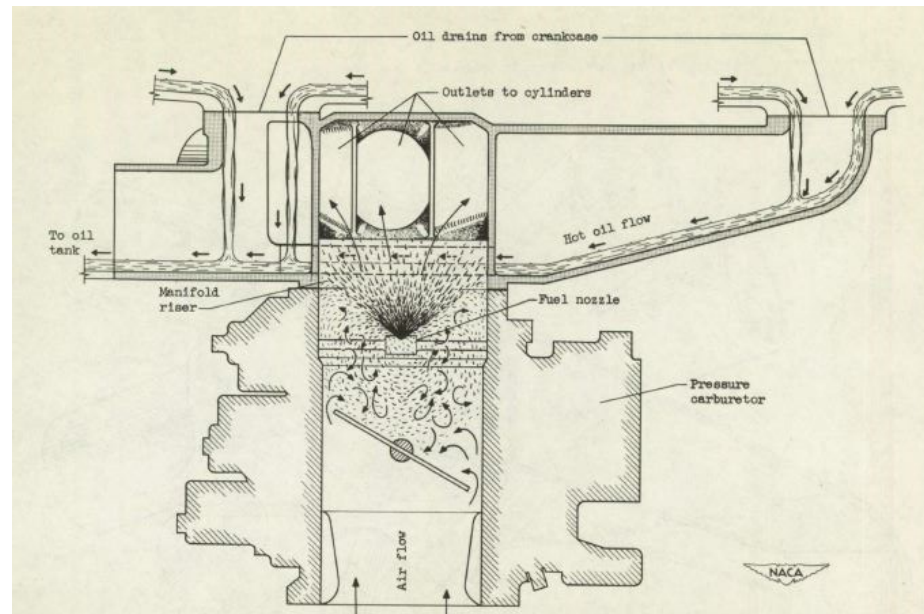
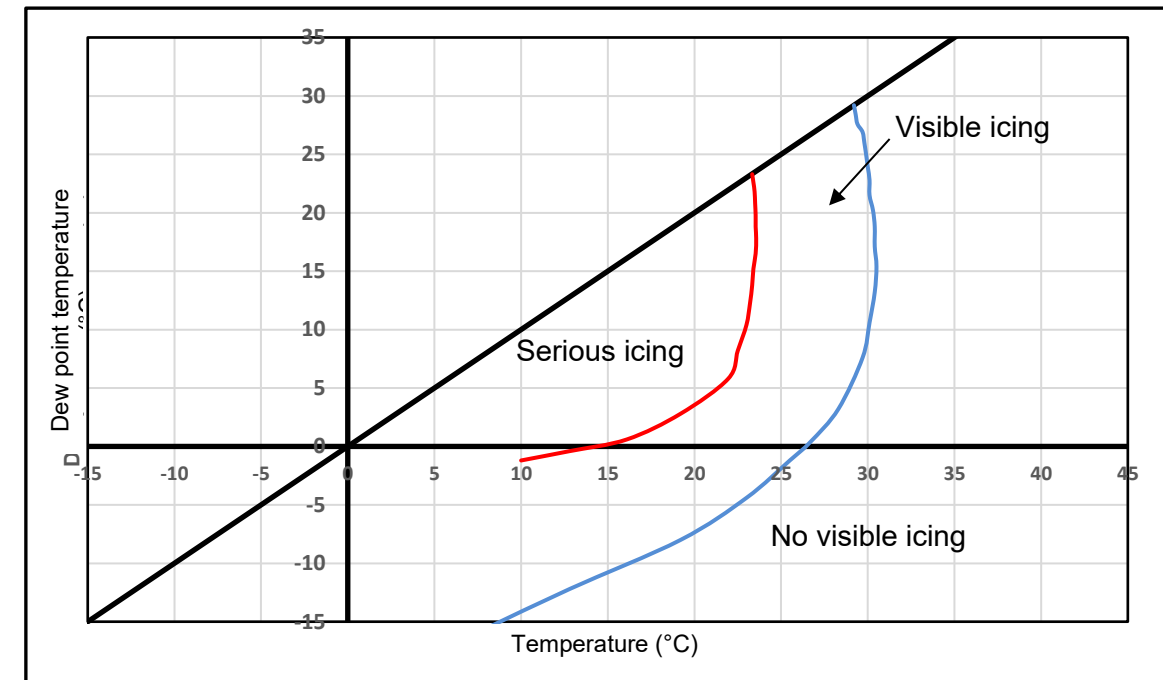


Figure 43: carburettor

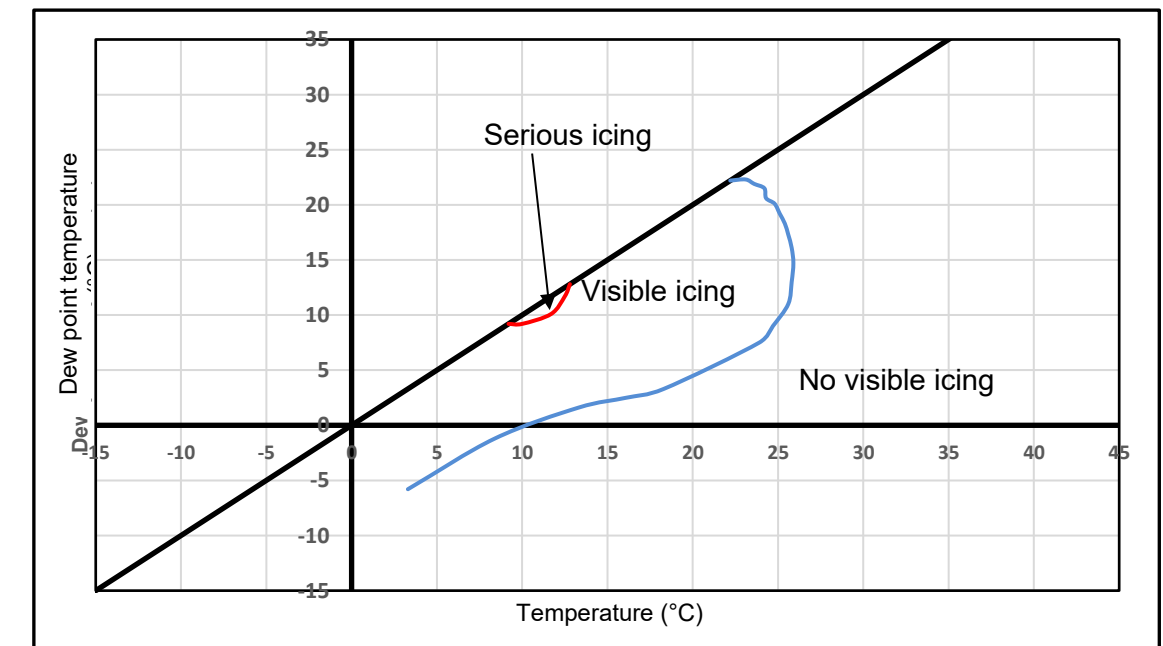
Source: Investigation of icing characteristics of typical light-airplane engine induction systems _ Willard D. Coles _ February 1947

Figure 44: graphs obtained for "Glide Power"



—	Limit between the serious icing zone and the visible icing zone
—	Limit between the visible icing zone and the no visible icing zone

Figure 45: graphs obtained for "Low Cruise Power"



3.9.3. Publications between 1950 and present day

Following the study programme launched by the NACA that gave rise to a large number of publications, we note regular publications on icing up to now.

Several of these publications indicate the performance of tests. Contrary to previous studies, the carburetors used during these tests are models used regularly in modern general aviation (Marvel-Schebler models).

However, very little accurate test data is provided. No data enabling the establishment of new graphs defining the limits of icing zones was identified in particular.

The publications reviewed are listed in the table below.

Article title	Author	Date of publication
Variables Affecting Carburetor Icing in Controlled Laboratory Tests https://www.sae.org/publications/technical-papers/content/630488/	G. R. Dunton, H. J. Scheule, J. D. Rogers	1963
Aircraft Carburetor Icing Studies https://www.sae.org/publications/technical-papers/content/710371/	Gardner, L; Moon, G.	1970
A study of carburetor/induction system icing in general aviation accidents https://ntrs.nasa.gov/citations/19750011136	L. Gardner, G. Moon and R. B. Whyte	March 1971
A STUDY OF CARBURETOR/INDUCTION SYSTEM ICING IN GENERAL AVIATION ACCIDENTS https://ntrs.nasa.gov/citations/19750011136	Richard W. Obermayer and William T. Roe	March 1975
Flight Test Results of the Use of Ethylene Glycol Monomethyl Ether (EGME) as an Anti-Carburetor Icing Fuel Additive https://www.researchgate.net/publication/235158226_Flight_Test_Results_of_the_Use_of_Ethylene_Glycol_Monomethyl_Ether_EGME_as_an_Anti-Carburetor_Icing_Fuel_Additive	Newman, Richard L	1979
LIGHT AIRCRAFT ENGINES, THE POTENTIAL AND PROBLEMS FOR USE OF AUTOMOTIVE FUELS PHASE I - LITERATURE SEARCH https://apps.dtic.mil/sti/citations/ADA094154	D. Patterson et al. UNIVERSITY OF MICHIGAN	January 1981
Light Aircraft Piston Engine Carburetor Ice Detector/Warning Device Sensitivity/Effectiveness https://apps.dtic.mil/sti/citations/ADA117745	Cavage, William; Newcomb, James; Biehl, Keith	June 1982
Calculational method for determination of carburetor icing rate https://www.osti.gov/biblio/5373635	Nazarov, V.I. ; Emel'yanov, V.E. ; Gonopol'ska, A.F. ; Zaslavskii, A.A.	1986
The use of automotive gasoline (mogas) in aviation	Transport Canada	March 1993
Carburetor Ice Test Methodology Evaluation Final Report / CRC Report No. AV-17-13 https://crcao.org/published-report/aviation/page/3/	J. M. Thom, Associate Professor, Purdue University B. Kozak, PhD., Purdue University T. Yother, Purdue University	December 2015

For the most part, these publications were published in the US.

The publication dated 1971, *A study of carburetor/induction system icing in general aviation accidents - L. Gardner, G. Moon and R. B. Whyte*, presents studies that were conducted to determine whether carburettor icing could be eliminated through the use of additives in fuel or the treatment of internal carburettor surfaces. These tests were conducted in serious icing conditions, in a laboratory (**Figure 46**), on a Marvel-Schebler MA4-5 carburettor.

The test conditions were as follows:

Engine power	Idling => Take off power
Fuel used	Aviation fuel grade 100/130 (MIL G 5572) or AVGAS 100 that differs from AVGAS 100 LL due to a higher content of tetraethyl lead.
Fuel temperature	45°F in line with the carburettor (i.e. 7.2°C)
Air temperature	37 to 40°F (i.e. 2.8 to 4.4°C)
Relative humidity	95-98% (an orifice was provided for the spraying of water droplets)

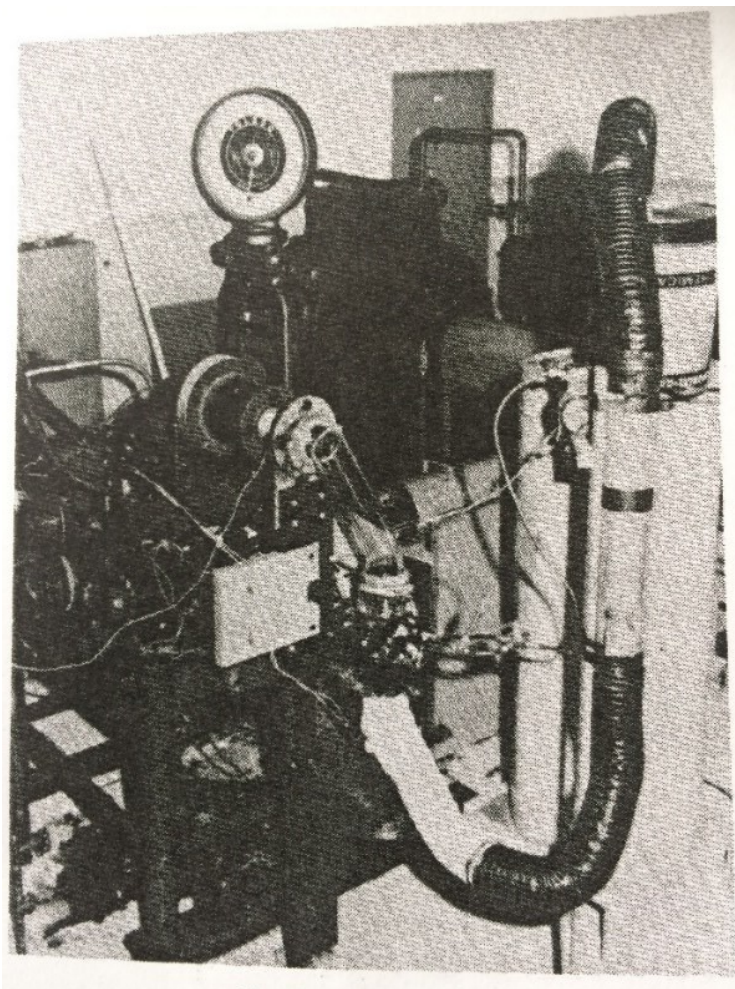


Figure 46: photo of the test setup

Source: *A study of carburetor/induction system icing in general aviation accidents* _ L. Gardner, G. Moon and R. B. Whyte _ March 1971

During the tests, the formation of ice was essentially observed on the butterfly valve. As a result of these tests, the use of a Teflon-type coating was prioritised over the use of an additive.

Documents published in 1981 and 1993 confirmed fuel volatility to be a factor having significant influence on the formation of ice in a carburettor. The higher the fuel volatility, the greater the icing risk.

The purpose of the most recent publication (December 2015) was to reproduce the tests conducted in 1951. Within the context of this study, the test setup in Figure 47 was implemented.



Figure 47: powerplant used

Source: *Carburetor Ice Test Methodology Evaluation Final Report / CRC Report No. AV-17-13 _ J. M. Thom, Associate Professor, Purdue University B. Kozak, PhD., Purdue University T. Yother, Purdue University _ December 2015*

The powerplant comprised a Continental C-85-12 engine, which is a four-cylinder, direct drive, horizontally opposed and air-cooled engine. This version of the engine delivers the maximum power of 85 hp,

and is associated with a Marvel-Schebler MA-3A carburettor (float-type carburettor). The carburettor was installed on the lower surface of the engine.

The engine was fixed to a metal support. During the tests, the assembly remained outside. It was therefore subjected to the outside conditions of the day.

The tests were conducted at a constant speed of 1,750 rpm⁻¹.
The fuel used was AVGAS 100LL.

A metal box was installed on the carburettor, as illustrated in Figure 48.



Figure 48: enclosure surrounding the carburettor to provide the required temperature and humidity conditions

Source: *Carburetor Ice Test Methodology Evaluation Final Report / CRC Report No. AV-17-13* _ J. M. Thom, Associate Professor, Purdue University B. Kozak, PhD., Purdue University T. Yother, Purdue University _ December 2015

The climatic condition reproducer illustrated in Figure 49 provides the carburettor with the required temperature and humidity conditions via a flexible metallic hose.



SPECIFICATIONS

- Temperature:**
 - Range: -17 to 49°C (1 to 120°F)
 - Accuracy: ±1°C (±1.8°F)
- Relative Humidity:**
 - Range: 2 to 98% RH
 - Accuracy: ±3% RH (@ 15 to 90% RH)
- Repeatability:** ±1% RH
- PC Interface:** USB
- USB Cable:** Integral to sensor, 2 m (6') (shielded) Type A plug
- Software (Included):** Requires Windows® 2000, XP, or Vista operating system
- Housing:** 316 stainless steel
- Dimensions:** 138 L x 16 mm D (5.5 x 0.625")
- Weight:** 67 g (0.18 lbs)

Figure 49: climatic condition reproducer used during the tests

Source: *Carburetor Ice Test Methodology Evaluation Final Report / CRC Report No. AV-17-13* _ J. M. Thom, Associate Professor, Purdue University B. Kozak, PhD., Purdue University T. Yother, Purdue University _ December 2015

Upon completion of the tests, several criteria for improving the test setup were noted:

- the importance of having the same conditions supplied by the climatic condition reproducer in the carburettor stream and also in its environment. Indeed, when the outside walls of the carburettor are subjected to conditions that are completely different from those produced by the climatic condition reproducer, icing can be delayed by the temperature of the walls.
- It is essential to check the barometric pressure in the carburettor air supply stream. The variation of the barometric pressure due to the atmospheric conditions on the day causes the humidity to vary. The pressure control quality is directly associated with the climatic condition reproducer used.
- However, the test setup allowing the operator to be as close to the engine as possible enabled the operator to gather audible evidence of icing.

Tests allowed ice to form in very specific conditions (temperature = 55°F, i.e.12.8°C, and a relative humidity of 95%). The engine used appeared to tolerate the ice. During the many adjustments and tests carried out, it was evident that after an initial minor formation of ice, resulting in a decrease of 50 to 200 rpm⁻¹, the engine continued to operate despite the ice and, in several cases, freed itself of the ice and restored full power.

This publication shows the following graphs illustrating the appearance and spread of icing.

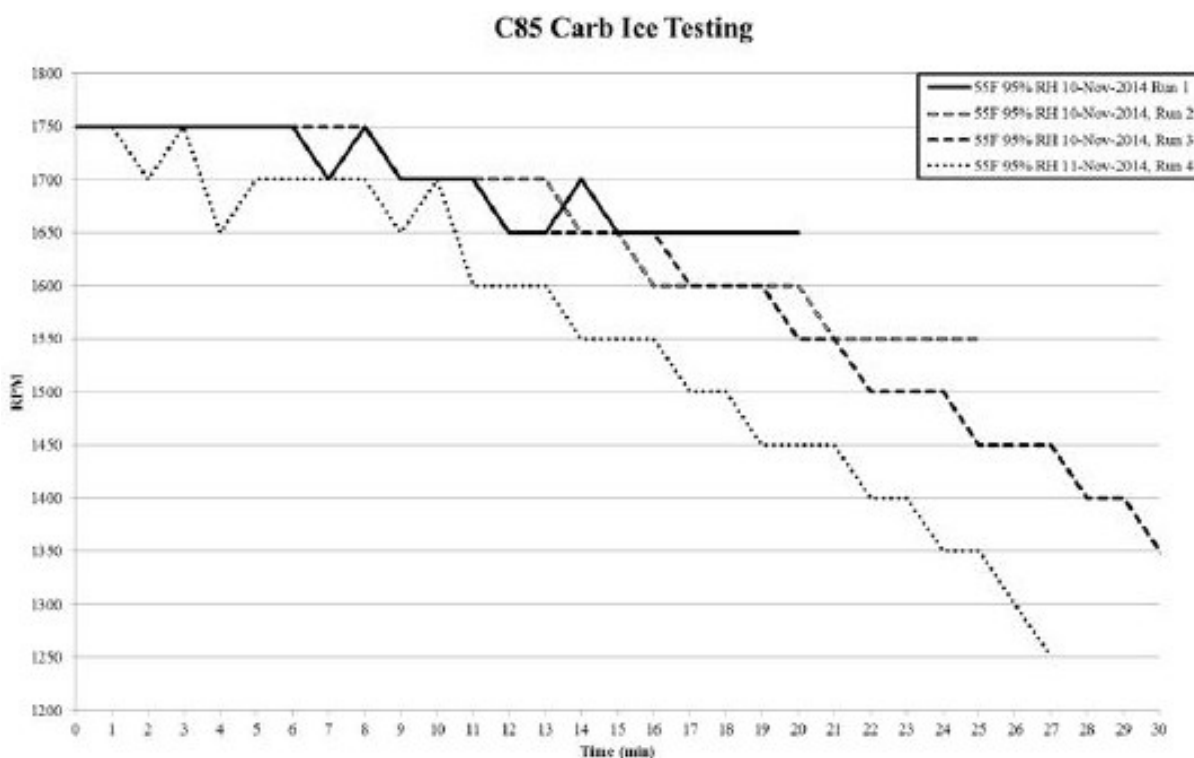


Figure 50: test results

Source: Carburetor Ice Test Methodology Evaluation Final Report / CRC Report No. AV-17-13 _ J. M. Thom, Associate Professor, Purdue University B. Kozak, PhD., Purdue University T. Yother, Purdue University _ December 2015

3.10. Comparison of the different graphs

3.10.1. Reminder of the sources identified

Two types of sources were used to identify the graphs defining the icing zones based on the air temperature and the dew point temperature:

- the main aviation authorities (EASA, FAA, Canada, Australia) and safety investigation authorities;
- various scientific articles mostly published between 1945 and 1950.

Each graph defines the zones of the envelope in which the probability of piston engine induction system icing varies depending on the engine speed.

For the graphs proposed by the authorities, the icing zones are not precisely defined and the nature of the data used to establish the graphs is unknown. Unverified information was identified in two articles:

- an article published in the FAA Safety Briefing: "The data is from a NASA study of carb ice accidents back in the 1980's";
- an article in the DSAC Safety Bulletin No.16, stating that these risk zones were established based on nearly 5,400 cases of carburettor icing with the temperature conditions observed on the ground.

The authorities do not specify whether these graphs are valid for all powerplants.

Reminder: the graphs proposed by the authorities are available at the addresses given in the table below:

EASA	https://www.easa.europa.eu/document-library/general-publications/egast-leaflet-ga-5-piston-engine-icing
FAA	https://rgl.faa.gov/Regulatory_and_Guidance_Library/rgSAIB.nsf/(LookupSAIBs)/CE-09-35?OpenDocument
Canada	https://www.tc.gc.ca/fra/aviationcivile/publications/tp2228-6036.htm
Australia	https://www.atsb.gov.au/publications/2009/carburettor-icing/

For scientific articles, these zones are defined as follows:

- no visible;
- visible: ice visible without decreasing the air flow;
- serious: ice causing a decrease in air flow of at least 2% within at least 15 minutes.

For these graphs, the following engine speeds are considered:

- glide power;
- low cruise power;
- high cruise power.

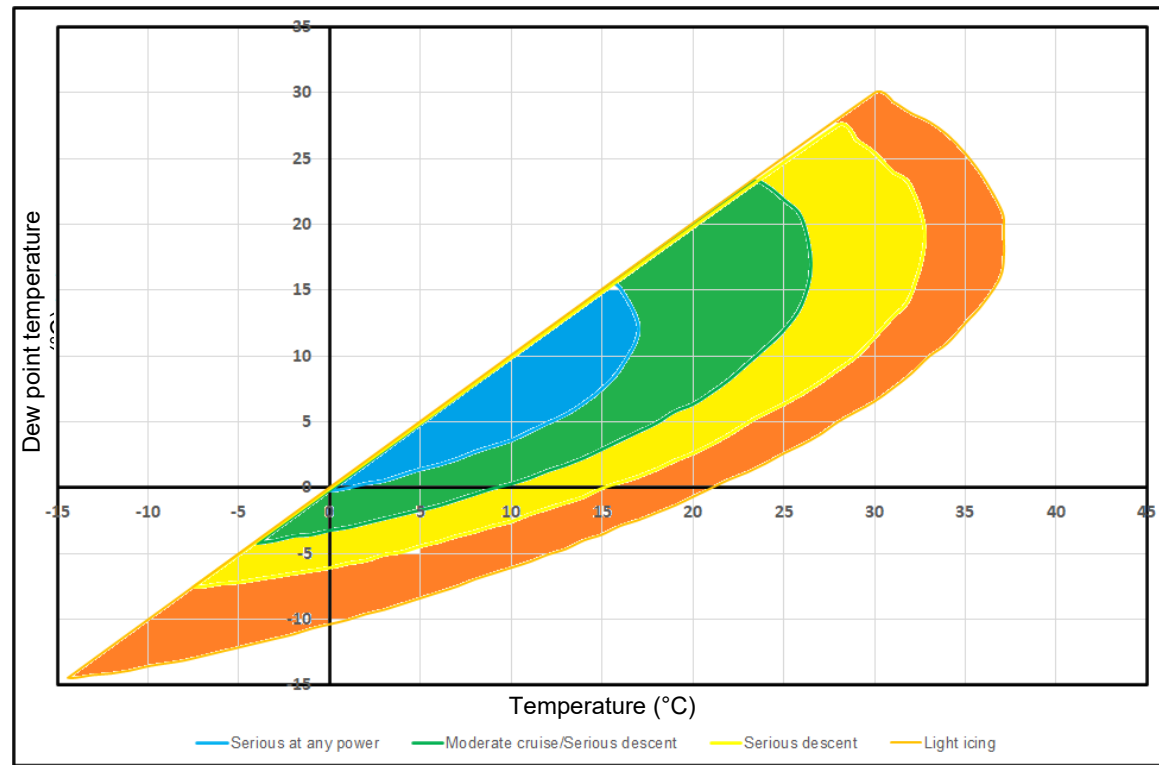
The tests used to establish these graphs were conducted for the most part in a laboratory. The conditions of these tests were more or less clearly defined, with the type of carburettor used being systematically defined.

The scientific articles containing the graphs are listed in the table below:

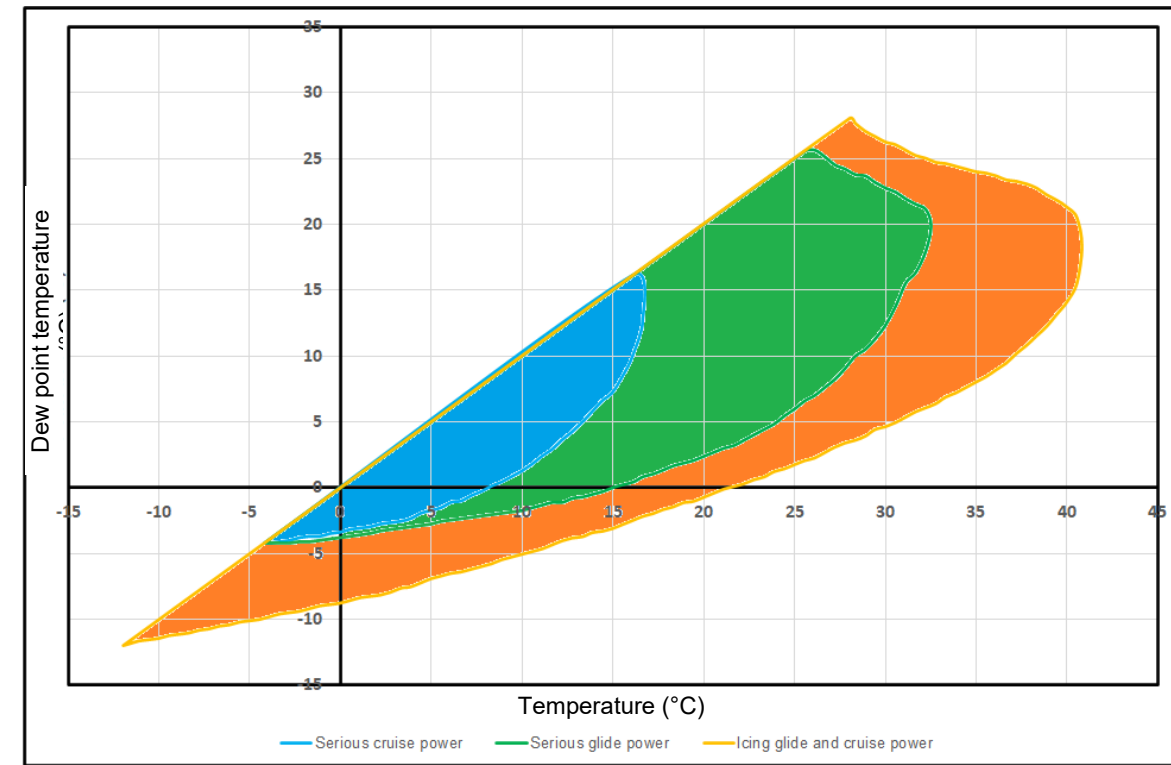
Article title	Author	Date of publication
Laboratory investigation of icing in the carburetor and supercharger inlet elbow of an aircraft engine / II - Determination of the limiting-icing conditions	Henry A. Essex, Wayne C. Keith, Donald R. Mulholland	12/1945
A Preliminary investigation of the Icing Characteristic of a Large Rectangular-Throat Pressure-Type Carburetor	Gilbert E. Chapman	07/1946
An investigation of the icing and heated-air de-icing characteristics of the R-2600-13 induction system	Gilbert E. Chapman	12/1946
Effects of Induction-System Icing on Aircraft-Engine Operating Characteristics	Stevens, Howard C., Jr.	01/1947
Investigation of icing characteristics of typical light-airplane engine induction systems	Willard D. Coles	02/1947
Icing protection requirements for reciprocating-engine induction systems	Willard D.Coles, Vern G.Rollin, Donald R.Mulholland	03/1950

3.10.2. Comparison of the graphs proposed by the different authorities

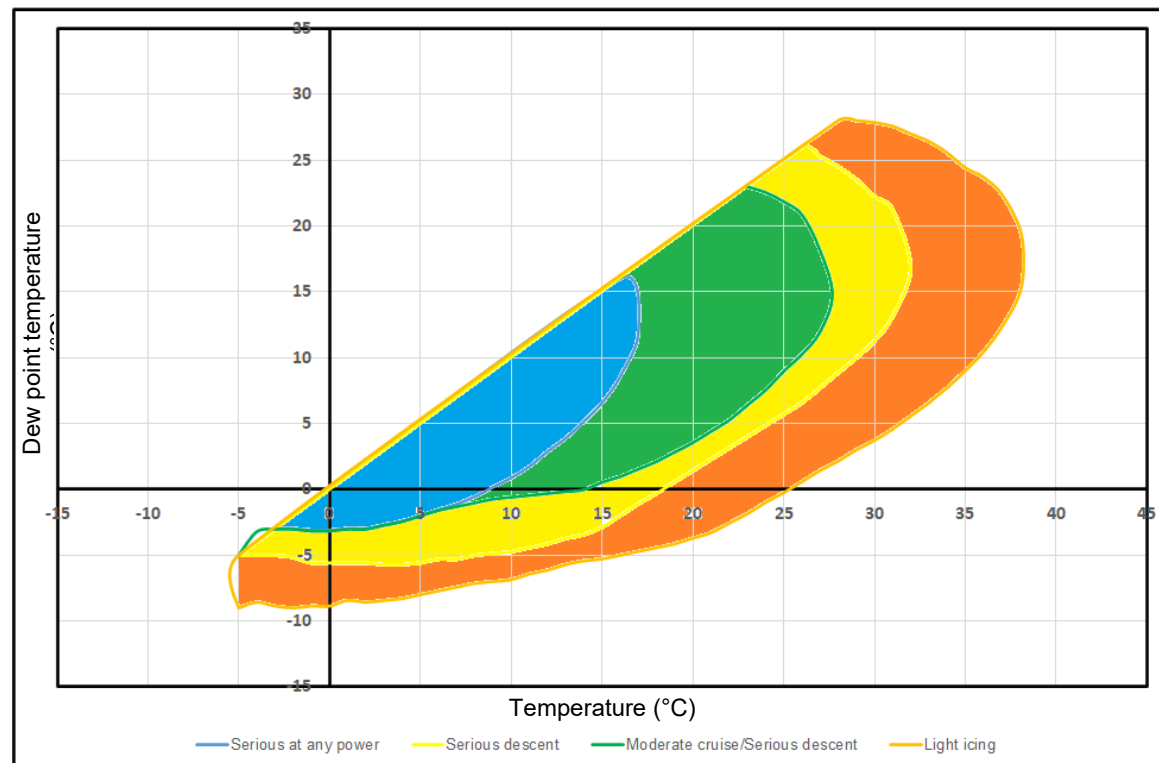
* The graph keys below are those used by the authorities.



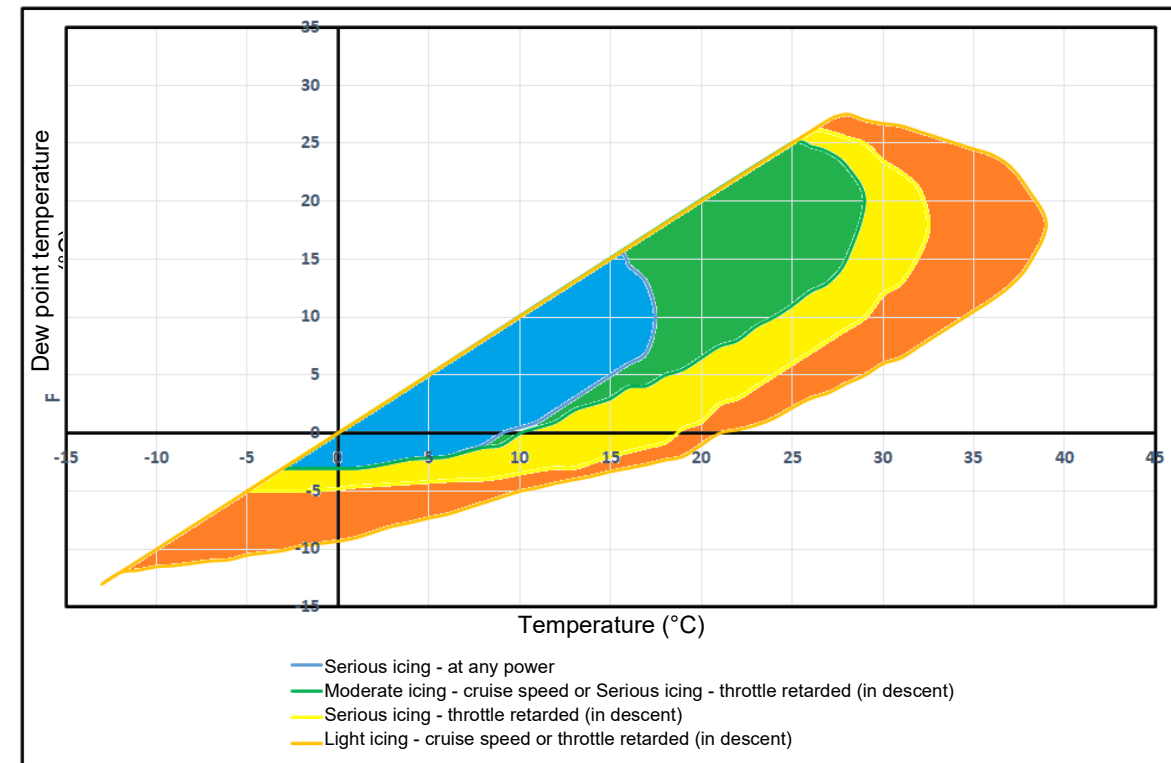
EASA



FAA



ATSB



Transport Canada

Figure 51: graphs proposed by the authorities
Source: established by the BEA

For the graphs proposed by the EASA, Canada and Australia, the envelope is divided into four zones. In these three graphs, these four zones are identified in exactly the same way:

- Serious at any power;
- Moderate cruise / Serious descent;
- Serious descent;
- Light icing.

Of these authorities, only Canada specifies that the graph should not be used when the engine is operated with MOGAS fuel (automotive gasoline), which is more volatile than aviation fuel.

The graph proposed by the FAA distinguishes two types of carburettor: float-type and pressure. The graph pertaining to pressure carburettors is not dealt with in this document.

For the pressure carburettor, the envelope concerned is very restricted.

For the float-type carburettor, the envelope is divided into three zones. These three zones are labelled differently from those in the graphs proposed by the EASA, Canada and Australia. Equivalences are however proposed by the BEA below to enable these four graphs to be compared. They are labelled as follows:

Zones identified on the FAA's graph	Equivalences proposed with the other three graphs
Serious cruise power	Serious at any power
Serious glide power	Serious descent and Moderate cruise/Serious descent
Icing glide and cruise power	Light icing

On the next page, the various graphs are superimposed by zones.

Comparison of “Serious at any power” zones (Figure 52):

For this zone, we observe that the zones on the graphs proposed by the FAA, Canada and Australia are practically identical. The zone on the graph proposed by the EASA is smaller for the lowest dew point temperature values.

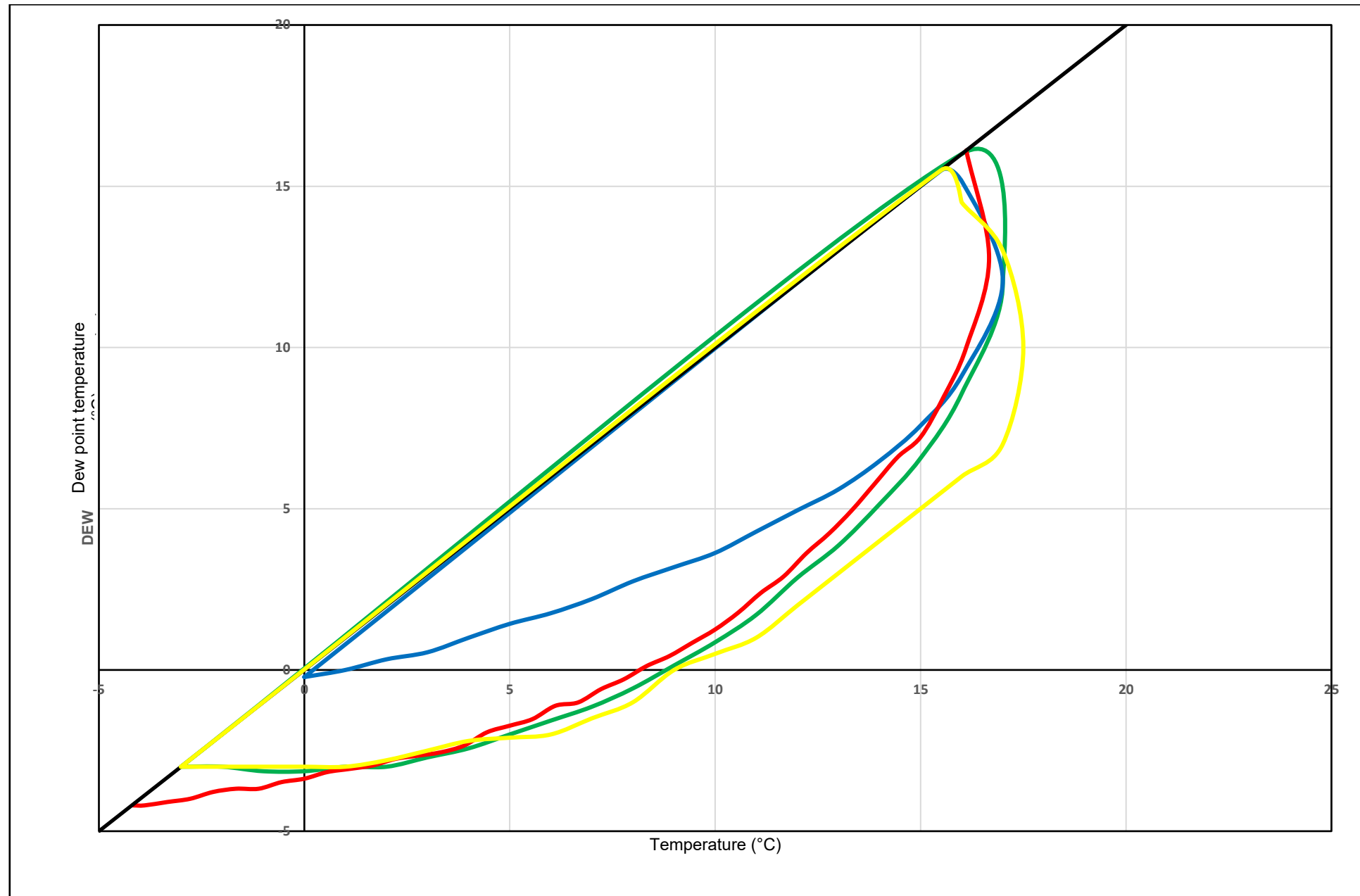
Comparison of “Serious descent - Moderate cruise/Serious descent” zones (Figure 53):

The “Moderate cruise/Serious descent” zone proposed by the EASA, Canada and Australia is included in the “Serious descent” zone proposed by the other four authorities. The graphs are very similar for this zone, slightly larger for the EASA for the low temperatures. The most restricted graph is that proposed by the FAA.

Comparison of “Light icing - Icing glide et cruise power” zones (Figure 54):

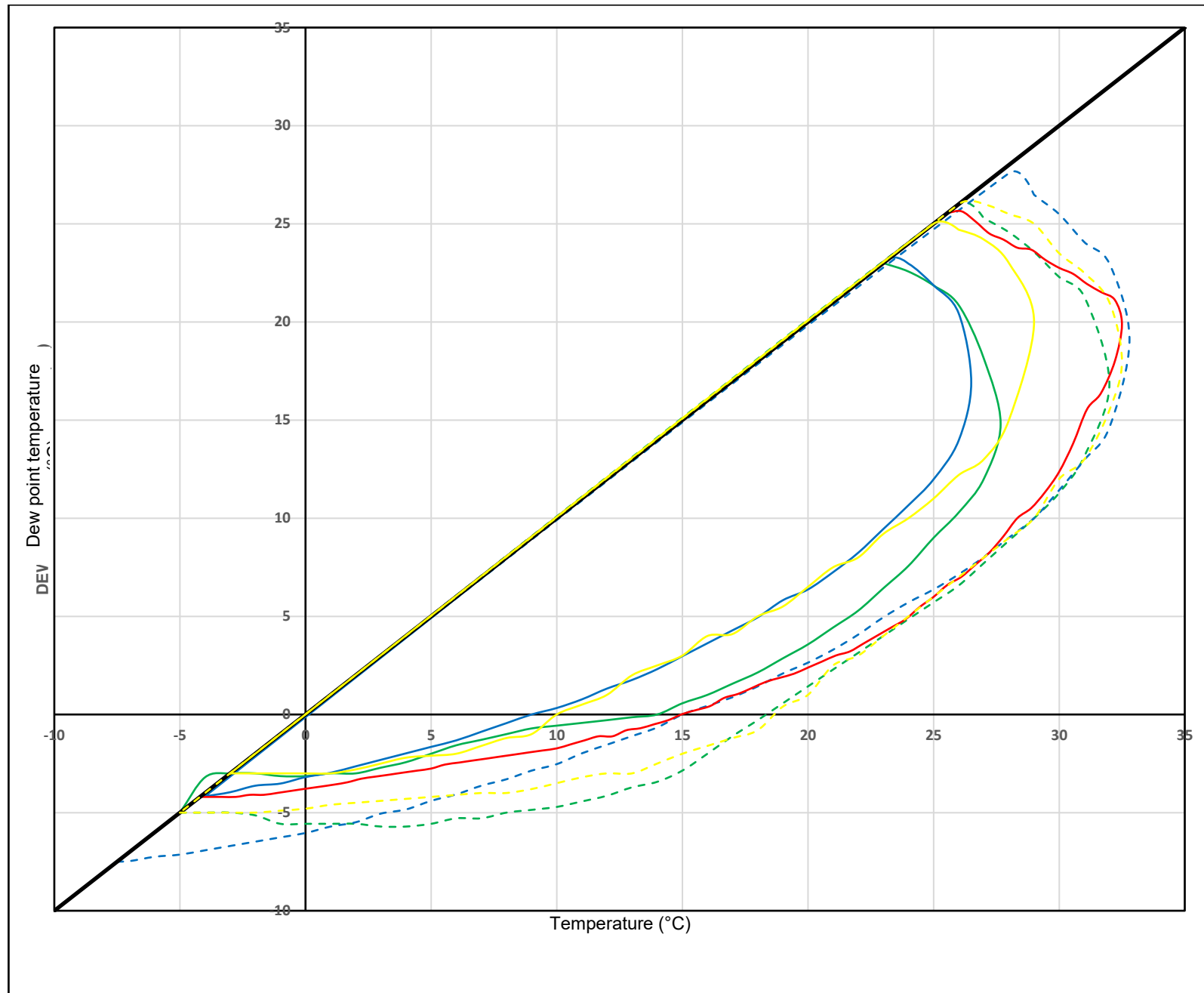
The four graphs are similar, with a slightly larger envelope on the FAA's graph in the higher temperatures.

To conclude, the authority graphs are different and therefore clearly based on different data.



—	EASA
—	FAA
—	Australia
—	Canada

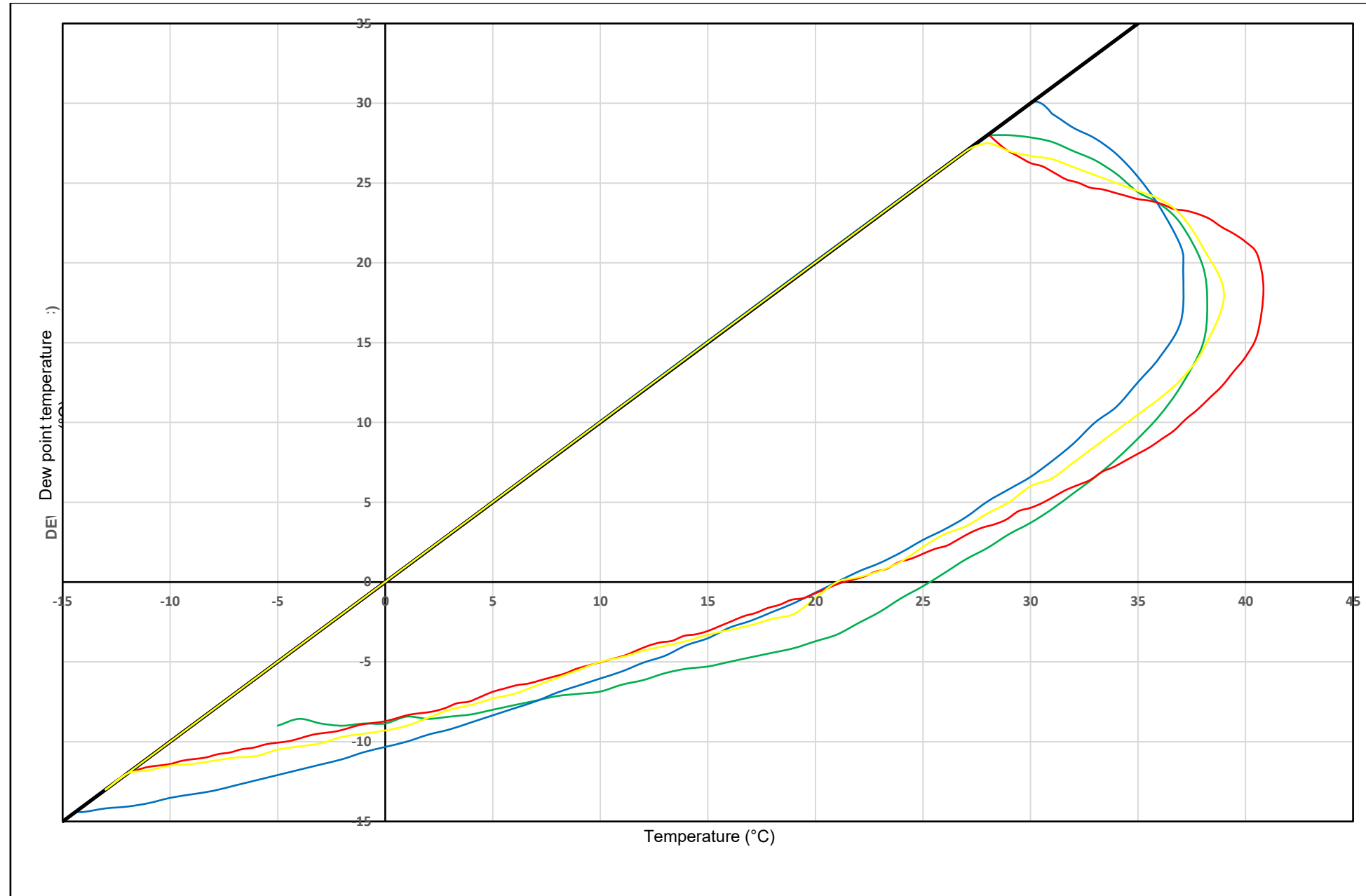
Figure 52: graphs proposed by the authorities for the “Serious Any Power” envelope
 Source: established by the BEA



	EASA / Moderate Cruise - Serious Descent
	EASA / Serious Descent
	FAA
	Australia / Moderate Cruise - Serious Descent
	Australia / Serious Descent
	Canada/ Moderate icing in cruise speed or Serious icing in descent
	Canada / Serious icing in descent

Figure 53: graphs proposed by the authorities for the “Serious descent and Moderate cruise/Serious descent” envelope
 Source: established by the BEA

Light Icing



—	EASA
—	FAA
—	Australia
—	Canada

Figure 54: graphs proposed by the authorities for the “Light Icing” envelope
Source: established by the BEA

3.10.3. Comparison of the graphs proposed by the scientific articles

For the graphs identified in the scientific articles, several parameters are used to differentiate the different icing envelope zones:

- The carburettor type:
 - float-type carburettor;
 - pressure carburettor.

- The engine power as follows (not all represented on each graph):
 - *Glide Power*;
 - *Low Cruise Power*;
 - *High Cruise Power*;

- The icing severity as follows:
 - the *No Visible* zone;
 - the *Visible* zone;
 - the *Serious* zone.

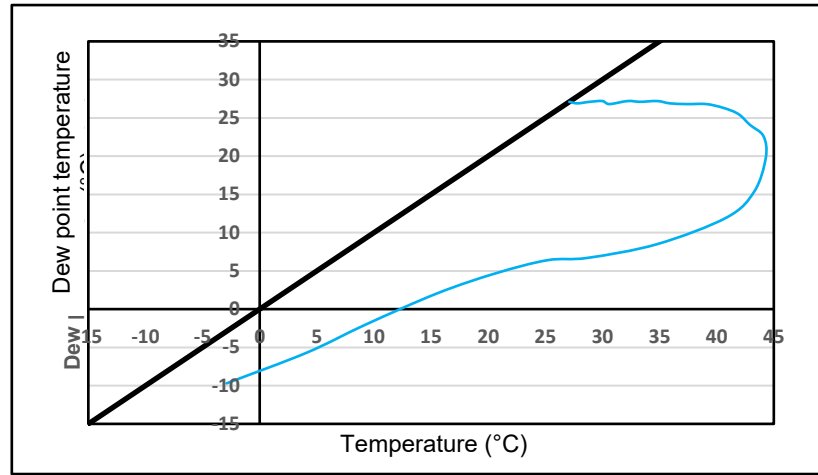
In terms of carburettor type, most of the graphs concern pressure carburettors. Only one scientific article presents data relating to a float-type carburettor.

In terms of engine power, most of the graphs provide data for *Low Cruise Power*.

In terms of icing severity, several of the graphs only show the limit between the *Visible* and *No Visible* envelopes. In these cases, *Serious* icing is only obtained for a relative humidity of 100%, with the addition of liquid water.

Due to these specificities, only the data from the different articles for *Low Cruise Power*, as well as the delimitation between the *Visible* and *No Visible* zones can be comprehensively compared. The data comparison for the other characteristics will only be very partial.

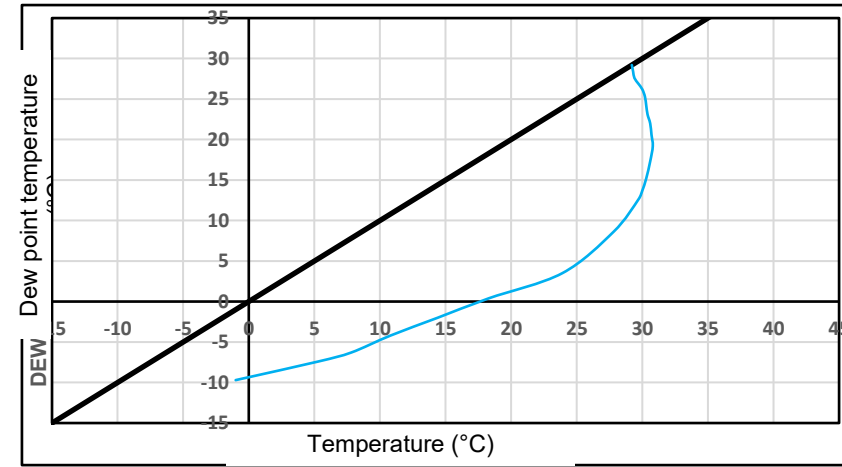
Publication: An investigation of the icing and heated-air de-icing characteristics of the R-2600-13 induction system - 12/1946



Refer to **Figure 31**

	Delimitation between visible icing and no visible icing
--	---

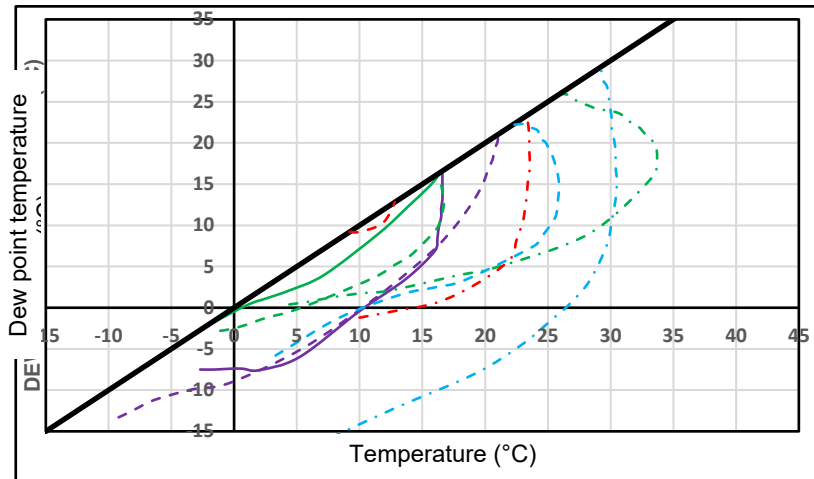
Publication: A Preliminary investigation of the Icing Characteristic of a Large Rectangular-Throat Pressure-Type Carburetor - 07/1946



Refer to **Figure 34**

	Delimitation between visible icing and no visible icing
--	---

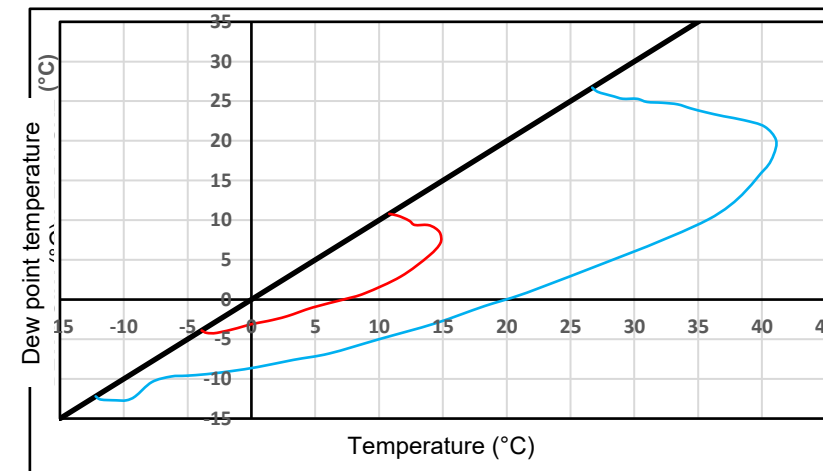
Publication: Investigation of icing characteristics of typical light-airplane engine induction systems - 02/1947



Refer to **Figure 39** and **Figure 43**

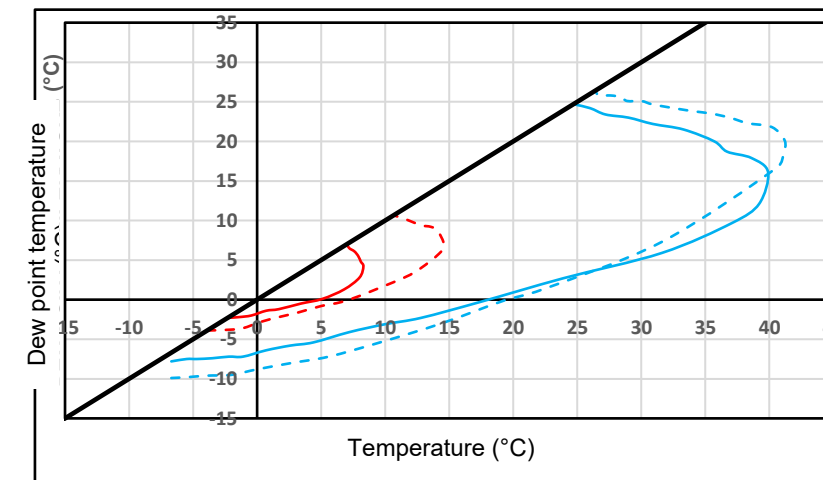
	Pressure carburettor / Low Cruise Power / serious icing - visible icing
	Pressure carburettor / Low Cruise Power / visible icing - no visible icing
	Pressure carburettor / Glide Power / serious icing - visible icing
	Pressure carburettor / Glide Power / visible icing - no visible icing
	Float-type carburettor / High Cruise Power / serious icing - visible icing
	Float-type carburettor / High Cruise Power / visible icing - no visible icing
	Float-type carburettor / Low Cruise Power / serious icing - visible icing
	Float-type carburettor / Low Cruise Power / visible icing - no visible icing
	Float-type carburettor / Glide Power / serious icing - visible icing

Publication: Effects of Induction-System Icing on Aircraft-Engine Operating Characteristics - 01/1947



	Delimitation between serious icing and visible icing
	Delimitation between visible icing and no visible icing

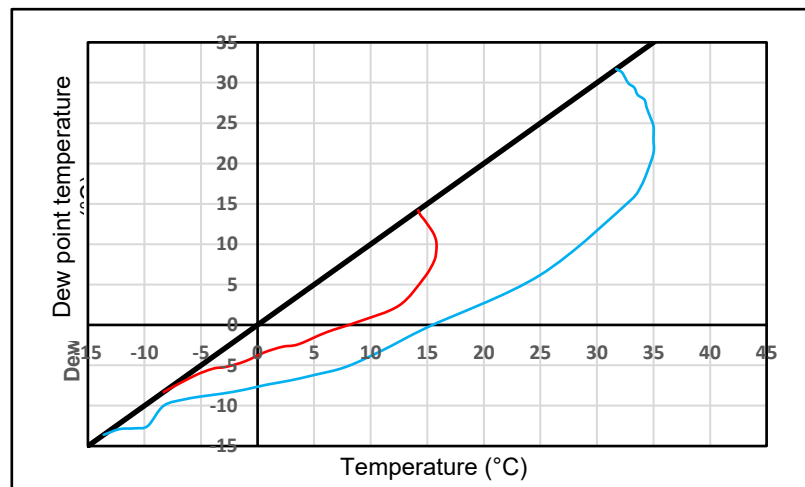
Publication: Laboratory investigation of icing in the carburetor and supercharger inlet elbow of an aircraft engine / II - Determination of the limiting-icing conditions - 12/1945



Refer to **Figure 36**

	Delimitation between serious icing and visible icing High Cruise Power
	Delimitation between visible icing and no visible icing High Cruise Power
	Delimitation between serious icing and visible icing Low Cruise Power
	Delimitation between visible icing and no visible icing Low Cruise Power

Publication: Icing protection requirements for reciprocating-engine induction systems - 03/1950

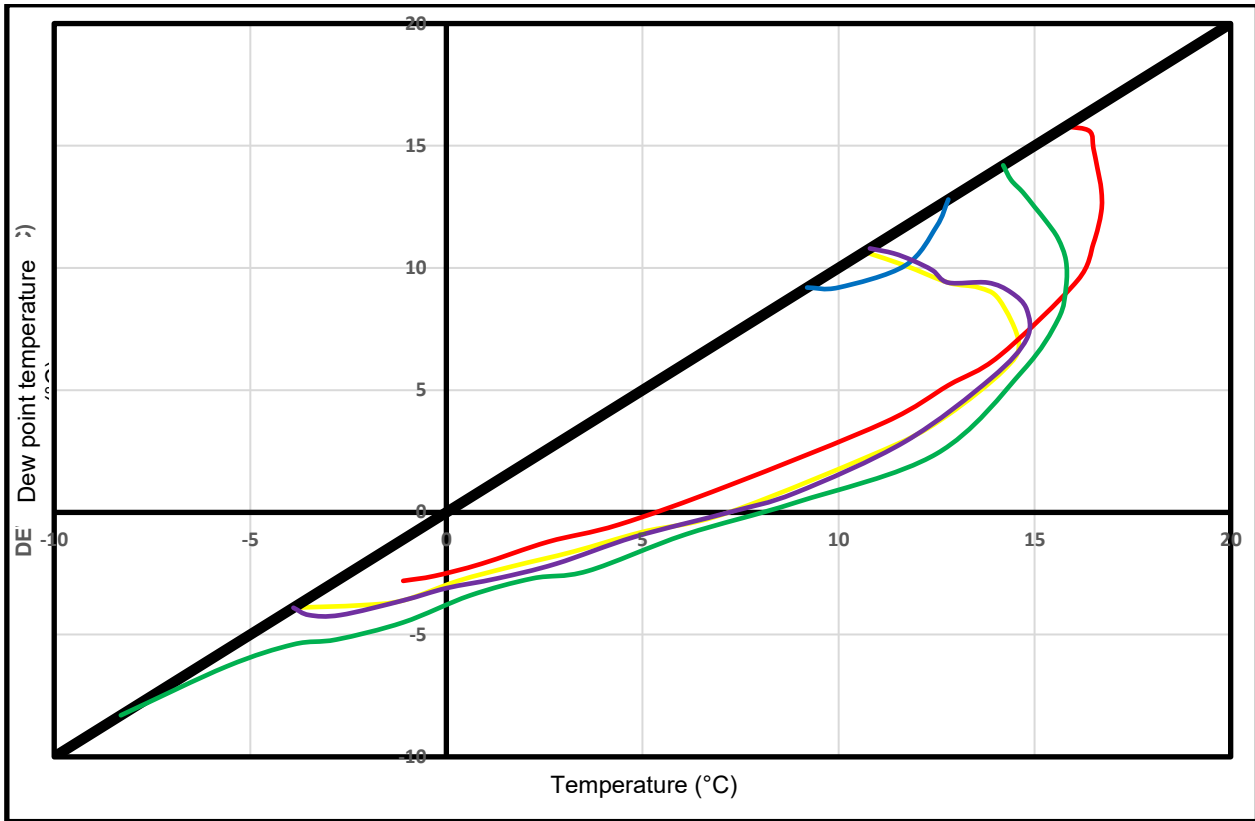


Refer to **Figure 28**

	Delimitation between serious icing and visible icing
	Delimitation between visible icing and no visible icing

Figure 55: graphs identified in the scientific publications - Source: established by the BEA

The first comparison concerns *Low Cruise Power* and the limit between the *Serious* and *Visible* zones (**Figure 56**).



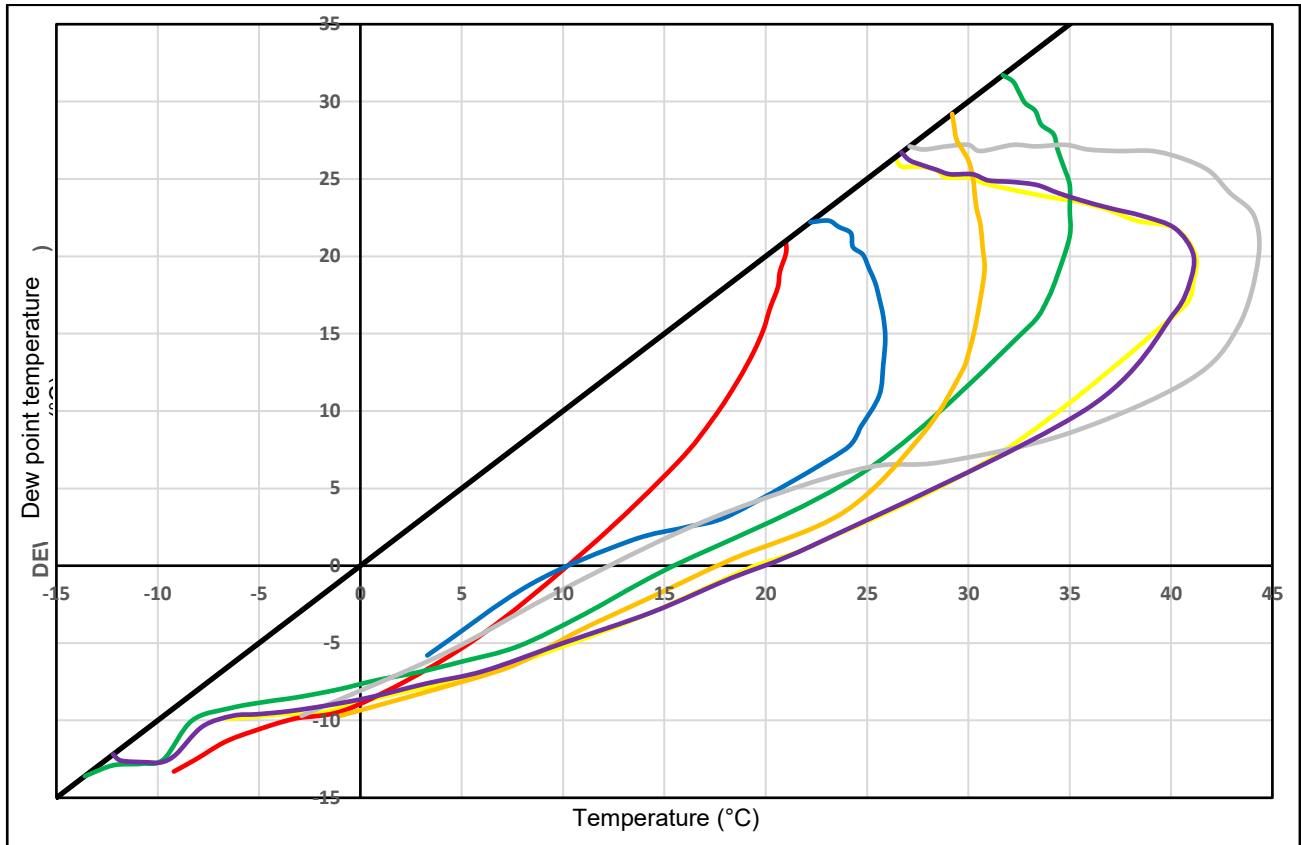
	Type of carburettor	Article
—	Pressure carburettor	Investigation of icing characteristics of typical light-airplane engine induction systems
—	Pressure carburettor	Effects of Induction-System Icing on Aircraft-Engine Operating Characteristics
—	Pressure carburettor	Laboratory investigation of icing in the carburetor and supercharger inlet elbow of an aircraft engine / II - Determination of the limiting-icing conditions
—	Pressure carburettor	Icing protection requirements for reciprocating-engine induction systems
—	Float-type carburettor	Investigation of icing characteristics of typical light-airplane engine induction systems

Figure 56: comparison of the graphs relating to the following parameters: *Low Cruise Power* / Delimitations between the *Serious* and *Visible* zones
 Source: established by the BEA

We note that the limit proposed for the pressure carburettor in the article “Investigation of icing characteristics of typical light-airplane engine induction systems” is very reduced and different from the other publications. According to the publication, this pressure carburettor was adapted to the engine with a much lower power than the other carburettors.

The limits provided by the other four articles follow the same trend. We note that the limit associated with the float-type carburettor creates a much larger zone than that of pressure carburettors.

The second comparison concerns *Low Cruise Power* and the limit between the *Visible* and *No visible* zones (**Figure 57**).



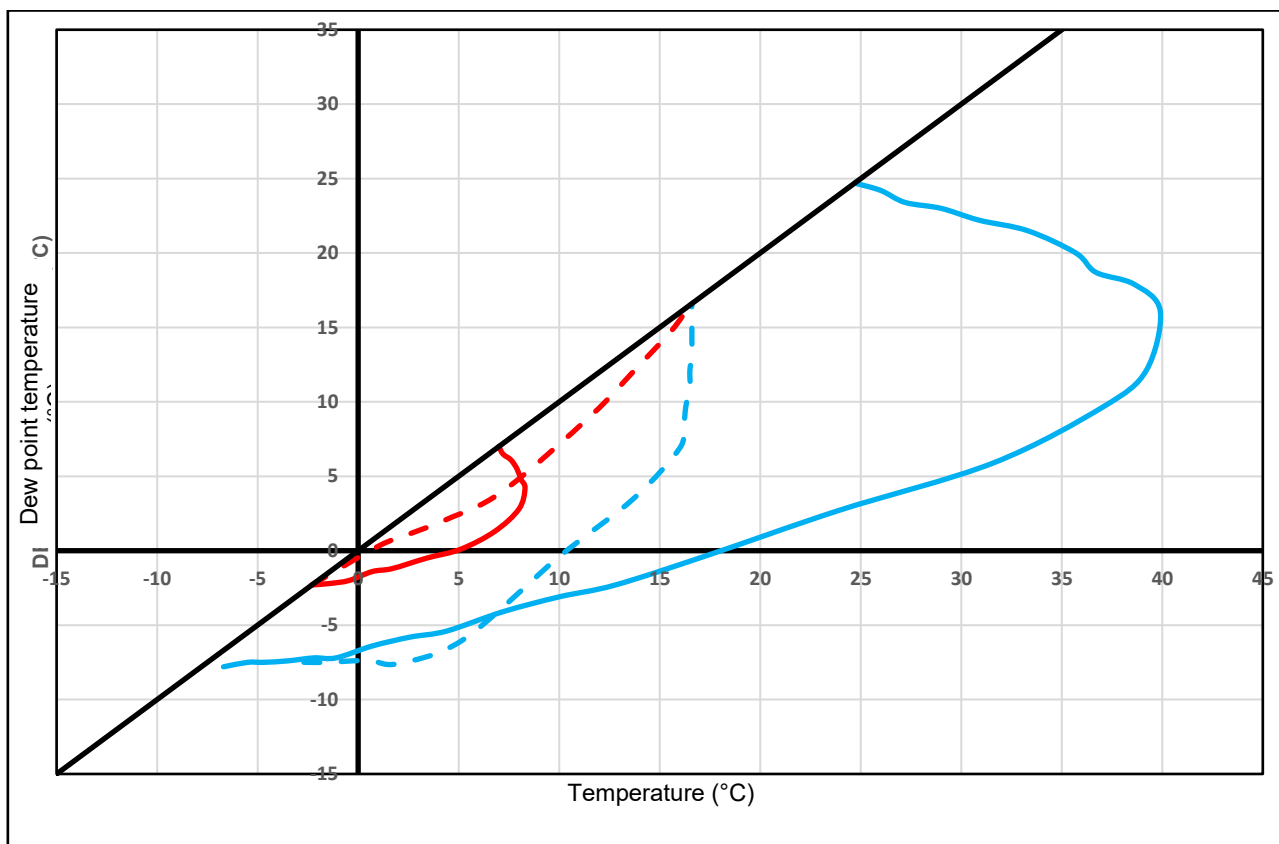
	Type of carburettor	Article
—	Pressure carburettor	Investigation of icing characteristics of typical light-airplane engine induction systems
—	Pressure carburettor	Effects of Induction-System Icing on Aircraft-Engine Operating Characteristics
—	Pressure carburettor	Laboratory investigation of icing in the carburetor and supercharger inlet elbow of an aircraft engine / II - Determination of the limiting-icing conditions
—	Pressure carburettor	Icing protection requirements for reciprocating-engine induction systems
—	Float-type carburettor	Investigation of icing characteristics of typical light-airplane engine induction systems
—	Pressure carburettor	A Preliminary investigation of the Icing Characteristic of a Large Rectangular-Throat Pressure-Type Carburetor
—	Pressure carburettor	An investigation of the icing and heated-air de-icing characteristics of the R-2600-13 induction system

Figure 57: comparison of the graphs relating to the following parameters: *Low Cruise Power* / Delimitations between the *Visible* and *No visible* zones
 Source: established by the BEA

We note that the limits provided vary significantly from one article to another. The narrowest zone is that provided for the float-type carburettor. This trend is therefore the reverse of that of the limit between the *Serious* and *Visible* zones described above.

The comparison concerning *High Cruise Power* and the limit between the *Serious* and *Visible* zones only concerns data from two articles: a set of data pertaining to a float-type carburettor and a set of data pertaining to a pressure carburettor. For this configuration, we note that the zones are completely different.

The comparison concerning *High Cruise Power* and the limit between the *Visible* and *No Visible* envelopes provides similar results, with a very significant difference depending on the configuration.



	Type of carburettor	Publication
—	Pressure carburettor	Laboratory investigation of icing in the carburetor and supercharger inlet elbow of an aircraft engine / II - Determination of the limiting-icing conditions Delimitation between <i>Serious</i> and <i>Visible</i>
—	Pressure carburettor	Laboratory investigation of icing in the carburetor and supercharger inlet elbow of an aircraft engine / II - Determination of the limiting-icing conditions Delimitation between <i>Visible</i> and <i>No Visible</i>
- -	Float-type carburettor	Investigation of icing characteristics of typical light-airplane engine induction systems Delimitation between <i>Serious</i> and <i>Visible</i>
- -	Float-type carburettor	Investigation of icing characteristics of typical light-airplane engine induction systems Delimitation between <i>Visible</i> and <i>No Visible</i>

Figure 58: comparison of the graphs relating to the following parameters: *High Cruise Power*
Source: established by the BEA

In terms of *Glide Power*, the data identified is taken from a single article, “Investigation of icing characteristics of typical light-airplane engine induction systems (02/1947)”. This data was already compared in para. 3.9.2. This comparison shows zones that are different, with the zone associated with *Serious* icing larger for the float-type carburettor than the pressure carburettor.

To conclude, the comparison of the various data from the scientific articles shows icing zones that vary greatly depending on the carburettor type, but also depending on the carburettor model for a given type (para. 3.9.2).

3.10.4. Comparison of the graph proposed by the EASA with those identified in the scientific articles

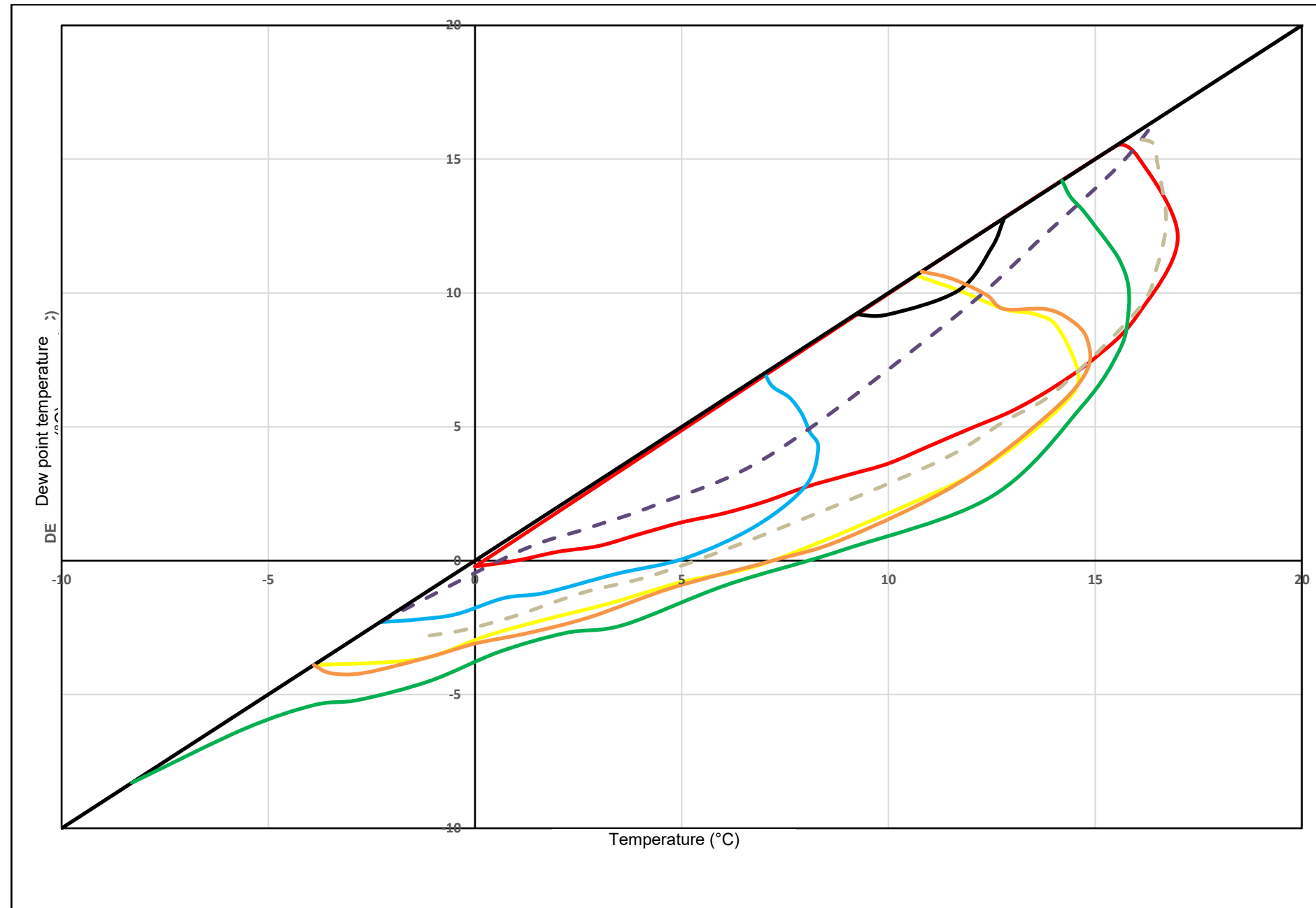
The previous chapters highlighted that the icing zones are identified based on different criteria in the scientific publications than in the authority graphs.

To compare the different graphs identified, the BEA proposes the equivalences indicated in the following table.

Envelope zone limits (simply defined by the BEA)	EASA	Scientific articles
1	Limit between the <i>Serious at any Power</i> zone and the <i>Moderate cruise/Serious descent</i> zone	Limit between the <i>Serious - Low Cruise Power</i> zone and the <i>Visible - Low Cruise Power</i> zone + Limit between the <i>Serious - High Cruise Power</i> zone and the <i>Visible - High Cruise Power</i> zone
2	Limit between the <i>Serious Glide Power</i> zone and the <i>Light Icing</i> zone	Upper limit of the <i>Serious - Glide Power</i> zone
3	Upper limit of the <i>Light Icing</i> zone	Limit between the <i>Visible - Low Cruise Power</i> zone and the <i>Non Visible - Low Cruise Power</i> zone + Limit between the <i>Visible - High Cruise Power</i> zone and the <i>Non Visible - High Cruise Power</i> zone

Identified limit 1:

- EASA: Limit between the Serious at any Power zone and the Moderate cruise/Serious descent zone
- Scientific articles: Limit between the Serious - Low Cruise Power zone and the Visible - Low Cruise Power zone + Limit between the Serious - High Cruise Power zone and the Visible - High Cruise Power zone



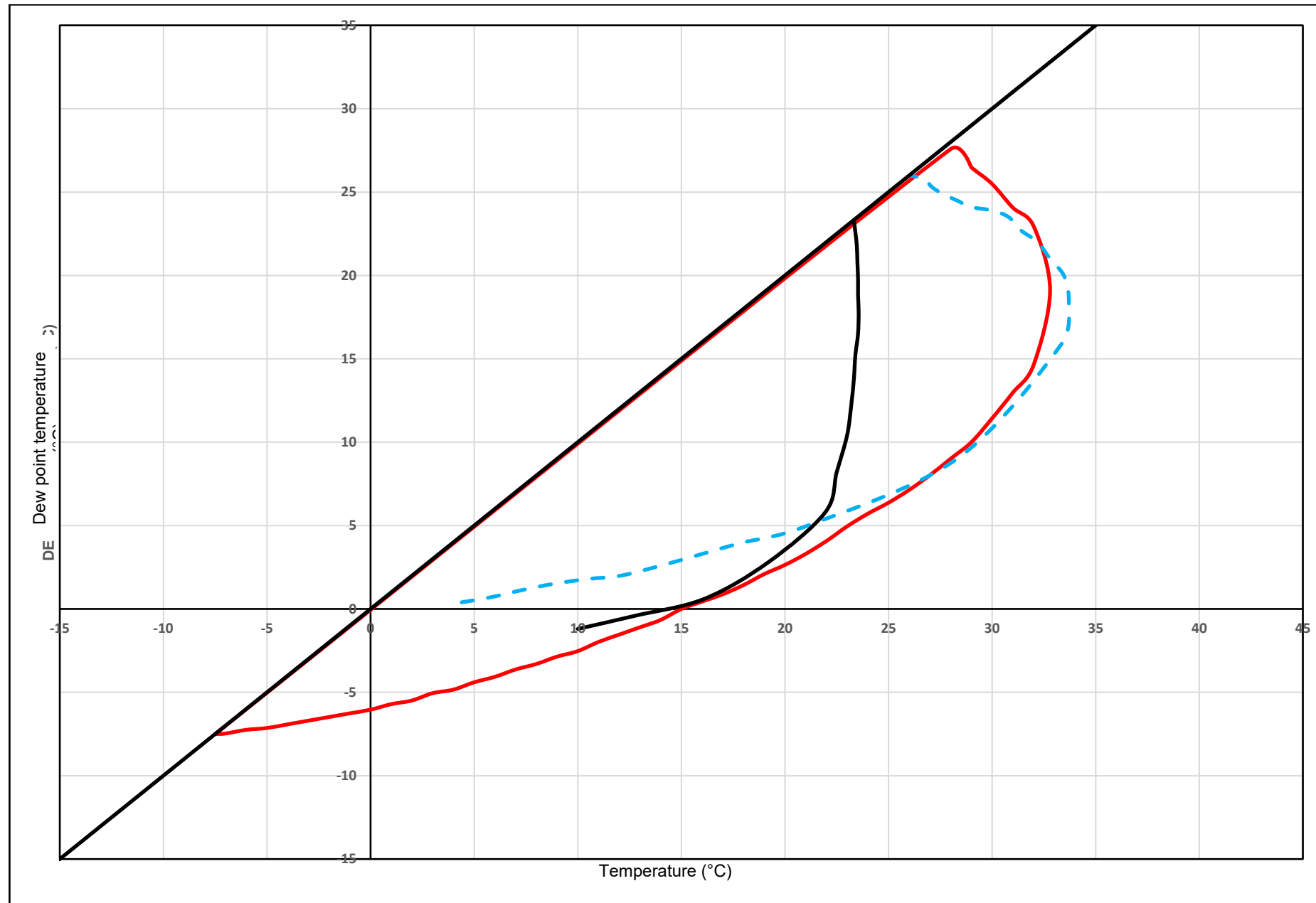
	EASA	Delimitation <i>Serious at any power / Moderate cruise/Serious descent</i>
	Pressure carburettor Investigation of icing characteristics of typical light-airplane engine induction systems	Limit between the Serious Low Cruise Power zone and the Visible Low Cruise Power zone
	Pressure carburettor Effects of Induction-System Icing on Aircraft-Engine Operating Characteristics	Limit between the Serious Low Cruise Power zone and the Visible Low Cruise Power zone
	Pressure carburettor Laboratory investigation of icing in the carburetor and supercharger inlet elbow of an aircraft engine / II - Determination of the limiting-icing conditions	Limit between the Serious Low Cruise Power zone and the Visible Low Cruise Power zone
	Pressure carburettor Laboratory investigation of icing in the carburetor and supercharger inlet elbow of an aircraft engine / II - Determination of the limiting-icing conditions	Limit between the Serious High Cruise Power zone and the Visible High Cruise Power zone
	Pressure carburettor Icing protection requirements for reciprocating-engine induction systems	Limit between the Serious Low Cruise Power zone and the Visible Low Cruise Power zone
	Float-type carburettor Investigation of icing characteristics of typical light-airplane engine induction systems	Limit between the Serious Low Cruise Power zone and the Visible Low Cruise Power zone
	Float-type carburettor Investigation of icing characteristics of typical light-airplane engine induction systems	Limit between the Serious High Cruise Power zone and the Visible High Cruise Power zone

Figure 59: comparison of the graphs for identified limit 1
Source: established by the BEA

Figure 59 shows that the graph proposed in the scientific articles, the closest to that proposed by the EASA, for temperatures higher than 10°C, is that associated with the float-type carburettor (which would appear coherent). The graphs differ for temperatures below 10°C.

Identified limit 2:

- EASA: Limit between the *Serious Glide Power* zone and the *Light Icing* zone
- Scientific articles: Upper limit of the *Serious - Glide Power* zone



—	EASA	Delimitation <i>Serious at any power / Moderate cruise/Serious descent</i>
—	Pressure carburettor Investigation of icing characteristics of typical light-airplane engine induction systems	Upper limit of the Serious Glide Power zone
- - -	Float-type carburettor Investigation of icing characteristics of typical light-airplane engine induction systems	Upper limit of the Serious Glide Power zone

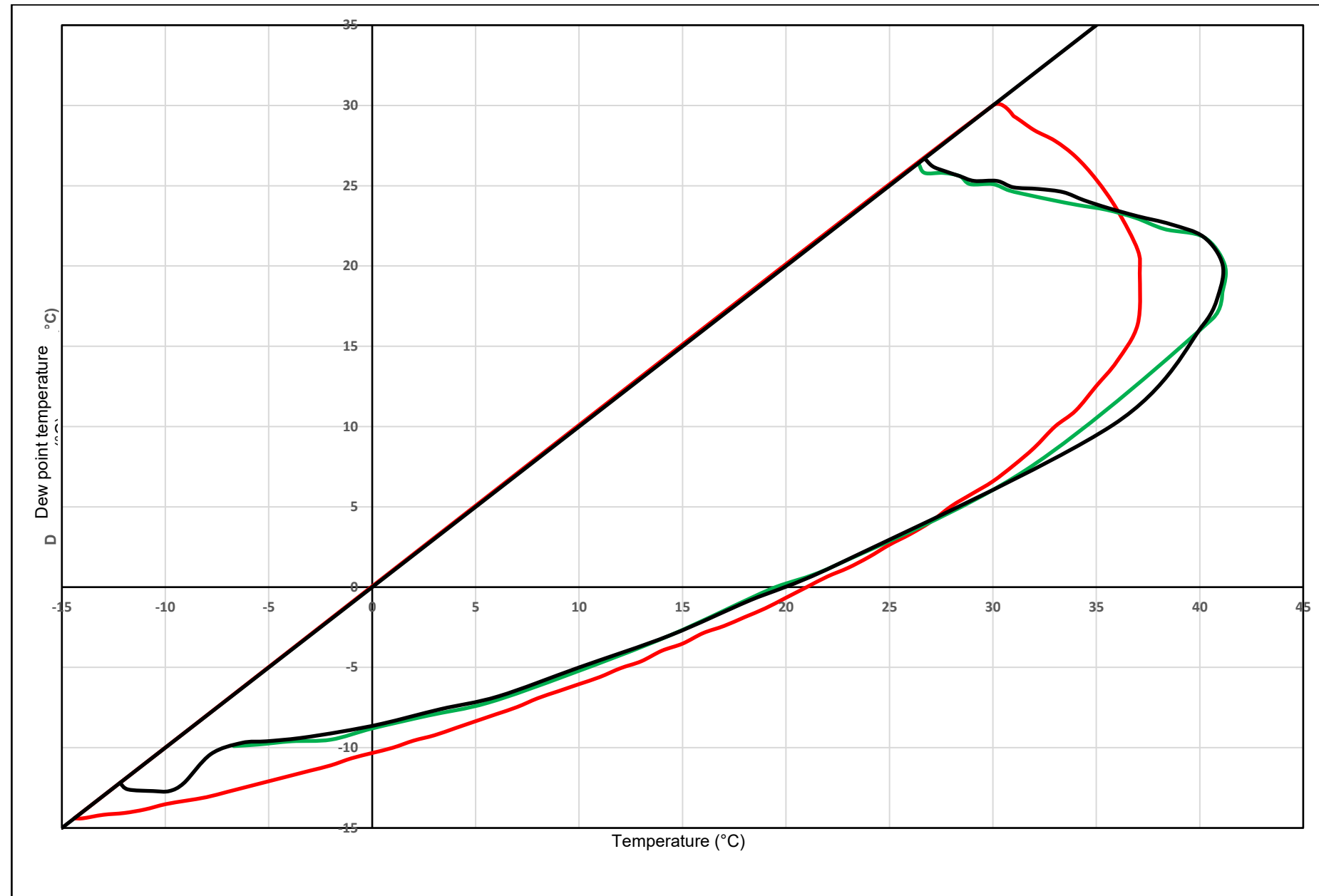
Figure 60: comparison of the graphs for identified limit 2
Source: established by the BEA

This illustration shows that the graph proposed in the scientific articles, the closest to that proposed by the EASA, for temperatures higher than 25°C, is that associated with the float-type carburettor. The graphs differ for temperatures below 25°C.

The other graph proposed in the scientific articles, corresponding to the icing zone in question, associated with a pressure carburettor, presents a completely different icing zone.

Identified limit 3:

- EASA: Upper limit of the *Light Icing* zone
- Scientific articles: Limit between the *Visible - Low Cruise Power* zone and the *No Visible - Low Cruise Power* zone + Limit between the *Visible - High Cruise Power* zone and the *No Visible - High Cruise Power* zone



—	EASA	Upper limit of the <i>Light Icing</i> zone
—	Pressure carburettor Low Cruise Power - Effects of Induction- System Icing on Aircraft- Engine Operating Characteristics	Limit between the <i>Visible</i> and <i>No Visible</i> zones
—	Pressure carburettor Low Cruise Power - Laboratory investigation of icing in the carburetor and supercharger inlet elbow of an aircraft engine / II - Determination of the limiting-icing conditions	Limit between the <i>Visible</i> and <i>No Visible</i> zones

Figure 61: comparison of the graphs for identified limit 3
Source: established by the BEA

The two graphs identified in the scientific articles differ significantly from the EASA graph with regards to temperatures higher than 30°C. The graphs are fairly similar for the remainder of the envelope.

3.11. Overview of the bibliographic research

Four graphs published by the aeronautical authorities are available to define the probability of icing and its severity, depending on the air temperature and the dew point temperature. They are all different. The bibliographic research did not enable the BEA to identify the data used to compile these graphs.

Older graphs, essentially taken from scientific studies conducted in the United States between 1945 and 1950, were identified and analysed. Most of these studies were conducted on pressure carburettors that differ greatly from the float-type carburettors equipping modern engines. These graphs are different from those proposed by the authorities. In addition, these studies were conducted for the most part in a laboratory, on carburettors separated from the propulsion system. The influence of the powerplant was not therefore taken into consideration.

The four graphs proposed by the authorities have the same philosophy and the same objective:

- they should be considered as a very broad envelope intended to incorporate all existing powerplants;
- the objective is to make pilots aware of the phenomenon of induction icing.

In these conditions, it is therefore reasonable not to use these graphs as investigative tools.

No other authority publication likely to provide information of investigative relevance was identified.

Certification requirements essentially focus on the heat system, defining minimal temperature increases for defined conditions. It is moreover important to note that the specified temperature is low (-1°C for the EASA).

Moreover, the reading of a number of investigation reports published in a number of countries would seem to suggest that induction system icing is considered and taken into account in a similar way. The analysis was based essentially on weather conditions and on one of the four available graphs. The specific nature of powerplants does not seem to have been a consideration.

The phenomenon is well cited by aircraft manufacturers and engine manufacturers. However, the available data do not seem sufficient to conduct a reasoned and constructed analysis.

To conclude, there is very little information available to investigators to analyse the phenomenon of induction system icing. In the very few cases studied by the BEA⁵ in which aircraft are equipped with data recording devices, this analysis is clearly facilitated and conclusive.

The scientific articles studied enable the following characteristics to be defined regarding the phenomenon of icing:

- icing was mostly observed at relatively low temperatures and very high relative humidity;
- fuel type seems to be a key factor: the more volatile the fuel, the more prone to icing the induction system;
- the temperature of the carburettor body also seems to be a dominant factor in icing;
- the most recent American study (published in 2015) seems to indicate that the phenomenon is slow to start and to spread.

⁵ The ATSB (Australia) has informed the BEA that the number of aircraft equipped with engine data recording devices, according to them, is significant and increasing. This observation is not shared by the BEA to date.

4 - POWERPLANT ICING TESTS

4.1. Test centre

This test campaign was carried out in partnership with DGA Essais propulseurs (DGA EP), which is an organisation of the French Defence Procurement Agency, attached to the Ministry of Defence.

DGA EP operates several test stands including the small icing ring stand dedicated to the testing of small items of equipment in icing conditions (e.g. probes, vanes, blade fragments, etc.). This stand has the following configuration (Figure 62) and the capacities specified in the table below (Figure 63).

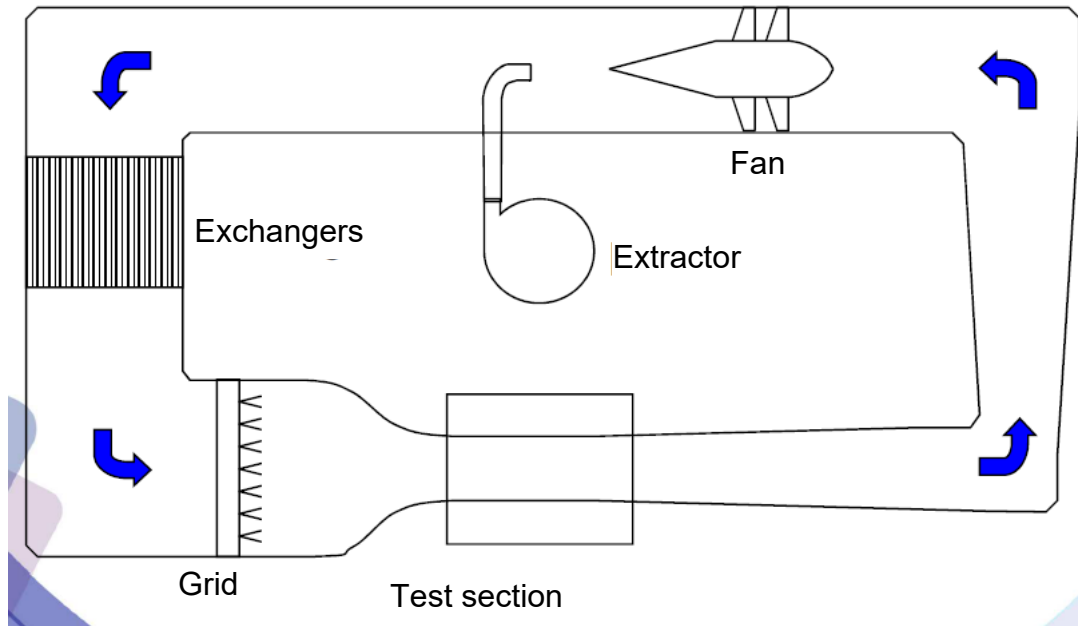


Figure 62: schematic diagram of the small icing ring test stand
Source: DGA EP

Mach envelope	Altitude	Temperature envelopes	LWC (<i>Liquid Water Content</i>)
0.1 - 0.3 0.2 - 0.6	Sea level	-35°C - 0 -40°C - 0	0.1 - 3 g.m ³ 0.15 - 3 g.m ³
MVD (<i>Median Volumetric Diameter</i>)	Intake section of the test section	Maximum air flow	
15 - 50 μm	0.2 x 0.5 m 0.2 x 0.2 m	14 kg.s ⁻¹	

Figure 63: capacities of the small icing ring test stand
Source: DGA EP

4.2. Test objectives

These tests are carried out to:

- explore the icing envelope of the graph proposed by the EASA in order to observe whether ice forms as well as the severity of any icing for the powerplant considered;
- simulate the conditions described in investigation reports for which induction system icing was confirmed;
- record engine parameters when icing occurs;
- film this phenomenon.

These tests aim at better understanding the icing phenomenon that may occur on an induction system and at attempting to define dominant factors in the initiation of this phenomenon.

4.3. Feasibility study

4.3.1. Phase one of the feasibility study

Phase one of the feasibility study consisted in defining:

- the specimen to be tested;
- the test points;
- the test setup to guarantee the completion and representativeness of the tests.

For the specimen to be tested, three work hypotheses were defined:

- a setup solely comprising a carburettor, as in the laboratory tests conducted as part of the NACA's study programme in the 1940s;
- an engine equipped with a carburettor and associated with a brake;
- a complete powerplant comprising the engine, the propeller and the aeroplane cowlings.

The first hypothesis was not selected despite being technically simpler. It is important to consider the engine environment and its consequences on the carburettor.

The second hypothesis was ruled out due to the unavailability of a brake.

The third hypothesis was therefore selected. It seemed to be the most coherent in ensuring the tests were sufficiently representative and in taking into account interactions that may occur on the aeroplane.

The test setup corresponded to the powerplant of the Socata TB10 (Figure 64 and Figure 65), with the exception of the propeller. The latter was replaced with a propeller specific to the test stand testing and is recognised by its four blades (two more than on the propeller installed on the aeroplane) and its reduced diameter (Figure 66).



Figure 64: ENAC TB10
Source: <https://www.flickr.com/photos/mduthet/43218769375>



Figure 65: TB10 propulsion system
Source: <https://www.aerobuzz.fr/breves-aviation-generale/le-silencieux-chabord-certifie-sur/>



Figure 66: specific propeller used during the tests
Source: BEA

The Socata TB10 is equipped with a Lycoming O-360-A1AD four cylinder, direct drive, horizontally opposed and air-cooled engine (Figure 67). This version of the engine delivers the maximum power of 180 hp at a speed of 2,700 rpm.



Figure 67: general view of a Lycoming O-360 engine
Source: <https://ww2.txtav.com/Parts/PartSearch/PartsDetail/O360A1AD-8089-N>

The main characteristics of this engine are as follows:

Cylinder capacity	5.916 litres
Dry weight	288 lbs, i.e. 130.6 kg
Dimensions	Length = 31.33 in (i.e. 79.6 cm), Width = 33.37 in (i.e. 84.8 cm), Height = 24.59 in (i.e. 62.5 cm)
Fuel	AVGAS 100LL
Compression ratio	8 : 5 : 1
Direction of rotation	clockwise
Maximum rotation speed	2,700 rpm

The powerplant installed included a very restricted section of the aeroplane's fuel system as illustrated in the diagram below. The remainder of the system will be that of the test stand.

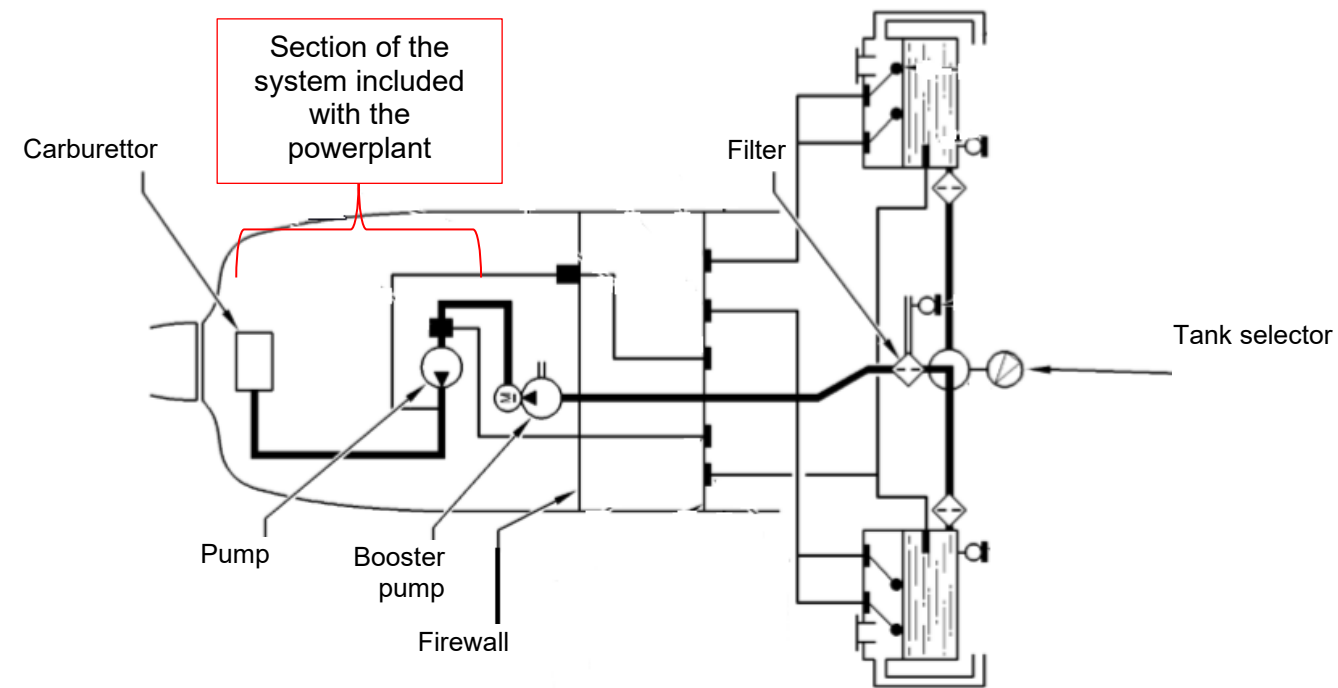


Figure 68: schematic diagram of the TB10 fuel system

Fuel system

Fuel pressure:

- maximum: 8 PSI;
- minimum: 0.5 PSI;
- Expected by the manufacturer: 3 PSI.

The engine is equipped with the Marvel-Schebler MA4-5 carburettor. This carburettor and its operation are described in chapter 3.2.

Lubrication system

Grade of oil used in the ambient temperature range 30-90°F (i.e. -1 to 32°C): SAE 40

Optimum quantity of oil: 8 US quarts (i.e. 7.57 litres)

Minimum quantity of oil: 2 US quarts (i.e. 1.89 litres)

Oil temperature for an outside air temperature of between -1 and 32°C:

- Expected by the manufacturer = 82°C;
- maximum = 118°C.

Specified maximum oil consumption:

- maximum speed = 0.76 litres/hour;
- 75% = 0.43 litres/hour;
- 65% = 0.37 litres/hour;

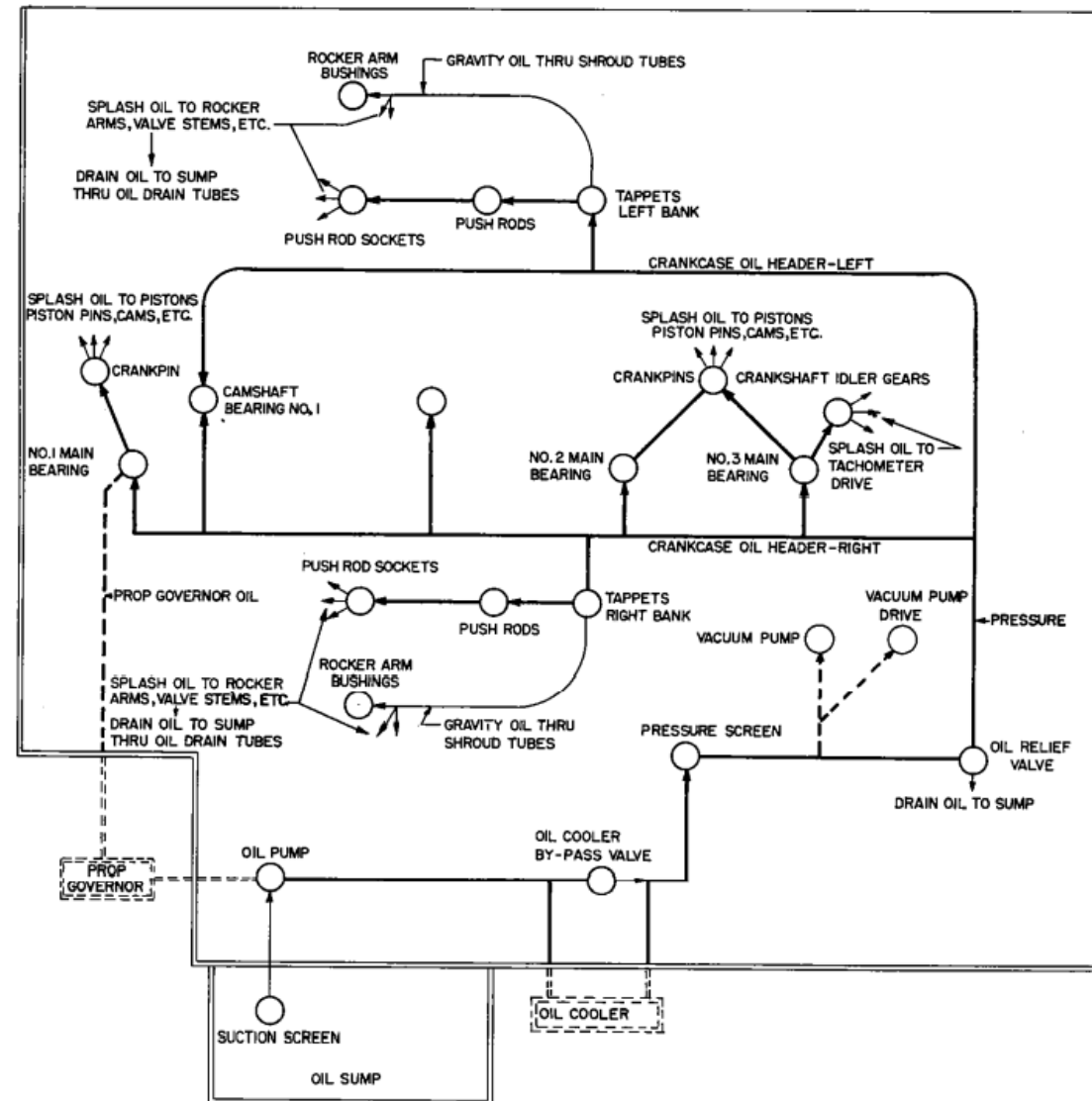


Figure 69: schematic diagram of the lubrication system
 Source: Lycoming - Overhaul Manual 6th edition December 1974

Ignition system

The engine ignition system comprises a double magneto installed on the engine accessory section, harnesses, and two spark plugs per cylinder.

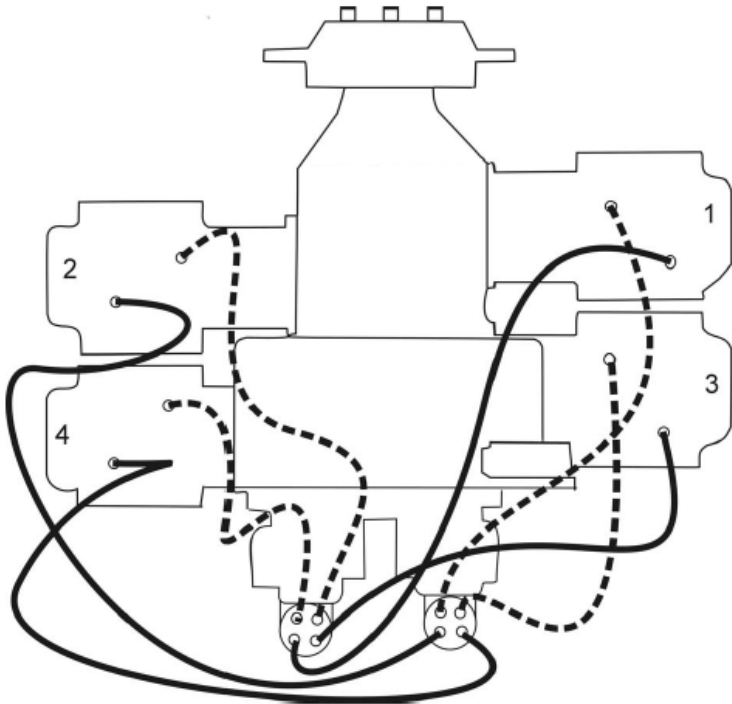


Figure 70: schematic diagram of the ignition system
Source: Lycoming - Operator Manual 8th edition October 2005

Ignition sequence: cylinder 1, cylinder 3, cylinder 2 then cylinder 4

Ignition advance: 25°

4.3.2. Phase two of the feasibility study

Phase two consists in conducting digital simulations in order to identify the type of test section that guarantees the establishment of the identified test points.

The test section of the DGA EP's small icing ring stand was initially designed to test very small items of equipment. The use of this stand to conduct tests on the powerplant of the Socata TB10 thus requires the complete reworking of the test section. Before modifying the test section, the configuration must be defined. The digital simulation tool is essential for this.

4.3.2.1 - Presentation of the simulation tool

Stage one of the simulation consists in obtaining a geometric model of the powerplant used for these tests that is as accurate as possible.

To obtain this model, the propeller and the cowlings were scanned in three dimensions. The files were then processed using the Catia software to produce the following model. We note the position of the air intake ensuring the supply of the carburettor on the LH side of the cowlings (Figure 71).



Source: <http://www.pictaero.com/fr/pictures/picture,255000>

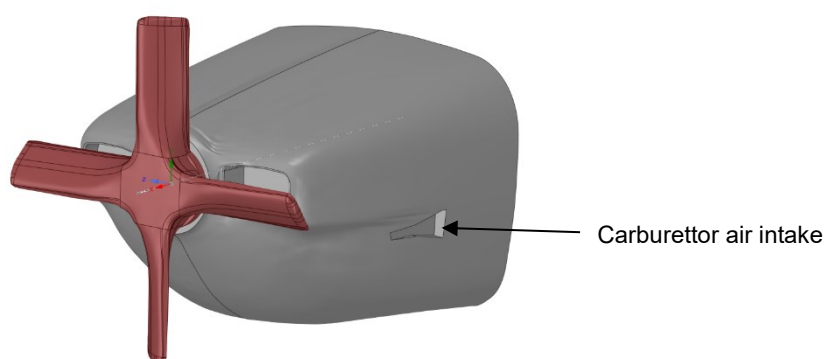


Figure 71: model obtained after scanning the propeller and the cowlings

Source: DGA EP

The simulations were carried out using the Ansys Fluent software, version 19-2.

The simulation conditions were as follows:

- Resolution model:

The aim is to model the flow of a Newtonian fluid (viscosity independent of the stress applied) and associated transportation phenomena. Newtonian fluid movements are described using Navier-Stokes equations.

In terms of the modelling, ANSYS FLUENT will therefore approximately solve the continuity and momentum continuity equations. For flows involving a transfer of heat, a supplementary energy continuity equation is solved.

Continuity equation:

$$\frac{\partial \rho}{\partial t} + \nabla \cdot (\rho \vec{v}) = S_m$$

ρ is the mass density of the fluid

∇ is the divergence operator

\vec{v} is the speed

S_m is the mass added to the continuous phase after the second dispersed phase (e.g. due to the vaporization of liquid droplets) and from all sources defined by the user

Momentum continuity equation:

$$\frac{\partial}{\partial t} (\rho \vec{v}) + \nabla \cdot (\rho \vec{v} \vec{v}) = -\nabla p + \nabla \cdot (\bar{\tau}) + \rho \vec{g} + \vec{F}$$

p is the static pressure

$\bar{\tau}$ is the stress tensor such that: $\bar{\tau} = \mu \left[(\nabla \vec{v} + \nabla \vec{v}^T) - \frac{2}{3} \nabla \cdot \vec{v} I \right]$ where

μ is the molecular viscosity

I is the unit tensor

$\rho \vec{g}$ is the gravitational force

\vec{F} are the external forces

Energy continuity equation:

$$\frac{\partial}{\partial t} (\rho E) + \nabla \cdot (\vec{v} (\rho E + p)) = -\nabla \cdot \left(\sum_j h_j J_j \right) + S_h$$

E designates the total energy per unit of mass such that $E = h - \frac{p}{\rho} + \frac{v^2}{2}$

S_h comprises the heat of the chemical reaction and any other source of volumetric heat defined

h_j is the enthalpy of the species j

Within the context of the simulations carried out, a RANS (*Reynolds-averaged Navier–Stokes*) approach was adopted. The Reynolds-averaged Navier-Stokes equation can be used to simplify the problem by eliminating short amplitude and period fluctuations. The resolution uses averaged measurements. The RANS method requires few resources.

- Turbulence model:

This turbulence model involves two transport equations:

- one for turbulent kinetic energy k ;
- one for the specific dissipation rate ω .

This model provides an optimum prediction in transitional areas (e.g. along walls).

The two transport equations are as follows:

$$\frac{\partial}{\partial t}(\rho k) + \frac{\partial}{\partial x_i}(\rho k u_i) = \frac{\partial}{\partial x_j} \left(\Gamma_k \frac{\partial k}{\partial x_j} \right) + G_k - Y_k + S_k$$

and

$$\frac{\partial}{\partial t}(\rho \omega) + \frac{\partial}{\partial x_i}(\rho \omega u_i) = \frac{\partial}{\partial x_j} \left(\Gamma_\omega \frac{\partial \omega}{\partial x_j} \right) + G_\omega - Y_\omega + S_\omega$$

In these equations, G_k represents the generation of turbulence kinetic energy due to mean velocity gradients. G_ω represents the generation of ω . Γ_k and Γ_ω represent the effective diffusivity of k and ω , respectively. Y_k and Y_ω represent the dissipation of k and ω due to turbulence. All of the above terms are calculated as described below. S_k and S_ω are user-defined source terms.

- Modeling the turbulent viscosity:

The proper transport behavior can be obtained by a limiter to the formulation of the eddy-viscosity:

$$\mu_t = \frac{\rho k}{\omega} \frac{1}{\max \left[\frac{1}{\alpha}, \frac{SF_2}{a_1 \omega} \right]}$$

S is the strain rate magnitude

F_2 is given by:

$$F_2 = \tanh \left(\Phi_2^2 \right)$$

$$\Phi_2 = \max \left[2 \frac{\sqrt{k}}{0.09 \omega y}, \frac{500 \mu}{\rho y^2 \omega} \right]$$

y is the distance to the next surface

- Wall boundary conditions:

The wall boundary conditions for the k equation in the k - ω models are treated in the same way as the k equation is treated when enhanced wall treatments are used with the k - ϵ models. This means that all boundary conditions for wall-function meshes will correspond to the wall function approach, while for the fine meshes, the appropriate low-Reynolds number boundary conditions will be applied.

In ANSYS Fluent the value of ω at the wall is specified as

$$\omega_w = \frac{\rho(u^*)^2}{\mu} \omega^+$$

Analytical solutions can be given for both the laminar sublayer

$$\omega^+ = \frac{6}{\beta_l (y^+)^2}$$

and the logarithmic region:

$$\omega^+ = \frac{1}{\sqrt{\beta_\infty}} \frac{du_{turb}^+}{dy^+}$$

Therefore, a wall treatment can be defined for the ω -equation, which switches automatically from the viscous sublayer formulation to the wall function, depending on the grid. This blending has been optimized using Couette flow in order to achieve a grid independent solution of the skin friction value and wall heat transfer. This improved blending is the default behavior for near-wall treatment.

- Fluid-related hypotheses:

Taking into consideration the test conditions selected, air is considered to be compressible.

Air is considered to be an ideal gas.

The ideal gas model is based on the hypothesis that molecular gas interactions can be negligible, with the exception of molecule collisions. Kinetic molecular theory is therefore used to explain the macroscopic behaviour of gases based on mechanical and statistical considerations of the movements of its molecules.

The fundamental hypothesis of ideal gases is that their internal energy (as well as their enthalpy) is independent of the pressure.

The equation of state for an ideal gas can be written:

$$P \cdot v = r \cdot T \text{ avec } r = \frac{R}{M} \text{ (exprimé en } kJ \cdot kg^{-1} \cdot K^{-1})$$

R being the universal constant such that $R = 8,314 \text{ kJ} \cdot kmol^{-1} \cdot K^{-1}$

M being the molar mass of the gas expressed in $kg \cdot kmol^{-1}$

Depending on the units used, the previous equation takes different forms:

- in units of mass: $P \cdot v = r \cdot T$
- in molar units: $P \cdot v_{mol} = R \cdot T$

In relation to the total volume V occupied by the fluid, where n is the number of kilomoles:

- in units of mass: $P \cdot V = m \cdot r \cdot T$
- in molar units: $P \cdot V = n \cdot R \cdot T$

Given that the internal energy and enthalpy of an ideal gas only depends on its temperature, and that $r = cp - cv$

This gives:

- $cv = \frac{du}{dT}$ expressed in $J \cdot kg^{-1} \cdot K^{-1}$
- $cp = \frac{dh}{dT}$ expressed in $J \cdot kg^{-1} \cdot K^{-1}$

The viscosity of the gas is calculated based on Sutherland's Law, which is based on an specific interatomic potential introduced by William Sutherland. Viscosity is defined as per the following formula:

$$\eta(T) \approx \eta(T_{ref}) \left(\frac{T}{T_{ref}} \right)^{\frac{3}{2}} \frac{T_{ref} + S}{T + S}$$

T_{ref} is the reference temperature, i.e. 273.11 K

S is an approximate numerical constant factor, i.e. 110.56 K

$$\eta(T_{ref}) = 1,716 \cdot 10^{-5} \text{ Pa} \cdot \text{s}$$

- Modelling method:

The selected modelling method is the *Multiple Reference Frames* (MRF), method, referred to more commonly as the frozen rotor modelling method.

When the problem involves moving parts (e.g. rotary blades, wheel, propeller, etc.), the problem is rendered unstable in the conventional fixed reference. The aim is therefore to use a moving reference to stabilise the problem. When a moving reference is activated, the momentum equations are modified to incorporate the supplementary acceleration terms produced by the transformation of the fixed reference into the moving reference. By solving these equations in a stable way, flows around moving parts can be modelled.

When the envelope contains both fixed and moving parts, the MRF method consists in dividing this envelope into several zones. This approach does not take into account the relative momentum of a moving zone in relation to adjacent zones (which may be moving or stationary), the chain remains fixed for the calculation. This is the same as the freezing of the moving section in a specific position and as the observation of the instant flow field with the moving part in this position.

This MRF approach is therefore an approximation, which generally provides a rational flow model for applications in which there is relatively little interaction between the moving section and the fixed section.

The interface between the chain of the moving section and of the fixed section is consistent, and there is no need for interpolation between the two fluid envelopes.

In terms of the processing of quantities at the interface, scalar quantities such as the pressure or the temperature do not need to be processed. In terms of speed, the momentum continuity equations for the moving zone are formulated with the absolute speeds. The interface does not therefore need to be processed as the speed components are all expressed in relation to the fixed reference.

Within the context of the powerplant selected, two zones were identified:

- a zone including the propeller, corresponding to the moving section;
- a zone including the rest of the environment, corresponding to the fixed section.

The simulations were systematically conducted considering a number of propeller positions to determine the influence of this parameter.

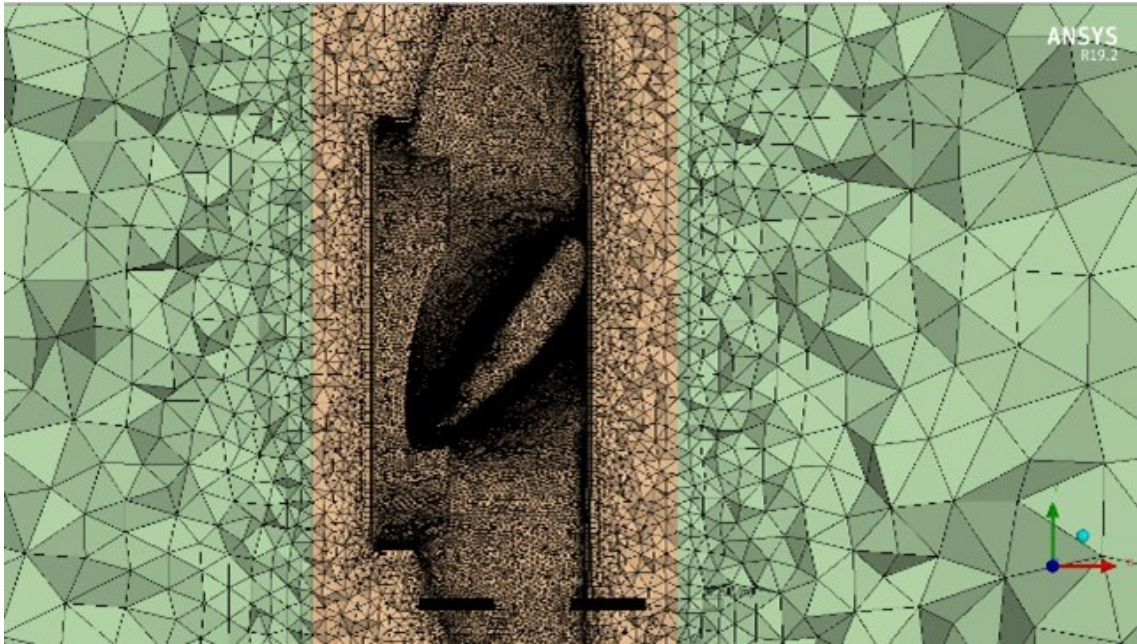
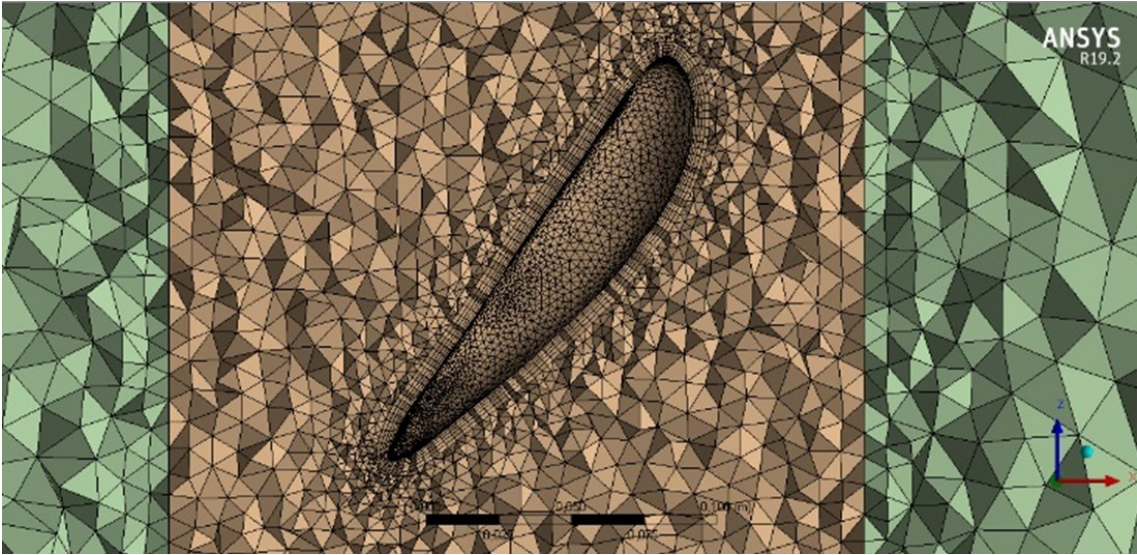
- Mesh:

The meshes having an orthogonality lower than 0.15 or an inclination higher than 0.94, are meshes of bad quality, they involve a more difficult convergence of calculation. The table below summarizes the statistics of the meshes used in the case of the propeller, the free field and the test section (§ 4.3.2.3). The meshes are different between the three test section configurations. However, the dimensioning parameters are identical, and consequently the mesh qualities are very close between the different configurations.

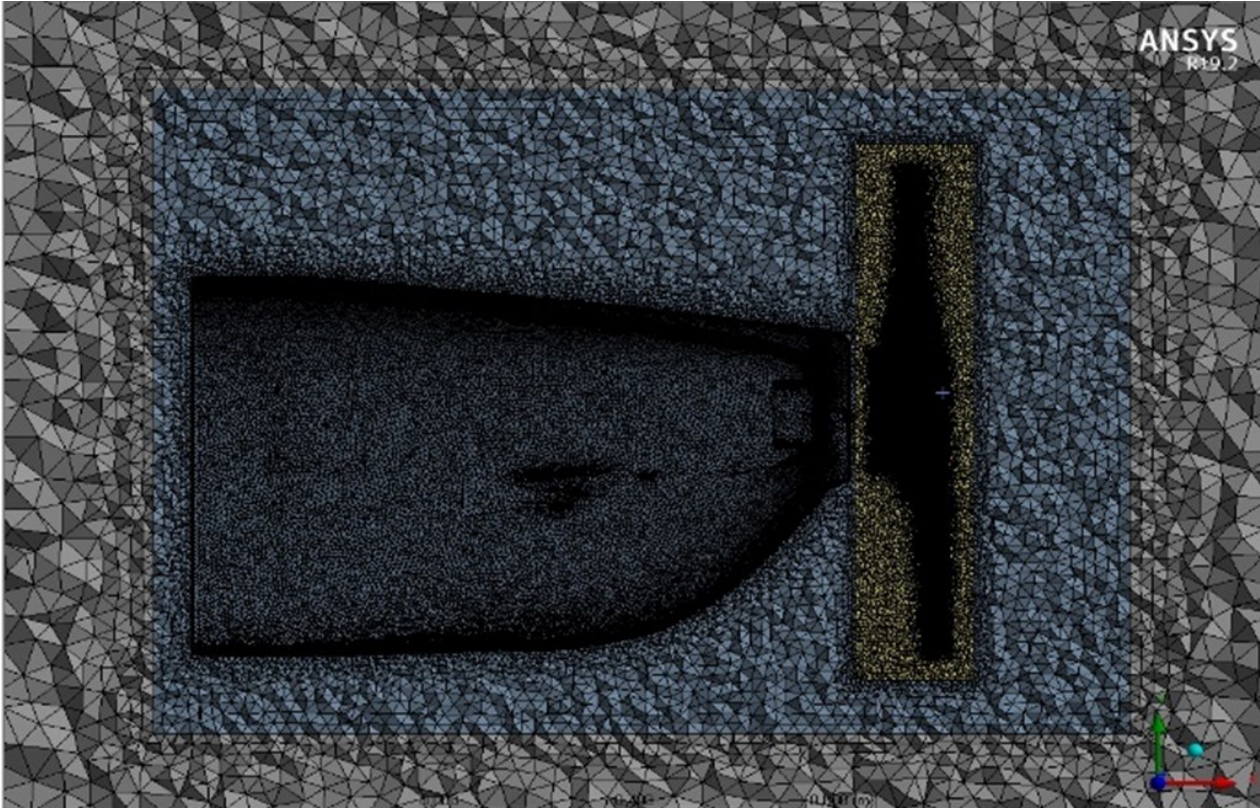
	Propeller	Free field	Test section – Configuration 2 (§ 4.3.2.3)
Number of meshes	8,6 M	12,7 M	29 M
Minimal orthogonality	0,15	0,109	0,102
Maximum orthogonality	0,999	0,999	1
Number of meshes ortho<0.15	0	17	17
Minimal inclination	9,8 e-11	9 e-11	1 e-10
Maximum inclination	0,8499	0,891	0,898
Number of meshes incli >0.94	0	0	0

The mesh must be constructed in such a way that it has enough meshes to guarantee the physics of the problem. But it is necessary to avoid having more than 30 million meshes because that lengthens the times of calculations and as well as the post-processing.

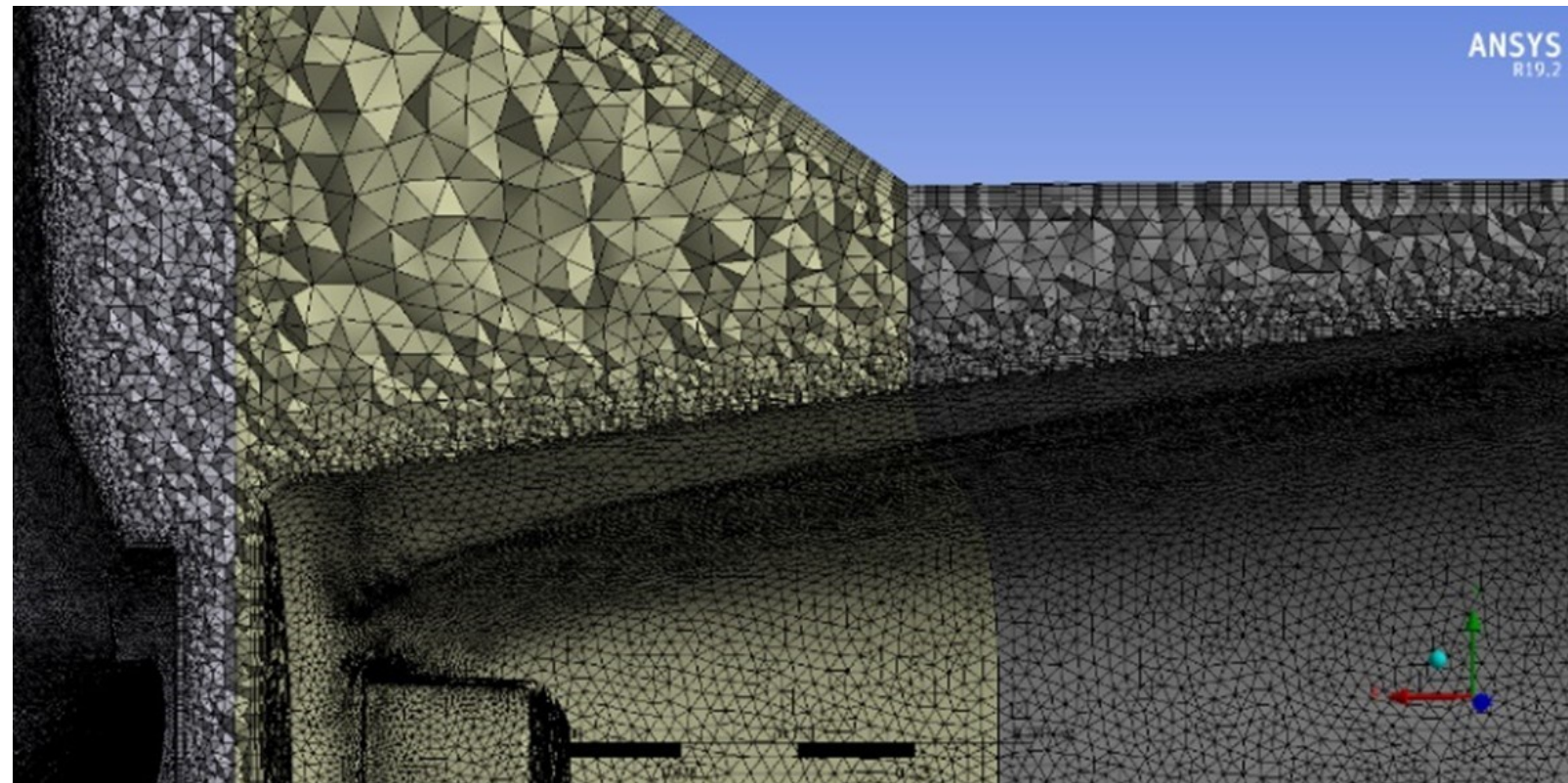
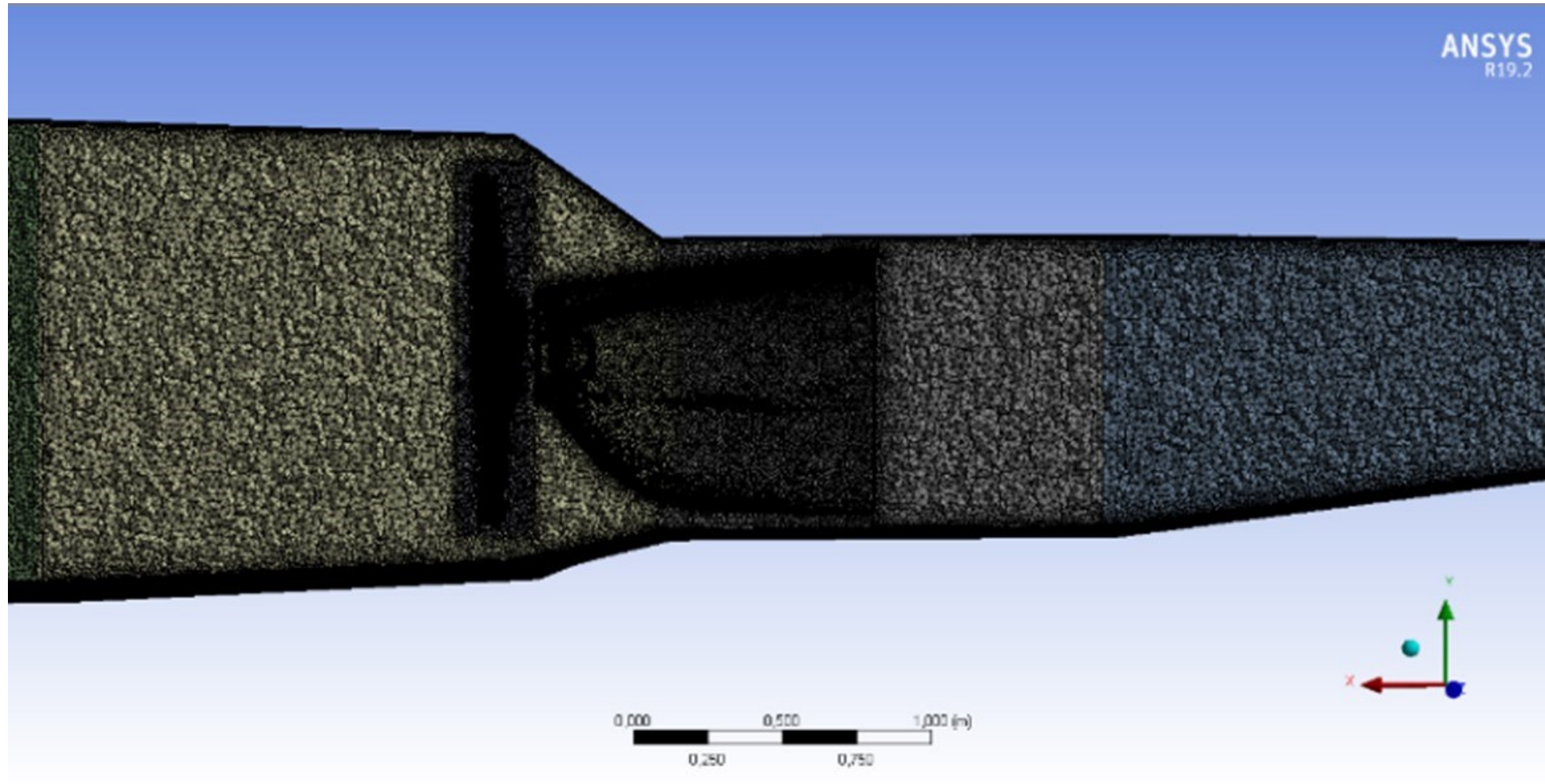
The meshes having an upper inclination of 0.94 or a lower orthogonality of 0.15 are few (about ten) and located on the engine cover, at the level of geometry defects linked to the 3D reconstruction of the cover from the scan, this number of meshes is low enough to continue the simulations with these meshes. The poor quality meshes being few in number, they will not influence the results of the simulations.



Propeller mesh



“Engine + Propeller” mesh

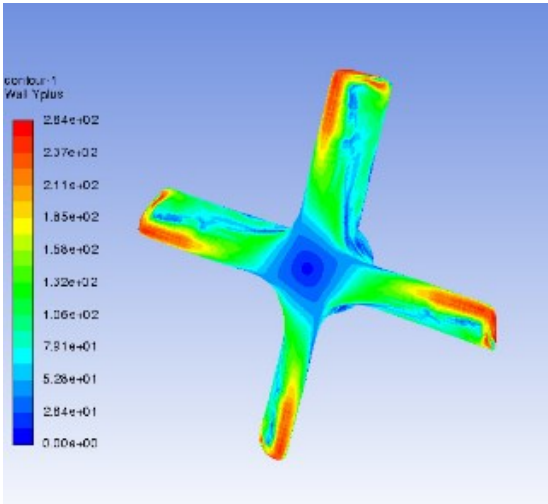
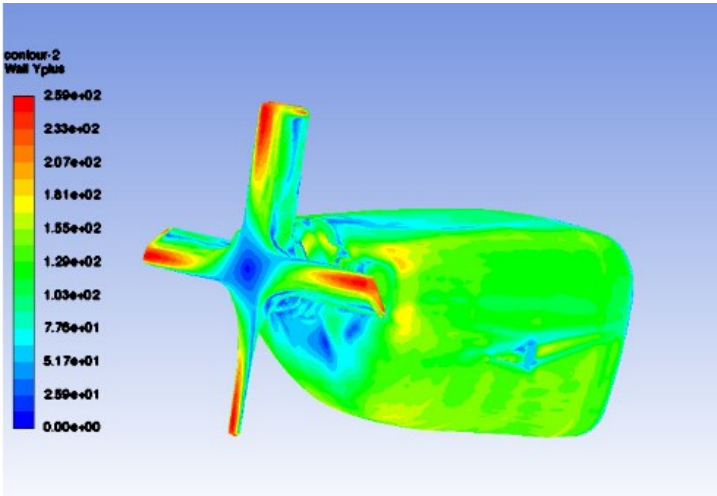


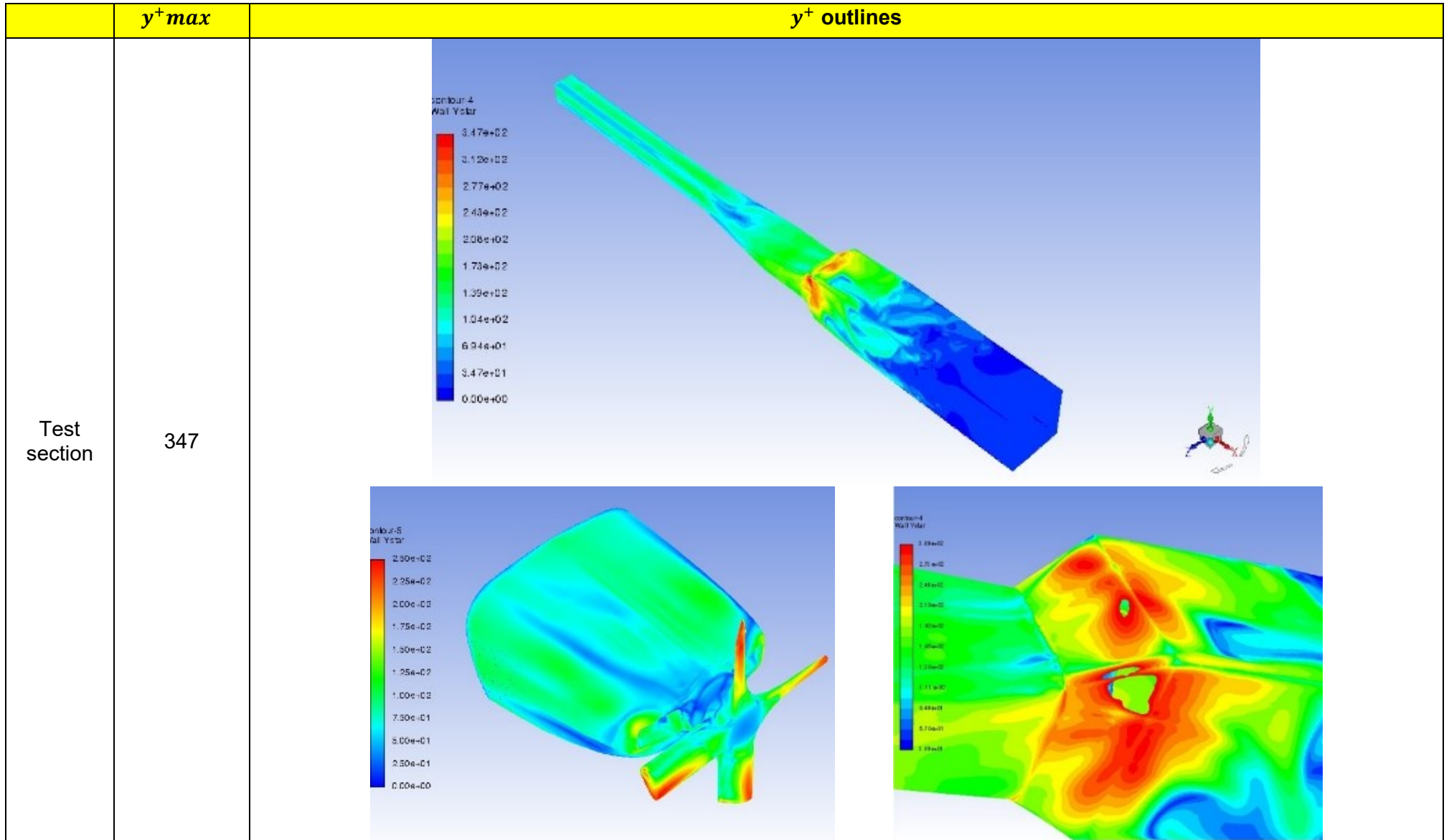
Test section mesh

A y^+ between 30 and 300 is necessary to consider that the boundary layer is modeled correctly. It is the choice of the height of the first mesh δ_y and the calculation of the friction speed which makes it possible to calculate y^+ . The choice of the heights of the first meshes was made in such a way as to best respect this range of y^+ . This is not necessarily easy because when you have a rotating propeller, the speed varies along the blade (from 0 to ωR and therefore the y^+ also varies). For the propeller we fix $\delta_y = 0.75$ mm, for the cowl $\delta_y = 1.2$ mm and for the walls of the test section $\delta_y = 2$ mm. In all cases, the number of boundary layer thicknesses was set to 5 with a growth rate of 1.2.

For the propeller, the most important thing is to respect the y^+ at the level of the intrados and the extrados of the propeller. At the level of the hub the speeds are close to $V=0$ m/s, consequently we have in this zone $y^+ < 30$, we cannot do otherwise. The table below summarizes the y^+ calculated in the case of the propeller alone, the free field and the test section.

The y^+ for the propeller alone and for the motor in free field are less than 300. On the other hand, for the case of the vein, there are small zones located in the corners of the convergent B where y^+ exceeds 300, the maximum value of y^+ is 347. Physically, this is due to the fact that a good part of the flow passing through the end of the blades of the propeller is accelerated and sent towards the walls of the convergent B. By decreasing the value of size of first mesh at the level of the corners of the convergent B of the vein one can make return the maximum y^+ below of 300, this was not done for reasons of time, it was estimated that this overshoot of the y^+ is not critical for the resolution of the flow.

	y^+_{max}	y^+ outlines
Propeller	262	
Free field	259	



- Hypotheses relating to the powerplant:

The air passing through the two air intakes located immediately behind the propeller plane was not modelled. The heating caused by the engine under the cowlings was also not modelled. In these conditions, the environment around the carburettor was not modelled.

The carburettor suction was modelled by a flow condition defined in the paragraph below.

- Selected test conditions:

The atmospheric pressure considered was 101.325 Pa.

The following test point was selected, the associated conditions were deemed to be conservative in relation to the other identified test points:

- air temperature = 273 K (i.e. 0°C);
- engine speed = 2,600 rpm, considered to be constant;
- airspeed upstream of the powerplant = $54 \text{ m} \cdot \text{s}^{-1}$

The air flow taken in by the engine, and therefore circulating in the carburettor stream, was calculated as a function of the engine speed selected and of the characteristics of the engine:

- Taking the engine cylinder capacity (5.916 litres), and considering that this volume enters the intake in every 2 revolutions, the corresponding air flow can be defined as:

$$Q_{v_{air}} = \frac{\text{Cylindrée}}{2} \cdot \text{Régime moteur} = \frac{5,916}{2} \cdot 2600 = 7690,8 \text{ L} \cdot \text{min}^{-1}, \text{ i.e. } 7.69 \text{ m}^3 \cdot \text{min}^{-1}$$

- Taking the mass density of the air equal to $\rho_{air} = 1.2 \text{ kg} \cdot \text{m}^{-3}$, we can define the mass flow of the intake air such that:

$$Q_{m_{air}} = Q_{v_{air}} \cdot \frac{\rho_{air}}{60} = 7,69 \cdot \frac{1,2}{60} = 0,15 \text{ kg} \cdot \text{s}^{-1}$$

It is important to note that this mass of intake air is calculated taking into consideration the cylinder fill rate of 100%, which is purely theoretical.

4.3.2.2 - Initial open field simulation

This purely theoretical simulation is required to obtain a reference and have therefore a critical impact on the results of simulations considering various types of test section.

To perform this simulation, the powerplant was placed in a cylinder of the following dimensions:

- diameter = 20 m;
- height = 20 m.

These dimensions significantly limit the edge effects, which are considered to be negligible.

The fixed limit condition is as follows:

- upstream airspeed = $54 \text{ m} \cdot \text{s}^{-1}$

In this configuration, we note that:

- the temperature and pressure conditions (Figure 75 and Figure 76), downstream of the propeller, along the length of the cowlings, was not at all or only very slightly influenced by the propeller;
- no recirculation was identified;
- the streamlines passing through the air intake ensuring supply of the carburettor are straight (Figure 73).

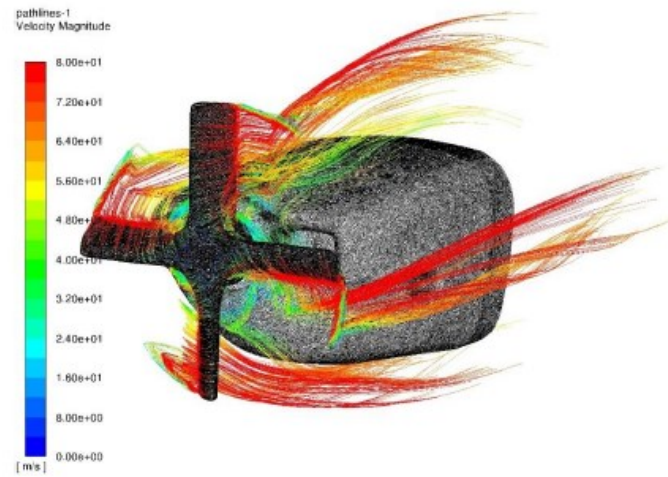


Figure 72: streamlines passing through the propeller

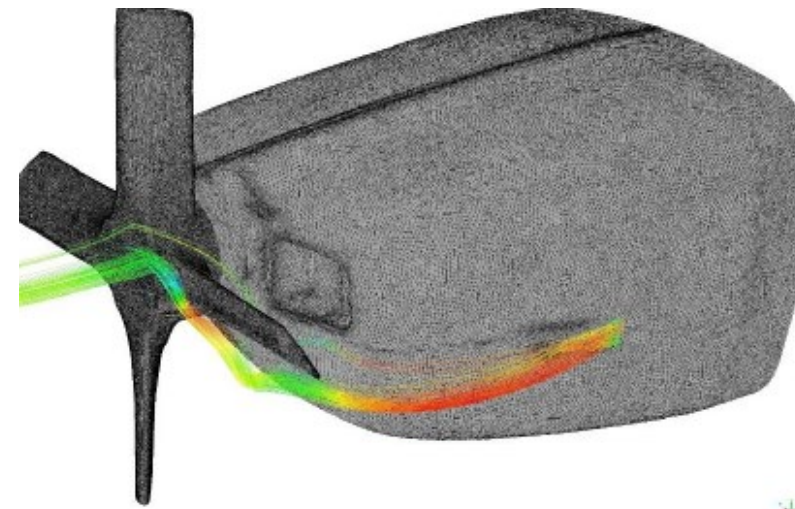


Figure 73: streamlines passing through the air intake supplying the carburettor

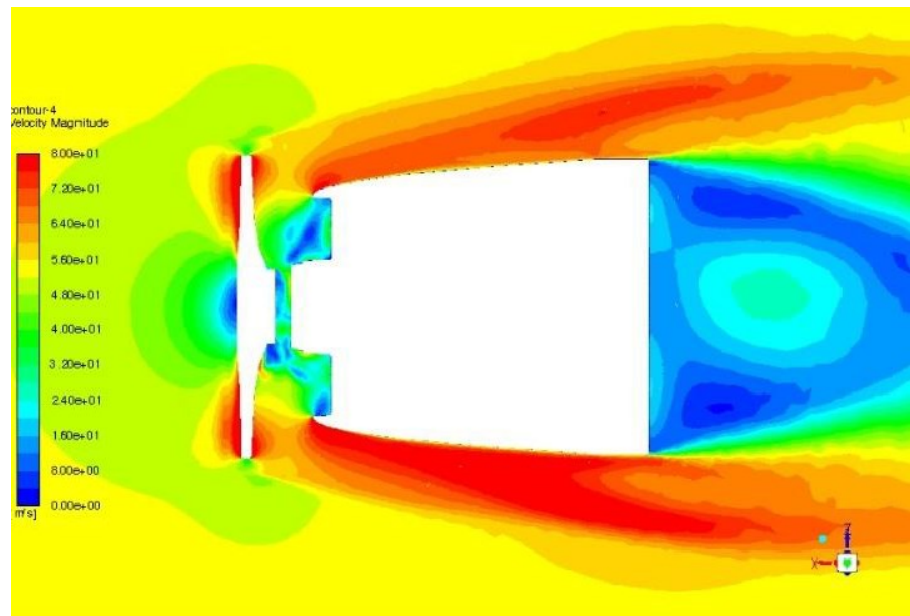


Figure 74: velocity field

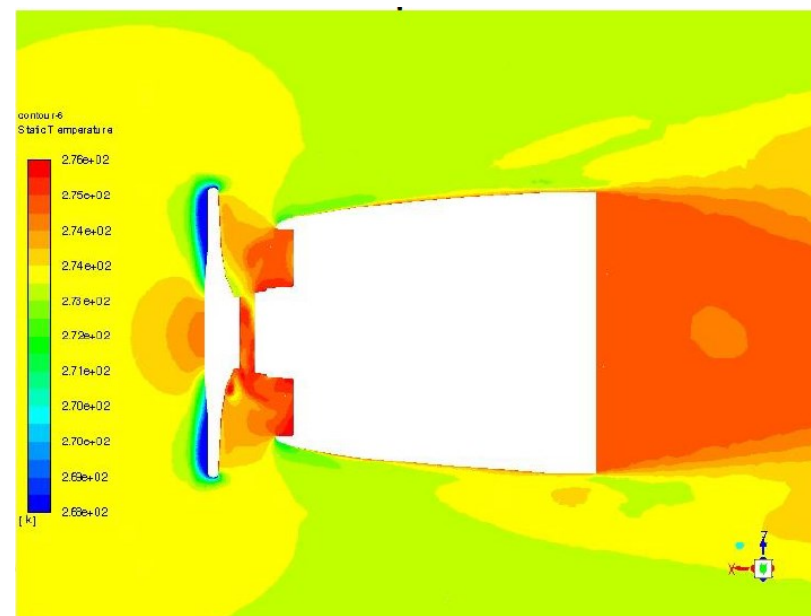


Figure 75: temperature mapping

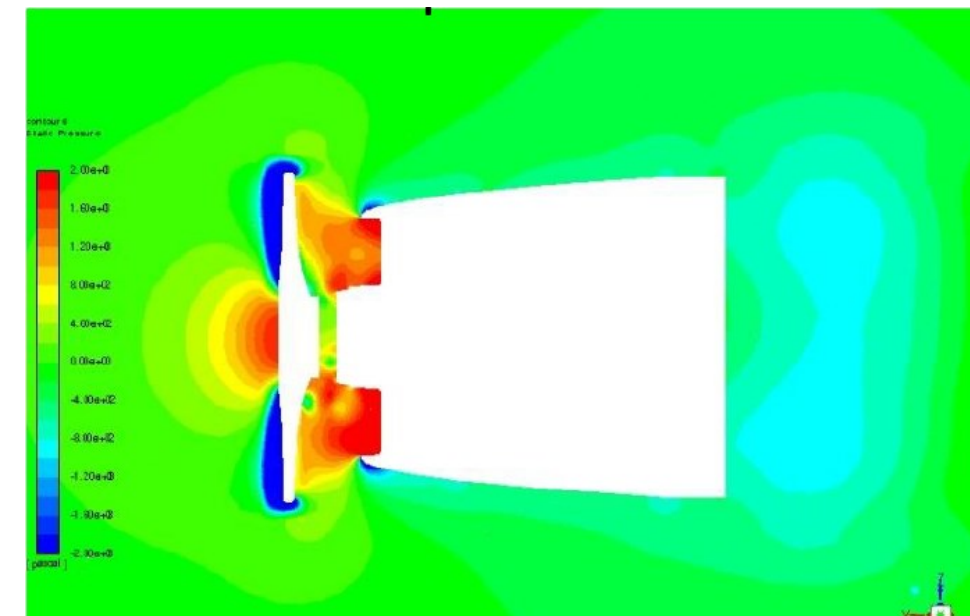


Figure 76: pressure mapping

Source: DGA EP

4.3.2.3 - Series of simulations considering different types of test section

The different types of test section considered are as follows:

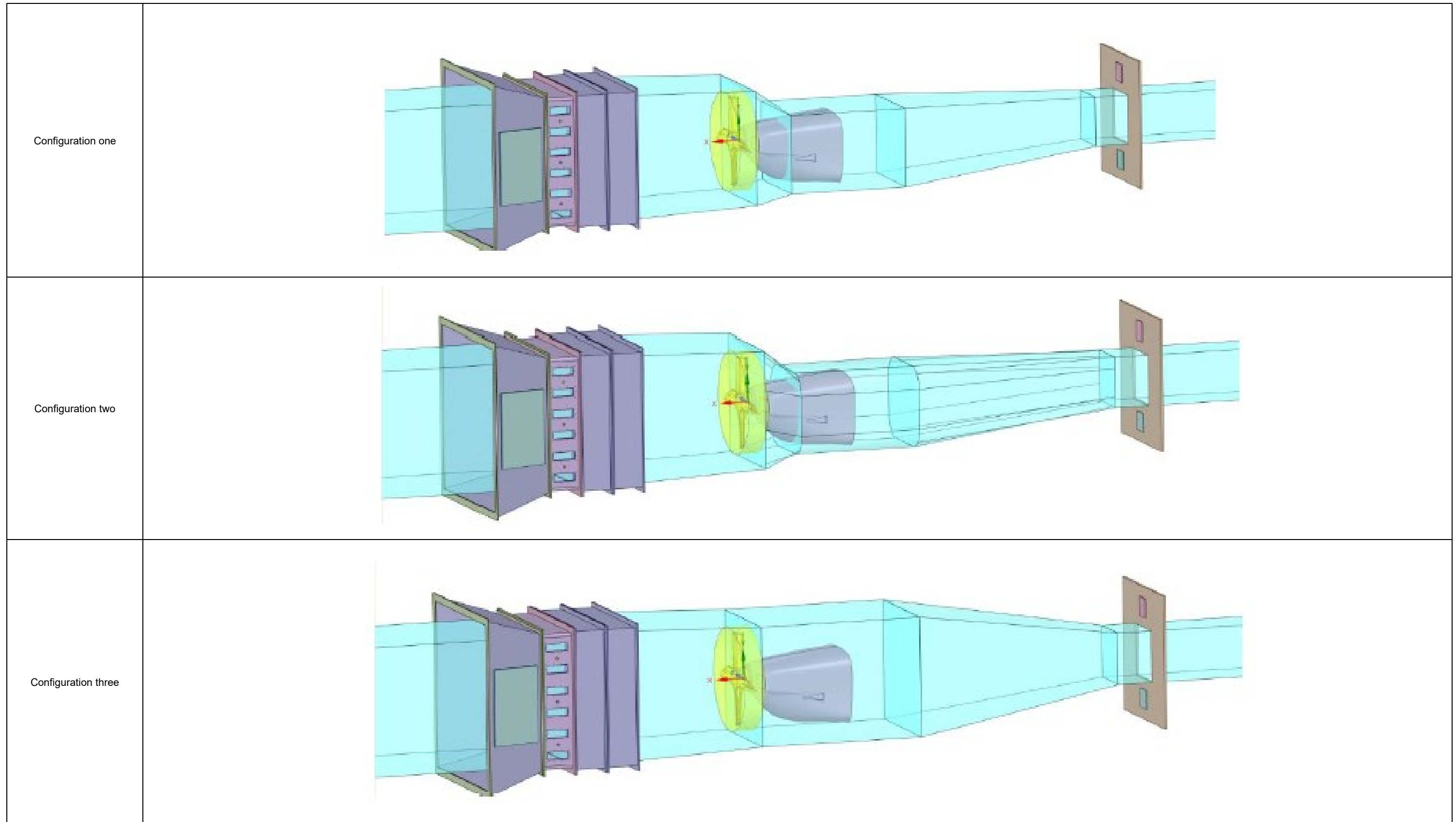


Figure 77: types of test section considered
Source: DGA EP

In the three configurations, the intake area and the outlet area of the section are invariable.

Configuration two differs from configuration one due to the rounded couplings between the section walls.

Configurations one and two differ from configuration three due to the very restricted space between the section walls and the cowlings: approximately 6 cm. In the case of configuration three, this space is significantly larger.

In all three configurations, the speed of air entering the section is set to 4.7 m.s^{-1} . This speed is obtained directly considering the maximum air flow of the test stand, i.e. 14 kg.s^{-1} , and the intake area of the test section $1.56 \times 1.56 = 2.43 \text{ m}^2$. I.e. $V_{air} = \frac{Q_{air}}{\rho \cdot S_{entrée\ veine}} = \frac{14}{2.43 \times 1.225} = 4.7 \text{ m.s}^{-1}$.

These simulations show that:

- the specified speed 54 m.s^{-1} cannot be reached (phenomenon amplified when the section is too wide);
- large recirculation zones appear upstream of the propeller due to the fact that this propeller “sends” most of the flow to the walls (Figure 79);
- these recirculations still occur but are much smaller with a wider section;
- these recirculations induce significant increases in temperature which do not guarantee the control of essential temperature/humidity parameters for this test campaign (Figure 81 and Figure 82).

To conclude, none of the configurations presented above enabled the specified tests to be carried out by placing the powerplant inside the small icing ring test stand section.

Another configuration must be proposed by removing the powerplant from the section and supplying the engine air intakes (air intake supplying the carburettor on the LH side and air intakes upstream of the cowlings, immediately behind the propeller) with air. In these conditions, the supply of the air intakes upstream of the cowlings requires the propeller to be distanced from the cowlings.

Velocity fields

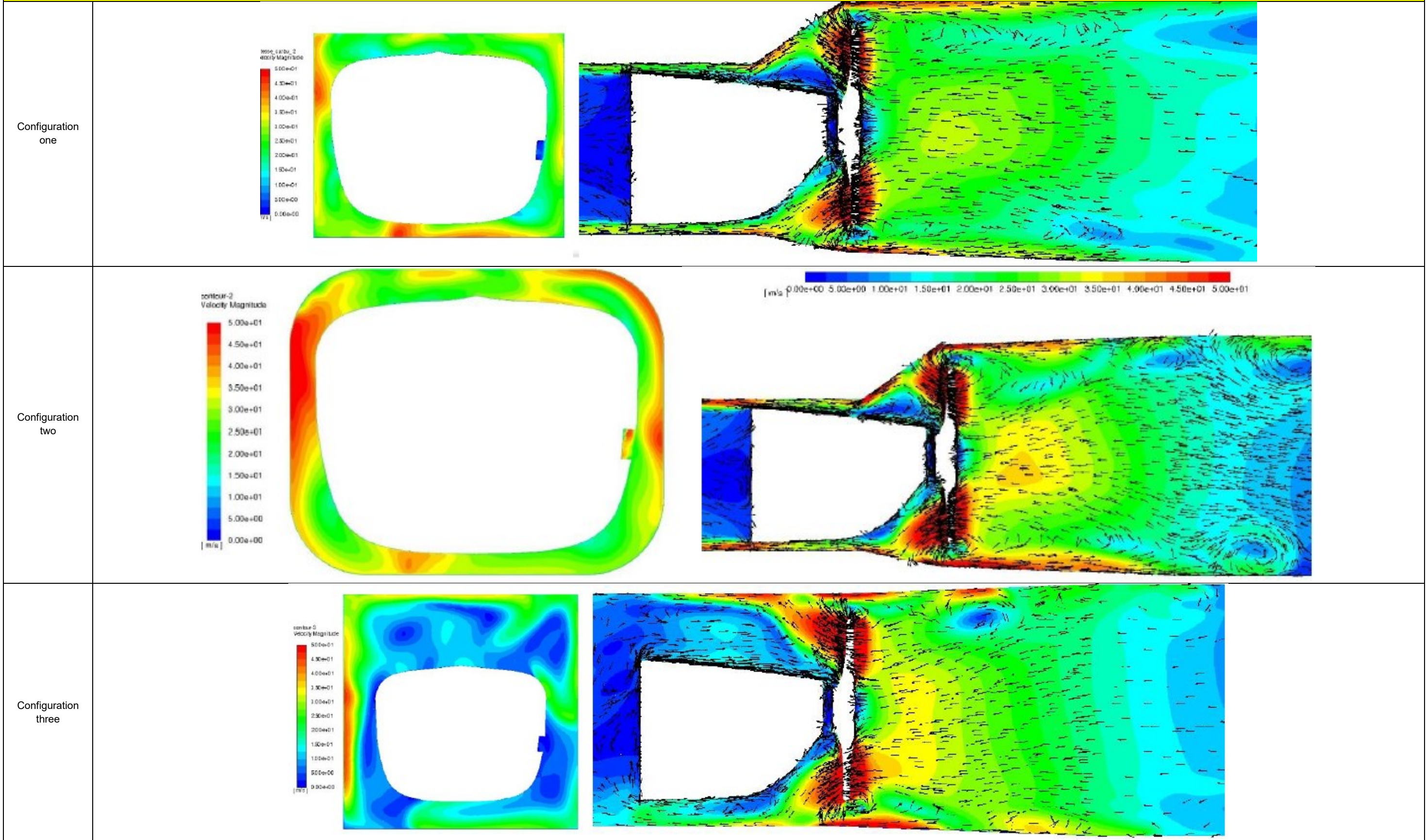


Figure 78: modelling of the velocity field for each configuration

Source: DGA EP

Configuration two

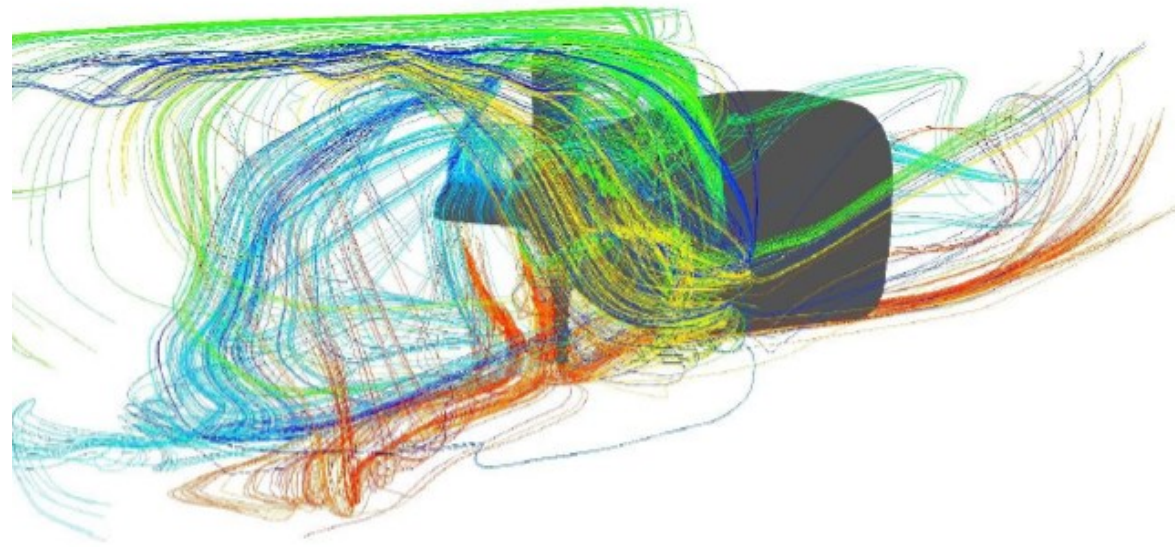


Figure 79: streamlines passing through each propeller blade

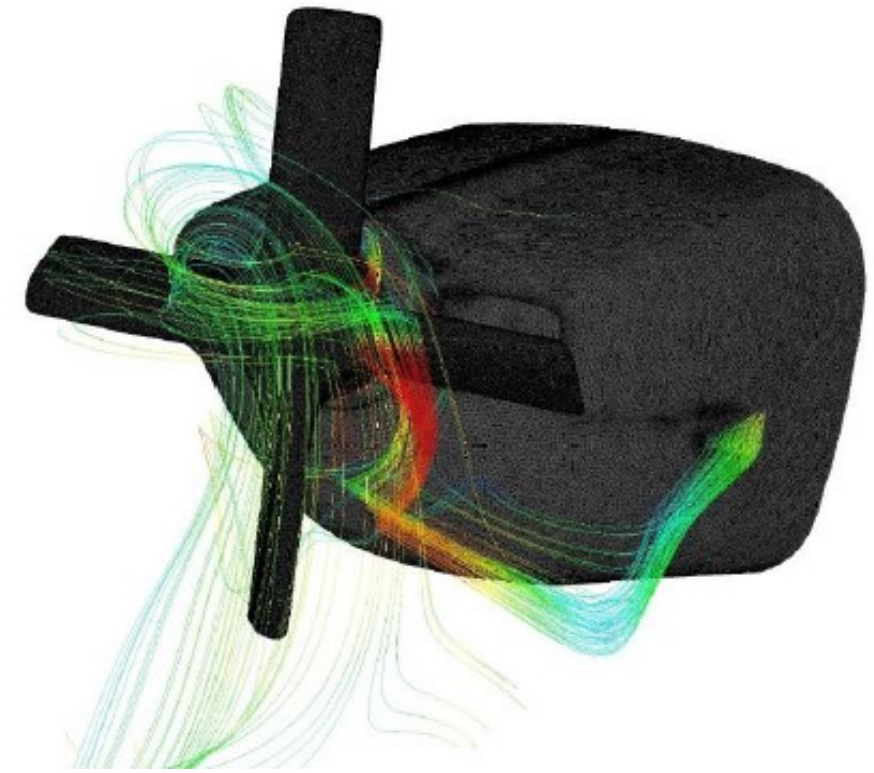
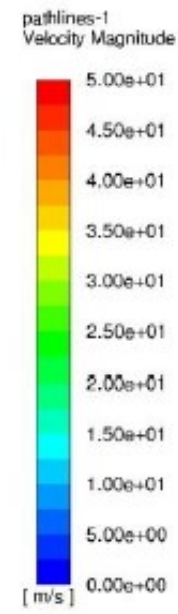


Figure 80: streamlines taken in by the carburettor

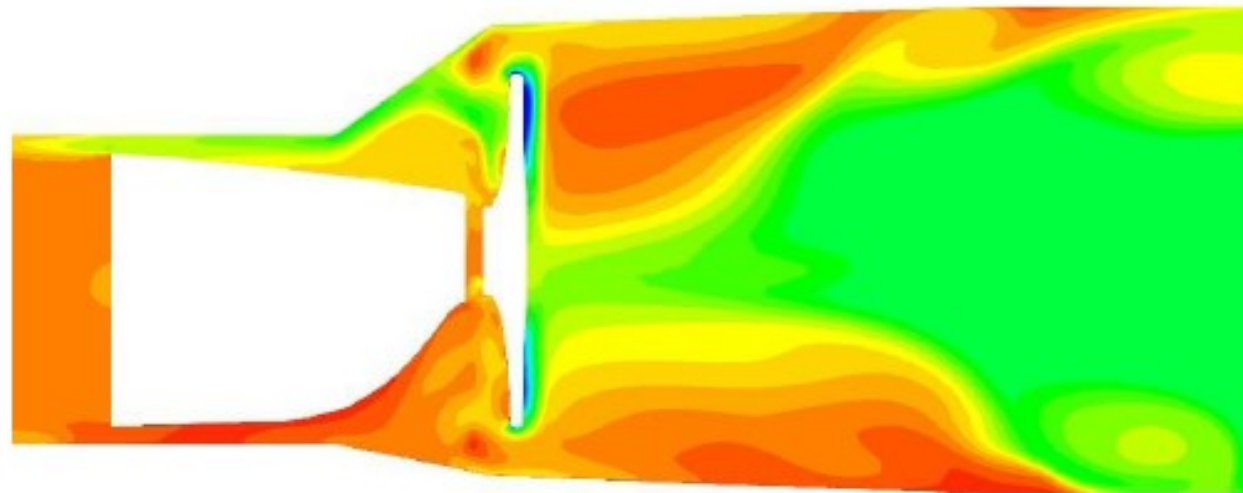


Figure 81: temperature increases caused by the recirculations

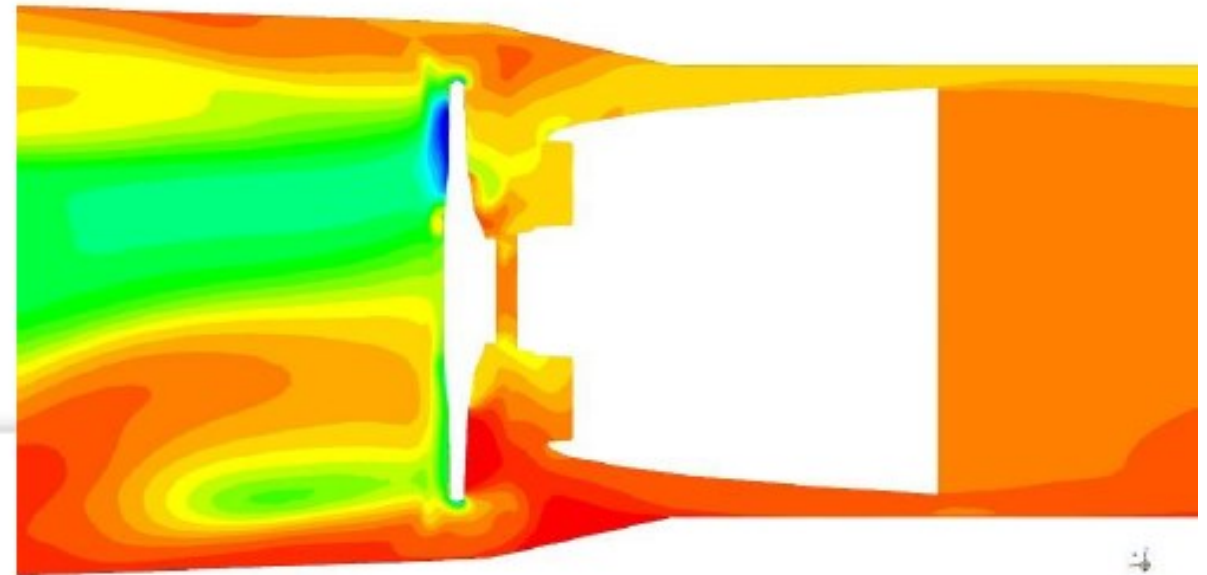


Figure 82: temperature increases caused by the recirculations

Source: DGA EP

4.3.2.4 - Series of simulations considering a new type of test section

Taking into account the results of the first series of simulations, the following test setup was studied (Figure 83).

In this configuration, the engine was installed on its stand, as on the aeroplane, itself attached to a very robust steel stand. On the first blank, a long extender was considered between the engine and the propeller as shown in the diagrams below. Thus, the supplying of air to the air intakes upstream of the cowlings seems to be completely practicable.

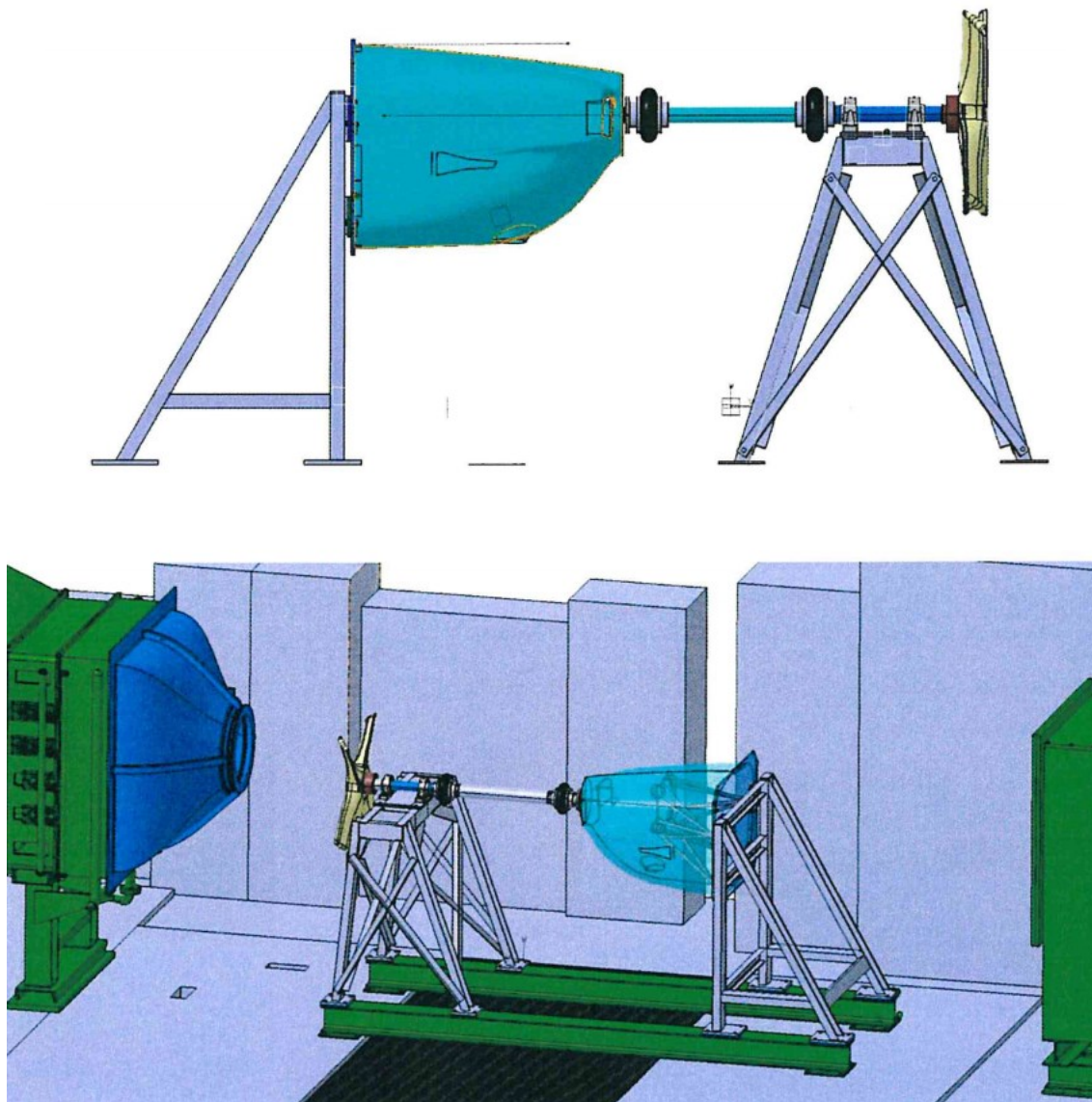


Figure 83: first blank of the new configuration

Source: DGA EP

This extender was not selected due to weight considerations. Indeed, the amplitude of the engine's movements during the start-up and shut-down phases would require the use of a system ensuring high degrees of freedom to guarantee the integrity of the setup.

The amplitude of the engine's movements during the start-up and shut-down phases was measured by the BEA at the ENAC's Castelnau test stand. These measurements were taken using the video resources described below.

- **Tools used:**

Two GOPRO cameras: one filming the underside of the engine and the other filming its right-hand side:

- one hero8 GOPRO: set to 240 im/s;
- one hero6 GOPRO: set to 240 im/s.

Stick-on targets were positioned on the engine. These targets are illustrated in Figure 84, they are the references used to define the engine's movements by video analysis.

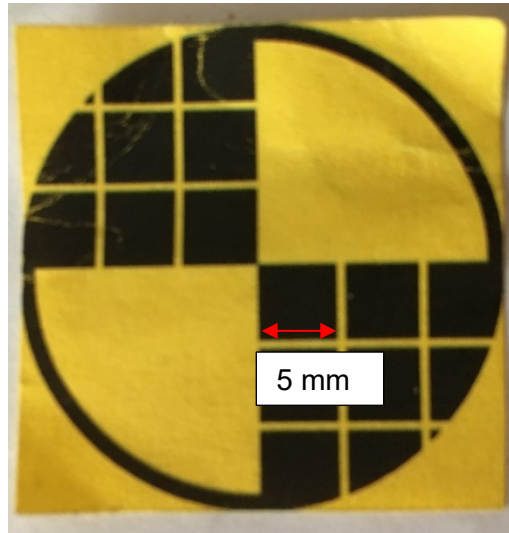


Figure 84: target affixed to several sections of the engine
Source: BEA

- **Position of GOPRO cameras in relation to the engine:**

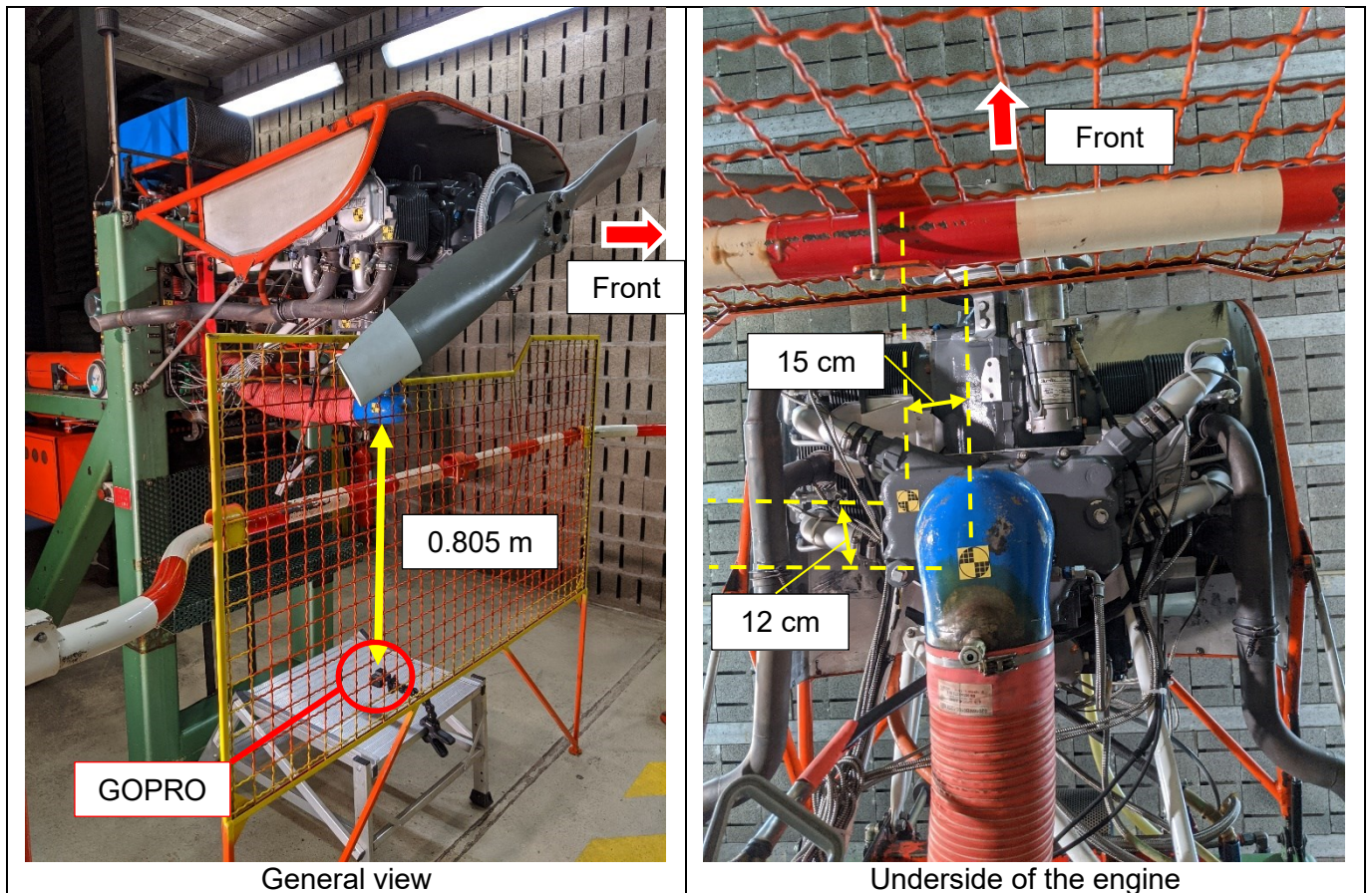


Figure 85: Position of the GOPRO under the engine
Source: BEA

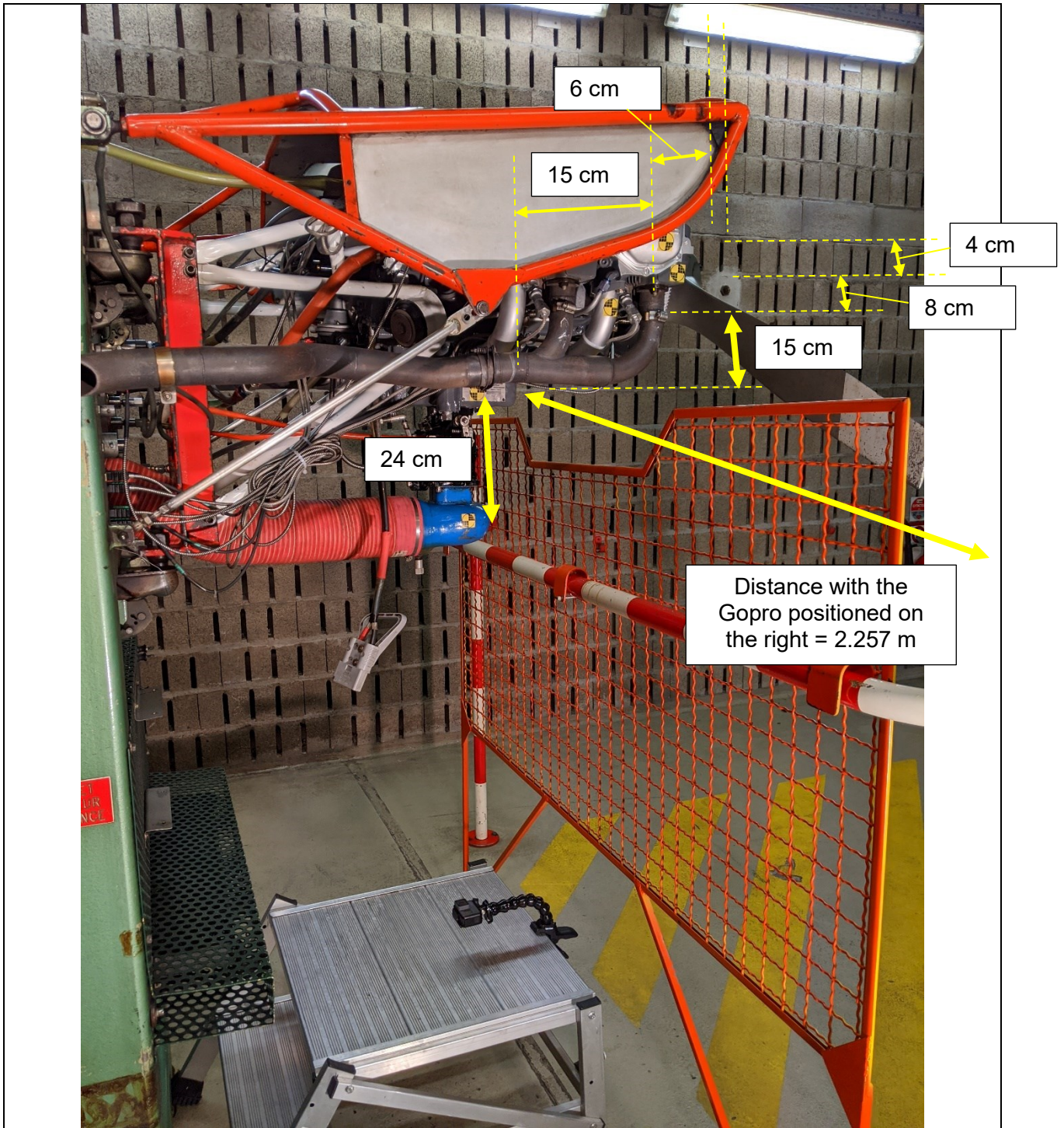
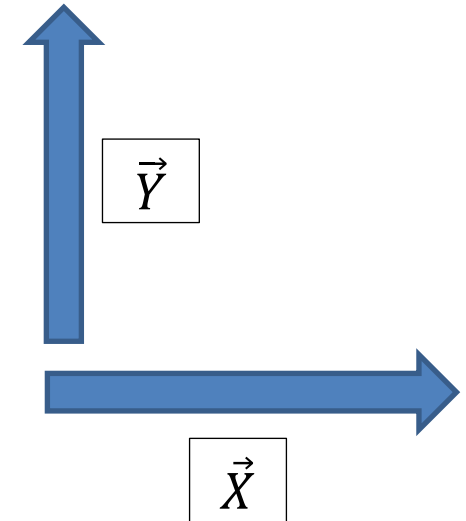
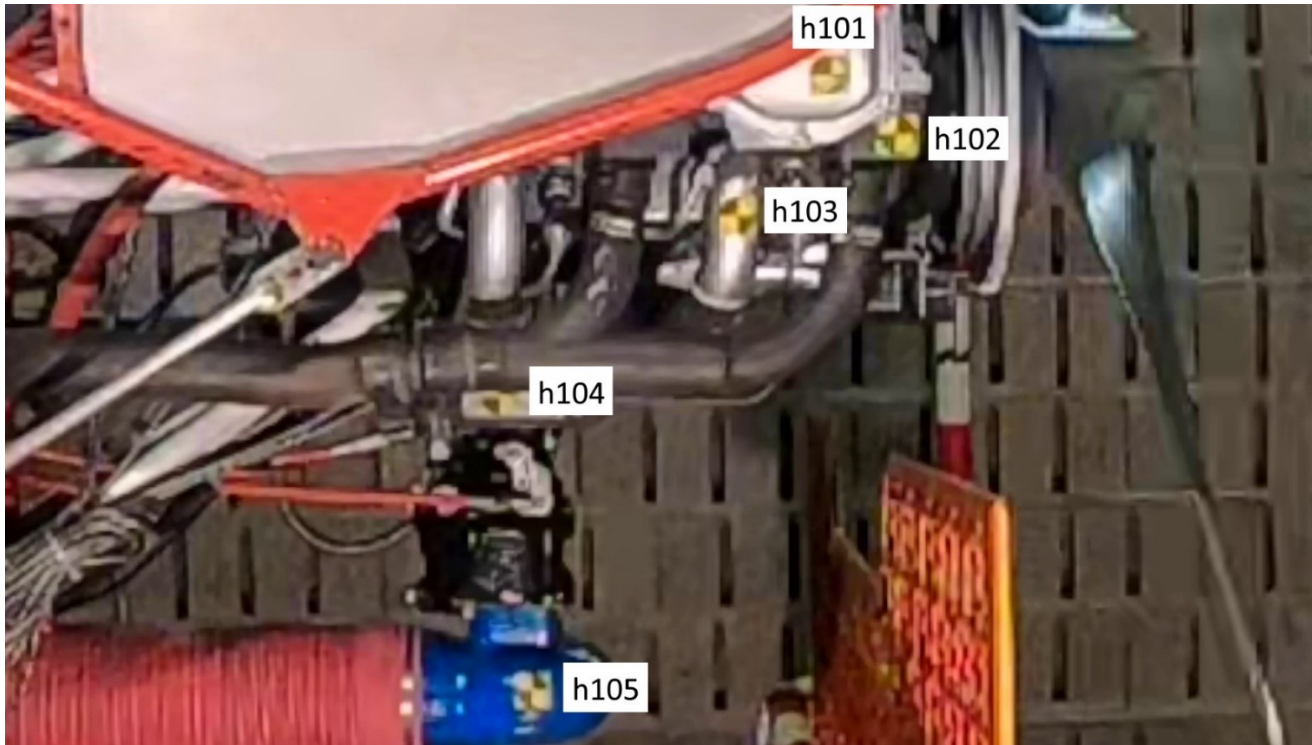


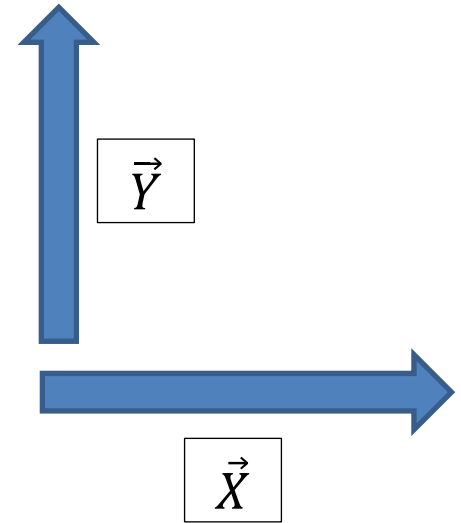
Figure 86: Position of the GOPRO on the right of the engine
Source: BEA

The peak amplitudes measured are indicated in **Figure 87** and **Figure 88**



	X	Y
h101	+ 2.8 mm - 5.96 mm	+ 5.4 mm - 13 mm
h102	+ 4.1 mm -3.1 mm	+3.6 mm -10.8 mm
h103	+3.8 mm -5.6 mm	+5 mm -9.5 mm
h104	+2.6 mm -4.2 mm	+2.9 mm -4.3 mm
h105	+3.4 mm -1.5 mm	+2 mm -2.4 mm

Figure 87: maximum amplitudes measured on axes \vec{x} and \vec{y}
 Source: BEA



	X	Y
v101	+ 20 mm - 8.3 mm	+ 4.2 mm - 3.3 mm
v102	+ 7.7 mm - 3.3 mm	+ 3.7 mm + -3.5 mm

Figure 88: maximum amplitudes measured on axes \vec{x} and \vec{y}
 Source: BEA

The test setup selected is therefore equivalent to the ENAC's setup with the exception of a 100 mm-long aluminium alloy spacer installed between the propeller and the engine (**Figure 89**). The positioning of such a spacer between the engine and the propeller enables ducts to run through this space to supply the air intakes at the front of the engine (**Figure 91**).

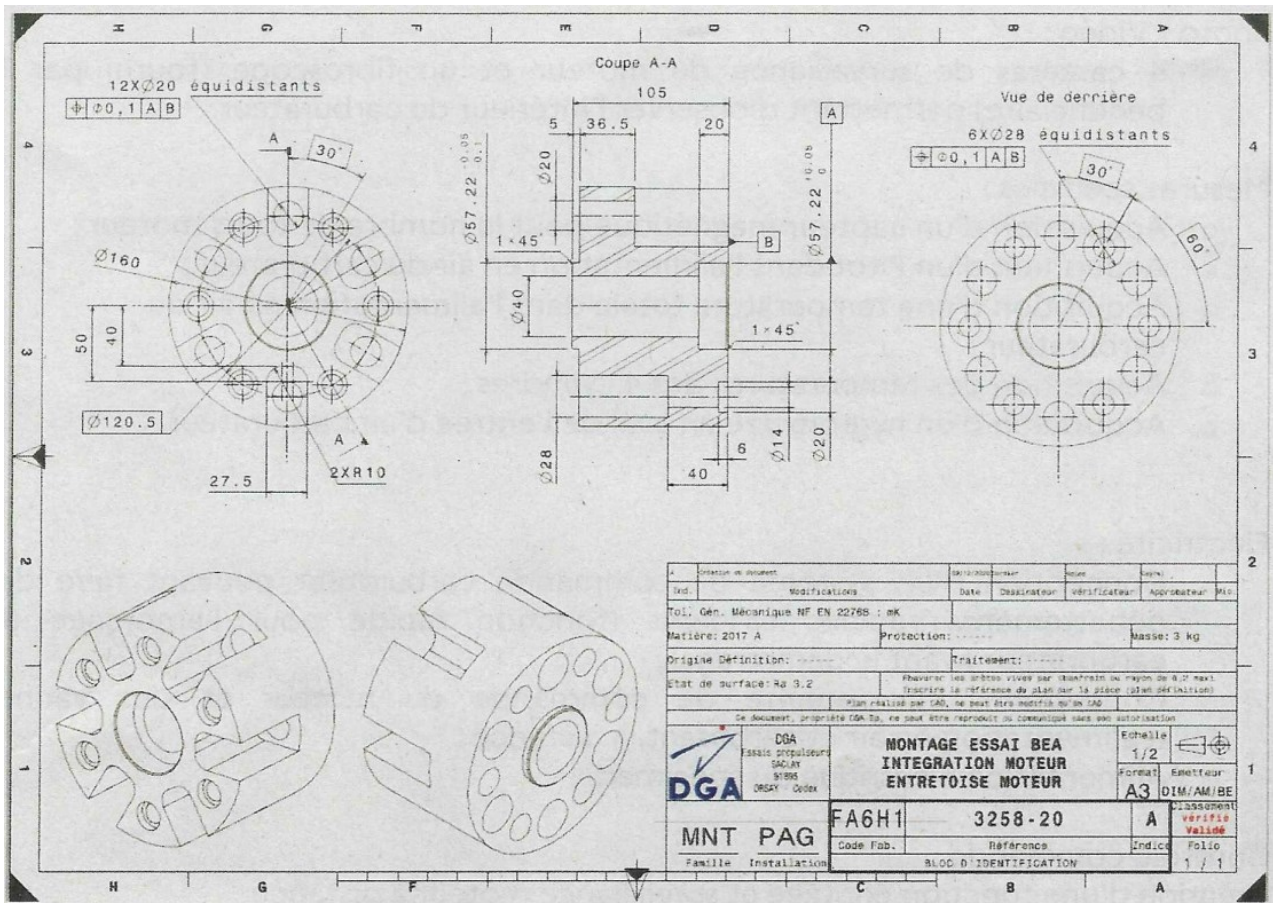


Figure 89: spacer installed between the engine and the propeller
Source: DGA EP

In line with its intake area, the section is divided into three separate ducts (**Figure 90** to **Figure 94**):

- a duct routed along the left side of the cowlings to supply the carburettor;
- two similar ducts supplying the air intakes located behind the propeller.

The connection between the engine cowlings and the firewall was sealed.

The air was introduced by the inlets at the intake and extracted in the lower section by two extraction ducts.

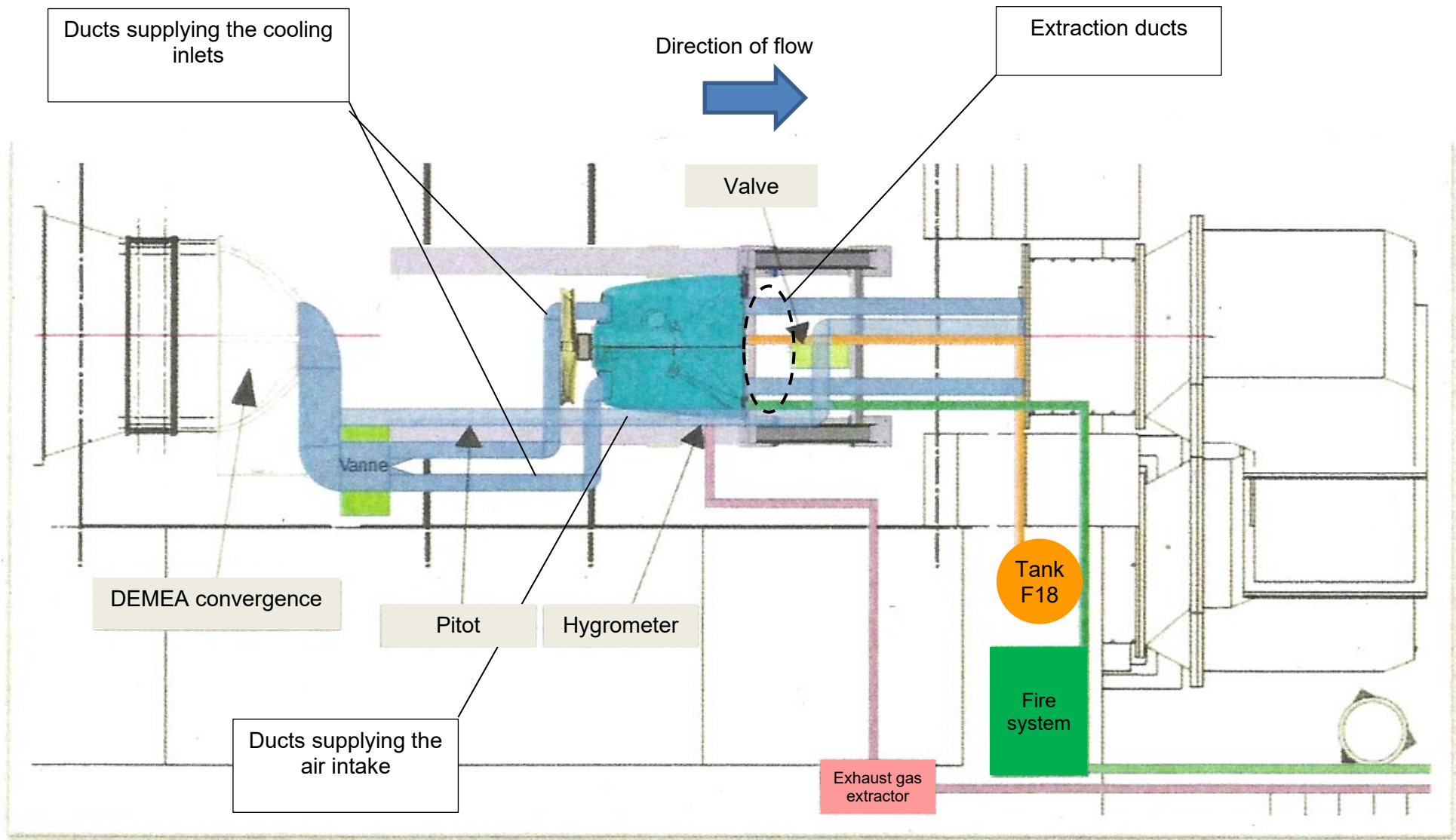


Figure 90: supply of "conditioned" air to the powerplant
 Source: DGA EP

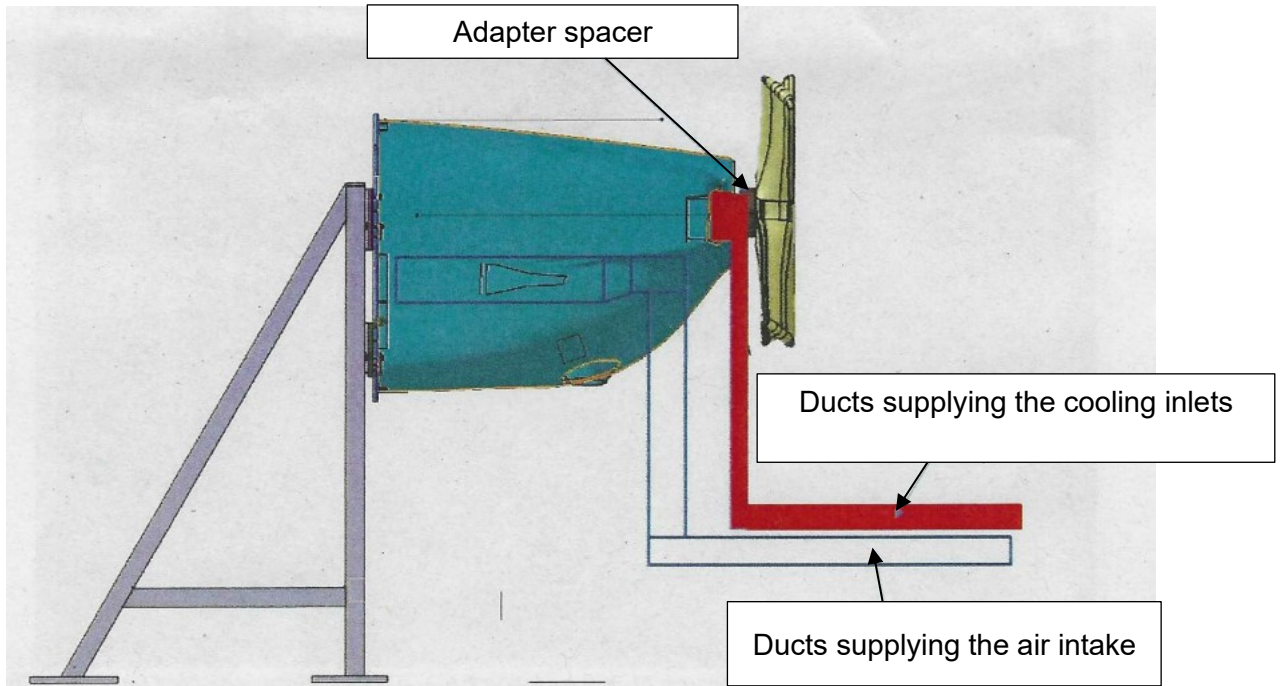


Figure 91: details of the installation
Source: DGA EP

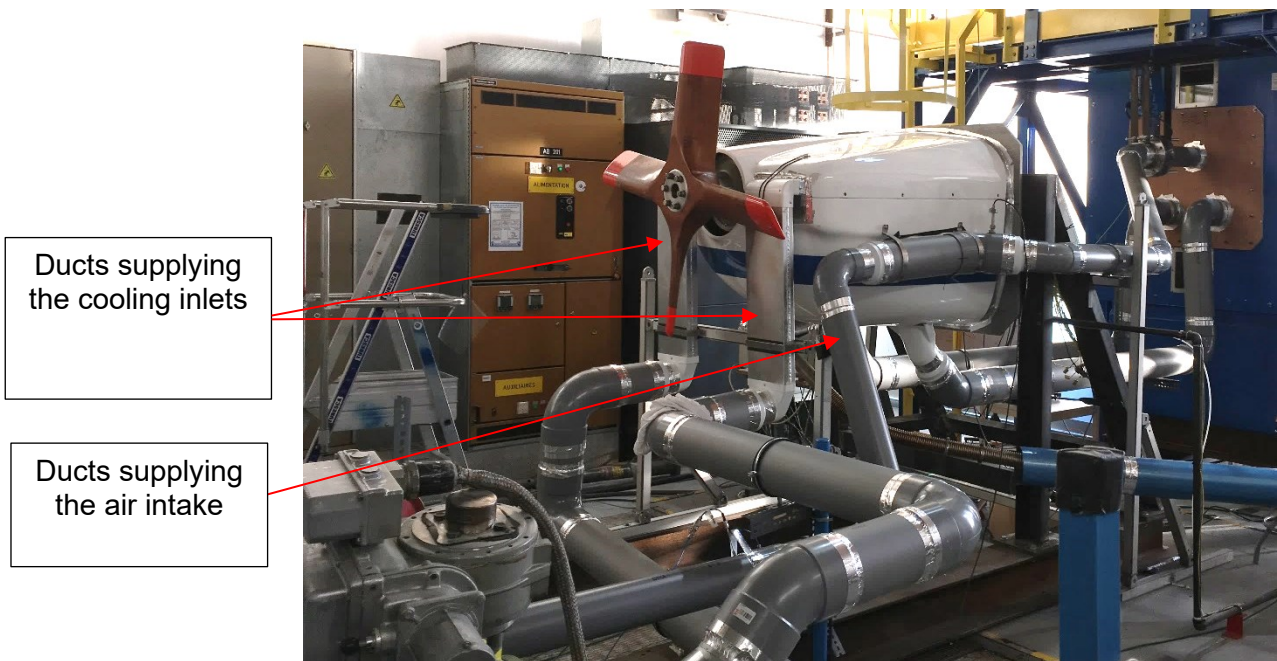
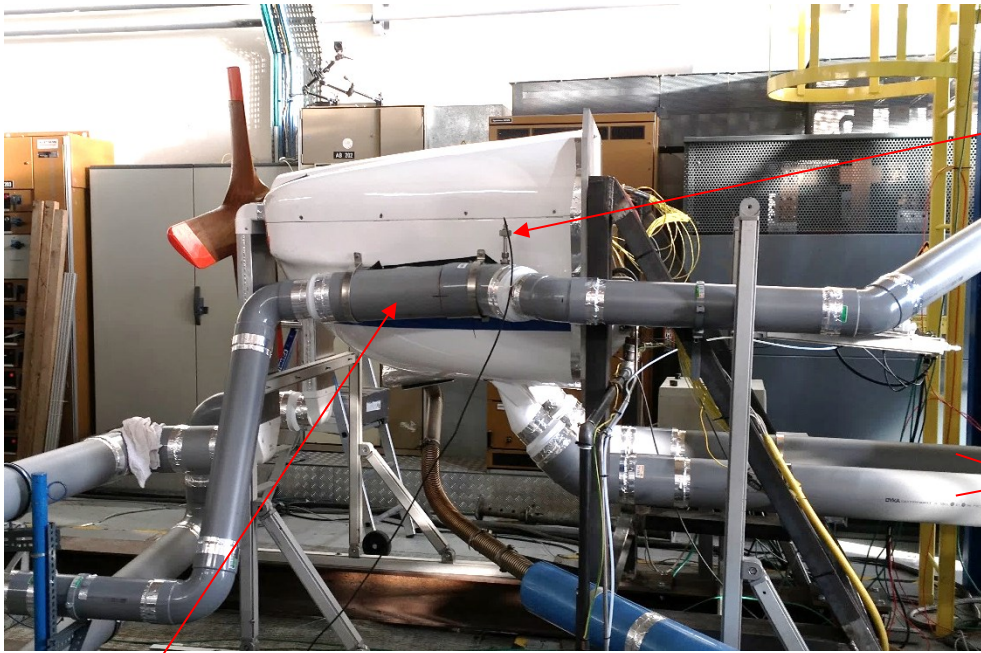


Figure 92: installation - 3/4 RH forwards view
Source: DGA EP

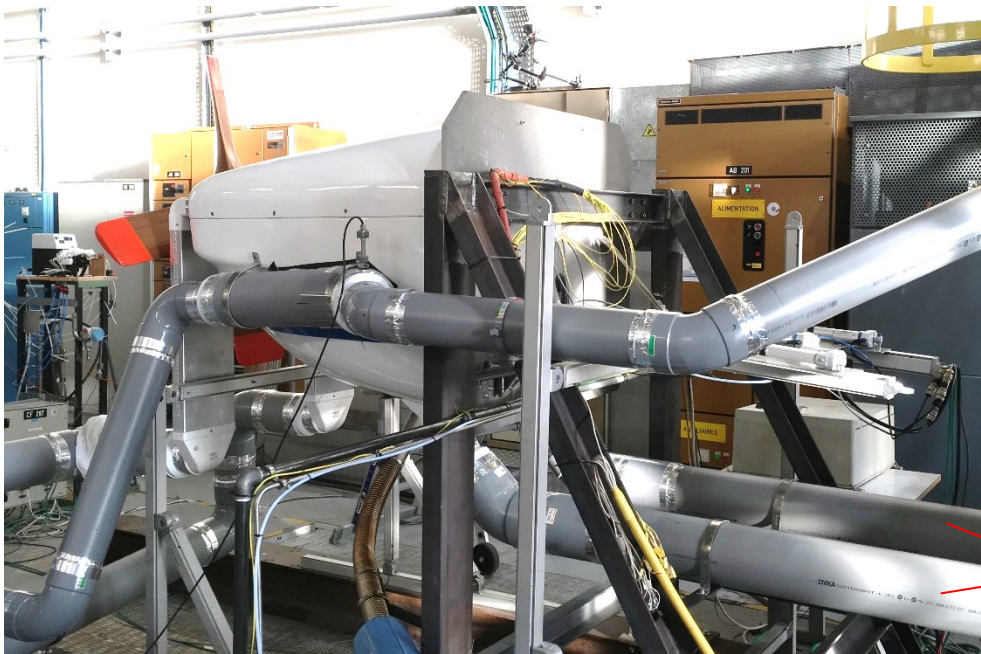


Temperature and humidity measurements

Ducts ensuring the extraction of air introduced at the front into the engine cowlings

Ducts supplying the air intake

Figure 93: installation - right side view
Source: DGA EP



Ducts ensuring the extraction of air introduced at the front into the engine cowlings

Figure 94: installation - 3/4 RH rearwards view
Source: DGA EP

4.3.3. Detailed overview of the test setup

4.3.3.1 - Assembly of the engine and its associated equipment

The schematic diagram showing the intakes and outlets is presented in Figure 95 below.

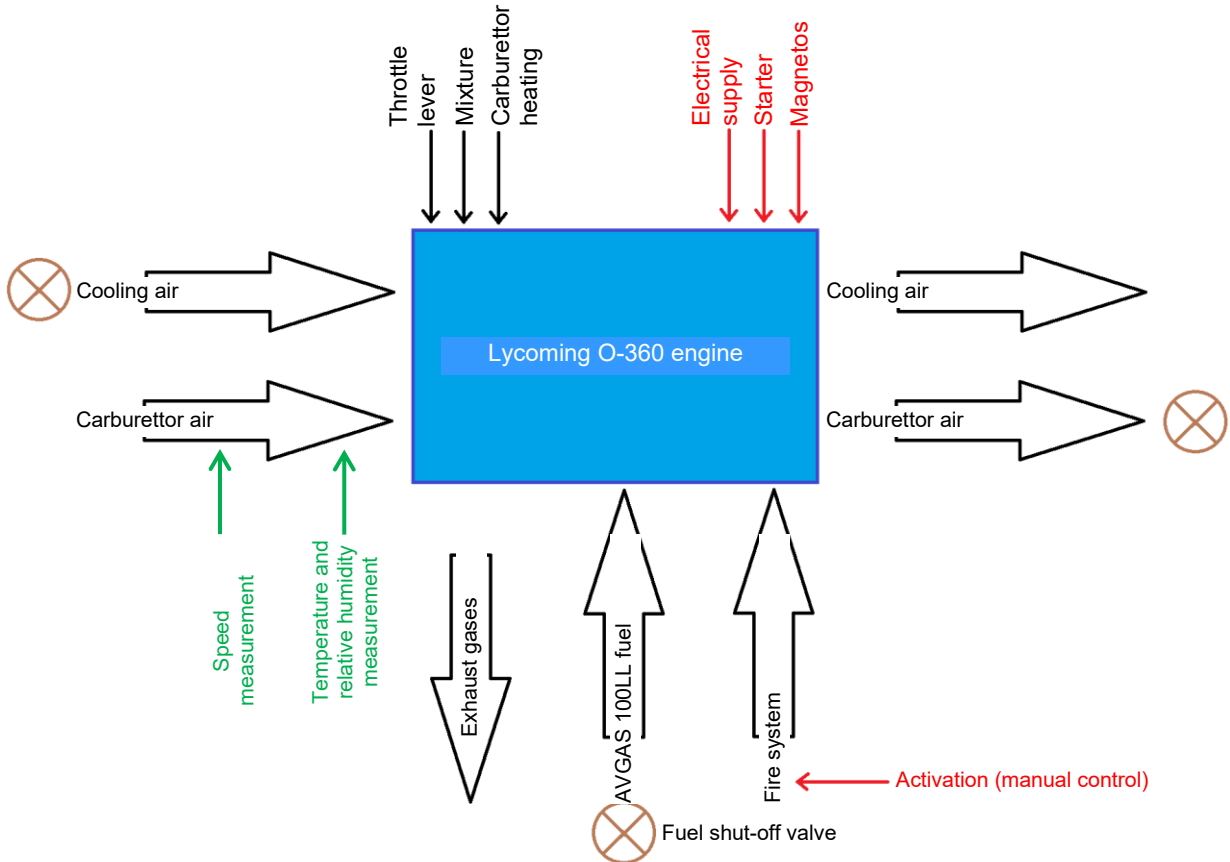


Figure 95: Schematic diagram of the installation

Source: BEA

( Valves)

The engine is equipped as it would be when installed on the aircraft.

The engine stand and the test stand are connected through a solid metal firewall (Figure 96). Fuel hoses and flight control linkages are routed through this firewall. Each routing orifice was sealed.

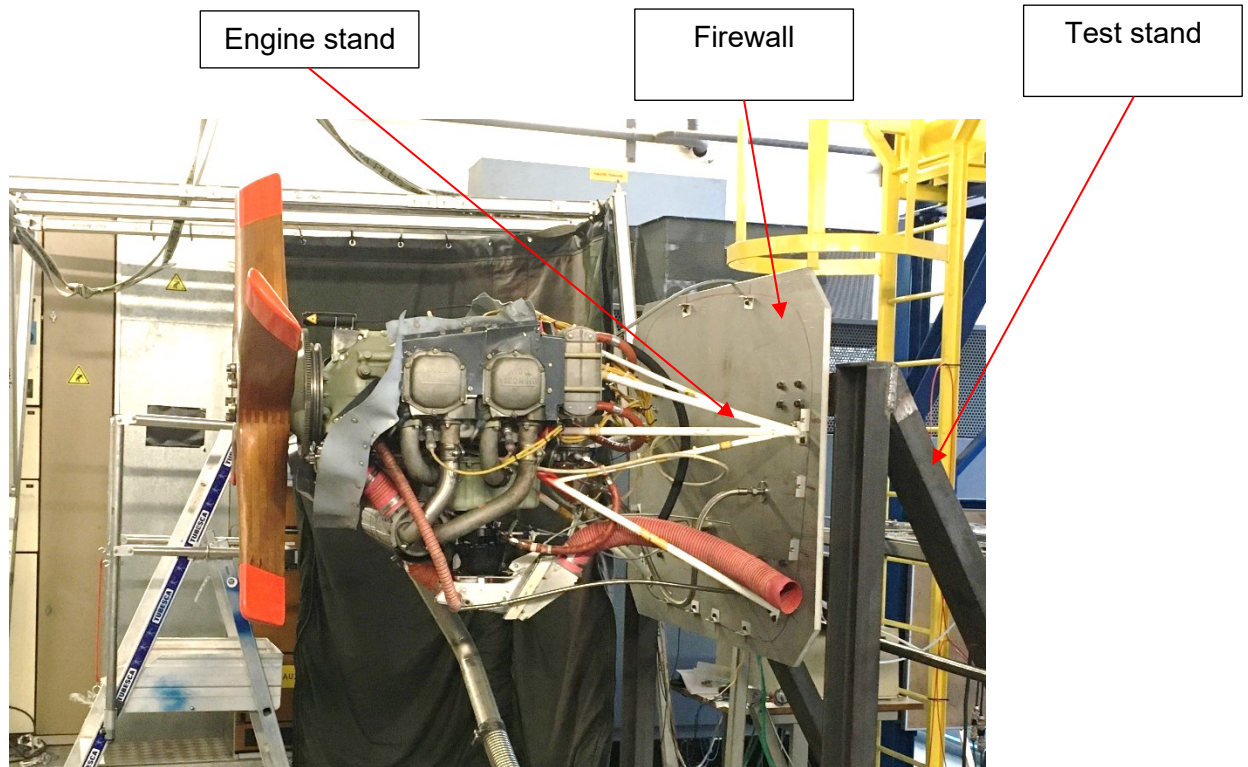


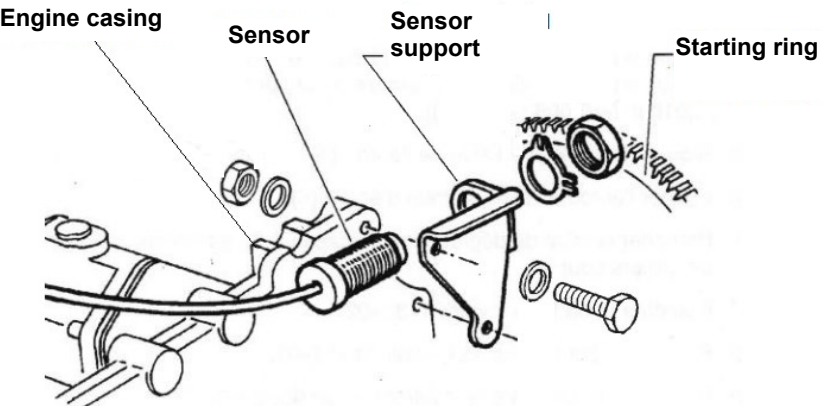
Figure 96: powerplant in position
Source: DGA EP

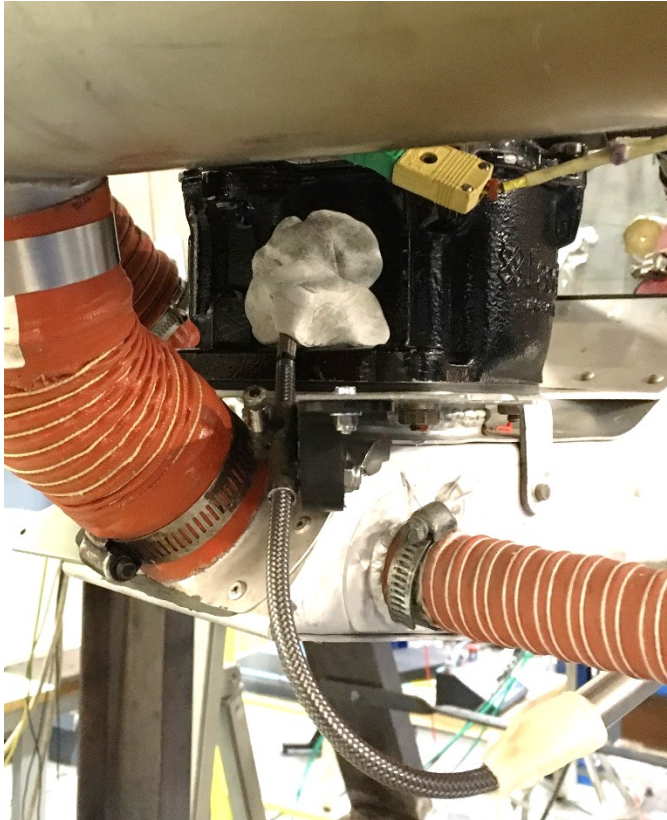
The engine is equipped with deflectors around the cylinders to enable cooling air to circulate.


The carb heat system is operational as it would be on the aircraft.

The carburettor and Airbox control linkages are controlled by pneumatic cylinders, which enable the engine to be controlled remotely.

4.3.3.2 - Sensors installed on the engine

Parameter measured	Sensor installed	Comments
Temperature of the outer surface of the cylinder head of cylinder 1	Type K thermocouple	/
Temperature of the outer surface of the cylinder head of cylinder 2	Type K thermocouple	/
Temperature of the outer surface of the cylinder head of cylinder 3	Type K thermocouple	/
Temperature of the outer surface of the cylinder head of cylinder 4	Type K thermocouple	/
RPM	Tachometer sensor using the Hall effect principle	<p>This sensor is the sensor installed on the ENAC TB10 and TB20. It is located just behind the starting ring.</p> <p>The principle</p>  <p>Figure 97: speed sensor installation diagram Source: ENAC</p> <p>The information provided by the sensor is processed by a DGA processing unit and is displayed on the control page in the test stand cabin.</p>
EGT	Type K thermocouple	Thermocouple located in the exhaust pipe associated with cylinder 3
Temperature of the outer surface of the carburettor	Type K thermocouple	Thermocouple located on the LH side of the carburettor
Temperature downstream of the carburettor butterfly valve	Thermocouple	Thermocouple specified for the carburettor considered, positioned in the purpose-made tapping on the carburettor

Parameter measured	Sensor installed	Comments
View of the venturi and the up-side of the butterfly valve	Borescope equipped with a 6 mm-diameter fibre	<p>The carburettor body was drilled to enable insertion of the borescope fibre.</p>  <p>Figure 98: insertion of the borescope fibre in the carburettor Source: DGA EP</p>
Temperature at the Airbox intake, upstream of the carburettor	Type K thermocouple	/
Manifold pressure	/	Measurement taken on the cylinder 1 intake duct

Parameter measured	Sensor installed	Comments
Oil pressure	/	
Oil temperature		<p>The sensor is that specified for the aircraft and the engine in question. It is located on the engine accessory section.</p> <div data-bbox="1389 470 1813 554" style="border: 1px solid black; padding: 2px; display: inline-block;">Position of the oil temperature probe</div>  <p>Figure 99: Rear face of the unequipped engine Source: BEA</p> <p>This sensor is associated with a conventional needle indicator located behind the firewall. This indicator is filmed continuously and the image is displayed in the bench control cabin.</p>

4.3.3.3 - Supply and extraction ducts

The engine is covered by the aeroplane's upper and lower cowlings. The connection between the cowlings and the firewall was sealed.

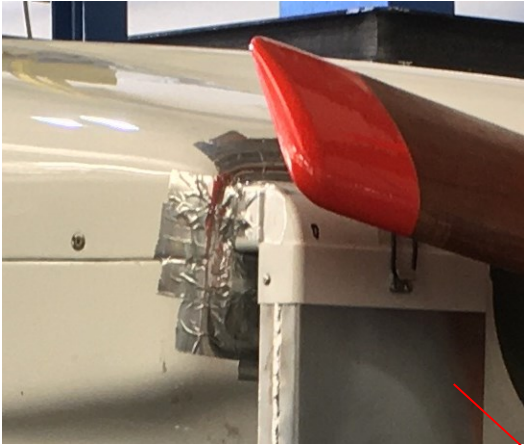
The air intake supply duct fits snugly against the cowling. The connection between the duct and the cowling was sealed.

Upstream of the air intake, the duct was equipped with a pitot probe used to measure the airspeed. Immediately downstream of the air intake, the duct was equipped with a probe used to measure the temperature and the humidity.

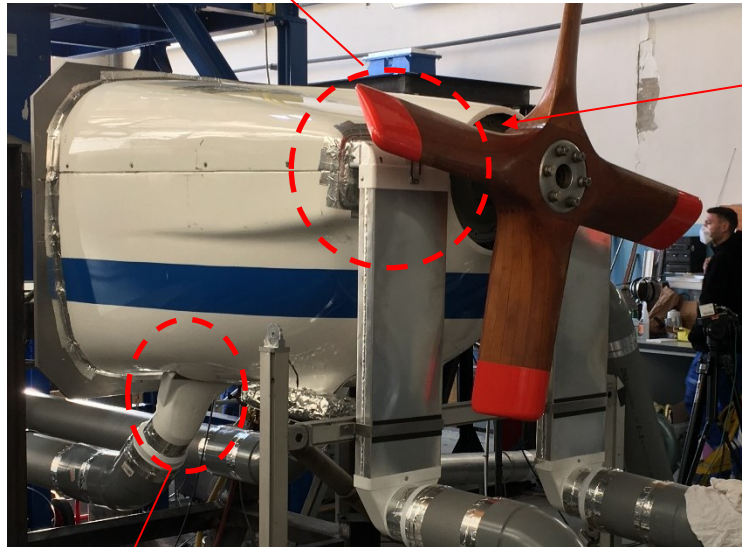
These instruments are used to accurately check the conditions permitted in the air intake.

The two cooling inlet supply ducts and the two extraction ducts are integrated into the cowlings to seal these connections.

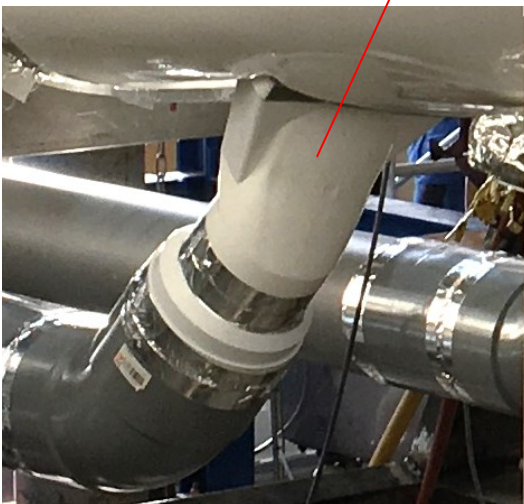
In the cowlings, the only unsealed zone was the rounded space behind the propeller. When the two cooling inlet supply ducts are supplied, the outside air is taken in through this unsealed zone. The flow of this unconditioned air remains very weak in relation to the controlled flow injected into the cooling inlets.



Engine supply/cooling duct



Unsealed zone



Extraction duct

Figure 100: air supply and extraction ducts

Source: DGA EP

4.4. Test results

4.4.1. Introduction

The tests were conducted in two phases.

Phase one was conducted with the powerplant as detailed in the chapter above. In this configuration, it is important to note that the carburettor is near the exhaust system.

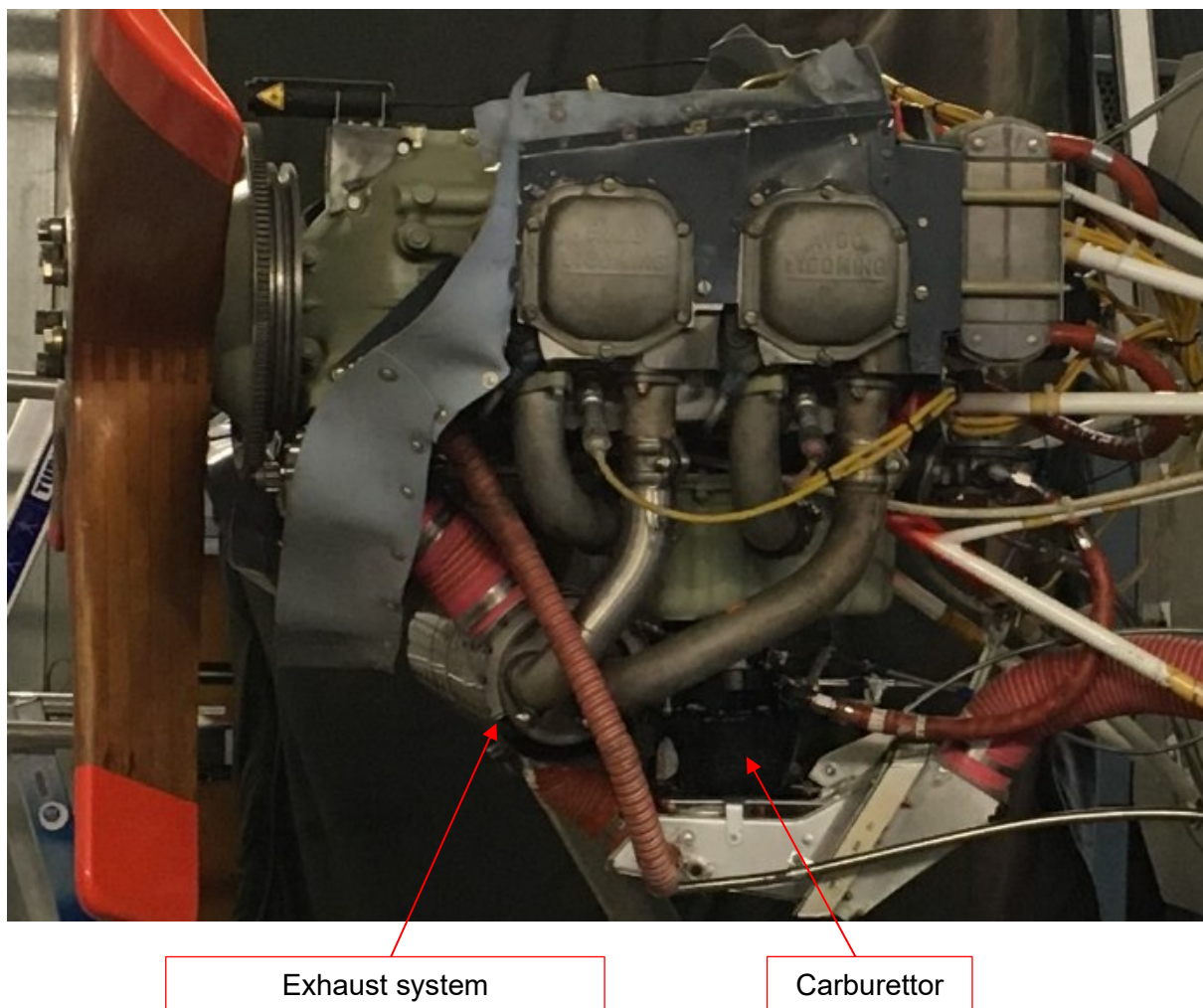


Figure 101: Position of the carburettor in relation to the exhaust system

Source: DGA EP

During this phase, the process was always the same:

- start-up of ventilation in the test stand;
- start-up of the engine and maintaining the engine at a speed between 1,200 and 1,500 rpm to ensure gradual heating;
- conditioning of the test stand according to the test point (temperature, relative humidity, airspeed);
- completion of the test point when the conditions are met.

Phase two consisted in positioning thermal insulation around the carburettor to try to reduce the impact of the temperature induced by the exhaust muffler. The engine was started after the test conditions were reached in order to limit the increase in temperature of the outer surface of the carburettor.

During this test campaign, the engine was operated for 35 hours and 18 minutes, comprising 15 start-ups and around 550 litres of fuel consumed.

4.4.2. Test points completed

The test points are listed in the table below.

Test phase one Engine in standard configuration				
Temperature (°C)	Relative humidity (%)	Dew point temperature (°C)	Engine speed (rpm)	Airspeed (kt)
-6	74	-9.1	2,100	99
-5.3	72	-8.9	2,100	82
-3.6	74	-7.6	2,500	105
0	77	-3.7	1,700	80
0	78	-3.5	2,100	99
0	75	-4.1	2,600	80
1	99	0.9	2,100	100
1.5	80	-1.4	1,500	80
1.5	80	-1.4	1,700	80
1.5	80	-1.4	1,900	80
1.5	84	-0.7	1,700	100
1.5	80	-1.4	1,900	100
2	80	-0.9	1,300	80
2	82	-0.6	1,700	80
2	80	-0.9	1,900	80
2.4	83	-0.1	1,700	80
2.4	83	-0.1	1,900	80
3	77	-0.5	1,700	80
3	99	2.9	2,100	100
3	97	2.6	1,500 => 2,100	80
3	97	2.6	1,500 => 2,100	100
3	97	2.6	1,800	100
3.4	83	0.8	1,700	80
3.4	97	3	1,500 => 2,100	80
3.6	83	1	1,700	80
3.6	83	1	1,900	80
3.6	83	1	2,100	80
3.6	83	1	2,500	80

Temperature (°C)	Relative humidity (%)	Dew point temperature (°C)	Engine speed (rpm)	Airspeed (kt)
3.7	28	-13	1,500	80
3.7	28	-13	1,700	80
3.7	28	-13	1,900	80
3.7	28	-13	2,100	80
3.8	81.7	0.9	1,300	80
3.8	84.4	1.4	1,700	80
3.8	81.7	0.9	1,900	80
3.8	78	0.3	1,700	80
3.8	77	0.1	1,900	80
3.8	77	0.1	2,100	80
4.2	82	1.4	1,700	80
4.2	82	1.4	1,900	80
4.2	82	1.4	2,100	80
4.2	83	1.6	2,500	80
4.7	99	4.6	2,100	104
4.8	97	4.4	1,500 => 1,900	100
5	86.9	3	1,700	80
5	83	2.4	1,900	80
5	82	2.2	2,000	80
5	83	2.4	2,100	80
5	83	2.4	2,500	80
5	83	2.4	1,700 => 1,900	80
5	80	1.9	2,100	103
5	80	1.9	2,500	103
5	76	1.1	2,400	80
5	76	1.1	2,400	99
5	78	1.5	2,400	121
5.1	97	4.7	1,500 => 1,900	100
5.1	97	4.7	2,100 => 1,900	100
5.2	99	5.1	2,100	104
5.2	97	4.8	1,500 => 2,100	100
6	83	3.3	1,800	80
6	83	3.3	2,500	103
6.3	99	6.2	1,900	102

Temperature (°C)	Relative humidity (%)	Dew point temperature (°C)	Engine speed (rpm)	Airspeed (kt)
6.8	99	6.7	2,100	104
7	97	6.6	1,800	100
7	97	6.6	1,900	100
7	97	6.6	2,100	100
7	98	6.7	2,400 => 1,500 => 2,400	100
7.2	99	7.1	1,700	102
7.2	99	7.1	1,500 => 2,300	102
7.3	62	0.5	2,000	80
7.7	99	7.5	1,700	100
9.3	98	9	2,100	100
9.5	97	9	1,700	102
9.6	96	9	1,900	104
9.7	97	9.2	1,500 => 2,100	100
9.9	96	9.3	2,100	104
10	87	7.9	1,700	80
10	82	7	1,900	80
10	83	7.2	2,100	80
10	74	5.6	2,100	80
10	76.1	6	2,100 => 1,300	80
10	62	3	1,700	99
10	96	9.4	1,900	100
10	84	7.4	2,100 => 1,700	99
10	75	5.8	2,400	99
10	76	6	1,700 => 2,400	99
10	99	9.8	2,300	106
11.8	96	11.2	1,700	100
12	67	6.1	1,700	99
12	97	11.5	1,700	102
12.3	38	-1.5	1,700	80
12.3	38	-1.5	1,900	80
12.3	74	7.8	2,100	80
12.7	43	0.4	1,700	80
12.7	42.3	0.2	2,500	80
13	98	12.7	1,900	102

Temperature (°C)	Relative humidity (%)	Dew point temperature (°C)	Engine speed (rpm)	Airspeed (kt)
13.5	97	13	1,900	102
13.6	97	13.1	2,300	104
13.9	98	13.6	2,100	104
14.7	97	14.2	2,300	106
15	90	13.4	1,700	80
15	87	12.9	1,900	80
15	97	14.5	2,100	104

**Test phase two
Thermally insulated carburettor**

Temperature (°C)	Relative humidity (%)	Dew point temperature (°C)	Engine speed (rpm)	Airspeed (kt)
2.1	94	1.2	1,700	80
2.1	95	1.4	1,900	80
2.5	90	1	2,200	82
3.1	94	2.2	1,700	80
3.3	95	2.6	1,700	80
3.4	94	2.5	2,000	80
3.7	95	3	1,500	82
3.7	95	3	1,700	80
3.7	95	3	2,000	82

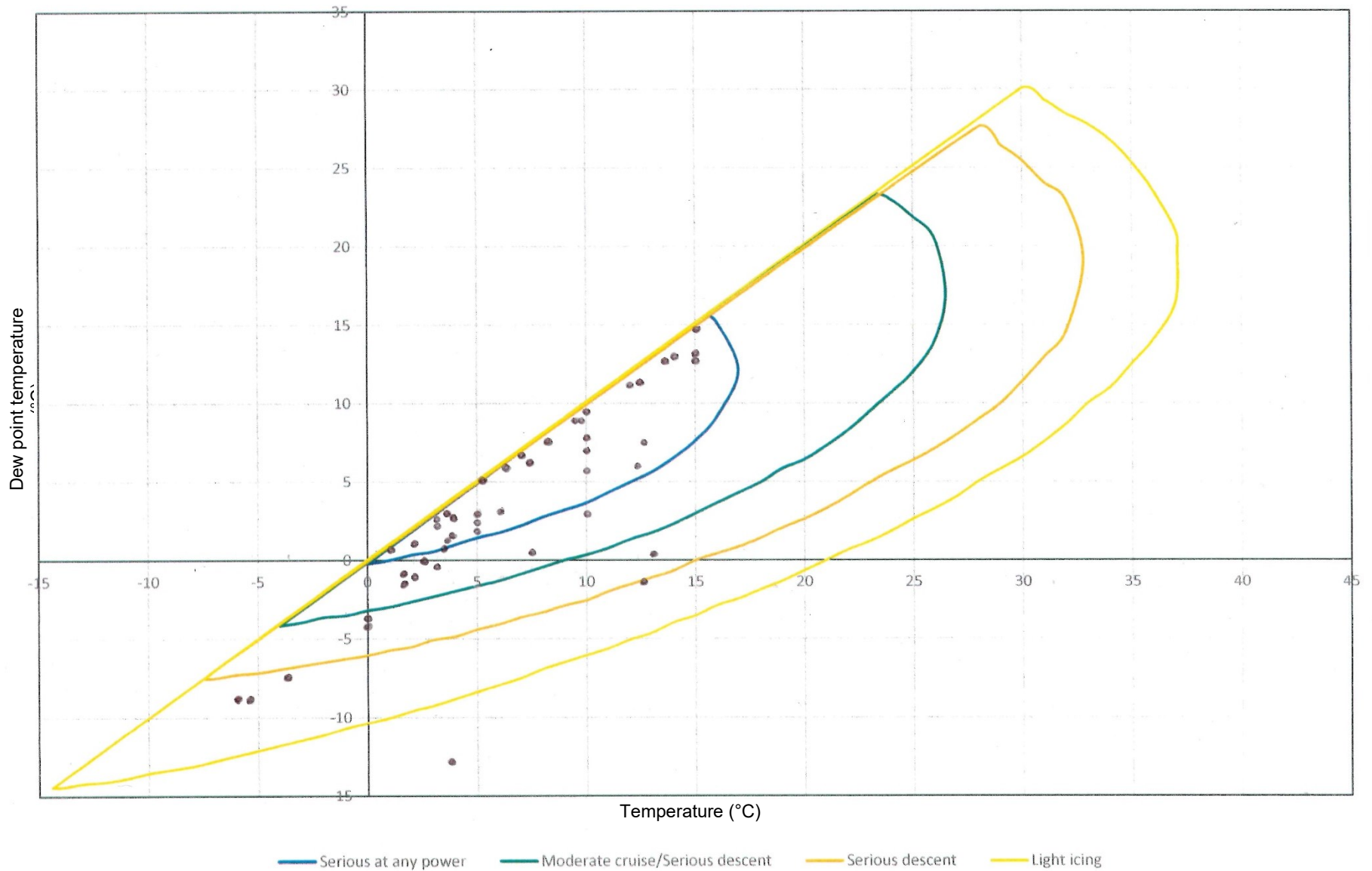


Figure 102: position of the test points on the graph proposed by the EASA
 Source: BEA

4.4.3. Observed occurrences of icing

Icing was observed during three test points only, during test phase two, when the carburettor was thermally insulated. The conditions associated with these three occurrences of icing are described in the following chapters. The third occurrence was identified during the data read-out, after the tests.

4.4.3.1 - 1st observed icing occurrence

Prior to engine start-up, the initial conditions were as follows:

- temperature in line with the air intake: between 3 and 4°C;
- relative humidity: approximately 87%;
- airspeed in line with the air intake: 80 kt.

This first icing occurrence is described below and is broken down into six phases.

Phase 1:

After engine start-up, the conditions were as follows:

Temperature (°C)	Relative humidity (%)	Dew point temperature (°C)	Engine speed (rpm)	Airspeed (kt)	Temperature of the outer surface of the carburettor (°C)	Temperature downstream of the butterfly (°C)
4°C	87%	2°C	1,500	80	5.5	-2.5

During this phase, the engine speed stabilised at 1,500 rpm.

The first symptoms were visual. A deposit of white ice formed very rapidly at the connection between the butterfly shaft and the butterfly, on one side (Figure 103). To facilitate understanding, this time is designated t_0 .



Figure 103: initiation of icing => time designated t_0
Source: BEA

The temperature of the outer surface of the carburettor and the temperature downstream of the butterfly valve decreased very slightly by around 1.5°C in the time period $[t_0, t_0 + 1 \text{ min}]$.

Ice gradually built up in the aforementioned zone. In addition, ice started to form on the other side of the butterfly valve. The figure below shows the situation at $t_0 + 2 \text{ min}$ (**Figure 104**). At this time, no modification of the engine speed and the EGT was observed.



Figure 104: progress of icing => time designated $t_0 + 2 \text{ min}$
Source: BEA

The formation of ice does not seem to follow a linear growth. Indeed, we note the amount of ice formed in the time period $[t_0, t_0 + 2 \text{ min}]$ is lower than that formed in the time period $[t_0 + 2 \text{ min}, t_0 + 4 \text{ min}]$ (**Figure 105**).



Figure 105: progress of icing => time designated t_{0+4min}
Source: BEA

A very slight decrease in engine speed of around ten revolutions was observed at $t_0 + 5 \text{ min } 43 \text{ s}$ (Figure 106). The decrease in engine speed reached around 50 to 60 rpm at $t_0 + 16 \text{ min}$ (Figure 107).



Figure 106: progress of icing => time designated $t_0 + 5 \text{ min } 43 \text{ s}$.
Source: BEA

The temperature of the outer surface and the temperature downstream of the butterfly increased linearly in the time period $[t_0 + 2 \text{ min}, t_0 + 10 \text{ min}]$, with different slopes. These temperature increases were associated with an increase in relative humidity of around 87% to 95%.

- The temperature of the outer surface of the carburettor increased from 5°C to 8°C during this time period.
- The temperature downstream of the butterfly valve rose from -4.5°C to -2°C.

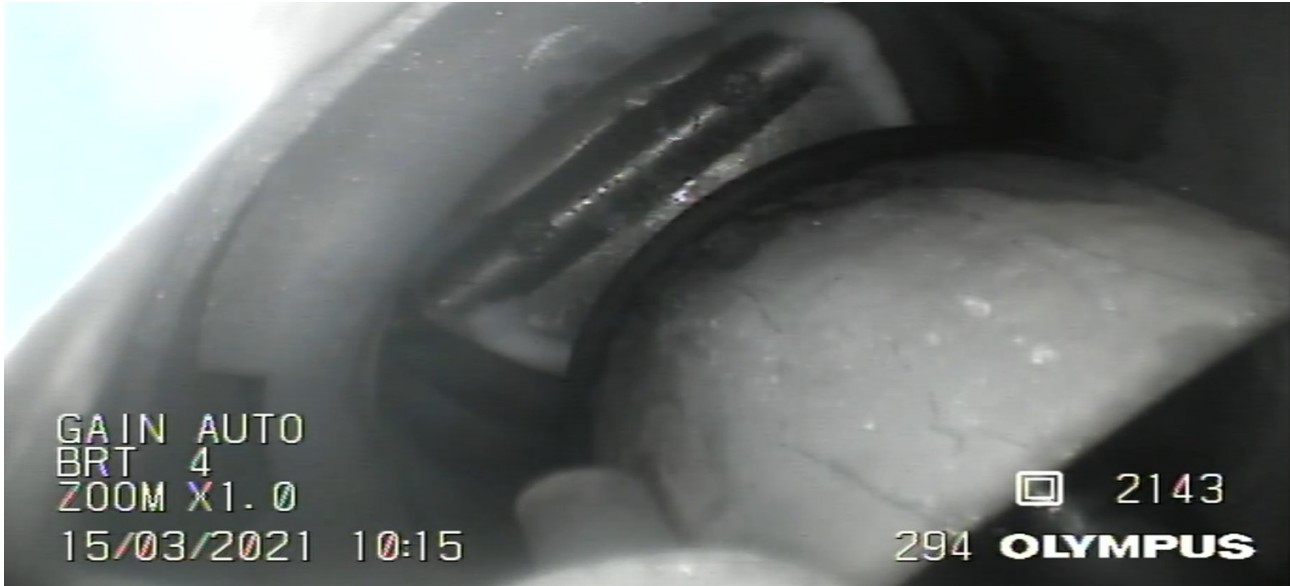


Figure 107: progress of icing => time designated $t_0 + 16\text{min}$
 Source: BEA

Phase 2:

During this phase, the engine speed rose to 1,700 rpm due to an input on the throttle lever. The time at which the speed rose to 1,700 rpm was designated t_1 (Figure 108).

The conditions were as follows:

Temperature (°C)	Relative humidity (%)	Dew point temperature (°C)	Engine speed (rpm)	Airspeed (kt)	Temperature of the outer surface of the carburettor (°C)	Temperature downstream of the butterfly (°C)
4°C	95%	3.2°C	1,700	80	10	-1.5

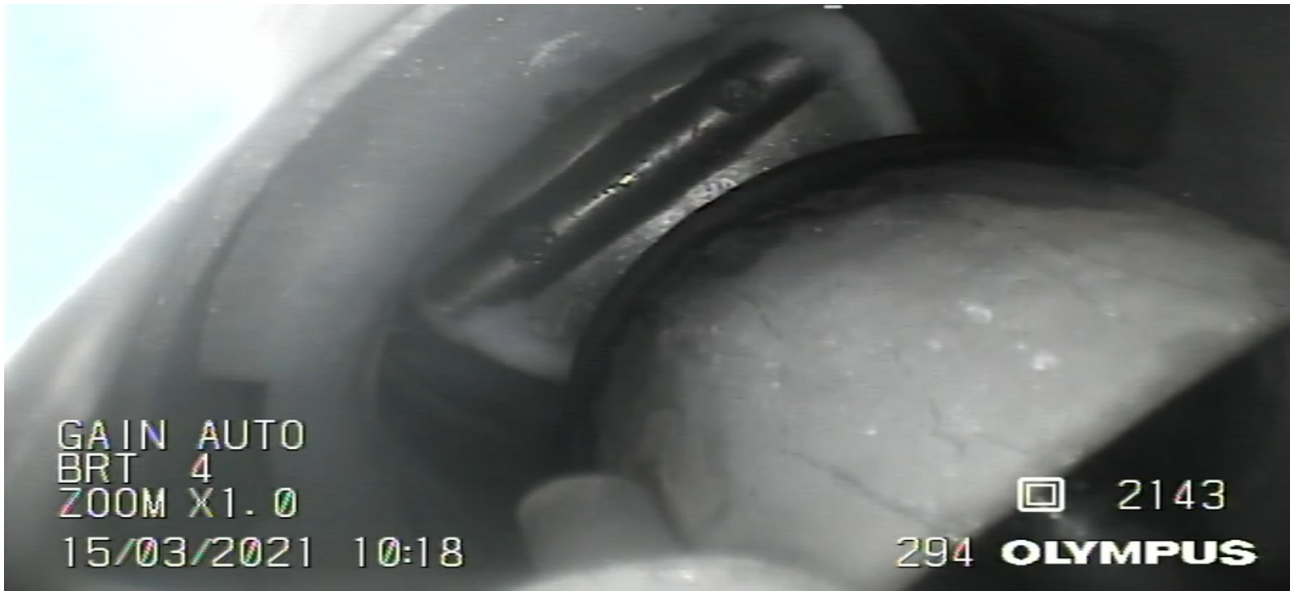


Figure 108: progress of icing => initiation of phase two => time designated t_1
 Source: BEA

When the speed reached 1,700 rpm, it started to decrease linearly. The speed decreased by 110 to 120 rpm during the time period $[t_1, t_1 + 11 \text{ min } 40 \text{ s}]$ (Figure 109).

During this same time period, the temperature of the outer surface and the temperature downstream of the butterfly increased linearly:

- the temperature of the outer surface increased by 1°C ;
- the temperature downstream of the butterfly valve rose by 0.5°C .

During this interval, the EGT decreased by around 80°C .



Figure 109: progress of icing => time designated $t_1 + 11\text{min}40\text{s}$
 Source: BEA

Phase 3:

During this phase, the engine speed rose to 1,700 rpm due to an input on the throttle lever.

The conditions were as follows:

Temperature (°C)	Relative humidity (%)	Dew point temperature (°C)	Engine speed (rpm)	Airspeed (kt)	Temperature of the outer surface of the carburettor (°C)	Temperature downstream of the butterfly (°C)
4°C	95%	3.2°C	1,700	80	10.5	-1

To facilitate understanding, the time at which the speed rose to 1,700 rpm was designated t_2 (Figure 110). At this time, the ends of the butterfly shaft and the outside edge of the butterfly were completely covered with ice.



Figure 110: progress of icing => initiation of phase three => time designated t_2
Source: BEA

As in phase two, when the speed reached 1,700 rpm, it started to decrease linearly. The speed decreased by 110 to 120 rpm during the time period $[t_2, t_2 + 7 \text{ min}]$ (Figure 111). The decrease in speed was more rapid than in phase two, which would suggest the non-linear formation of ice.



Figure 111: progress of icing => time designated $t_2 + 7$ min
 Source: BEA

The speed of 1,700 rpm was maintained for 18 minutes. We noted that the amount of visually identifiable ice appeared to stagnate from $t_2 + 7$ min. The EGT, the temperature of the outer surface and the temperature downstream of the butterfly remained stable.

Phase 4:

During this phase, the engine speed rose to 1,800 rpm due to an input on the throttle lever. The time at which the speed rose to 1,800 rpm due to an input on the throttle lever was designated t_3 (Figure 112).

The conditions were as follows:

Temperature (°C)	Relative humidity (%)	Dew point temperature (°C)	Engine speed (rpm)	Airspeed (kt)	Temperature of the outer surface of the carburettor (°C)	Temperature downstream of the butterfly (°C)
4°C	95%	3.2°C	1,800	80	10.5/11	0/-0.5



Figure 112: progress of icing => initiation of phase four => time designated t_3
Source: BEA

When the speed reached 1,800 rpm, it started to decrease linearly. The speed decreased by 80 to 90 rpm during the time period [t_3 , $t_3 + 3 \text{ min } 20 \text{ s}$] (Figure 113). The EGT, the temperature of the outer surface and the temperature downstream of the butterfly remained stable:

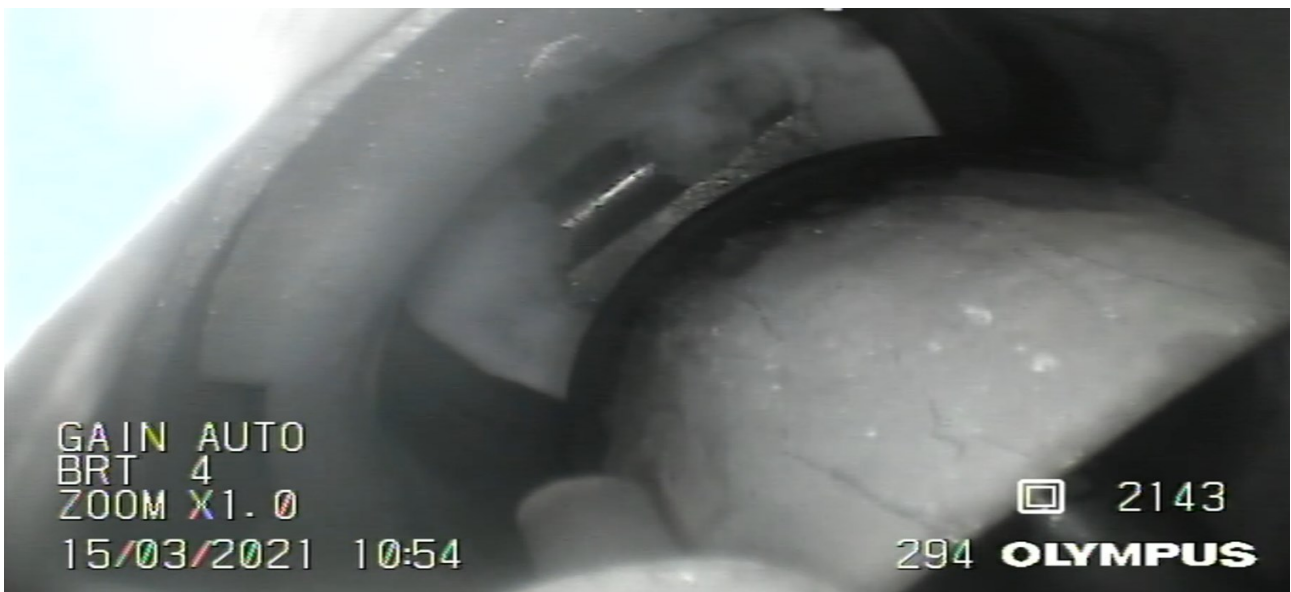


Figure 113: progress of icing => time designated $t_{3+3\text{min}20\text{s}}$
Source: BEA

Phase 5:

During this phase, the engine speed rose to 1,900 rpm due to an input on the throttle lever. The time at which the speed rose to 1,900 rpm due to an input on the throttle lever was designated t_4 .

The conditions were as follows:

Temperature (°C)	Relative humidity (%)	Dew point temperature (°C)	Engine speed (rpm)	Airspeed (kt)	Temperature of the outer surface of the carburettor (°C)	Temperature downstream of the butterfly (°C)
4°C	95%	3.2°C	1,900	80	10.5 to 11	0



Figure 114: progress of icing => initiation of phase five => time designated t_4
Source: BEA

When the speed reached 1,900 rpm, it started to decrease linearly. The speed decreased by 80 to 90 rpm during the time period $[t_4, t_4 + 4 \text{ min}]$ (Figure 115). The EGT, the temperature of the outer surface and the temperature downstream of the butterfly remained stable:



Figure 115: progress of icing => time designated $t_{4+4\text{min}}$
Source: BEA

Phase 6:

During this phase, the heat system was activated, without any input on the throttle lever.

To facilitate understanding, the following times were designated:

- $t_{5:5}$: immediately before activation of the heat system (Figure 116);
- t_6 : time when no fragments of ice could be seen (Figure 119);
- t_7 : deactivation of the heat system.

The following time periods were identified:

- $[t_5, t_6] = 11$ s;
- $[t_5, t_7] = 21$ s.



Figure 116: designated time t_5
Source: BEA



Figure 117: designated time $t_5 + 4$ s
Source: BEA



Figure 118: designated time $t_5 + 7$ s
Source: BEA



Figure 119: designated time t_6
Source: BEA

When the heat system was activated, there was an abrupt decrease in speed of around 150 rpm. The speed then increased very rapidly (without any input on the throttle lever):

- at t_5 , the speed was 1,800 rpm;
- at t_6 , the speed was 2,090 rpm;
- after t_7 , the speed was 2,180 rpm⁶.

The graph to be used presents the changes in engine speed during this first occurrence of visible icing.

⁶ The engine speed after the ice had melted was markedly greater than the last speed established manually at the start of phase five. The engine power had effectively increased on several occasions despite the presence of ice, without knowing the equivalent position of the throttle lever without icing. The post-icing engine speed was then unknown.

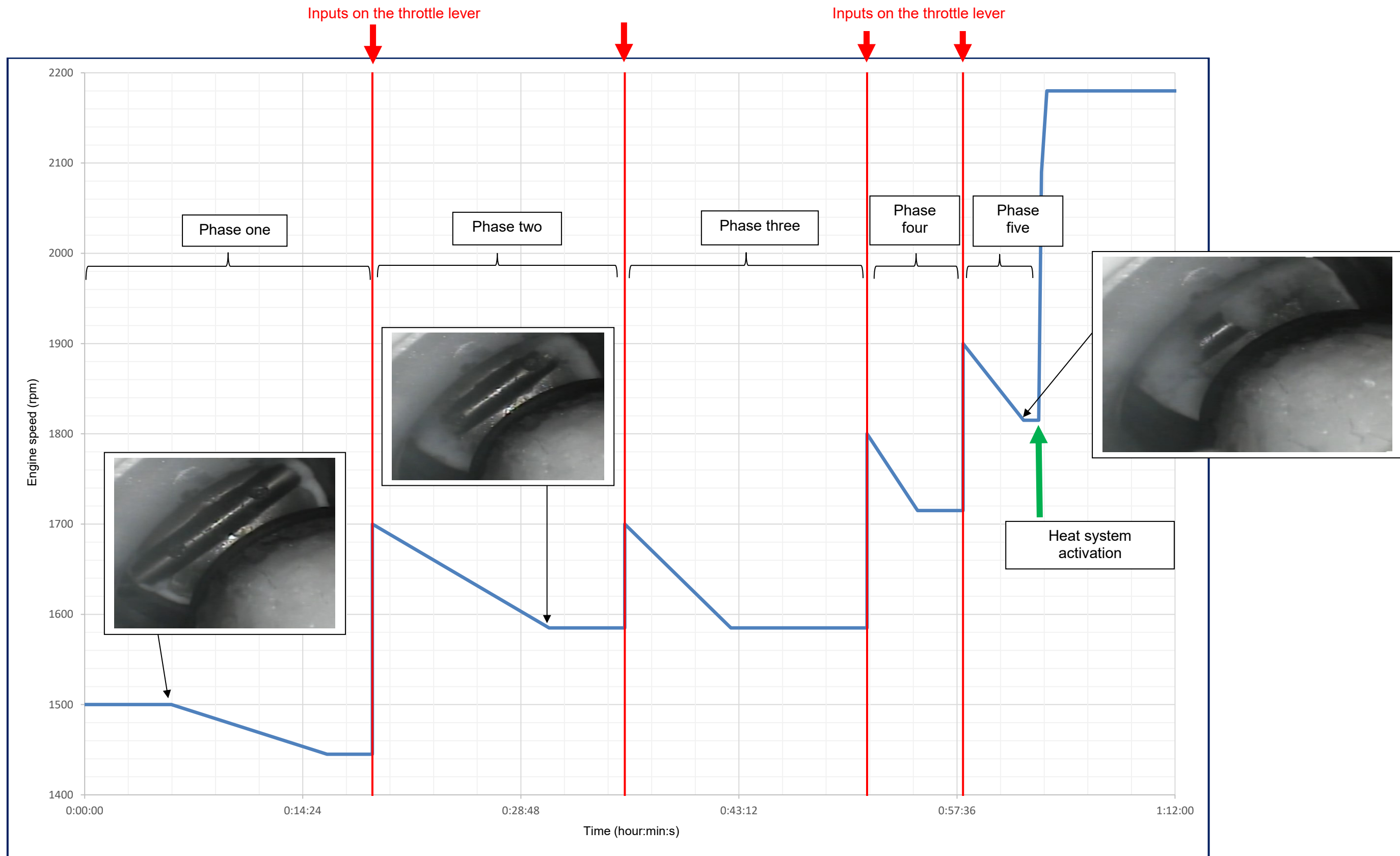


Figure 120: variation in engine speed during the 1st identified occurrence of icing
 Source: BEA

4.4.3.2 - 2nd observed icing occurrence

Prior to engine start-up, the fixed conditions were as follows:

- temperature in line with the air intake: between 3 and 4°C;
- relative humidity; approximately 90%;
- airspeed in line with the air intake: 80 kt.

The various phases of this test are summarised in the table below:

Phases	Air temperature in line with the air intake (°C)	Relative humidity (%)	Airspeed in line with the air intake (kt)	Engine speed (rpm)	Comments
1	3.5 to 4	90 to 95	80	1,500	The observations, the change in the temperature of the outer surface and the change in temperature downstream of the butterfly valve were identical to those described in the previous chapter, during phase one.
2	3.2 to 3.7	93 to 94	80	1,830	When the speed had increased again, it started to decrease linearly. The speed decreased by 170 to 180 rpm during a period of around three minutes. During this period, the temperature of the outer surface increased by around 1°C. The temperature downstream of the butterfly valve remained relatively constant. This phase continued for around five minutes.
3	3.4 to 3.8	93 to 95	80	2,000	When the speed had increased again, it started to decrease linearly. The speed decreased by around 120 rpm during a period of around three minutes. During this period, the temperature of the outer surface increased by around 0.5°C. The temperature downstream of the butterfly valve remained relatively constant. The amount of visible ice no longer increased and some fragments broke away. The temperature of the outer surface was around 1°C higher than that measured during the 1 st observed occurrence of icing described above.
4	3.5 to 3.8	93 to 95	80	1,800	This phase lasted for seven minutes. The amount of visible ice no longer increased. No variation in speed was measured.
5	3.5 to 3.7	94 to 95	80	1,700	This phase lasted for five minutes. The amount of visible ice no longer increased. No variation in speed was measured.
6	3.5 to 3.8	94 to 95	80	2,000	The amount of ice increased for approximately four minutes and 45 seconds. During this period, the speed decreased by around 60 rpm. The temperature of the outer surface and the temperature downstream of the butterfly valve remained constant. The ice melted after around 10 minutes of operation in the considered conditions, without activation of the heat system. After the ice had melted, the speed increased by 150 rpm, without any input on the throttle lever. The temperature of the outer surface and the temperature downstream of the butterfly valve remained constant. Before the ice disappeared, the temperature of the outer surface was around 1°C higher than that measured during the 1 st observed occurrence of icing described above.

4.4.3.3 - 3rd observed icing occurrence

Ice was observed from time to time in the following conditions (Figure 121). Ice did not develop and melted without modifying the conditions after around nine minutes and 30 seconds.

Temperature (°C)	Relative humidity (%)	Dew point temperature (°C)	Engine speed (rpm)	Airspeed (kt)	Temperature of the outer surface of the carburettor (°C)	Temperature downstream of the butterfly (°C)
3.4 to 4.1	82 to 83	0.6 to 1.4	1,700	80	14.4 to 15.2	-1.7 to -0.3

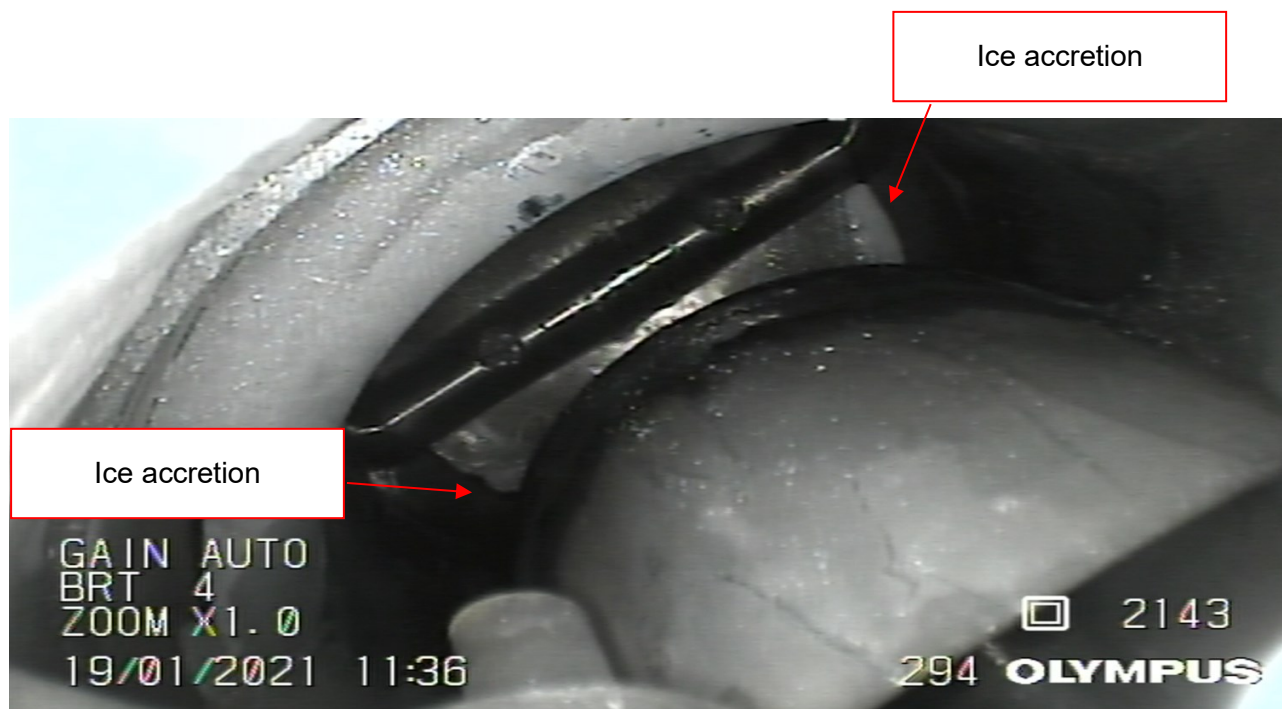


Figure 121: ice present on the edge of the butterfly valve
Source: BEA

4.4.3.4 - Another phenomenon

Rime ice was identified on several occasions on the outer surface of the venturi (Figure 122). This ice formation was very localised and superficial. During this phenomenon, no other ice formation was observed.

This formation of rime ice was identified during the very rapid increase in speed, beyond 2,000 rpm. During this increase in speed, the variation in temperature downstream of the butterfly valve was the parameter that varied the most. We noted an immediate decrease in this temperature of 3 to 9°C depending on the configurations.

After it had formed, the rime ice did not develop. It melted almost immediately as the speed decreased.

This phenomenon had no observable impact on engine operation.



Figure 122: presence of rime ice on the outer surface of the venturi
Source: BEA

4.4.3.5 - Conclusion

The formation of ice in line with the butterfly valve was only rendered possible after thermal insulation of the carburettor in relation to the exhaust muffler. This observation suggests the importance of the temperature of the carburettor body.

Without thermal insulation of the carburettor, icing was not observed.

The ice that formed in line with the butterfly valve was associated with an unstable icing phenomenon, heightened by low and established engine speeds. The initiation and development of icing required a significant operating time of around a few minutes.

When icing had initiated, maximum decreases in speed of around 150 rpm were observed within a few minutes.

When the heat system was activated, the formed ice melted almost instantly and was accompanied by a very brief decrease in speed followed by an increase in this speed.

4.4.4. Identification of parameters contributing to the phenomenon of icing in the carburettor

4.4.4.1 - Temperature of the outer surface of the carburettor and temperature downstream of the butterfly

- **Change as a function of the airspeed in line with the air intake:**

The temperature of the outer surface of the carburettor and the temperature downstream of the butterfly valve increases when the airspeed in line with the air intake increases, and vice versa (Figure 123).

The figure below illustrates the decrease in temperatures when the airspeed changes from 98.8 kt to 81 kt at a given engine speed, a given relative humidity and a given air temperature in line with the air intake (1,900 rpm, 82% and 4°C).

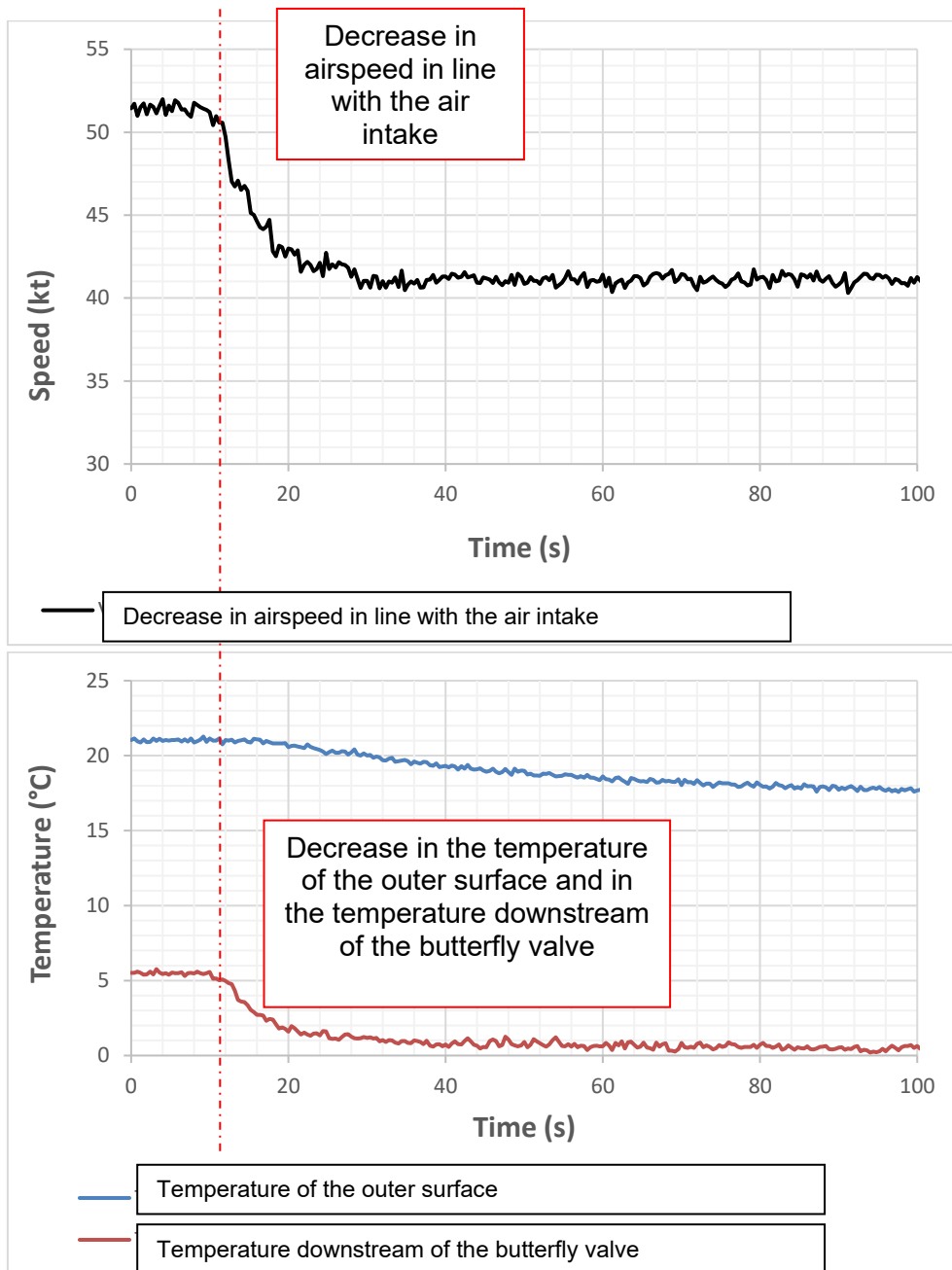


Figure 123: change in the temperature of the outer surface and the temperature downstream of the butterfly valve as a function of the airspeed in line with the air intake

Source: BEA

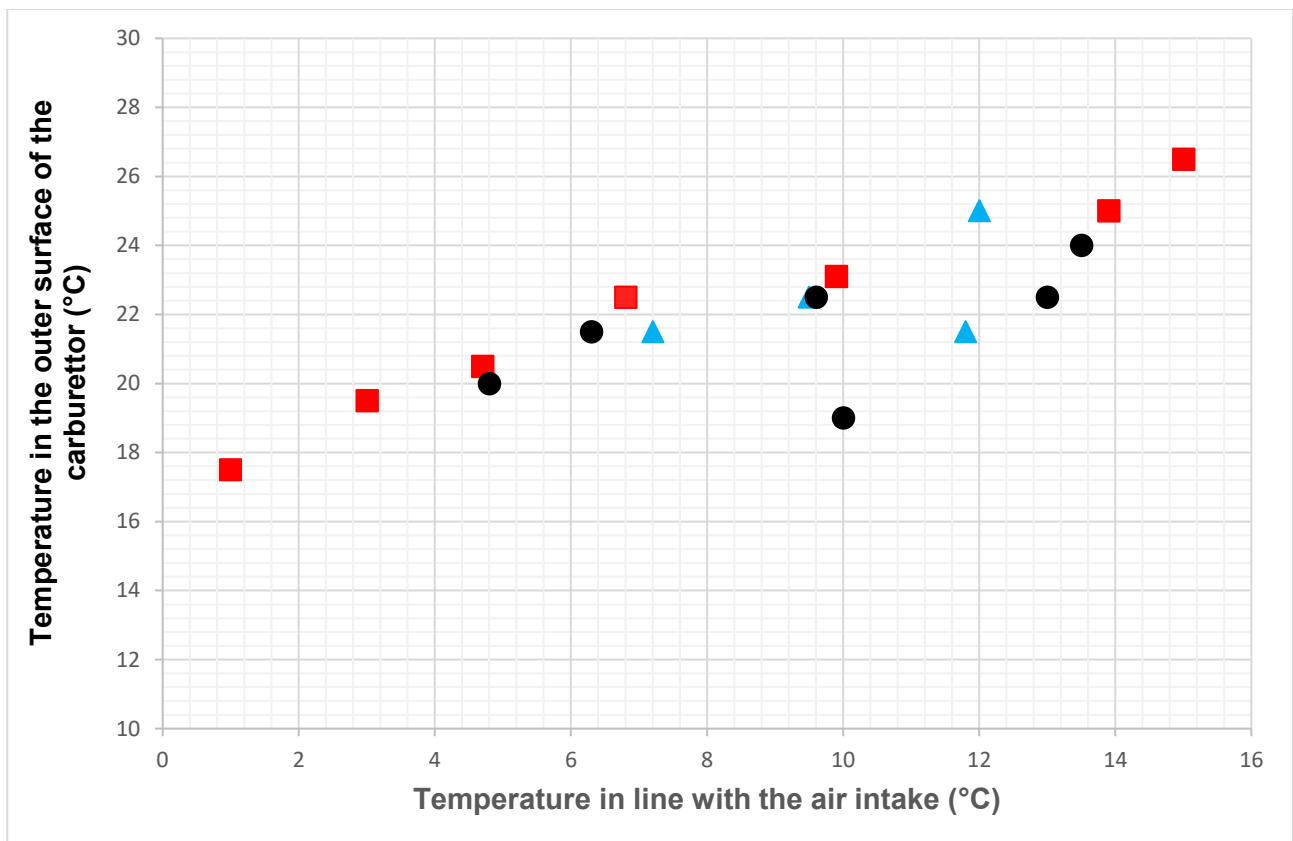
The temperature of the outer surface systematically presents a profile of very gradual change, suggestive of a certain inertia. In the case illustrated above, the temperature decreased by around 3.5°C, from 20.8 to 17.5°C in one minute and 45 seconds.

The temperature downstream of the butterfly valve changed more abruptly, with a profile practically similar to that of the speed graph. In the case illustrated above, the temperature decreased by around 4°C, from 5.3 to 1°C in 25 seconds.

- **Change as a function of the temperature of the air in line with the air intake:**

The general trend suggests that the temperature of the outer surface and the temperature downstream of the butterfly increase when the temperature of the air in line with the air intake increases, and vice versa.

Figure 124 and **Figure 125** below illustrate the change in the temperature of the outer surface and the temperature downstream of the butterfly valve when the temperature of the air in line with the air intake changes, at various engine speeds, with a relative humidity of around 97 to 99% and an airspeed in line with the air intake of around 100 kt.



Key:




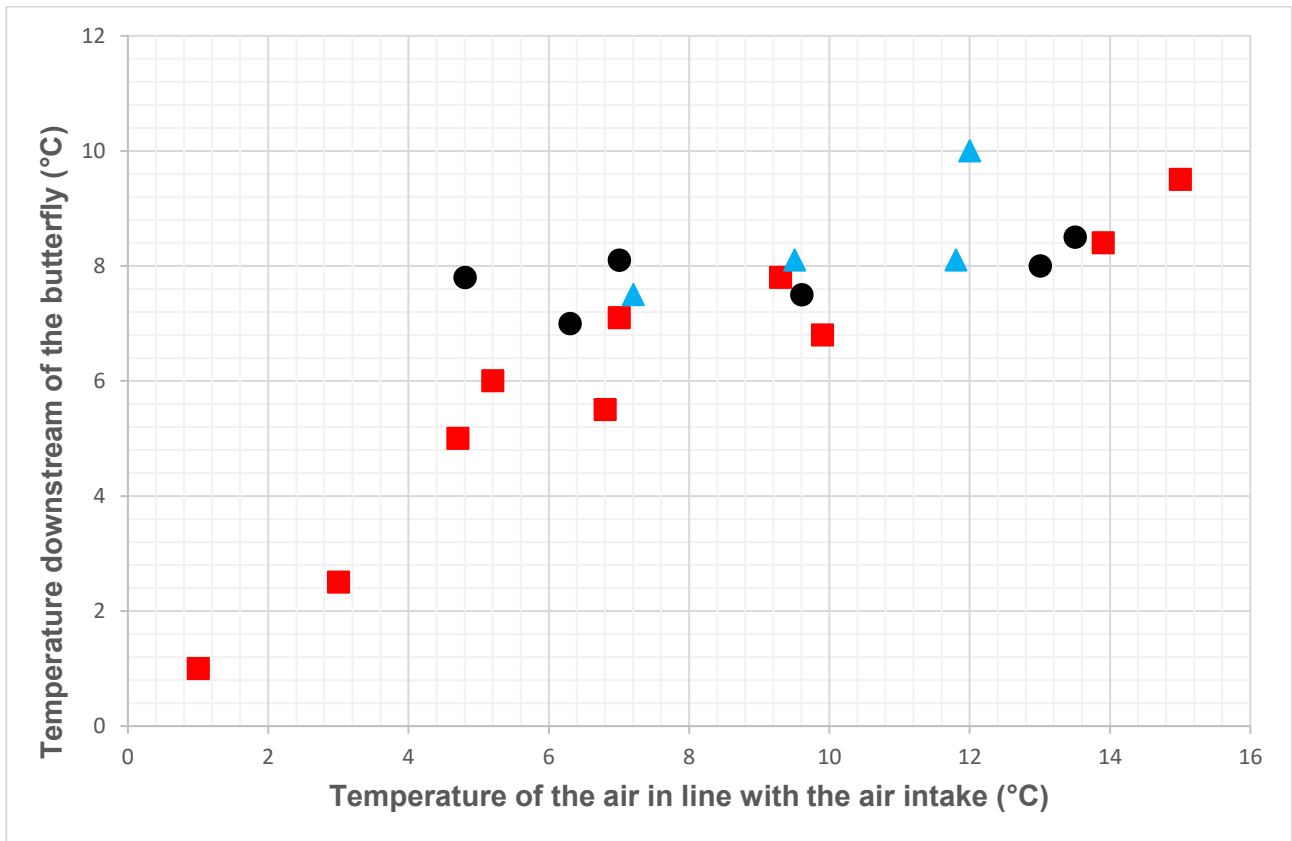
	1,700 rpm
	1,900 rpm
	2,100 rpm

Figure 124: change in the temperature of the outer surface as a function of the temperature in line with the air intake (relative humidity of around 97 to 99%, airspeed in line with the air intake of around 100 kt).



Key:




	1,700 rpm
	1,900 rpm
	2,100 rpm

Figure 125: change in the temperature downstream of the butterfly valve as a function of the temperature in line with the air intake (relative humidity of around 97 to 99%, airspeed in line with the air intake of around 100 kt).

Figure 126 illustrates the variation in temperature of the outer surface and the temperature downstream of the butterfly valve during a test session.

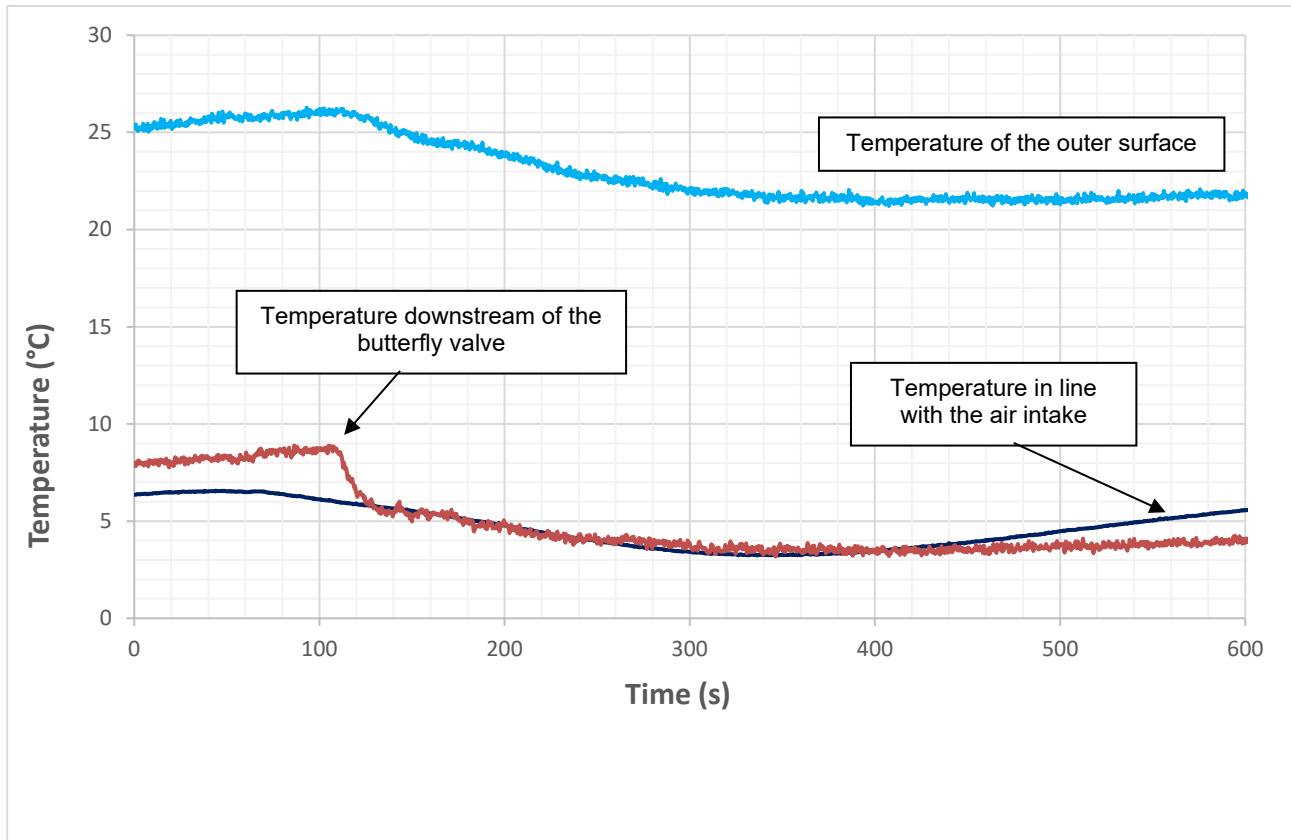


Figure 126: change in the temperature of the outer surface and the temperature downstream of the butterfly valve as a function of the temperature in line with the air intake

- **Change as a function of the relative humidity:**

The test points did not result in an exact and precise definition of the influence of relative humidity. The few points that could be used seem to suggest:

- an influence clearly less impactful than that of the temperature in line with the air intake;
- that the temperature of the outer surface and the temperature downstream of the butterfly valve increase when the relative humidity increases, and vice versa.

5 - POWERPLANTS EQUIPPED WITH A ROTAX ENGINE

5.1. Rotax engines considered

This document considers the following Rotax (*) engines:

- 912 Series engines equipped with carburetors (**Figure 127**);
- 914 Series engines (**Figure 128**).

(*) only engines with a composition as provided by Rotax are considered. Modifications not specified by Rotax and their consequences on the operation of the propulsion system are not considered.

These engines are four-cylinder boxer, four-stroke, mixed air (cylinders) - water (cylinder heads) cooled engines. They are currently used on microlights, light aeroplanes and some drones.

The difference between the 912 Series and the 914 Series is the addition of a turbocharger.

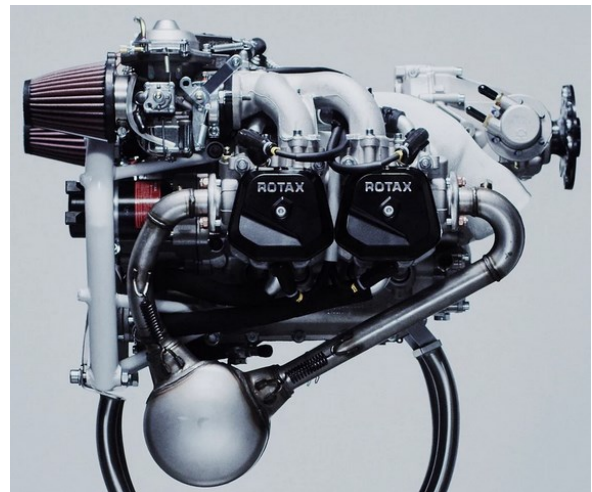
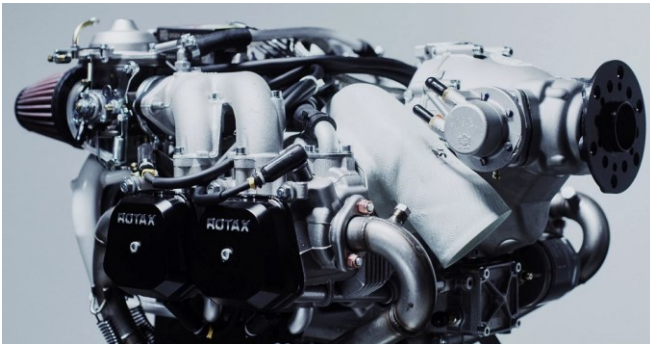


Figure 127: Rotax 912 Series engine
Source: <https://www.flyrotax.com/fr/products/912-ul-a-f>

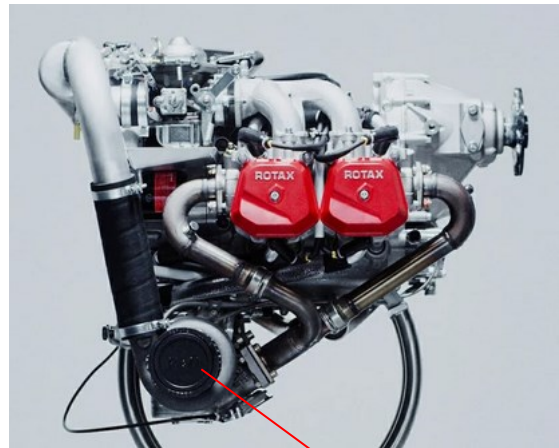
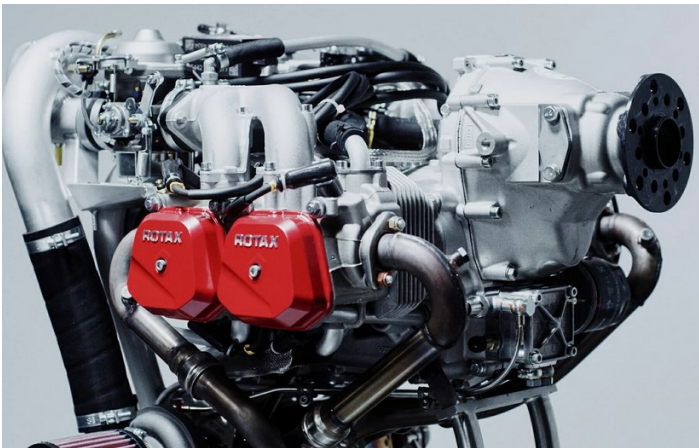
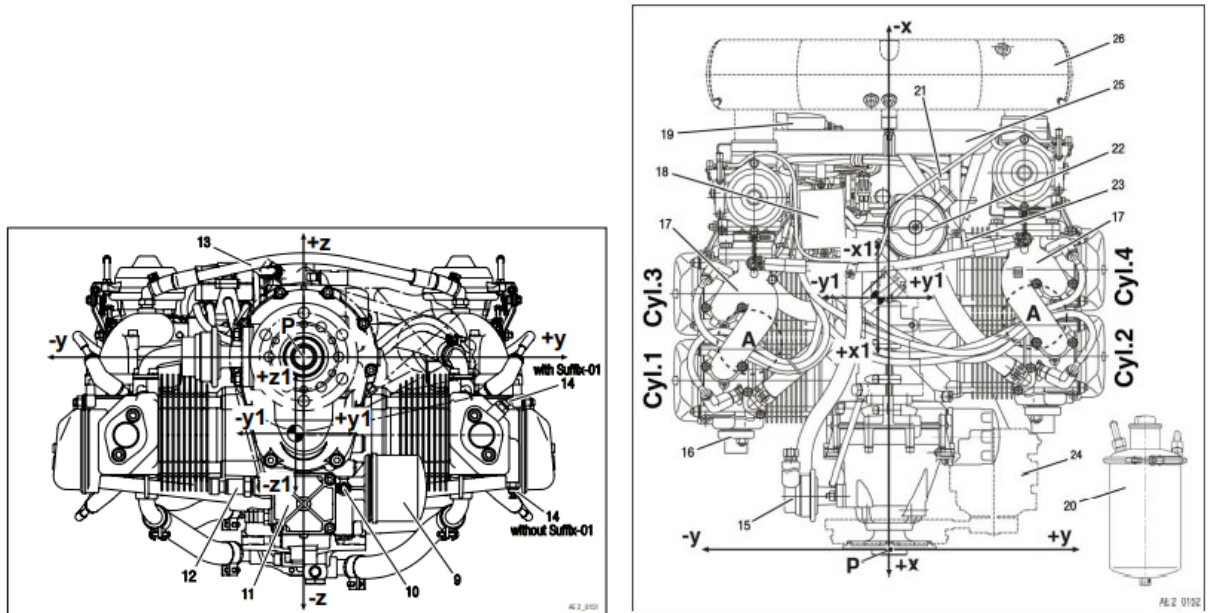
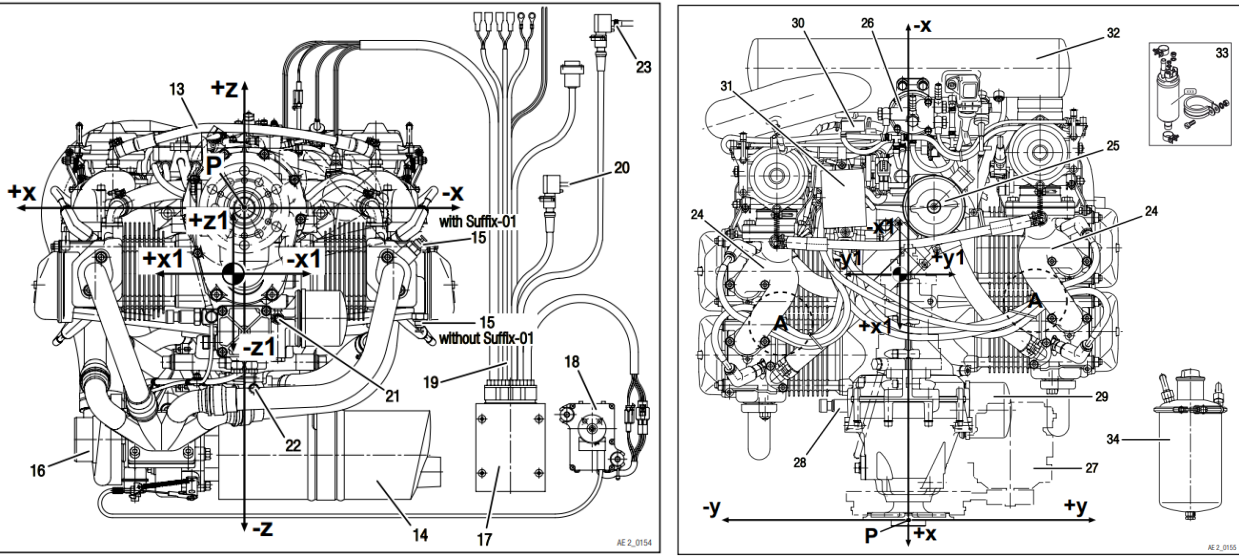


Figure 128: Rotax 914 Series engine
Source: <https://www.flyrotax.com/fr/products/914-ul-f>

The tables below list the main characteristics of these engines.

The parts common to these two engine series are: the technology of the engine unit, the ignition system, the cooling system, the lubrication system and the reduction gearbox.

However, the fuel system equipping these two engine series is technologically different.

	912 Series	914 Series
Cylinder capacity	1,211 or 1,352 cm^3 depending on the versions	1,211 cm^3
Dry weight	57.1 to 61 kg depending on the versions	70 to 74.4 kg depending on the versions
Dimensions	 <p>Source: Rotax documentation - Installation Manual - version updated on 28.01.2022</p> <p>On the \vec{x} axis = 589.5 mm max On the \vec{y} axis = 576 mm max On the \vec{z} axis = 394 mm max</p>	 <p>Source: Rotax documentation - Installation Manual - version updated on 28.01.2022</p> <p>On the \vec{x} axis = 665.1 mm max On the \vec{y} axis = 576 mm max On the \vec{z} axis = 531 mm max</p>
Fuels	MOGAS (recommended) or AVGAS 100LL When using MOGAS, RON (Research octane number = represents the performance of a fuel at low speed and in acceleration) values are given: <ul style="list-style-type: none"> 912 Series: min RON 90 or min RON 95 depending on the versions 914 Series: min RON 95 	
Compression ratio	9 :1 or 10.8 :1 depending on the versions	9 :1
Performance	Take-off = 80 to 100 hp depending on the versions Max continuous = 78 to 90 hp depending on the versions 75% = 58 to 68 hp depending on the versions 65% = 50 to 60 hp depending on the versions 55% = 43 to 50 hp depending on the versions	Take-off = 115 hp Max continuous = 100 hp 75% = 74 hp 65% = 64 hp 55% = 54 hp
Direction of rotation	clockwise	
Rotation speeds	Take-off = 5,800 $tr.min^{-1}$ Max continuous = 5,500 $tr.min^{-1}$ Min idle = 1,400 $tr.min^{-1}$	

912 Series

Consumption:

- take-off = 24 or 27 $l \cdot h^{-1}$
- max continuous = 22.6 or 25 $l \cdot h^{-1}$
- 75% = 16.2 or 18.5 $l \cdot h^{-1}$

Fuel pressure:

- maximum = 0.4 bars
- minimum = 0.15 bars

The powerplant comprises a restricted section of the aeroplane's fuel system: both carburettors and a mechanical pump.

The carburettors are Bing 64/3 models, which are covered in more detail in the next chapter. The carburettors are positioned in the upper section of the engine, on either side of its longitudinal axis.

The schematic diagram of a fuel system associated with this type of engine is presented below:

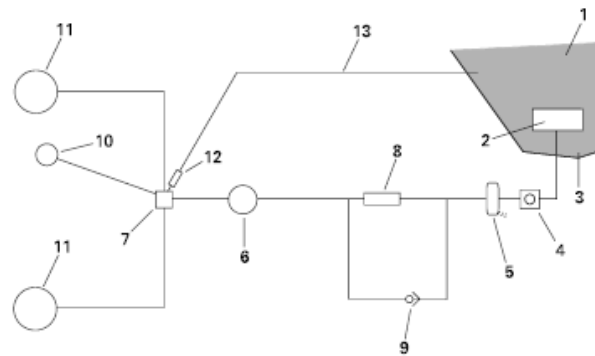


Figure 129: fuel system diagram

Source: Rotax Documentation - Installation Manual - version updated on 28.01.2022

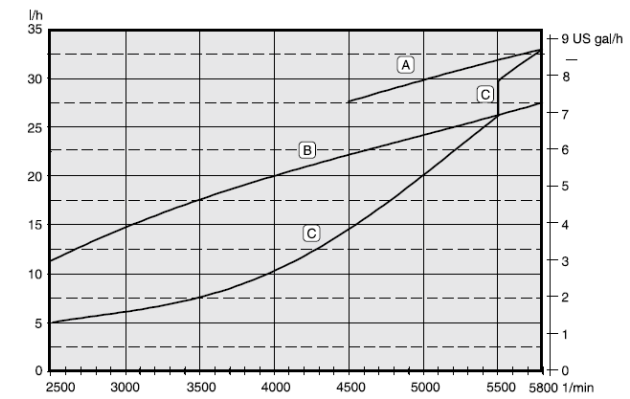
Key:

1	Tank	8	Electric pump
2	Strainer	9	Bypass
3	Drain	10	Pressure gauge
4	Valve	11	Carburettors
5	Filter	12	Reduction gear
6	Mechanical pump	13	Fuel return line
7	Pressure controller		

Fuel system

914 Series

Consumption:



- A: engine curve (take-off)
- B: engine curve (max continuous)
- C: curve of power required for the propeller

Fuel pressure:

- maximum = Airbox Pressure + 0.35 bars
- minimum = Airbox Pressure + 0.15 bars
- normal = Airbox Pressure + 0.25 bars

The schematic diagram of the fuel system is presented below. The carburettors are Bing 64/3 models, which are covered in more detail in the next chapter.

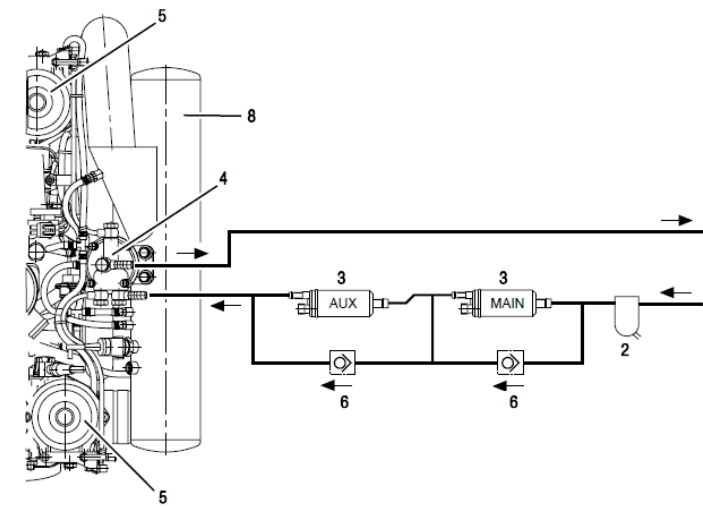


Figure 130: fuel system diagram

Source: Rotax Documentation - Installation Manual - version updated on 28.01.2022

Key:

1	Supply	5	Carburettor
2	Filter	6	Bypass
3	Electric pump	7	Return
4	Pressure regulator	8	Airbox

Oil pressure:

- maximum = 7 bars
- minimum = 0.8 bars if <3,500 rpm
- normal = 2 to 5 bars

Oil temperature:

- maximum = 140°C or 130°C
- minimum = 50°C

Maximum consumption = 0.06 l.h⁻¹

Oil grades that can be used at an OAT of between 0 and 20°C: SAE 15W50, SAE 15W40, SAE 10W40, SAE 10W30

The engines are equipped with a forced lubrication system with a dry casing and a main oil pump with an integrated pressure regulator.

Lubrication system

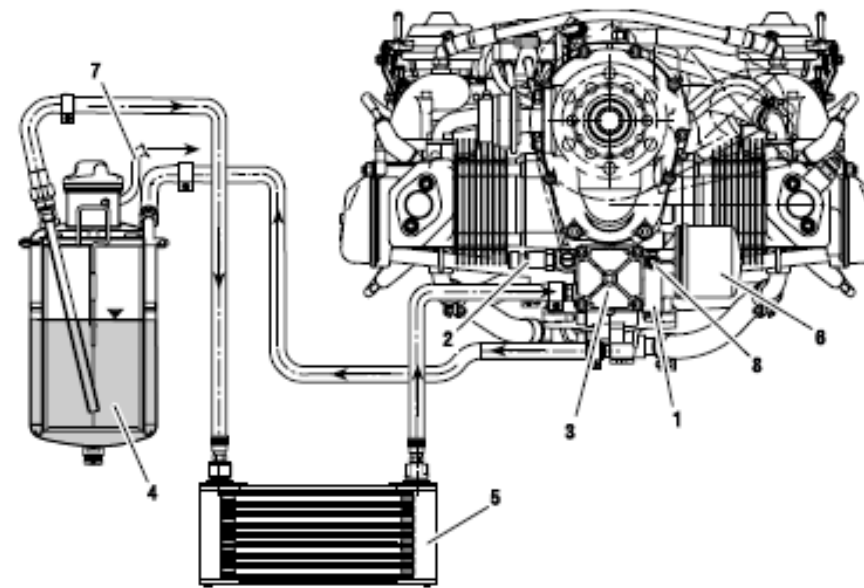


Figure 131: lubrication system diagram

Source: Rotax Documentation - Installation Manual - version updated on 28.01.2022

Key:

1	Pressure regulator	5	Cooler
2	Pressure sensor	6	Filter
3	Pump	7	Vent
4	Tank		

On 914 Series engines, the turbocharger is lubricated via a separate oil duct (coming from the main oil pump). Oil coming from the turbocharger collects in a small casing and is sucked towards the pump, then pumped to the main oil tank via the oil duct.

Ignition

Ignition sequence: 1-4-2-3

The ROTAX engine is equipped with a dual capacitor discharge ignition system with integrated generator.

The system therefore comprises:

- an integrated generator located behind the engine;
- two electronic ignition units;
- four coils;
- harnesses;
- two spark plugs per cylinder.

The schematic diagram of the system is presented below:

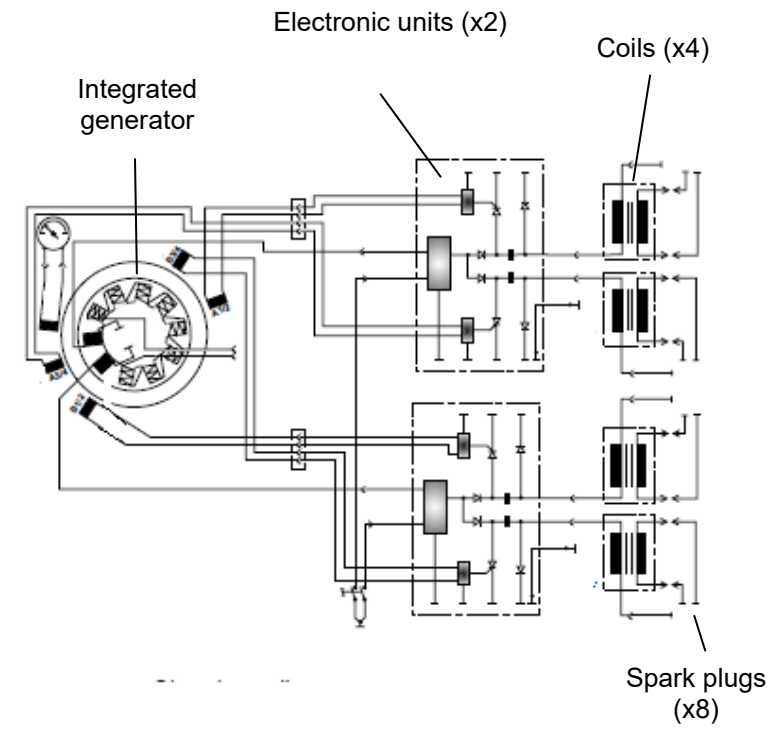


Figure 132: diagram of the ignition system

Source: Rotax documentation - Operator Manual - version updated on 28.01.2022

912 Series

914 Series

The engine cooling system is designed to cool the cylinder heads with liquid and to cool the cylinders with dynamic air. The cylinder head cooling system is a closed system with an expansion tank as illustrated in the diagram below.

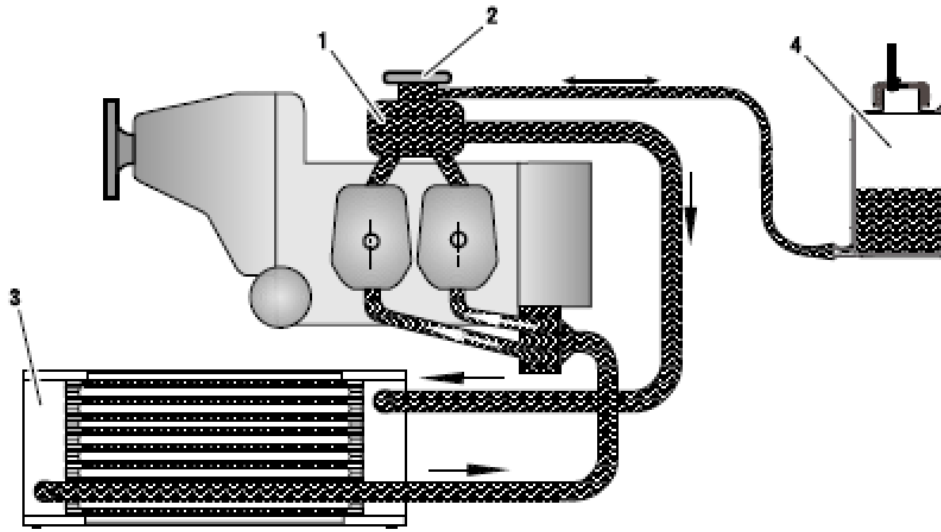


Figure 133: diagram of the cooling system

Source: Rotax documentation - Installation Manual - version updated on 28.01.2022

Key:

1	Expansion tank	3	Cooler
2	Pressure plug	4	Overflow tank

Cooling system

Reduction gear

Each engine is equipped with a reduction gearbox with a reduction ratio of 2.27 :1 or 2.43 :1 depending on the versions.
The majority of the reduction gearboxes are equipped with a torque reducing system. The objective of this type of system is to limit the torque on the crankshaft in case the propeller makes contact with the ground.

Each engine is equipped with a reduction gearbox with a reduction ratio of 2.43 :1.
The majority of the reduction gearboxes are equipped with a torque reducing system. The objective of this type of system is to limit the torque on the crankshaft in case the propeller makes contact with the ground.

Turbocharger

The engine is equipped with a turbocharger using the energy contained in the exhaust gases to pre-charge the intake air (boost pressure).
This boost pressure in the Airbox is controlled using a bleed valve associated with the turbine section of the turbocharger. This valve is opened and closed by a TCU (Turbocharger Control Unit).

5.2. Presentation of types of powerplants

Powerplants equipped with Rotax 912 and 914 Series engines vary greatly.

These engines can be installed on conventional three-axis aircraft in the forward position, under the cowlings. For the 912 Series engines in this configuration, there are two types of carburettor air supply:

- Type 1:
Each carburettor is equipped with an air filter. The air that is sucked in by the engine is the air present under the cowlings. This air is renewed by the air intakes that differ in size and position depending on the aircraft. The position of these air intakes in relation to the carburettors also differs depending on the aircraft.
In this case, the air that is therefore sucked in by the engine is a mix of outside air and the air heated in the engine environment.

Powerplant installed on a TECNAM P92

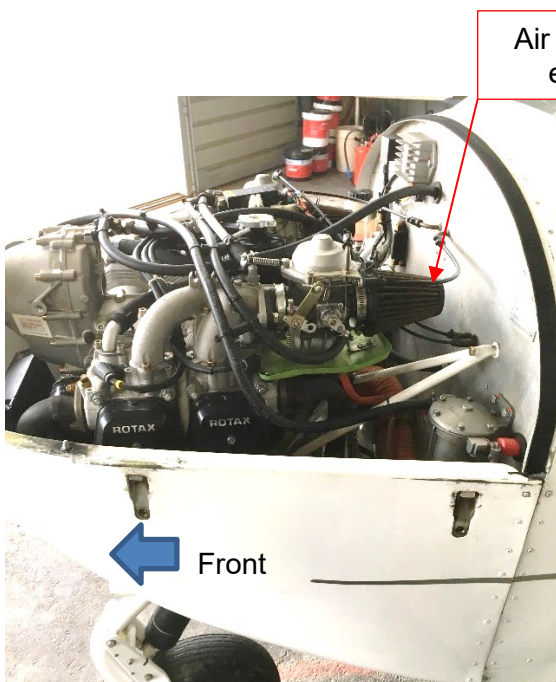


Figure 134: side view of the propulsion system

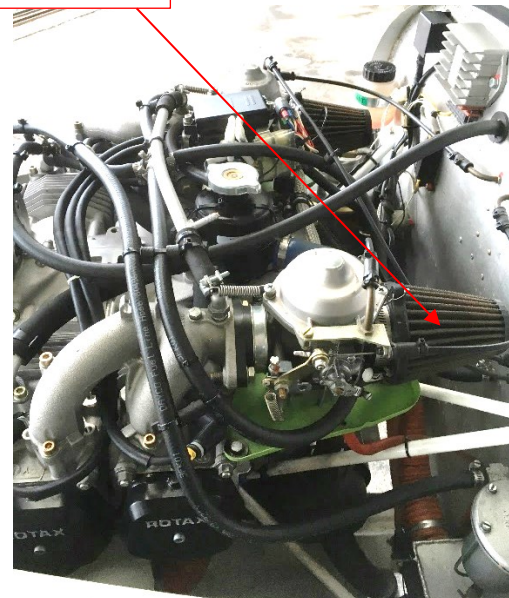
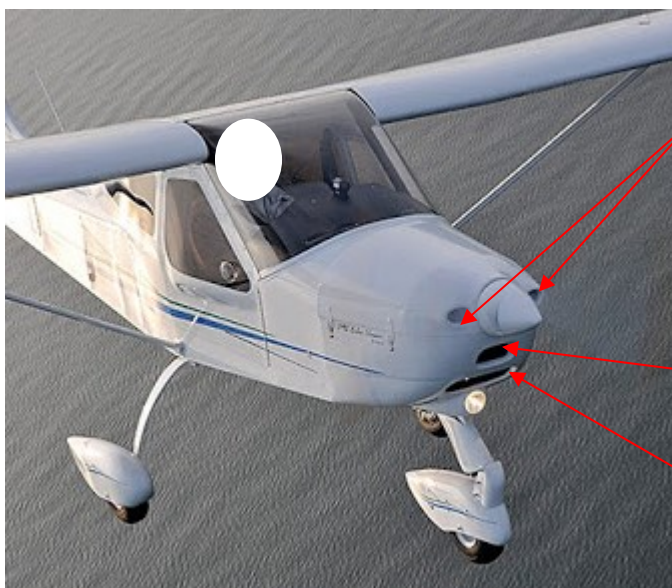


Figure 135: view from above of the propulsion system



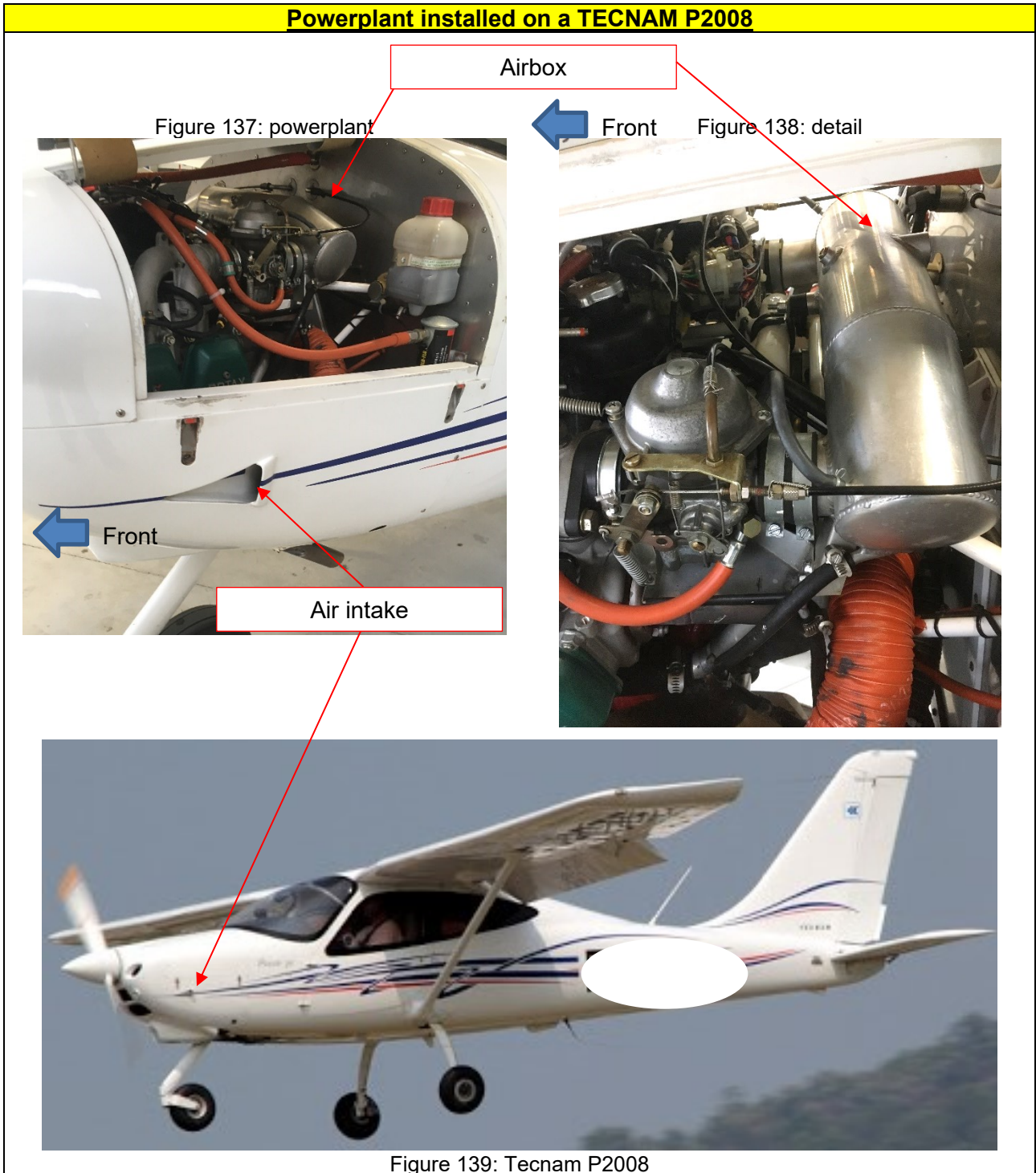
Air inlets

Inlet for the lubrication system cooler

Inlet for the cooling system cooler

Figure 136: Tecnam P92

- Type 2:
 Each carburettor is connected to an Airbox located just behind the carburettors, along the length of the firewall. This Airbox is connected via a flexible hose to an air intake. The air that is sucked in by the engine is the outside air. This type of powerplant enables installation of a system to heat the air supplied to the carburettors. The process consists in introducing air heated around the exhaust muffler into this Airbox. For 914 Series engines, only this configuration is used.



These engines can also be installed on aircraft with a powerplant in *Push* configuration (pusher propeller) or in very specific configurations (e.g. above the airframe, secured by a mast). The engine may or may not be positioned under cowlings.

The *Push* configuration more particularly applies to gyroplanes.

The two types of carburettor air supply described above, which equip the 912 series, are associated with this configuration.



Source: <https://www.flywhale.fr/>



Source: <http://www.magnigyro.it/fr/produits/m16-tandem-trainer/>



Source: <http://www.magnigyro.it/fr/produits/m24-orion/>



Source: <http://www.locagyro.com/gamme-ela>



Source: <https://www.flickr.com/photos/jeanpierredewam/33093079968>

Figure 140: various powerplant configurations

5.3. Presentation of the 912 and 914 Series carburetors

The Rotax 912 and 914 Series engines are equipped with two Bing 64/3 carburetors (Figure 141).

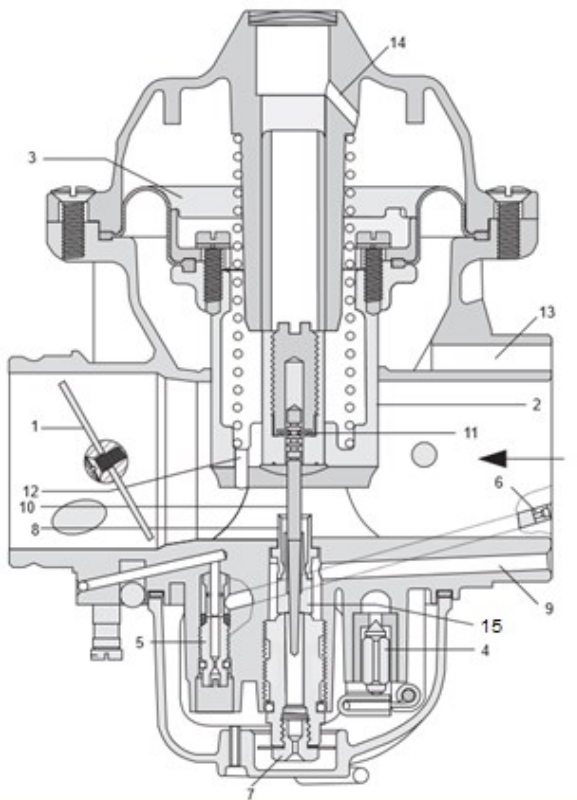


Figure 141: outside view of a Bing 64/3 carburettor

Source: <https://www.gyros-evasion.com/fr/carburateurs/508-carburateur-bing-64-pour-moteur-4-temps-rotax.html>

The Bing 64/3 carburettor is a constant depression carburettor (refer to chapter 3.2 for its operating principle).

The diagram below shows a sectional view of the carburettor with its components (Figure 142).



Key:

1	Butterfly valve
2	Throttle valve
3	Diaphragm
4	Needle valve
5	Idle jet
6	Idle jet air duct
7	Main nozzle
8	Diffuser tube
9	Main nozzle air duct
10	Needle
11	Elastic ring
12	Duct carrying air to the upper chamber
13	Duct carrying outside air to the lower chamber
14	Air duct
15	Needle jet

Figure 142: sectional view of the carburettor

Source: Rotax

5.4. Icing prevention systems

Three types of systems were identified:

- On powerplants equipped with an Airbox, the most common solution consists in introducing heated air that has circulated around the exhaust muffler. The arrival of this heated air is controlled by the pilot in the cabin using a pull-type control that activates a flap as shown in the diagram below.

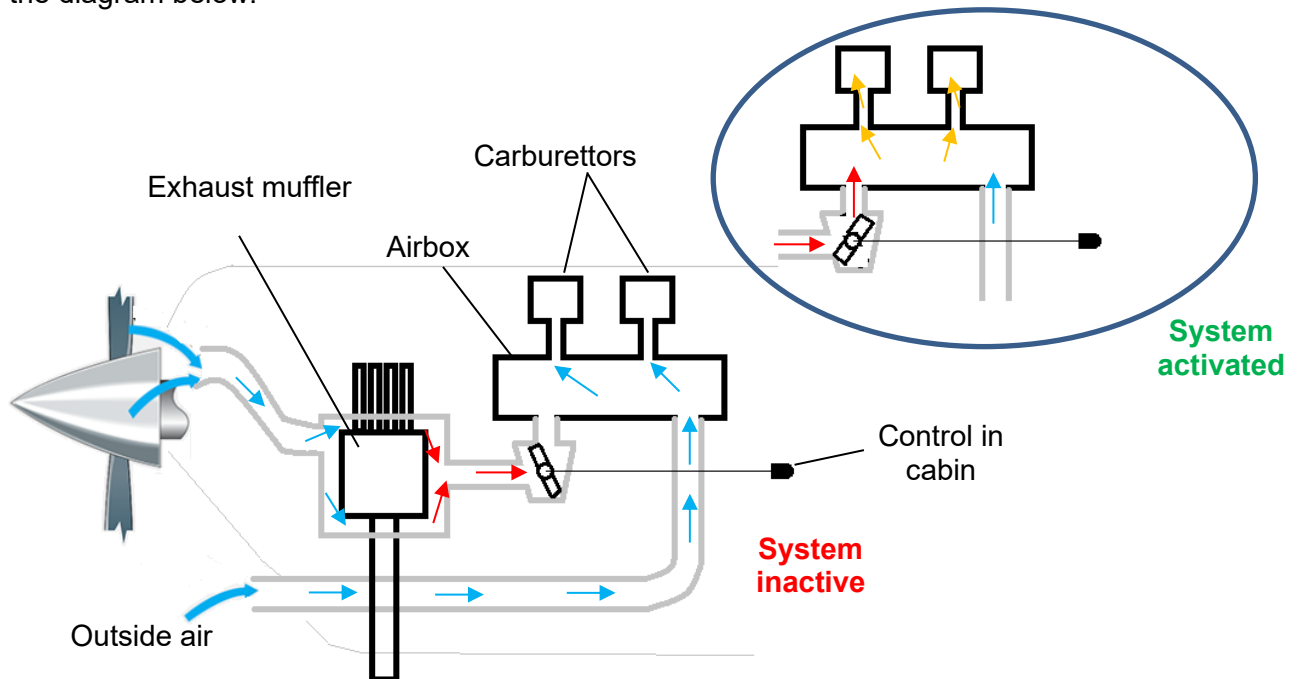


Figure 143: schematic diagram of the system

Source: BEA

- The second system consists in circulating coolant around the carburettor outlet section in which the butterfly valve is located (Figure 144). This heated coolant is used to keep the zone in question at a temperature that is high enough to prevent ice forming. This type of system is proposed by a number of equipment manufacturers, although not by Rotax.

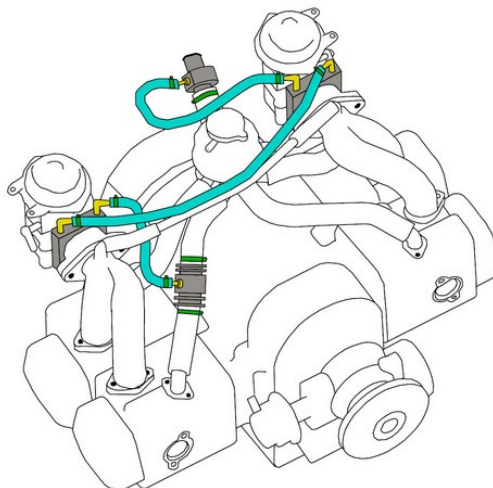


Figure 144: schematic diagram of the system

Source: <https://www.aero-parts.eu/PBSCProduct.asp?itmID=29290872>

- The third system consists in positioning heat resistors on the outer surface of the carburetors. This solution is clearly used to a very limited extent.



Figure 145: positioning of the heat resistor on the outer surface of the carburettor

Source: <https://mcr01passion.forumperso.com/t66-qivrage-carburateur-rotax>

5.5. Publications

5.5.1. Aircraft manufacturer

This research consisted in identifying information pertaining to the phenomenon of induction system icing and provided by aircraft manufacturers in their flight manuals. Thirty-one different aircraft manuals were looked at; 27 concerned three and four-axis aircraft and four concerned gyroplanes. These aircraft are listed in the following tables.

The reading of these manuals showed the following:

- No flight manual refers to a document about icing by an authority.
- The information published in these manuals can vary greatly and can be very limited or non-existent. The technical contents can differ from manual to manual.
- Fourteen manuals (45%) do not refer to this phenomenon.
- Eight manuals (25%) list the most common symptoms of icing (decrease in power, decrease in RPM, vibration, increase in temperature of the engine) and, in most cases, indicate the use of the heat system and the importance of exiting the zone in question.
- Six manuals (19%) contain a whole chapter on icing. In most of these cases, this chapter is divided into two sections:
 - section one lists the symptoms of icing, including the most common symptoms as listed above;
 - section two corresponds to a power restoration procedure.

In three cases, this procedure is similar in terms of the following points:

- indication of a speed, which varies between 80 and 130 km/h depending on the aircraft;
- the throttle lever in the 1/3 position, then a gradual increase after one to two minutes;
- if possible, the need to exit the zone in question;
- if the speed does not increase, a precautionary landing is recommended.

In the other three cases, the information is variable. In two cases, the probability of such a phenomenon occurring is very unlikely due to the powerplant.

- The temperature ranges in which icing is likely to occur are indicated in four manuals. The temperatures differ:
 - Case 1: phenomenon usually occurring between 5 and 15°C.
 - Case 2: phenomenon can occur at temperatures of around 10°C.
 - Case 3: phenomenon can occur when the temperature falls below 10°C.
 - Case 4: minimise the flight time between -5 and 5°C.

Manufacturer	Aircraft	Engine	Version of the manual used	Information published
Aero Ltd	Skyranger	912 UL	December 2006	None
Aeroprakt	A22LS	912 UL or 912 ULS	?	None
Aeropro	Eurofox	912 UL, 912 ULS, 912 iS and 914 UL	?	The manual contains a whole chapter on icing. The contents of this chapter are as follows: <ul style="list-style-type: none"> • Icing usually occurs when the temperature is between 5 and 15°C. • The symptoms of the phenomenon are: a decrease in power, a decrease in speed and an increase in temperature of the engine. • The power restoration procedure is as follows: <ul style="list-style-type: none"> - speed: 80 - 90 km/h IAS; - position of the throttle lever at 1/3 (around 3,500 RPM); - descend, when possible; - gradually increase the power after one to two minutes; - if power is not restored, prepare for a precautionary landing.
Aeroservices Guépard	Super Guépard	912 UL or 912 ULS		None
Aerospool	WT9 Dynamic	912 ULS	December 2011	It is simply indicated that a decrease in performance or an irregular operation of the engine can be caused by icing.
Aquila	AT01	912 S3	February 2003	It is simply indicated that if icing is identified, the heat system must be used. Recommendations on operating the system is presented.
Gyroplane	Calidus		March 2016	It is indicated that a decrease in speed and vibrations can be symptoms of icing. If icing is identified, continued full power and a change in altitude are requested.
Gyroplane	MTO sport 2010	912 ULS or 914 UL	February 2016	
Gyroplane	MTO sport 2017		April 2018	
ATEC v.o.s.	Zephyr	912 UL or 912 ULS	April 2001	None
BRM aero	Bristell LSA	912 ULS	July 2011	The manual contains a whole chapter on icing. The contents of this chapter are as follows: <ul style="list-style-type: none"> • The symptoms of the phenomenon are: a decrease in power and an increase in engine temperature. • The power restoration procedure is as follows: <ul style="list-style-type: none"> - speed: 70 kt IAS; - position of the throttle lever at 1/3; - descend, when possible; - gradually increase the power after one to two minutes; - if power is not restored, prepare for a precautionary landing.
BRM Land Africa	Okavango	912 UL or 912 ULS	January 2010	None
Comco Ikarus	C42	912 UL or 912 ULS	June 2019	It is simply indicated that if icing is identified (decrease in speed, increase in fuel consumption, vibration), the heat system must be used and a change in altitude must be made.
Czech sport aircraft	PS28 cruiser	912 S2	June 2014	It is simply indicated that if icing is identified (decrease in power and increase in temperature), the heat system must be used.
DTA	J-RO	912 ULS or 914	December 2012	It is simply indicated that if icing is identified (decrease in power, fluctuating speed and vibrations), the heat system must be used, the speed must not be decreased and a change in altitude must be made.
Dynaero	MCR 4S	912 S or 914	August 2003	None
Ekolot	Topaz	912 UL	May 2017	None
Ekolot	JK-05L Junior		September 2001	None

Manufacturer	Aircraft	Engine	Version of the manual used	Information published
Evektor	Eurostar SL	912 UL or 912 ULS	February 2008	The manual contains a whole chapter on icing. The contents of this chapter are as follows: <ul style="list-style-type: none"> • The symptoms of the phenomenon are: a decrease in power and an increase in engine temperature. • The power restoration procedure is as follows: <ul style="list-style-type: none"> - speed: 60 kt IAS; - position of the throttle lever at 1/3; - descend, when possible; - gradually increase the power after one to two minutes; - if power is not restored, prepare for a precautionary landing.
FKlightplanes	FK14B	912 ULS or 912 iS	October 2015	None
Flight design	CT2K	912 UL or 912 ULS	June 2005	It is simply indicated that if icing is identified, the heat system must be used.
Humbert Aviation	Tetras	912 UL	January 2004	The manual contains a whole chapter on icing. The contents of this chapter are as follows: <ul style="list-style-type: none"> • The type of carburettor used and its position prevents icing. • If icing is identified, the engine must be at full power.
I.C.P.	Savannah	912 UL, 912 ULS or 912 iS	August 2012	None
Issoire Aviation	APM 20 Lionceau	912 A2	December 2010	It is simply indicated that if icing is identified, the heat system must be used and the engine must be at full power.
Pipistrel	Virus SW	912 UL or 912 ULS	January 2009	The manual contains a whole chapter on icing. The contents of this chapter are as follows: <ul style="list-style-type: none"> • The symptoms of the phenomenon are: a decrease in power and a low-frequency engine noise. • Icing can occur at temperatures of around 10°C. • The risk of icing is low as the air intake is located near the cooling system cooler, thus increasing the temperature. • If icing is identified, a change in altitude must be made or a precautionary landing must be performed in the event of complete loss of power.
Rans Aircraft	S-6S Coyote II	912 UL	October 1993	None
Tecnam	P92	912 UL or 912 ULS	February 2007	None
Tecnam	P2008	912 S2	July 2013	The manual contains a whole chapter on icing. The contents of this chapter are as follows: <ul style="list-style-type: none"> • Icing can occur when the speed is low, visibility is poor and the temperature is below 10°C. • If icing is identified, the procedure is as follows: <ul style="list-style-type: none"> - activate the heat system; - exit the zone in question; - increase the engine speed.
Tomark Aero	Viper SD4	912 ULS	February 2017	It is indicated that a decrease in power and a modification of the mixture can be symptoms of icing. To prevent icing, flight time must be minimised between -5 and 5°C and a heat system must be used.
Van's Aircraft	RV12	912 ULS	June 2018	None
Zenair	Zodiac CH650B	912 UL or 912 ULS	June 2012	None

5.5.2. Rotax

This research consisted in identifying information pertaining to the phenomenon of icing and provided by the manufacturer Rotax in its various manuals. The manuals used were systematically the most recent versions (March 2020) available at:

<https://www.flyrotax.com/services/technical-documentation.html>.

For each engine series, 912 and 914, the information identified is published in the following manuals:

- installation manual;
- operator manual;
- maintenance manual.

here is the information common to both engine series published in these manuals:

- Icing is a common cause of engine malfunction.
- Icing can occur in the venturi and the butterfly valve due to fuel evaporation. This results in a decrease in power and a modification of the mixture.
- The only effective solution against this phenomenon is the heat system. However, the latter causes a decrease in performance due to the lowering of the resultant air density.
- The presence of water in the fuel can cause ice to form in the pipes, filters and injectors.

For 914 Series, it is specified that this type of engine does not normally require a heat system due to the use of the turbocharger, which naturally heats the air taken into the carburetors.

5.5.3. Articles, websites and forums

Only two scientific articles dealing with in-flight tests performed on aircraft equipped with Rotax engines were identified. These two articles were published by the same author, and these works were published as part of studies conducted at Poland's Military University of Technology. These articles are as follows:

Article
Author: Ryszard Chachurski Date of publication: 2008 INVESTIGATION OF SUSCEPTIBILITY TO ICING OF AIRCRAFT PISTON ENGINE ROTAX 447 UL SDCI https://www.google.com/url?sa=t&rct=j&q=&esrc=s&source=web&cd=&cad=rja&uact=8&ved=2ahUKEwi248PpyKz2AhWk4YUKHSB_JBgkQFnoECAUQAQ&url=https%3A%2F%2Fyadda.icm.edu.pl%2Fyadda%2Felement%2Fbwmeta1.element.baztech-article-BUJ5-0034-0007%2Fc%2Fhttpwww_bg_utp_edu_plartjok32008jo20kones20200820no20320vol201520chachurski.pdf&usq=AOvVaw3wsslxnrY9kQsXdjaZw7Qt
Author: Ryszard Chachurski Date of publication: 2016 IN-FLIGHT TESTING OF THE SUSCEPTIBILITY TO ICING OF THE INDUCTION SYSTEM OF THE ROTAX 582 ENGINE https://www.academia.edu/35612894/IN_FLIGHT_TESTING_OF_THE_SUSCEPTIBILITY_TO_ICING_OF_THE_INDUCTION SYSTEM OF THE ROTAX 582 ENGINE

In these studies, the following Rotax engine models are considered:

- Rotax 447;
- Rotax 582.



Figure 146: Rotax 447 engine
Source: Rotax



Figure 147: Rotax 582 engine
Source: Rotax

These two engines are in-line two-cylinder, two-stroke engines.

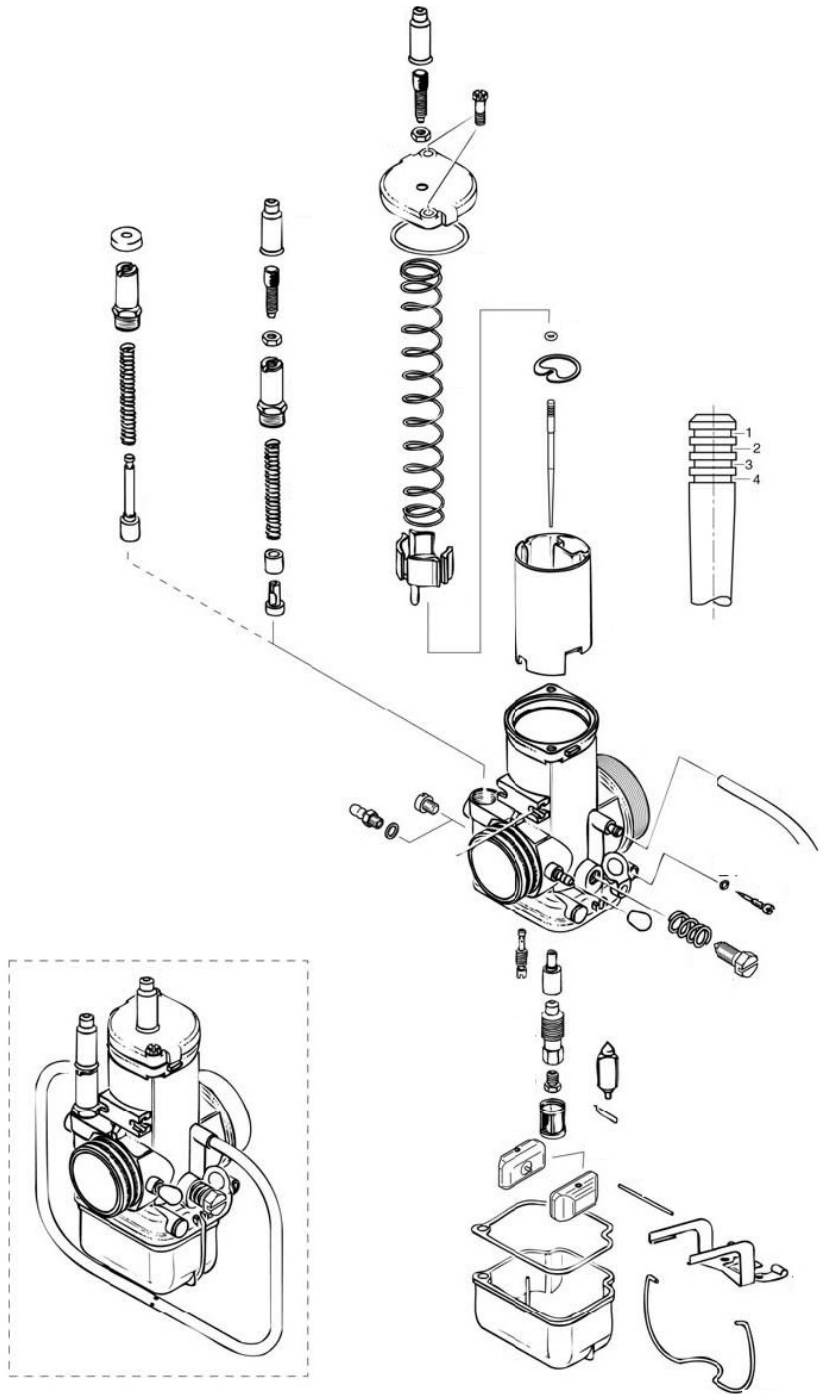
Model 447 is an air-cooled engine equipped with a Bing 54 carburettor.

Model 582 is a liquid-cooled engine equipped with two Bing 54 carburettors.

The Bing 54 carburettor is a constant depression carburettor. It differs from the Bing 64/3 model presented in chapter 7.3 due to the direct control of the throttle valve by the throttle lever.



Figure 148: outside view of a Bing 54 carburettor
Source: <https://www.finesse-max.com/rotax/1015-pointeau-de-carburateur-bing-54.html>



These articles present the results of measurements taken in flight. To take these measurements, the author installed thermocouples on the carburettor and in its direct environment. The diagram below shows the instruments used on a 582 engine carburettor.

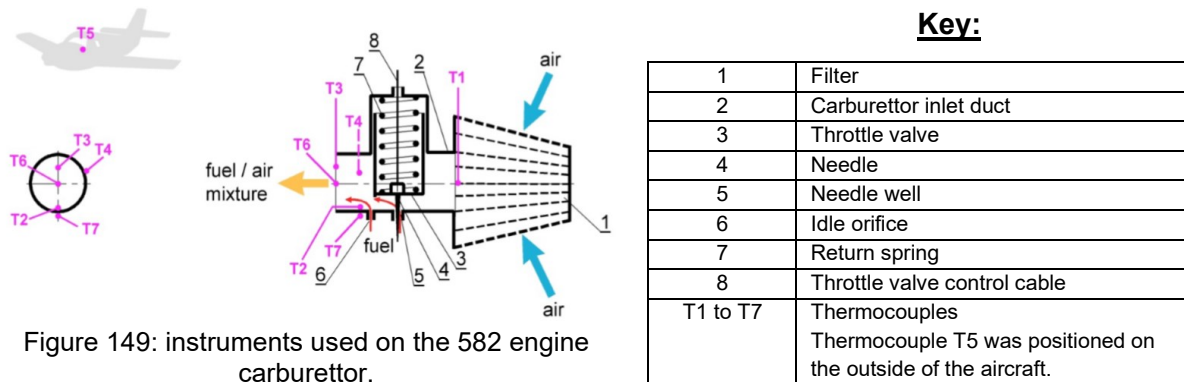


Figure 149: instruments used on the 582 engine carburettor.

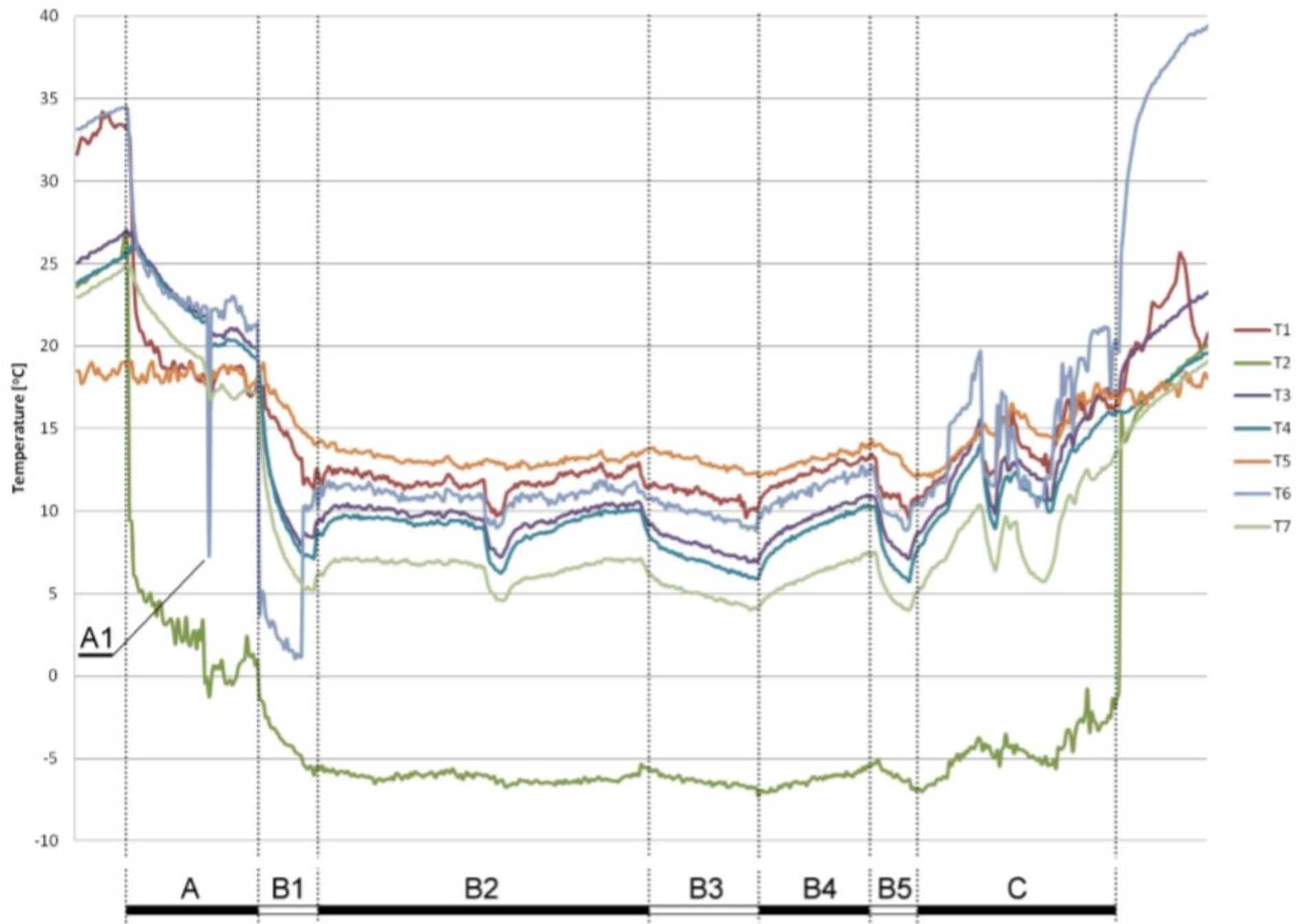
Source: *IN-FLIGHT TESTING OF THE SUSCEPTIBILITY TO ICING OF THE INDUCTION SYSTEM OF THE ROTAX 582 ENGINE* _ Ryszard Chachurski _ 2016

These tests showed that:

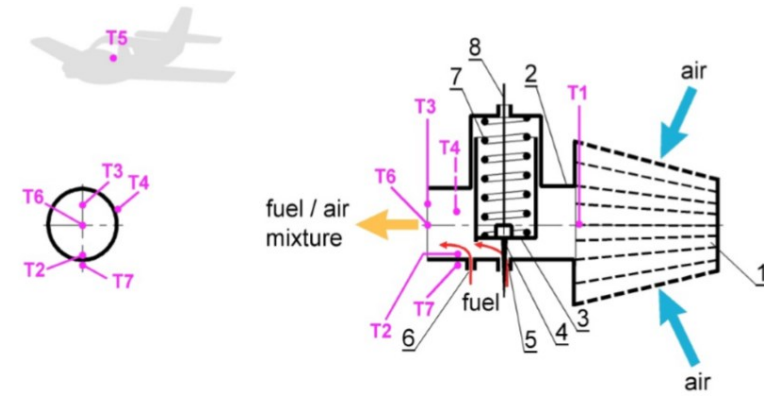
- Despite weather conditions during the tests that were conducive to icing (as per the graph proposed by the EASA), icing had not occurred.
- The maximum decrease in temperature was recorded in the fuel vaporization zone, which demonstrates the importance of icing in this type of carburettor (decrease in temperature of up to 30°C on the 447 engine and up to 20°C on the 582 engine).
- However, there was very little decrease in temperature of the carburettor walls.

In the most recent article, the author explained the lack of icing by the fact that the carburettor walls were not subject to a significant decrease in temperature in operation, therefore preventing ice from forming.

The graph below shows the data logged for a flight with the 582 engine. For this flight, the ground conditions, at take-off, were as follows: temperature = 18°C / relative humidity = 35 to 45%.



- A: Aircraft on ground
- B1: Climb
- B2: Cruise
- B3: Avoidance of obstacle
- B4: Cruise
- B5: Avoidance of obstacle
- C: Approach, descent and landing



Source: IN-FLIGHT TESTING OF THE SUSCEPTIBILITY TO ICING OF THE INDUCTION SYSTEM OF THE ROTAX 582 ENGINE _ Ryszard Chachurski _ 2016

The forums listed below were browsed in order to identify information issued on icing associated with Rotax engines:

- <https://www.rotax-owner.com/en/forum>
- <https://www.rotaryforum.com/threads/rotax-carb-ice.32926/>
- https://groups.google.com/forum/#!topic/rec.aviation.homebuilt/DDHtvq_ZwhU
- <https://forums.flyer.co.uk/viewtopic.php?t=81862>
- <http://www.microlightforum.com/archive/index.php/t-7287.html>
- <https://www.pprune.org/archive/index.php/t-601742.html>
- <http://www.vansairforce.com/community/archive/index.php?t-93548.html>
- <https://www.recreationalflying.com/threads/carb-ice-and-912-rotax.14053/>
- <https://www.homebuiltairplanes.com/forums/threads/carb-ice.22849/page-3>
- <https://forums.bmaa.org/forum/aircraft-specific-forums/shadow/16644-rotax-582-carb-icing?17656-Rotax-582-Carb-Icing=>
- <https://www.euroga.org/forums/hangar-talk/7915-how-do-some-aircraft-designs-avoid-carburettor-icing>
- <https://teamkitfox.com/Forums/threads/2132-912S-Carb-Heat-or-Not/page3>
- <https://backcountrypilot.org/forum/carb-ice-rotax-582-2-stroke-23420>
- <https://mcr01passion.forumperso.com/t66-givrage-carburateur-rotax>

The suggestions of users on these forums are generally cautious. Many of them write about their experience of icing, both on the ground and in flight. They focus essentially on the use of the heat system. A very small number of users seem to underestimate the probability of icing occurring on Rotax engines with no scientific proof. These users do not refer to or hardly refer to the graphs proposed by the authorities.

5.6. Measurements on aircraft

5.6.1. Objectives

The objective is to better understand the operating conditions of carburetors equipping Rotax 912 and 914 Series engines, on “standard” aircraft. The case of “confidential” constructions is not dealt with in this document.

This better understanding of the operating conditions should enable the BEA to be more critical of the tendency of such powerplants to be influenced by icing.

To ensure this, a series of measurements were taken in flight on aircraft in service equipped with Rotax engines, and on the ground on an engine installed on a test stand.

For engines with carburetors equipped with filters (designated as “type 1” in para. 5.2), the measurements consisted in measuring the temperature and humidity in the immediate vicinity of the carburetors, under the cowlings, and in comparing these measurements with those taken outside of the aircraft.

Indeed, to date, the post-accident study of icing is essentially based on outside conditions and often those on the ground provided by Météo-France at the time of the event. These measurements must be used to identify any discrepancies between these outside conditions and the conditions “experienced” by the carburetors.

For engines with carburetors associated with an Airbox (designated as “type 2” in para. 5.2), the measurements consisted in measuring the temperature and humidity in the Airbox, and in comparing these measurements with those taken outside of the aircraft.

To complete these measurements taken on various aircraft, additional measurements were made on a Rotax 914 engine belonging to the BEA, at the ENAC’s Castelnaudary test stand. On this engine, carburetors are associated with an Airbox. The test stand used enabled this engine to be tested in the atmospheric conditions prevailing on the day. During these tests, the engine was coupled to a three-blade DUC WINDSPOON propeller.

The main objective of the tests conducted on this 914 engine was to better comprehend the consequences of adding a turbocharger to an engine of this type (associated increase in temperature).

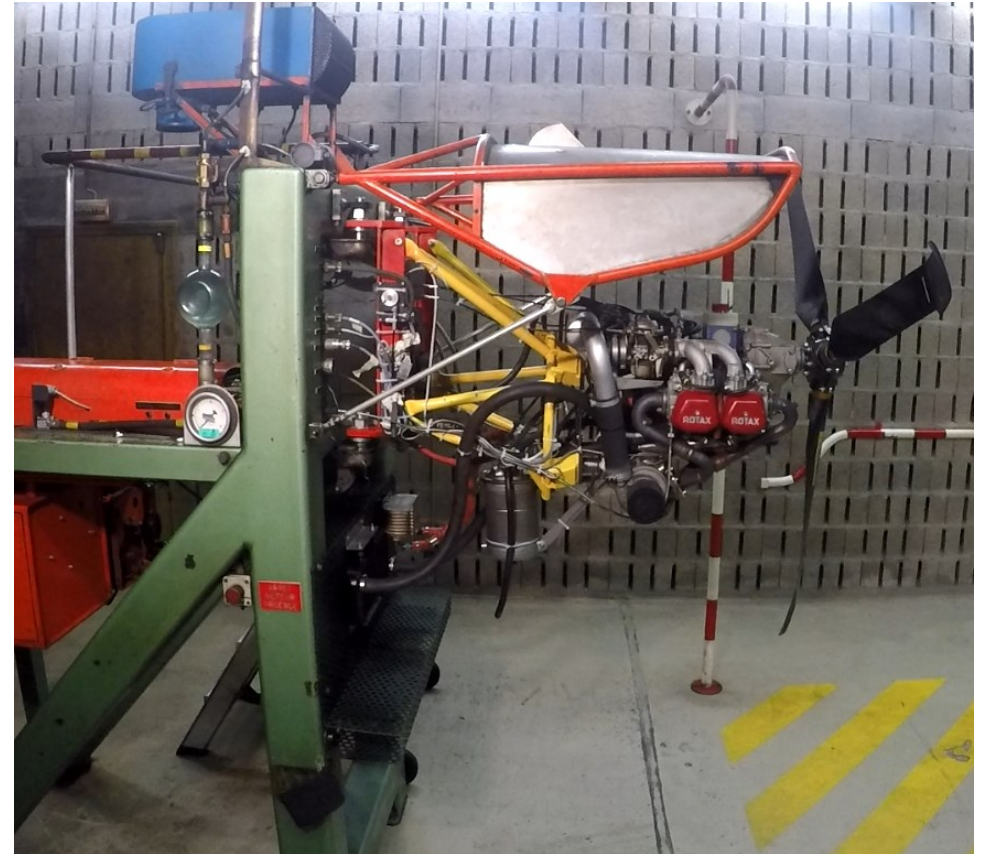


Figure 150: BEA Rotax 914 engine installed on the ENAC's Castenaudary test stand

Source: BEA

5.6.2. Measuring resources

Two types of sensors were used:

- **Hygrochron iButton sensor, reference DS1923:**

These very small sensors are used to record the temperature and the humidity at several recording frequencies. These sensors are “autonomous” and do not need to be plugged into a processing unit or another external energy source to log the data.

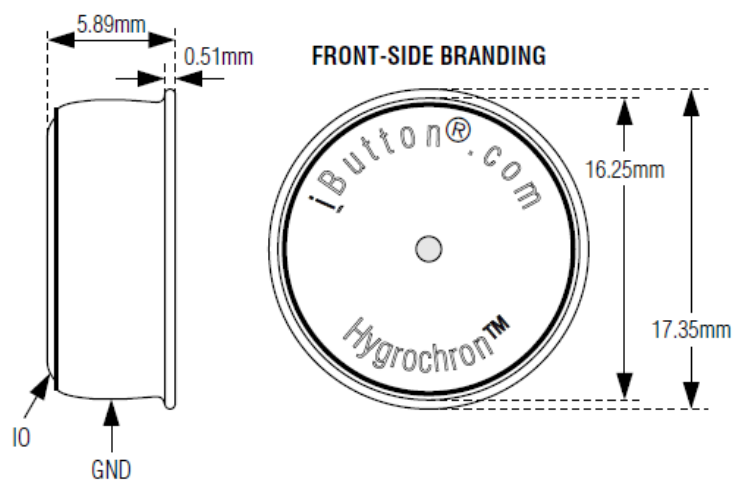
The sensors are programmed before they take the series of required measurements. When they have logged the necessary data, this data is simply retrieved using a PC and a dedicated interface. The sensors acquired by the BEA were initially controlled before the measurement campaign by being positioned in a controlled climatic condition reproducer.



Figure 151: iButton sensors

Source: https://www.embeddeddatasystems.com/DS1923-F5--Hygrochron-Temperature-Humidity-iButton_p_101.html

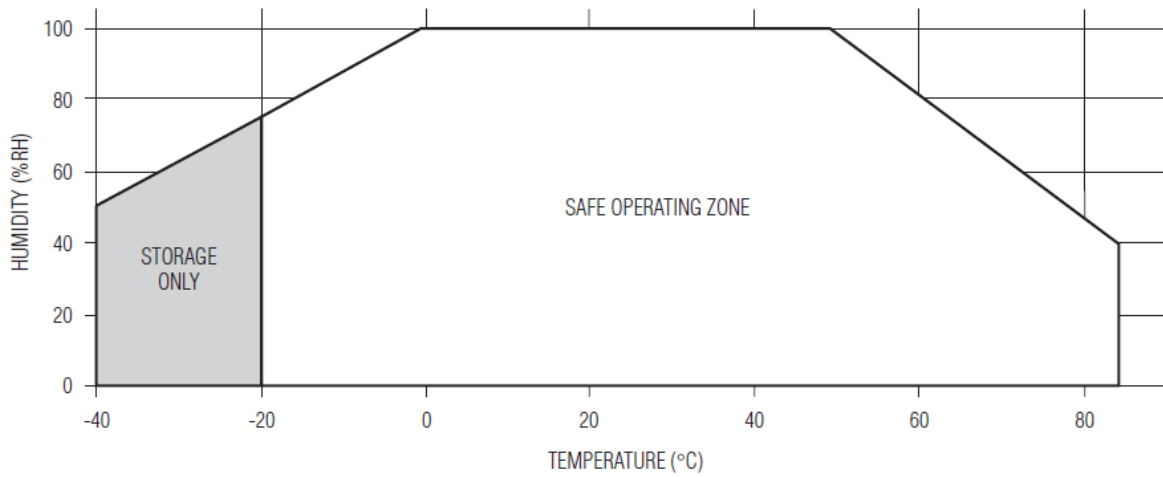
Dimensions:



Source: <https://www.ibuttonshop.com/ds1923-f5>

Sampling rate: 1 second to 273 hours

Conditions of use:



Source: <https://www.ibuttonshop.com/ds1923-f5>

- Type K thermocouples associated with a data logger:



Figure 152: thermocouple

Source: <https://www.onsetcomp.com/products/sensors/tc6-k/>



Figure 153: data logger

Source: <https://www.onsetcomp.com/products/data-loggers/ux120-014m>

The data logger is autonomous and does not need to be plugged into an external energy source to log the data. It can receive four thermocouples and log their data simultaneously.

5.6.3. Measurements taken on aircraft

5.6.3.1 - First series of measurements

A first series of measurements was taken on the three aircraft listed below. These aircraft belong to the fleet proposed by the company which is owned by the Safety Manager of the French Microlight Federation.

- Magny M16 (unducted powerplant) equipped with a Rotax 914 engine with carburettors associated with an Airbox (Figure 154);
- Magny M24 (ducted powerplant) equipped with a Rotax 914 engine with carburettors associated with an Airbox (Figure 155);
- Aeroprakt A22 (Figure 156) equipped with a Rotax 912is engine with an injection system. An injection system prevents the problem of icing. However, the conditions in the engine environment are the same as those found in an identical engine equipped with a carburettor. It is therefore still useful to consider this aircraft.



Figure 154: Magny M16

Source: <https://vaocluse-ulm.com/appareils/>



Figure 155: Magny M24

Source: <https://vaocluse-ulm.com/>



Figure 156: Aeroprakt A22

Source: <https://vaocluse-ulm.com/appareils/>

This first series of measurements consisted in using only iButton sensors, in checking their functionality and in adapting new measuring resources to the next series of measurements. The position of the sensors on each engine is specified in the table below.

Magny M16

Two sensors were positioned:

- one sensor on the LH landing gear strut to log the environmental conditions;
- one sensor positioned on the upper section of the Airbox, on the LH side.

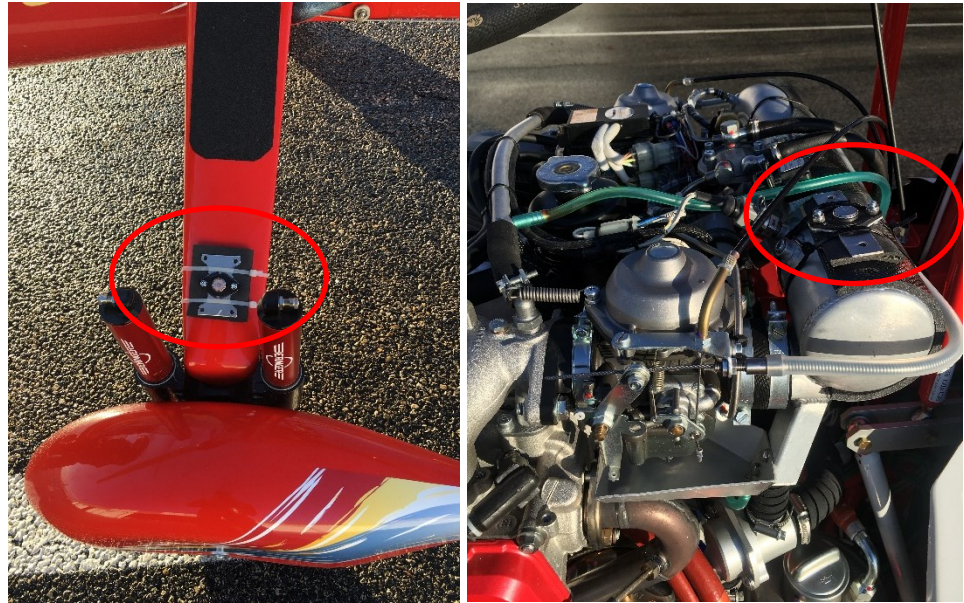


Figure 157: position of the sensors

Source: Vaucluse ULM

Magny M24

Two sensors were positioned:

- one sensor on the LH landing gear strut to log the environmental conditions;
- one sensor positioned on the upper section of the Airbox, on the LH side.

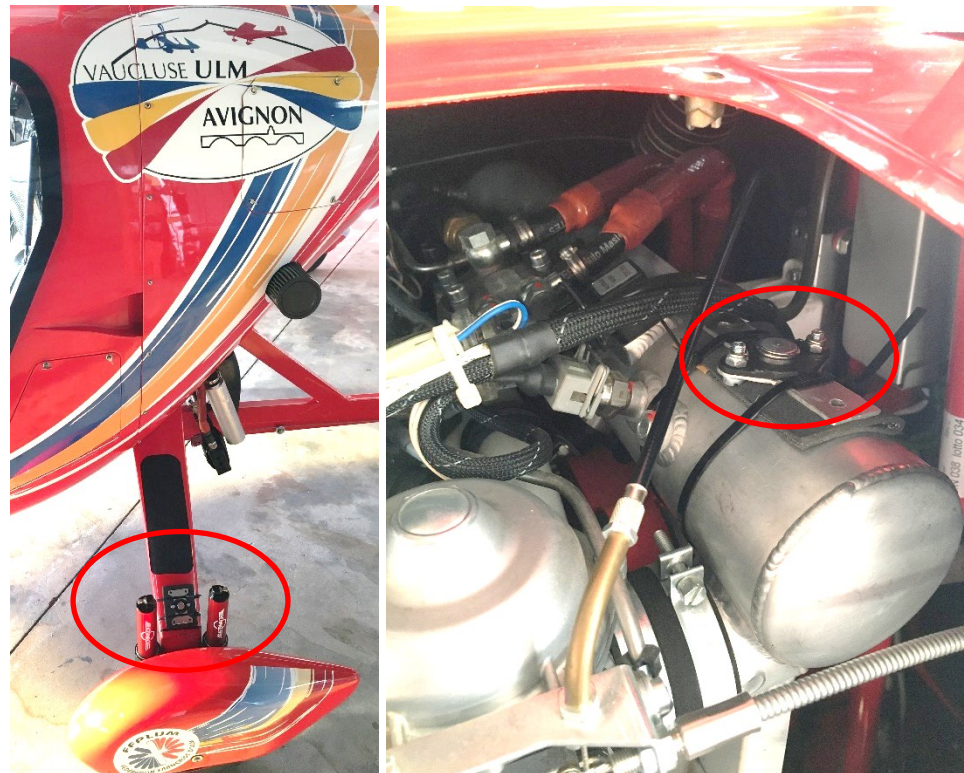


Figure 158: position of the sensors

Source: Vaucluse ULM

Aeroprakt A22	Two sensors were positioned: <ul style="list-style-type: none">• one sensor on the RH brace to log the environmental conditions;• one sensor under the cowlings, equidistant between the two carburettors.
---------------	---

Before each flight, the procedure applied consisted in retrieving the weather conditions at the time, then, at the end of every flight, in noting whether symptoms of icing had been felt.

The results obtained are presented in the tables below:

Magny M16

The measurements for which the data is presented below were taken on 12 December 2019.

The weather conditions available on the ground before this flight were as follows:

- wind of 7 kt, at 300;
- temperature = 9°C;
- dew point temperature = 1°C;
- atmospheric pressure = 1,011 hPa.

If we reposition these conditions on the graph proposed by the EASA, these conditions were conducive to serious icing in descent and to moderate icing in cruise flight.

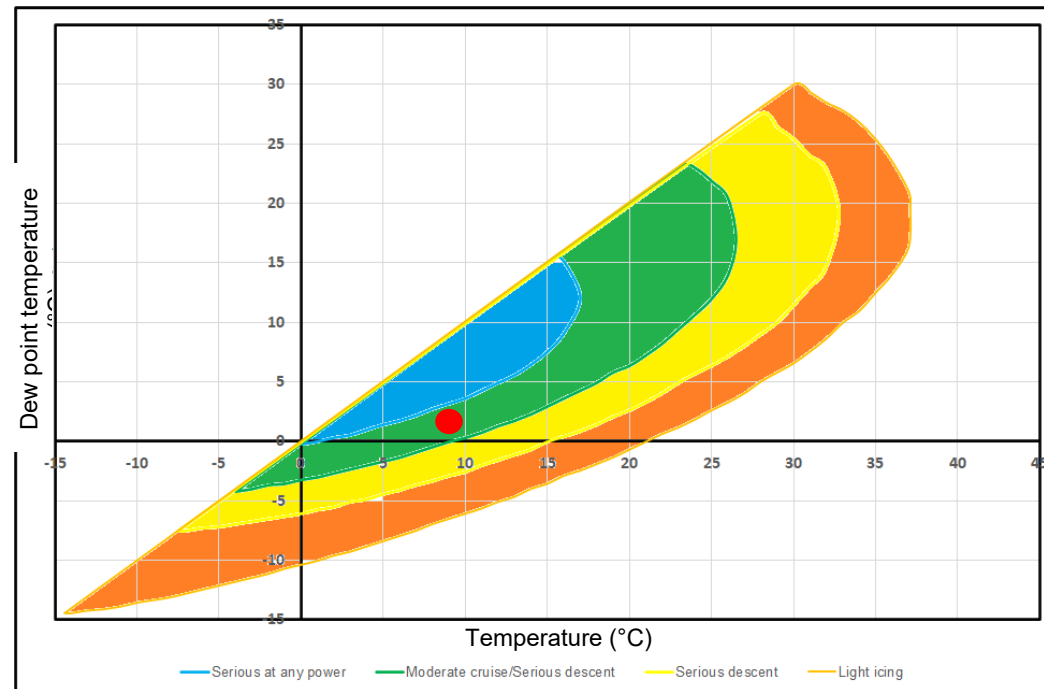


Figure 159: repositioning the weather conditions on the EASA graph
Source: BEA

No symptoms of icing were identified during this flight.

Temperature measurements

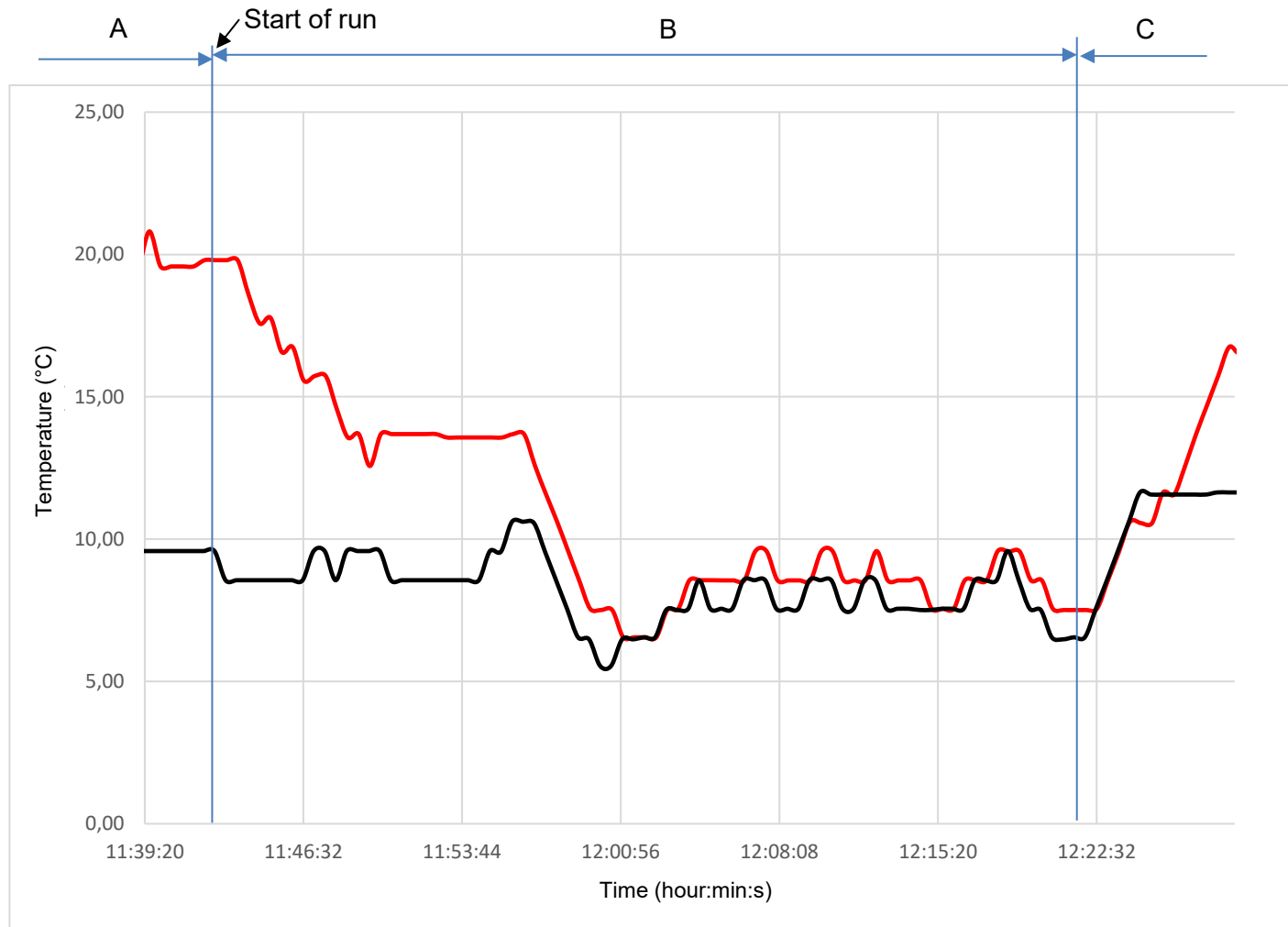


Figure 160: Temperature measurements
Source: BEA

Sensor positioned above the engine: — (red line)
Sensor positioned on the landing gear strut: — (black line)

A: aircraft on the ground, at shut-down
B: flight incorporating run, take-off, cruise and landing
A: aircraft on the ground, at shut-down

The measurements show that on the ground, prior to the first run, the temperature above the engine was around 10°C higher than the outside air temperature. At the start of run, the temperature above the engine will gradually decrease until it is similar to the outside air temperature after around 20 minutes. The temperature above the engine will increase in relation to the outside air temperature when the aircraft is stopped on the ground.

Relative humidity measurements

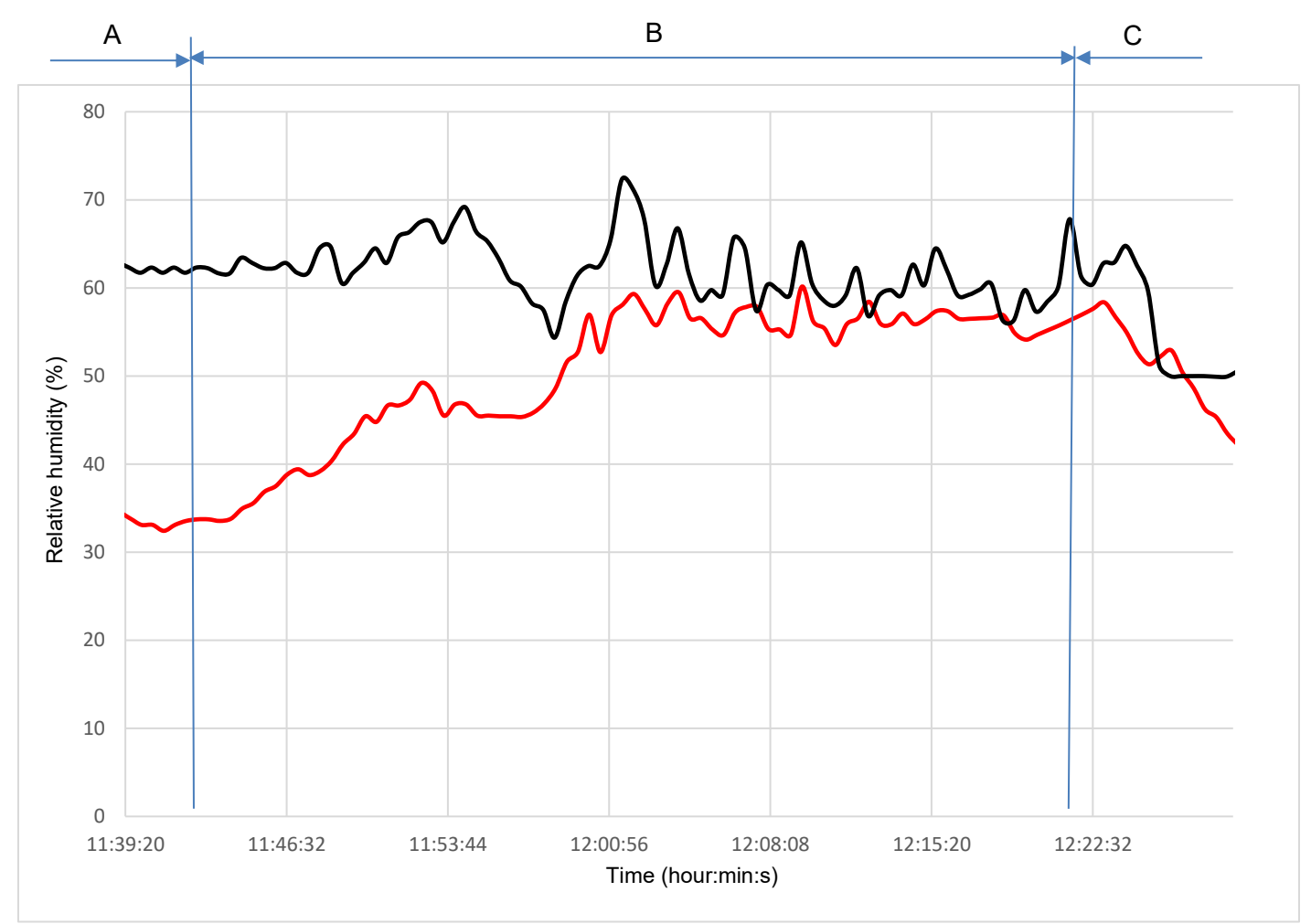


Figure 161: Relative humidity measurements
Source: BEA

Sensor positioned above the engine: — (red line)
Sensor positioned on the landing gear strut: — (black line)

The variations in relative humidity were inversely proportional to variations in temperature. Before the first run, the relative humidity above the engine was around 30% lower than the outside relative humidity.

Magny M24

The measurements for which the data is presented below were taken on 05 December 2019.

The weather conditions available on the ground before these flights were as follows:

- wind of 4 kt, variable 340/070;
- temperature = 5°C;
- dew point temperature= 3°C;
- atmospheric pressure = 1,022 hPa.

If we reposition these conditions on the graph proposed by the EASA, these conditions were conducive to serious icing at all speeds.

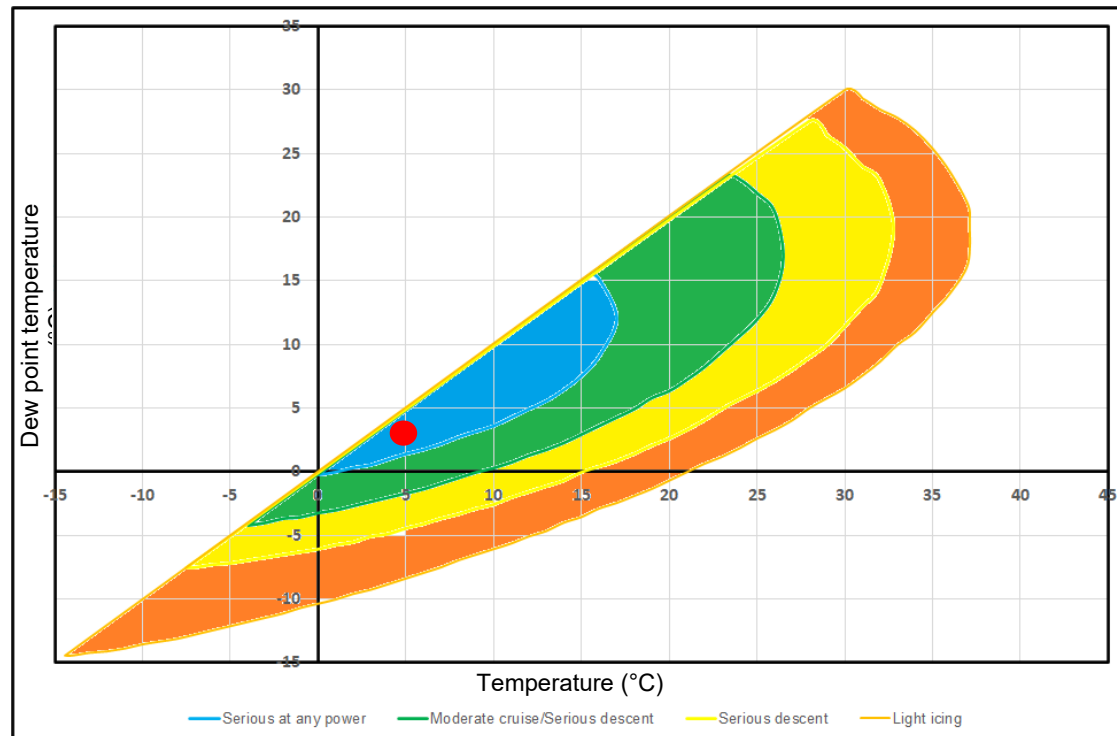


Figure 162: repositioning the weather conditions on the EASA graph

Source: BEA

The symptoms of icing were identified (vibration, hoarse engine sound) on the ground during the static phase (engine heating). No symptoms were then identified.

Temperature measurements

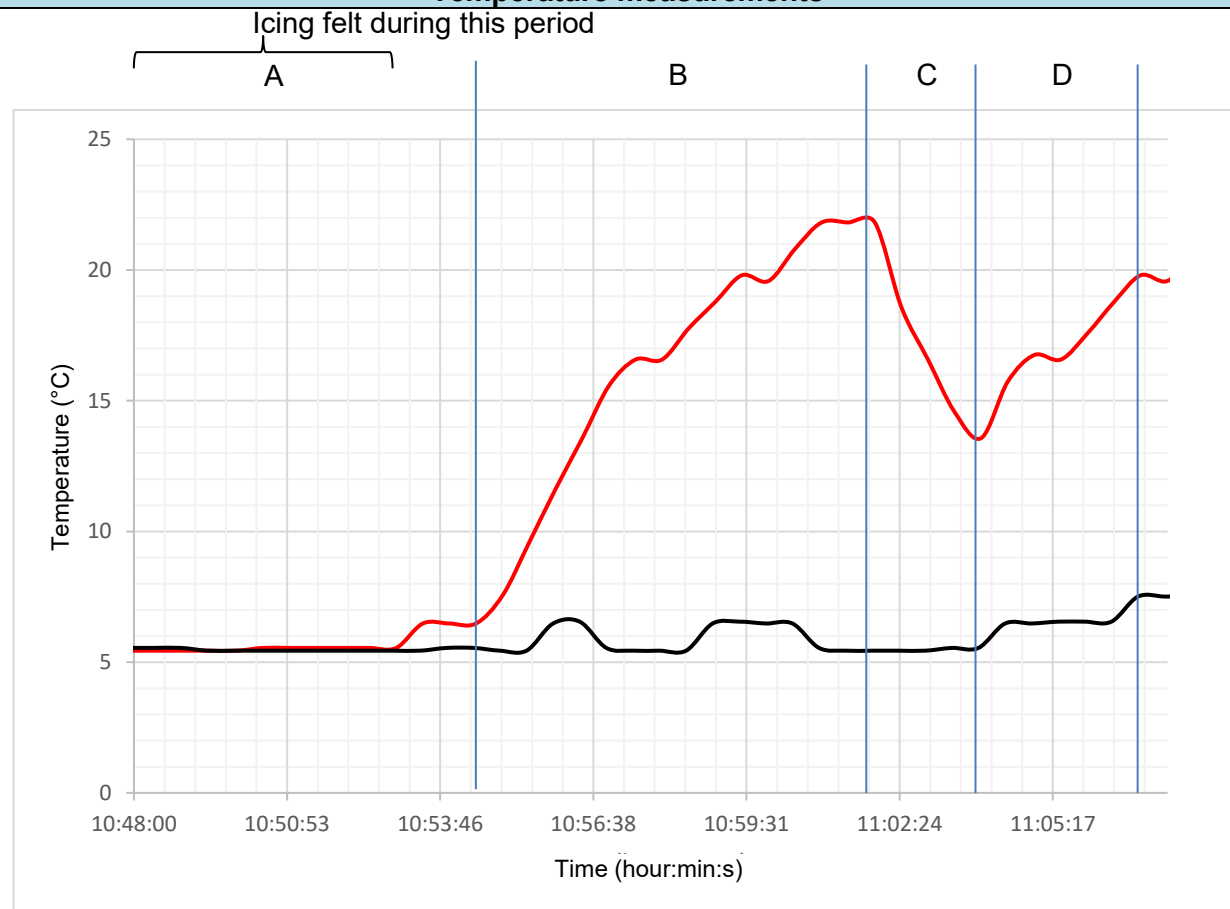


Figure 163: Temperature measurements
Source: BEA

Sensor located in the upper section of the engine compartment: — (red line)
Sensor located on the landing gear strut: — (black line)

A: aircraft on ground
B: run, take-off, climb and cruise
C: descent and landing
D: ground phase

On the ground, at engine start-up, the temperature recorded in the upper section of the engine compartment remained stable and equivalent to the outside air temperature. The temperature in the engine compartment then gradually increased to reach a temperature in the upper section of the engine compartment of higher by around 15°C than the outside air temperature. During descent, the temperature difference reduced to 7°C before rising again during the next ground phase.

Relative humidity measurements

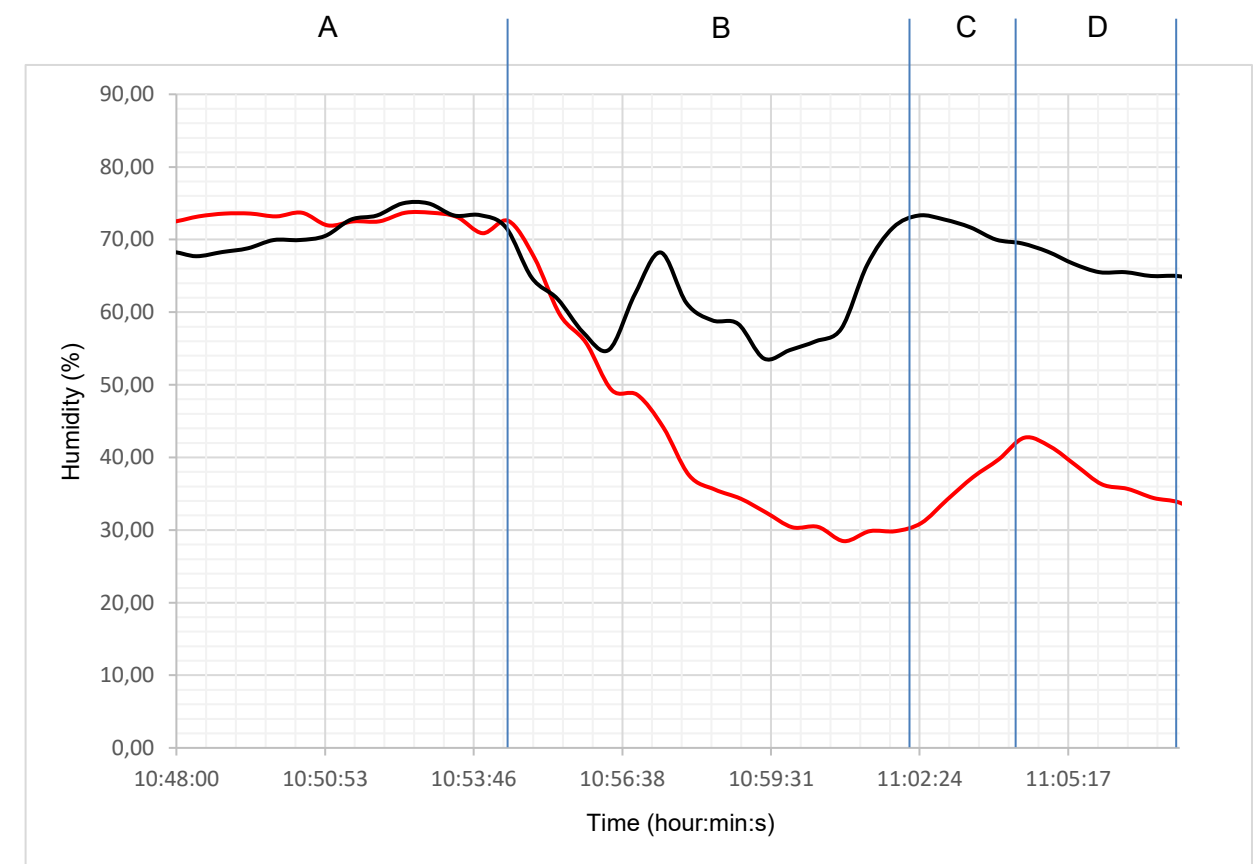


Figure 164: relative humidity measurements
Source: BEA

Sensor located in the upper section of the engine compartment: — (red line)
Sensor located on the landing gear strut: — (black line)

The variations in relative humidity were inversely proportional to variations in temperature. Before the first run, the relative humidity in the upper section of the engine compartment remained stable and equivalent to the outside relative humidity. The relative humidity in the engine compartment then gradually decreased until it was around 40% lower than the outside relative humidity. During descent, the difference reduced to 26% before rising again during the next ground phase.

Magny M24

During the flights made in this aircraft, all made in conditions conducive to serious icing at any engine speed as per the graph proposed by the EASA, the symptoms of icing were identified on the ground, after the start-up. During the other phases, these symptoms did not exist anymore.

According to the data recorded, the temperature in the engine compartment did not increase or increased only slightly on the ground following start-up. The conditions were therefore similar to those prevailing outside the aircraft. This observation can explain the onset of the symptoms of icing during this period, all the more strengthened that the butterfly valve of the carburetors was practically closed when the engine was idling.

The temperature in the engine compartment then increased gradually and markedly, which seemed to eliminate the symptoms of icing.

The performance of the engine after start-up could be explained by the powerplant illustrated in the two photographs below.

Firstly, we can see that this powerplant is ducted, with, in the engine compartment, a panel separating the upper section of the engine from its lower section containing the cylinders.

We then observe a very wide opening at the rear in line with the exhaust system.

These characteristics could create a reduced temperature in the upper section of the engine when the aircraft is on the ground and when the engine speed has not increased. To complete these observations, it seemed essential to record the outside temperature of the body of carburetors, and this will be considered for future measurements.

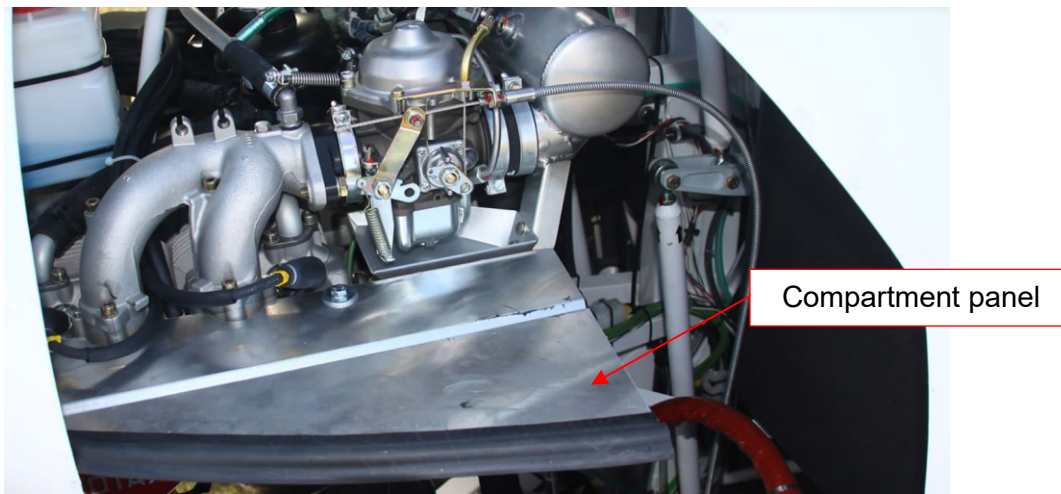


Figure 165 : engine compartment
Source: <http://www.magniqyro.it/en/products/m24-orion/>

Wide opening in line with the exhaust system



Figure 166: rear view of the aircraft
Source: <http://www.magniqyro.it/en/products/m24-orion/>

Aeroprakt A22

The measurements for which the data is presented below were taken on 26 November 2019 during two successive flights.

The weather conditions available on the ground before these flights were as follows:

- variable wind at 1 kt;
- temperature = 13°C;
- dew point temperature= 9°C;
- atmospheric pressure = 1,008 hPa decreasing.

If we reposition these conditions on the graph proposed by the EASA, these conditions were conducive to serious icing at all speeds.

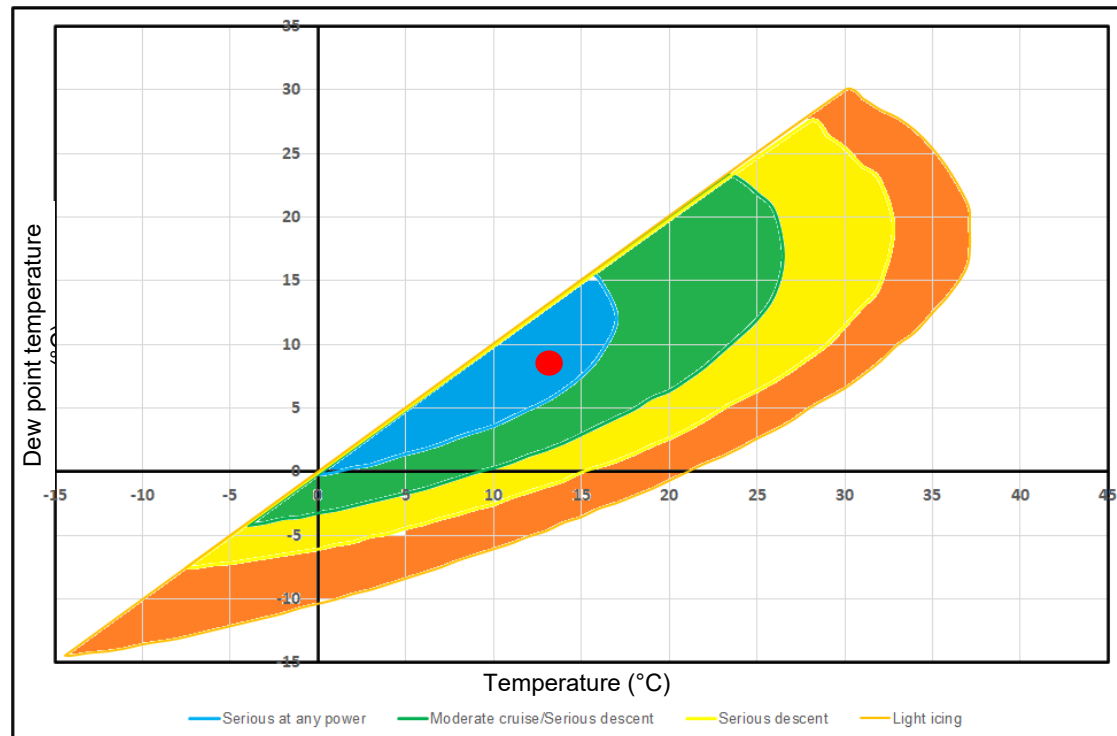


Figure 167: repositioning the weather conditions on the EASA graph

Source: BEA

No symptoms of icing were identified during this flight.

Temperature measurements

Relative humidity measurements

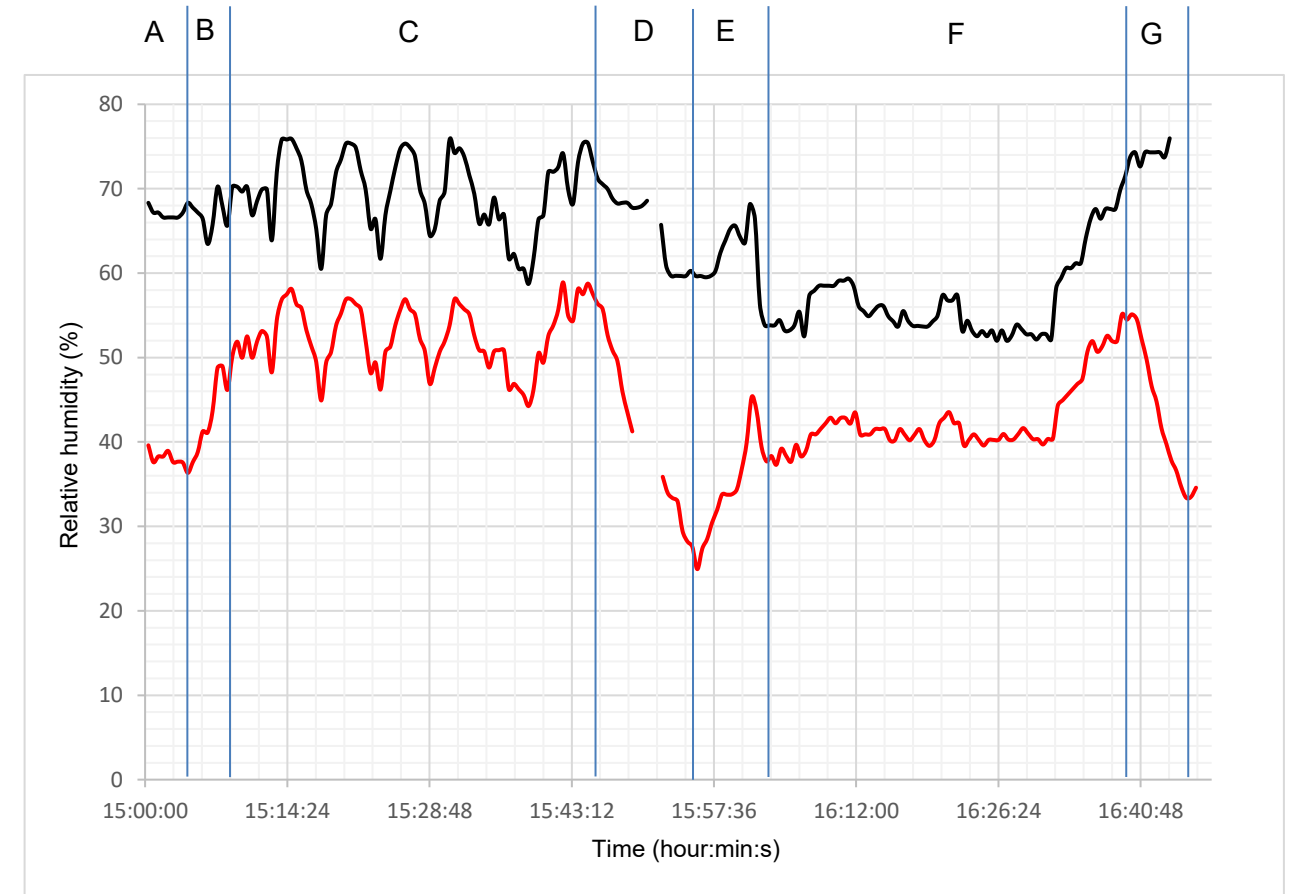
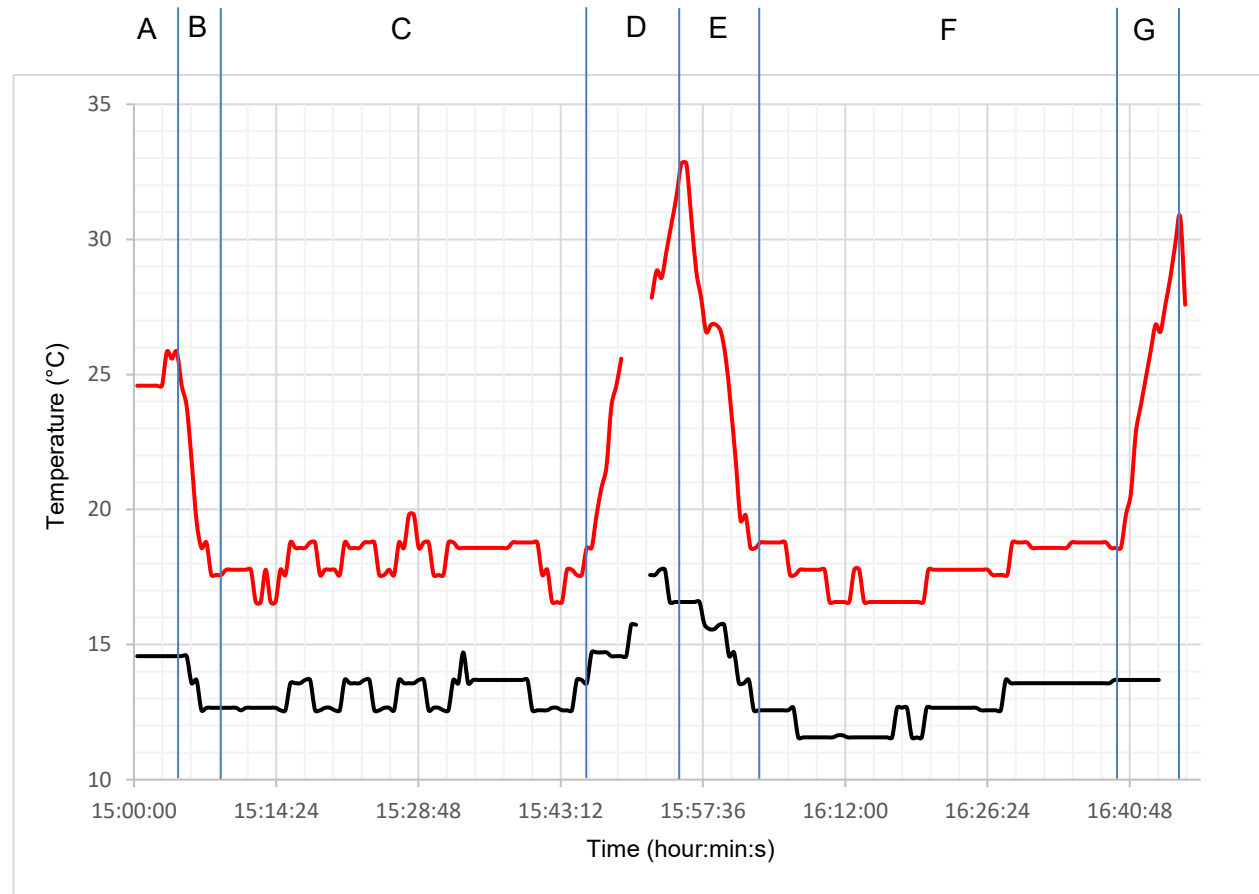


Figure 168: temperature measurements
Source: BEA

Figure 169: relative humidity measurements
Source: BEA

Sensor located under the cowlings: — (red line)
Sensor located on the brace: — (black line)

A: aircraft on ground	E: ground phase, take-off and climb
B: take-off and climb	F: cruise
C: cruise	G: descent and landing
D: descent and landing	

Sensor located under the cowlings: — (red line)
Sensor located on the brace: — (black line)

The variations in relative humidity were inversely proportional to variations in temperature. Before the first run, the relative humidity under the cowling was around 30% lower than the outside relative humidity. In cruise flight, the relative humidity under the cowling was around 20% lower than the outside relative humidity.

Before the first run, the temperature under the cowlings was around 10°C higher than the outside air temperature. After the first run, this difference in temperature decreased to around 5°C from the start of cruise. These observations on flight time slots A, B and C demonstrate the impact of air circulating around the engine when the aeroplane is in motion. During cruise flight, the difference in temperature between the outside and under the cowlings stabilised at around 5°C. During the descent phase up to the stop position, the difference between the two temperatures gradually increased to around 15°C. The figures were very similar for the second successive flight.

Aeroprakt A22

The measurements appeared to clearly show a difference between the outside conditions and those theoretically taken in by the carburettors (this aircraft is equipped with a Rotax engine associated with an injection system, versions of this aircraft use carburettors with a type 1 powerplant).

If we simulate the conditions recorded under the cowlings, during cruise flight, i.e.:

- temperature = 18°C;
- relative humidity = 52%;
- dew point temperature = 8°C.

If we reposition these conditions on the graph proposed by the EASA, these conditions were conducive to moderate icing in cruise flight and to serious icing in descent. We therefore changed the icing envelope in relation to the taking into account of the environmental conditions.

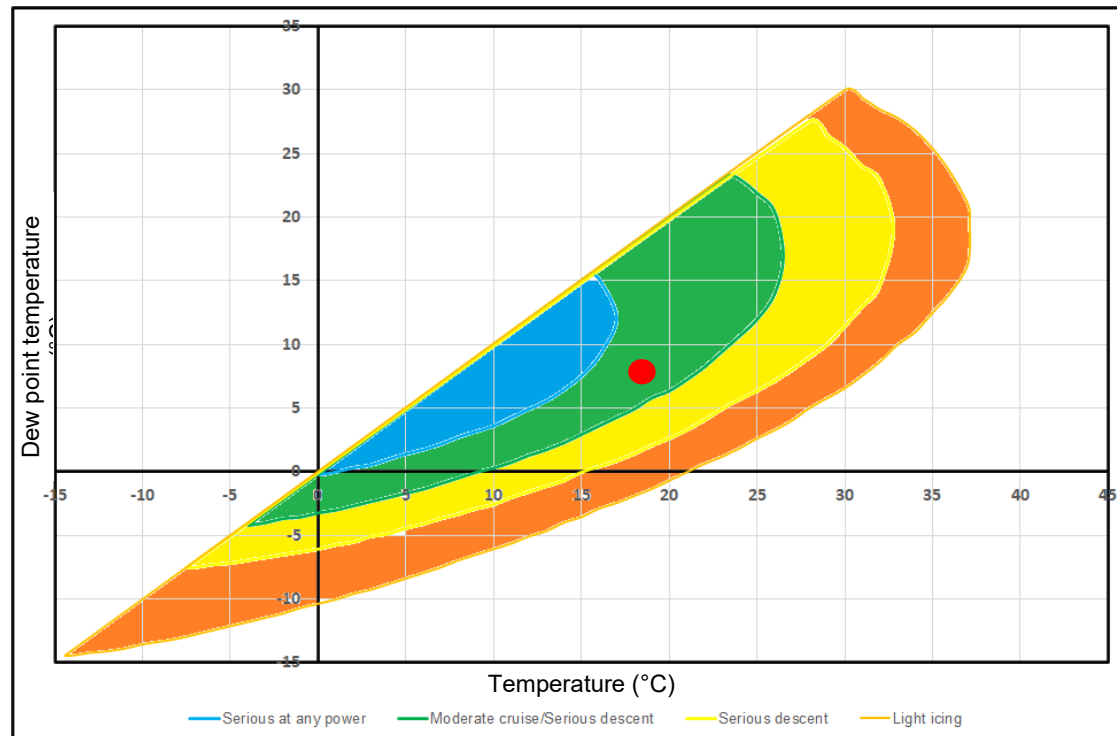


Figure 170: repositioning the weather conditions on the EASA graph

Source: BEA

This first series of measurements on three aircraft, all with different powerplants, showed that the temperature and relative humidity conditions in the engine environment varied very differently in relation to the environmental conditions. It showed that:

- On the M16, on which the powerplant is unducted, the temperature in the engine environment was initially higher than the outside air temperature before it gradually decreased until it was equal to the outside air temperature (humidity varied inversely). We may consider that the time required to reach equal temperatures varies depending on the environmental conditions.
- On the M24, on which the powerplant is ducted, with an additional separation between the upper section of the engine compartment and the lower section, the temperature in the upper section of the engine compartment was initially similar to the outside air temperature before it gradually increased. This increase was then reversed in relation to that observed on the M16.
During the tests conducted, the symptoms of icing were moreover observed only on the ground, after the first start-up. No symptoms were then identified anymore.
- On the Aeroprakt A22, the temperature in the engine compartment still remained at least 5°C higher than the outside air temperature. This difference increased very markedly at shut-down.

This first series of measurements seemed to justify the use of the iButton sensor to log the environmental conditions and the conditions in the engine environment.

The additional logging of the outer surface of at least one carburettor seemed however necessary to correlate with that of the engine environment and to be more precise in terms of carburettor operating conditions. Use of a thermocouple, bonded to the surface of a carburettor, seems to be the most simple solution.

5.6.3.2 - Second series of measurements

5.6.3.2.1 - Introduction

This second series of measurements was taken on the aircraft illustrated below. This series of measurements differed from the first through the additional use of multiple thermocouples. The position of the sensors is detailed in the presentation of each test below.



Figure 171: TECNAM P92 ECHO Light

Source: <https://www.ekeraviation.com/en/products/detail/111-p92-echo-light>



Figure 172: AEROPRAKT A-22L

Source: BEA



Figure 173: TECNAM P2002 JF

Source: BEA



Figure 174: TECNAM P2008 JC

Source : <http://tagazous.free.fr/affichage2.php?img=57907>

5.6.3.2.2 - TECNAM P92 Echo Light

Information pertaining to the aircraft and its propulsion system:

Aircraft category	Microlight
Engine installed on the aircraft	912 UL delivering a maximum power of 80 hp
Powerplant type	Type 1 / carburetors equipped with filters

Sensors installed on the aircraft:

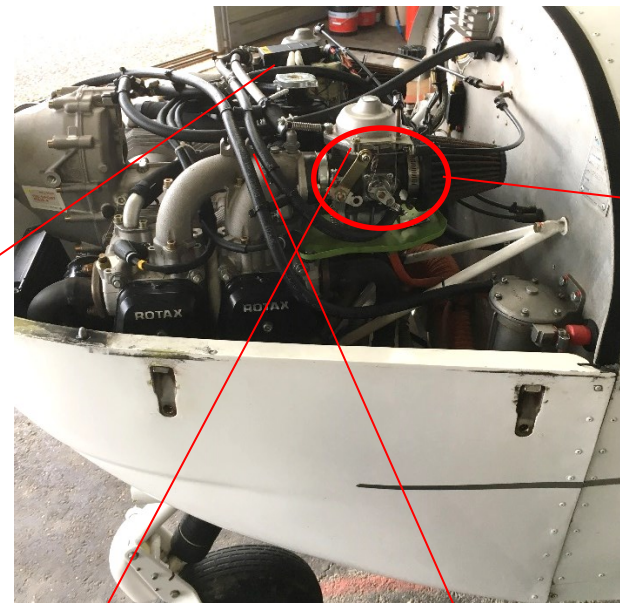
One iButton sensor positioned outside the aircraft (temperature and relative humidity measurement)



Figure 175: TECNAM P92 ECHO Light

Source: <https://www.ekeraviation.com/en/products/detail/111-p92-echo-light>

Source: BEA
Figure 176: powerplant



One iButton sensor positioned under the engine cowlings, in the immediate vicinity of the LH carburettor (temperature and relative humidity measurement)

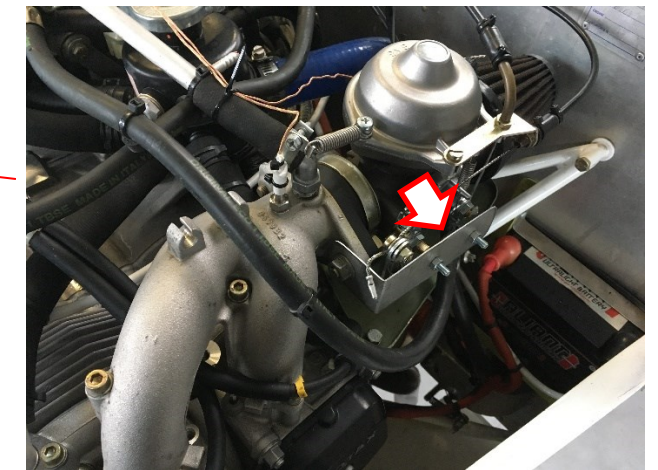


Figure 177: temperature/relative humidity sensor
Source: BEA

One thermocouple attached to the outer surface of the body of the LH carburettor (temperature measurement)

One thermocouple attached immediately downstream of the LH carburettor butterfly valve (temperature measurement)

One thermocouple attached immediately downstream of the RH carburettor butterfly valve (temperature measurement)

One thermocouple attached between the two ignition units (temperature measurement)



Figure 178: temperature sensor
Source: BEA

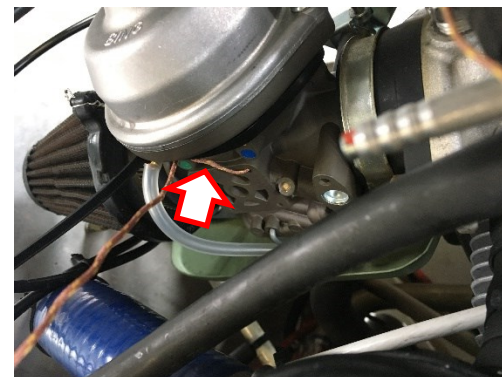


Figure 179: temperature sensor
Source: BEA

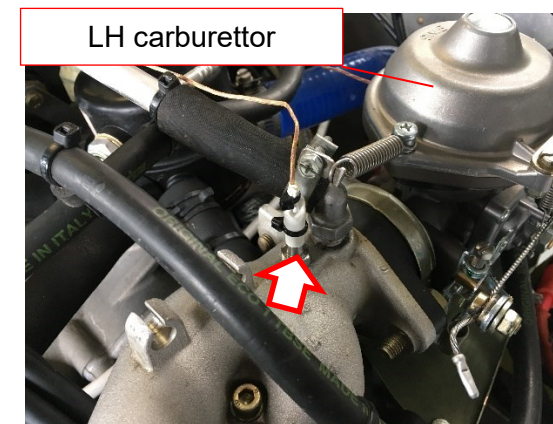


Figure 180: temperature sensor
Source: BEA

The thermocouple is located in the air flow in line with the carburettor output.

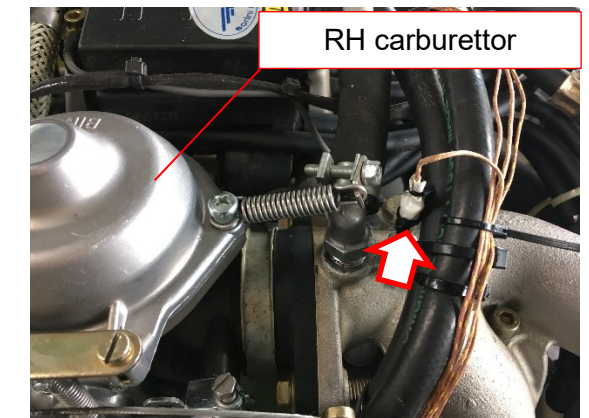


Figure 181: temperature sensor
Source: BEA

The thermocouple is located in the air flow in line with the carburettor output section.

Conditions during the flight:

Weather report from Chambéry station retrieved just before the flight

050830Z AUTO 16006KT 130V200 9999 BKN049 OVC060 14/11 Q1006 TEMPO SHRA

- temperature = 14°C;
- dew point temperature = 11°C.

If we reposition these conditions on the graph proposed by the EASA, these conditions were conducive to serious icing at all output powers.

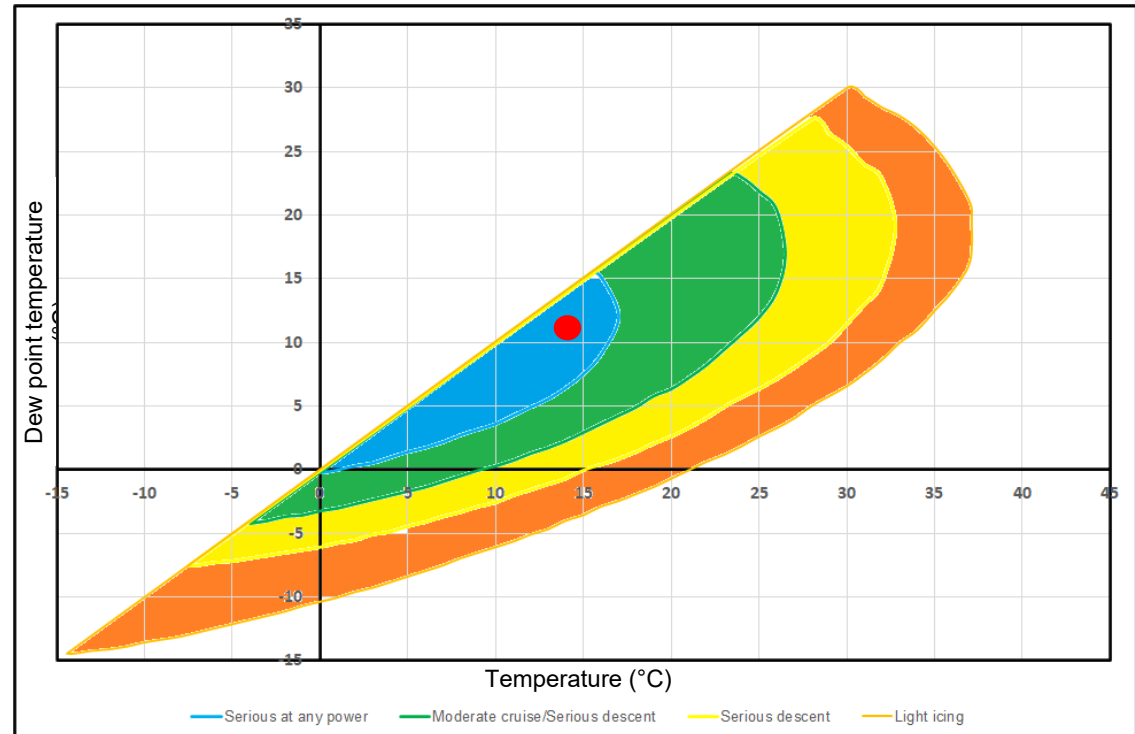


Figure 182: repositioning the weather conditions on the EASA graph

Source: BEA

Measurement results:

During the flight made, no symptoms of icing were identified.

Temperature measurements

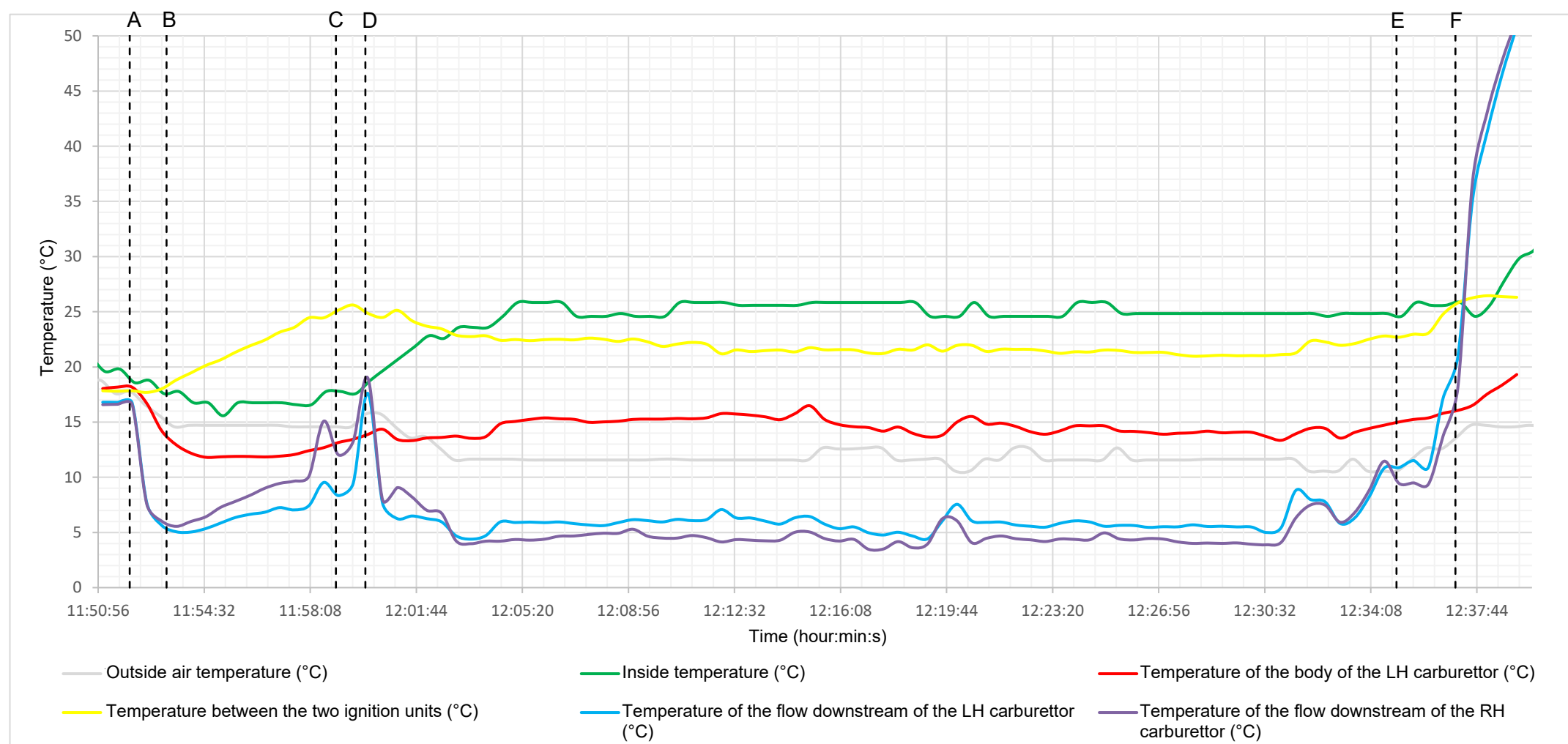


Figure 183: temperature measurements

Source: BEA

Key:

A: Engine start-up	B: Aeroplane at holding point	C: Start of take-off run
D: Take-off	E: Landing	F: Engine shut-down

Comments:

The difference between the environmental conditions and the conditions prevailing under the cowlings remained very negligible up to take-off (around 2°C). The temperature under the cowlings then gradually increased to reach a constant value up to engine shut-down. The maximum difference between the outside air temperature and the temperature under the cowlings was around 14°C.

After start-up of the engine, the temperature in the air flow, downstream of the butterfly valves, instantly decreased by around 10°C but remained above zero. The temperature in the flow increased again during the approach phase and after landing. The temperature then increased markedly after engine shut-down.

The maximum difference between the outside air temperature and the temperature of the flow downstream of the butterfly valve was around 6°C. This difference was around 20°C between the temperature under the cowlings and the temperature of the flow downstream of the butterfly valve.

relative humidity measurements

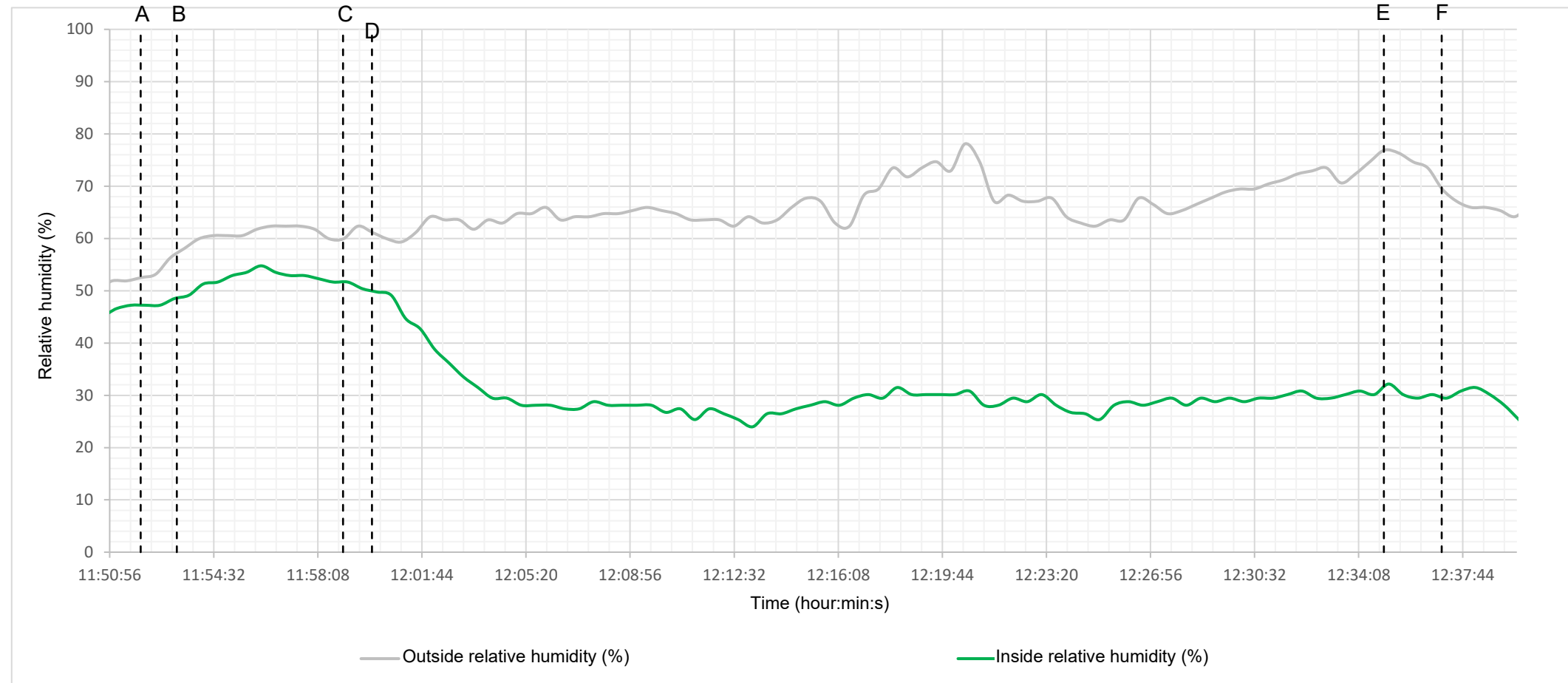


Figure 184: relative humidity measurements
Source: BEA

Key:

A: Engine start-up	B: Aeroplane at holding point	C: Start of take-off run
D: Take-off	E: Landing	F: Engine shut-down

Comments:

The relative humidity under the cowlings was around 10% lower than the outside relative humidity up to take-off. This difference then gradually increased due to the decrease in the relative humidity under the cowlings. The latter was then around 40% lower than the outside relative humidity.

5.6.3.2.3 - AEROPRAKT A-22L

The flight of this aircraft took place on 23 July 2020.

Information pertaining to the aircraft and its propulsion system:

Aircraft category	Microlight
Engine installed on the aircraft	912 UL delivering a maximum power of 80 hp
Powerplant type	Type 1 / carburetors equipped with filters



Figure 185: AEROPRAKT A-22L

Source: BEA

Sensors installed on the aircraft:

One iButton sensor positioned outside the aircraft, attached to the RH brace (temperature and relative humidity measurement)



Figure 186: temperature/relative humidity sensor
Source: BEA

One iButton sensor positioned under the engine cowlings, between the two carburetors (temperature and relative humidity measurement)



Figure 187: temperature/relative humidity sensor
Source: BEA

One thermocouple attached to the outer surface of the body of the LH carburettor (temperature measurement)

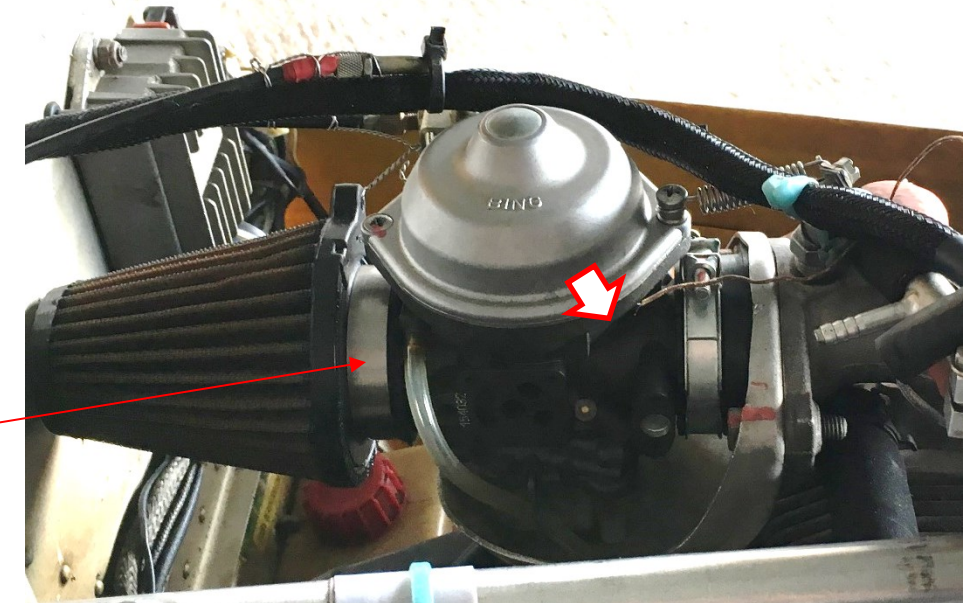


Figure 188: temperature sensor
Source: BEA

One thermocouple attached immediately downstream of the RH carburettor butterfly valve (temperature measurement)



Figure 189: temperature sensor
Source: BEA

Conditions during the flight:

Key:

	On the ground, before take-off
	In flight

If we reposition these conditions on the graph proposed by the EASA:

- on the ground, these conditions were conducive to serious icing in descent and to moderate icing in cruise flight;
- in flight, these conditions were conducive to serious icing in descent and to moderate icing in cruise flight;

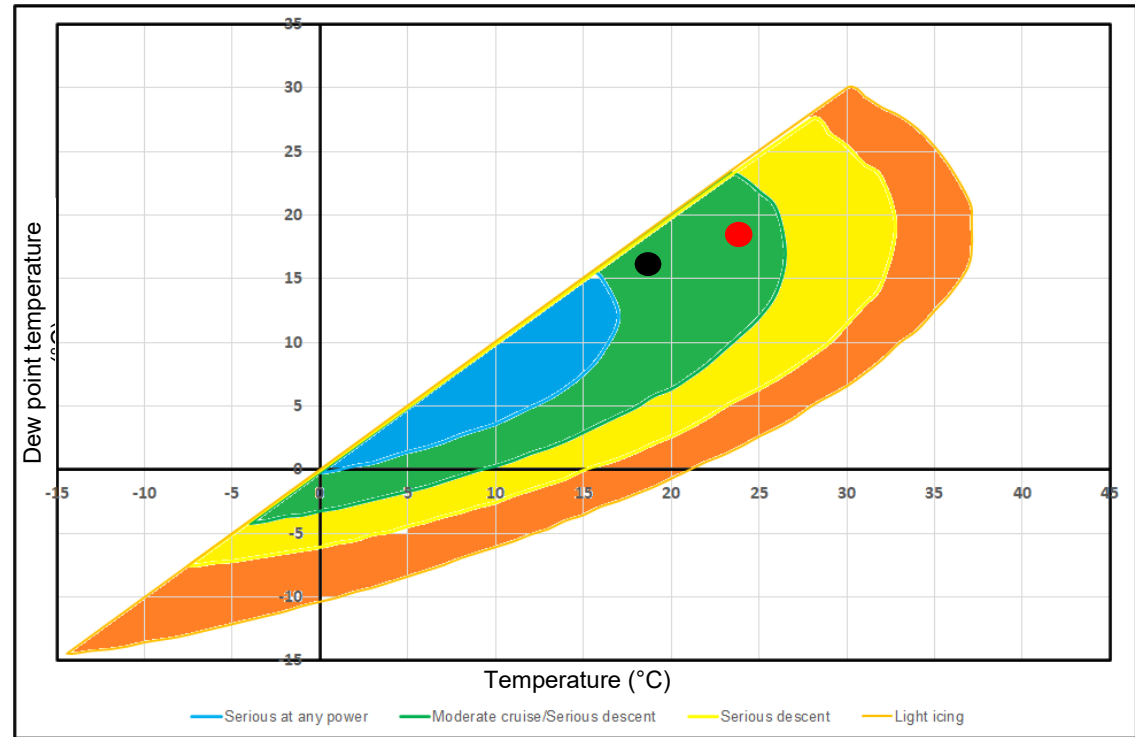


Figure 190: repositioning the weather conditions on the EASA graph
Source: BEA

Temperature

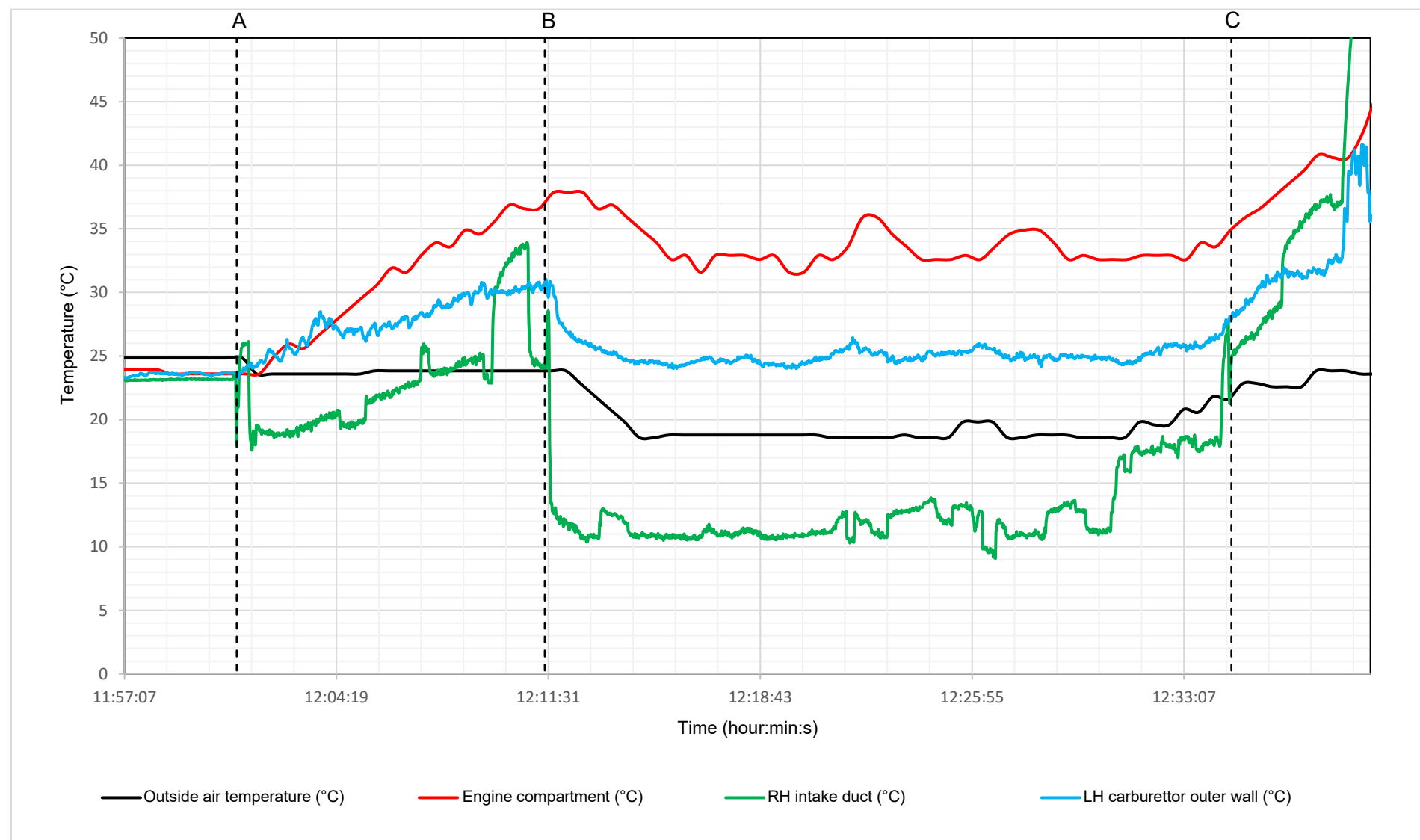


Figure 191: temperature measurements

Source: BEA

Key:

Reference line	Phase	Reference line	Phase
A	Engine start-up	B	Take-off / Power-up
C	Engine shut-down		

Comments:

On the ground, with engine stopped, the temperature under the cowlings was almost identical to the outside air temperature.

During start-up, the temperature in the RH intake duct suddenly decreased by around 7°C in relation to the outside air temperature.

From start-up to take-off, the temperature under the cowlings gradually increased. During take-off, the temperature under the cowlings was around 12°C higher than the outside air temperature.

In cruise flight, we can observe that:

- the temperature under the cowlings was around 14°C higher than the outside air temperature;
- the temperature in the RH intake duct was around 20°C lower than the temperature under the cowlings and around 6°C lower than the outside air temperature;
- the temperature of the carburettor outer wall was around 6°C higher than the outside air temperature.

After engine shut-down, the temperature under the cowlings, that of the carburettor outer wall and the temperature in the RH intake duct increased very markedly.

Relative humidity

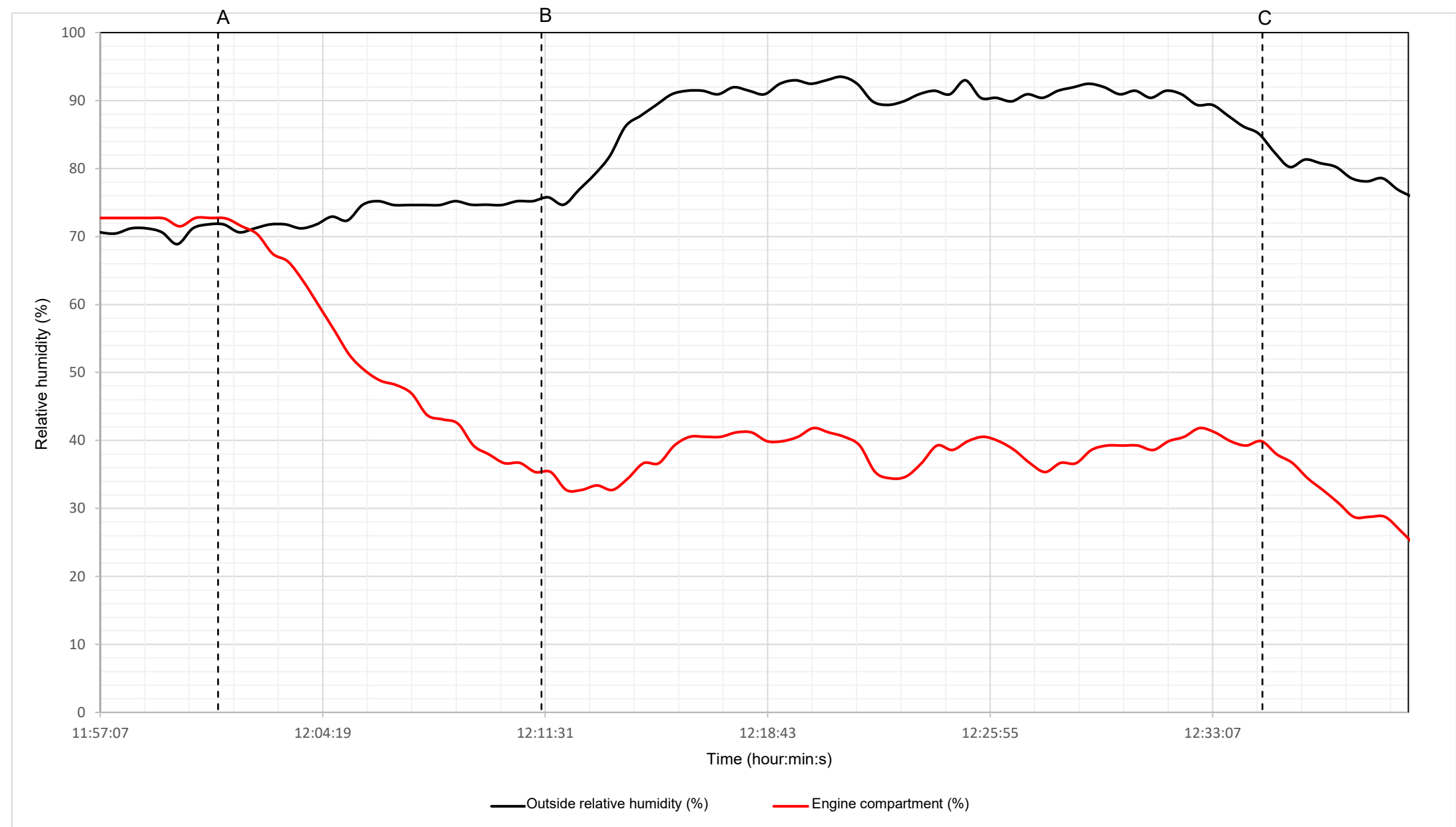


Figure 192: relative humidity measurements
Source: BEA

Key:

Reference line	Phase	Reference line	Phase
A	Engine start-up	B	Take-off / Power-up
C	Engine shut-down		

Comments:

On the ground, with engine stopped, the relative humidity under the cowlings was almost identical to the outside relative humidity. After engine start-up, the relative humidity gradually decreased in the engine compartment. In cruise flight, the relative humidity in the engine compartment was around 50% lower than the outside relative humidity.

5.6.3.2.3 - TECNAM P2002 JF

The two flights of this aircraft took place on 08 January 2021.

Information pertaining to the aircraft and its propulsion system:

Aircraft status*	Registered aeroplane Certification: CS-VLA
Engine installed on the aircraft	912 S2 delivering a maximum power of 100 hp (EASA Type Certificate No. EASA.E.121)
Powerplant type	Type 2 / carburettors associated with an Airbox

*: <https://www.easa.europa.eu/document-library/type-certificates/aircraft-cs-25-cs-22-cs-23-cs-vla-cs-lsa/easaa006-tecnam-p2002>



Figure 193: aeroplane on which the measurements were taken
Source: BEA



Figure 194: powerplant of the aeroplane used
Source: BEA

To conduct these tests, an approval was obtained from the EASA (EASA Approval Number: 60075728), then from the DGAC (No. 0637/20/NO/NAV).

European Union Aviation Safety Agency		60075728	Form												
Application for Approval of Flight Conditions for a Permit to Fly															
1. Applicant TECNAM FRANCE		2. Applicant's Reference TECNAM_FRANCE-F_GTFC-Measures in flight													
3. Aircraft manufacturer/type TECNAM / P2002JH / Registration: FGTFC		4. Serial number(s) 036													
5. Purpose (i.a.w. 21.A.701 a)															
1	2	3	4	5	6	7	8	9	10	11	12	13	14	15	16
<input checked="" type="checkbox"/>	<input type="checkbox"/>	<input type="checkbox"/>	<input type="checkbox"/>	<input type="checkbox"/>	<input type="checkbox"/>	<input type="checkbox"/>	<input type="checkbox"/>	<input type="checkbox"/>	<input type="checkbox"/>	<input type="checkbox"/>	<input type="checkbox"/>	<input type="checkbox"/>	<input type="checkbox"/>	<input type="checkbox"/>	<input type="checkbox"/>
Initial duration for Permit to Fly: From: 31 October 2020 Until: 1 st October 2021 Urgent - AOG <input type="checkbox"/>															
6. Aircraft configuration															
7. Substantiations															
8. Conditions/Restrictions															
9. Statement															
10. Approved under Organisation Approval Number (if applicable):															
11. Date of issue		12. Applicant name and signature													
20/10/2020		Lutz FRANCK													
Date		Name													
		Signature													
Important Note: EASA cannot accept applications without signature. Please make sure that you sign the application and the Flight Conditions for a Permit to Fly - Approval Form															
13. EASA Approval - To be filled in only by the European Aviation Safety Agency															
EASA Approval Number: 60075728		Name: Ralph MENZEL													
30 Oct 2020		Signature													
Date		Signature													

Figure 195: EASA approval
Source: BEA

LAISSEZ-PASSER PERMIT TO FLY		DIRECTION GENERALE DE L'AVIATION CIVILE	
N°0637/20/NO/NAV		1. Marques de nationalité et d'immatriculation Nationally and registration marks F-GTFC	
Ce laissez-passer est délivré conformément à l'article 5(4)(a) du règlement (CE) 216/2008 et certifie que l'aéronef est capable d'effectuer le(s) vol(s) prévus(s) en sécurité dans les conditions énumérées ci-dessous et est valide dans tous les Etats Membres. This permit to fly is issued pursuant to Regulation (EC) 216/2008, Article 5(4)(a) and certifies that the aircraft is capable of safe flight for the purpose and within the conditions listed below and is valid in all Member States. Cette autorisation de vol est également valable pour le vol vers et au-dessus des Etats non membres de l'UE sous réserve de l'obtention d'une approbation séparée des autorités compétentes de ces Etats. This permit is also valid for flight to and within non-Member States provided separate approval is obtained from the competent authorities of such States.			
2. Constructeur et type de l'aéronef Aircraft manufacturer and type COSTRUZIONI AERONAUTICHE TECNAM S.R.L P2002-JF		3. Numéro de série Serial number 036	
4. Ce laissez-passer couvre The permit to fly covers Vois de développement Development			
5. Détenteur Holder TECNAM FRANCE Aérodrome 01200 BELLEGARDE			
6. Conditions/Remarques Conditions/Remarks Les conditions de vols sont définies dans le document TECNAM_FRANCE-F_GTFC-Measures in flight du 20/10/2020, approuvé 60075728 le 30/10/2020, qui doit être en permanence associé au présent laissez-passer. The flight conditions are defined in the document TECNAM_FRANCE-F_GTFC-Measures in flight dated 20/10/2020, approved under/by 60075728 on 30/10/2020, which must be associated to this permit-to-fly. Remarques: a. Une autorisation de convoyage comprend un ou des vols de réception technique à l'aérodrome de départ et le convoyage proprement dit avec les escales techniques indispensables b. Le détenteur indique au §5 est responsable du respect de toutes les conditions associées à ce laissez-passer c. L'utilisation de l'aéronef doit être faite conformément aux règles d'exploitation des aéronefs applicables et les pilotes doivent être détenteurs des licences et qualifications adéquates valides en France, même s'ils sont mentionnés sur le laissez-passer ou un document associé. d. Si des marques provisoires ont été délivrées à l'aéronef, elles ne sont utilisables que pendant la durée de validité du laissez-passer ; ces marques ne permettent pas l'inscription au registre français d'immatriculation des aéronefs.			
7. Période de validité du 15/12/2020 au 28/02/2021 inclus Validity period			
8. Lieu et date de délivrance Paris, le 15/12/2020 Place and date of issue			
9. Signature du représentant de l'autorité compétente Signature of the competent authority representative		Benoit PINON Chef du pôle DSAG/NO/NAV	
AESA Form 20a			

Figure 196: DGAC approval
Source: BEA

The content of the tests validated by these approvals is specified below:

- **Take-off and landing aerodrome:**

LFHN BELLEGARDE Vouvray (Ain).

GPS location:

- latitude: 46° 07' 27" N;
- longitude: 005° 48' 22" E.

Altitude: 1,624 ft (495 m).

- **Flight programme:**

Two flights, each lasting 30 to 40 minutes.

Flight #1:

- Aircraft check
- Start-up and operation at stop position for at least 5 minutes
- Take-off
- Climb over the Plateau du Retord (France) - Altitude 5,000 to 5,500 ft - Rate of climb = 500 to 600 ft/min depending on the conditions of the day
- Descent and return to the aerodrome
- Touchdown then climb to an altitude of 3,300 ft
- High speed flight (115 to 120 kt) for two minutes, then low speed flight (65 to 70 kt) for three minutes
- Return to the aerodrome and landing
- Engine shut-down

Pause of around 30 to 40 minutes

Flight #2:

Content of flight #2 identical to that of flight #1.

Sensors installed on the aircraft:

One iButton sensor positioned on the outside of the aircraft, attached to the lower surface of the RH wing, at the root (temperature and relative humidity measurement)



Figure 197: temperature and relative humidity measurement sensor
Source: BEA

One iButton sensor positioned under the engine cowlings, in the immediate vicinity of the LH carburettor (temperature and relative humidity measurement)

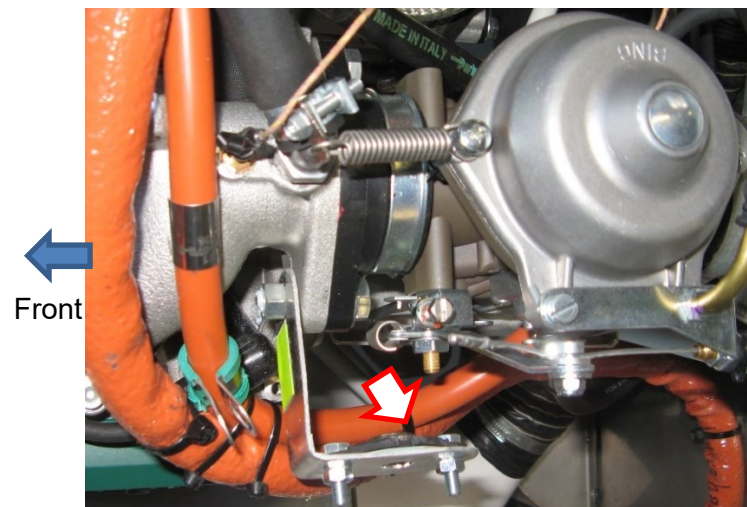


Figure 198: temperature and relative humidity measurement sensor
Source: BEA

One thermocouple attached to the outer surface of the body of the LH carburettor (temperature measurement)

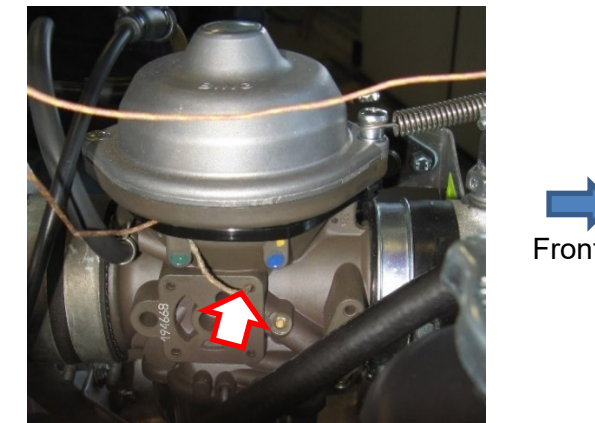


Figure 199: temperature measurement sensor
Source: BEA

One thermocouple attached immediately downstream of the LH carburettor butterfly valve (temperature measurement)

The thermocouple is located in the air flow in line with the carburettor output section.

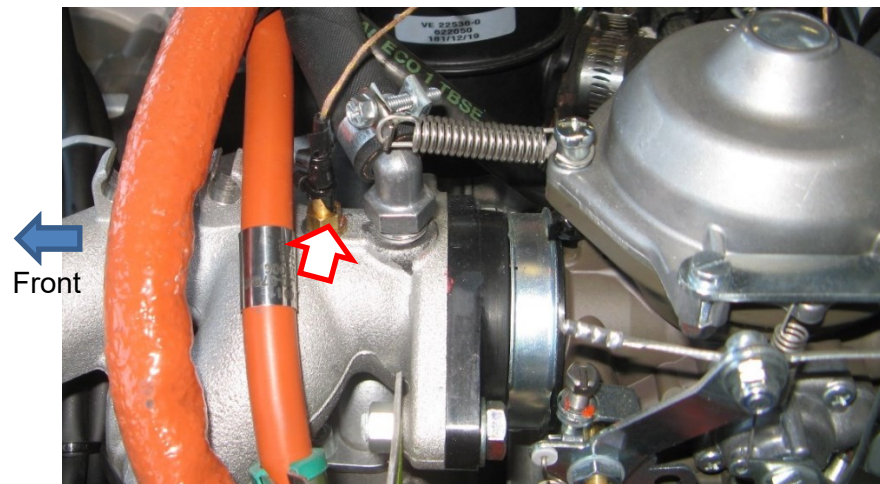


Figure 200: temperature measurement sensor
Source: BEA

One thermocouple attached in the Airbox (temperature measurement)

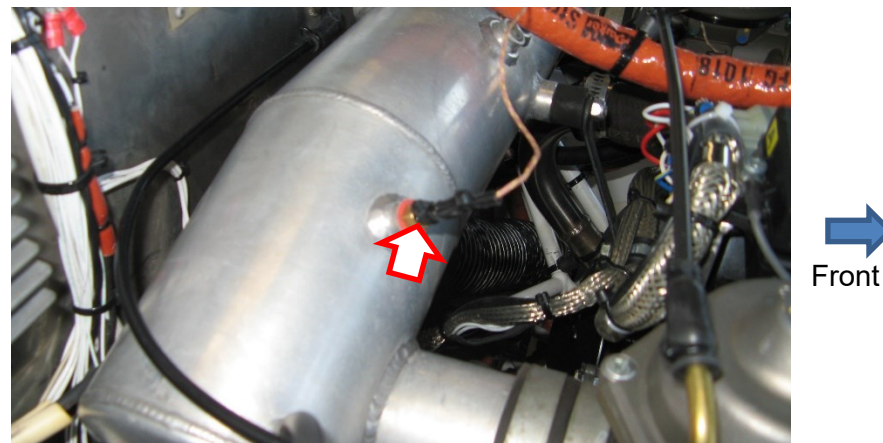


Figure 201: temperature measurement sensor
Source: BEA

One thermocouple attached at the Airbox intake (temperature measurement)

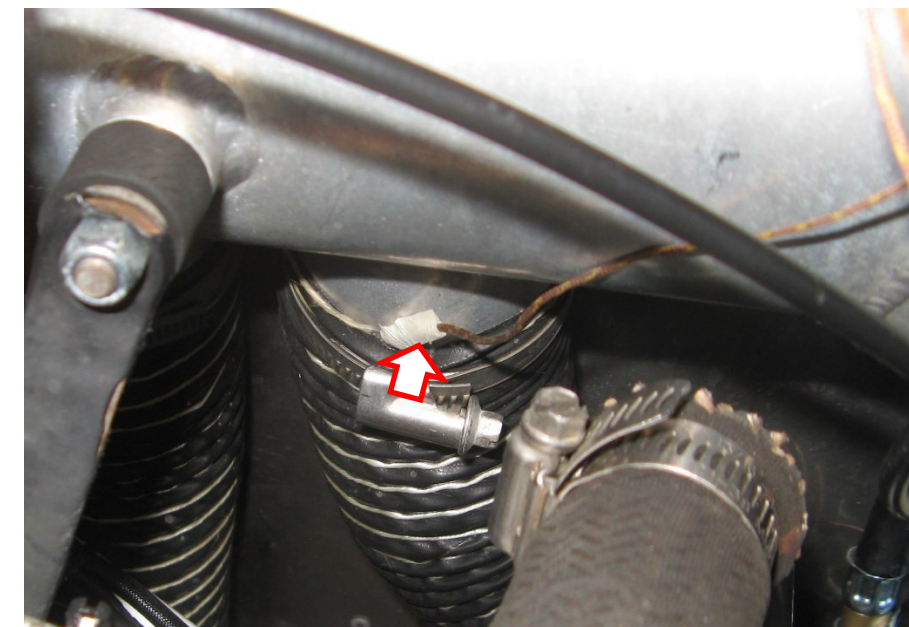


Figure 202: temperature measurement sensor
Source: BEA

Conditions during the flight:

Key:

	On the ground, before flight 1
	On the ground, before flight 2
	In descent, at the end of flights 1 and 2

If we reposition these conditions on the graph proposed by the EASA:

- on the ground, before flight 1, these conditions were conducive to serious icing in descent;
- on the ground, before flight 2, these conditions were conducive to serious icing in descent and to moderate icing in cruise flight;
- during the final descent of flights 1 and 2, these conditions were conducive to serious icing in descent and to moderate icing in cruise flight.

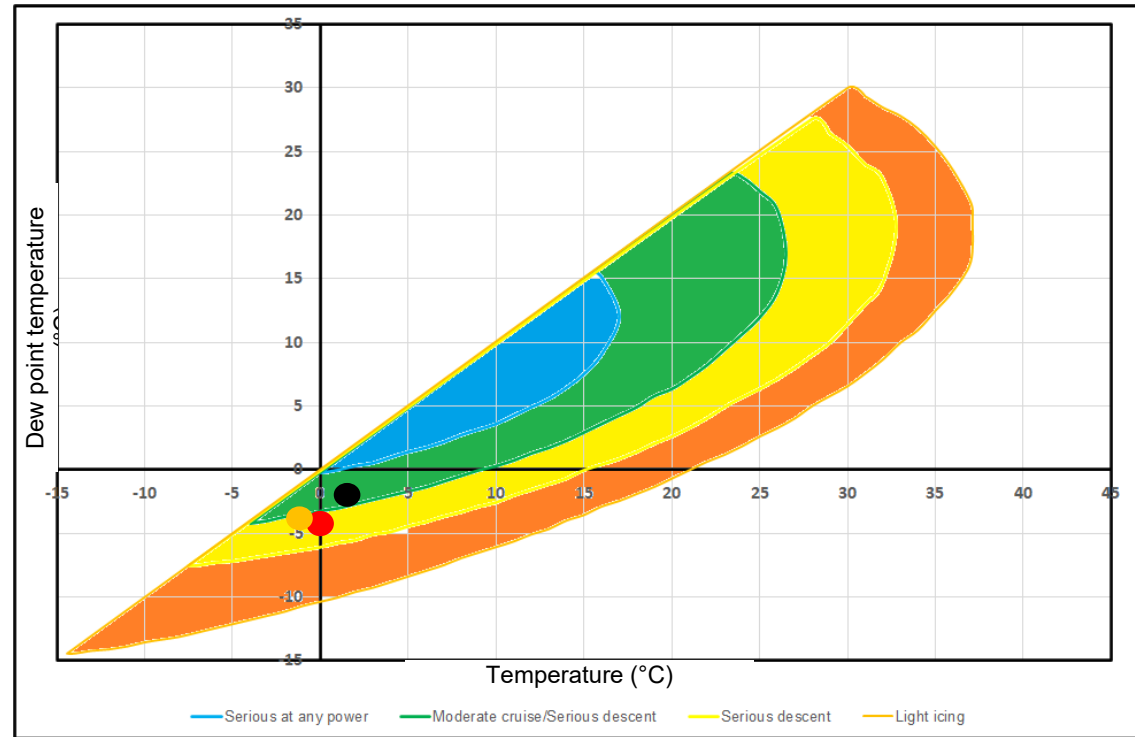


Figure 203: repositioning the weather conditions on the EASA graph
Source: BEA

Temperature

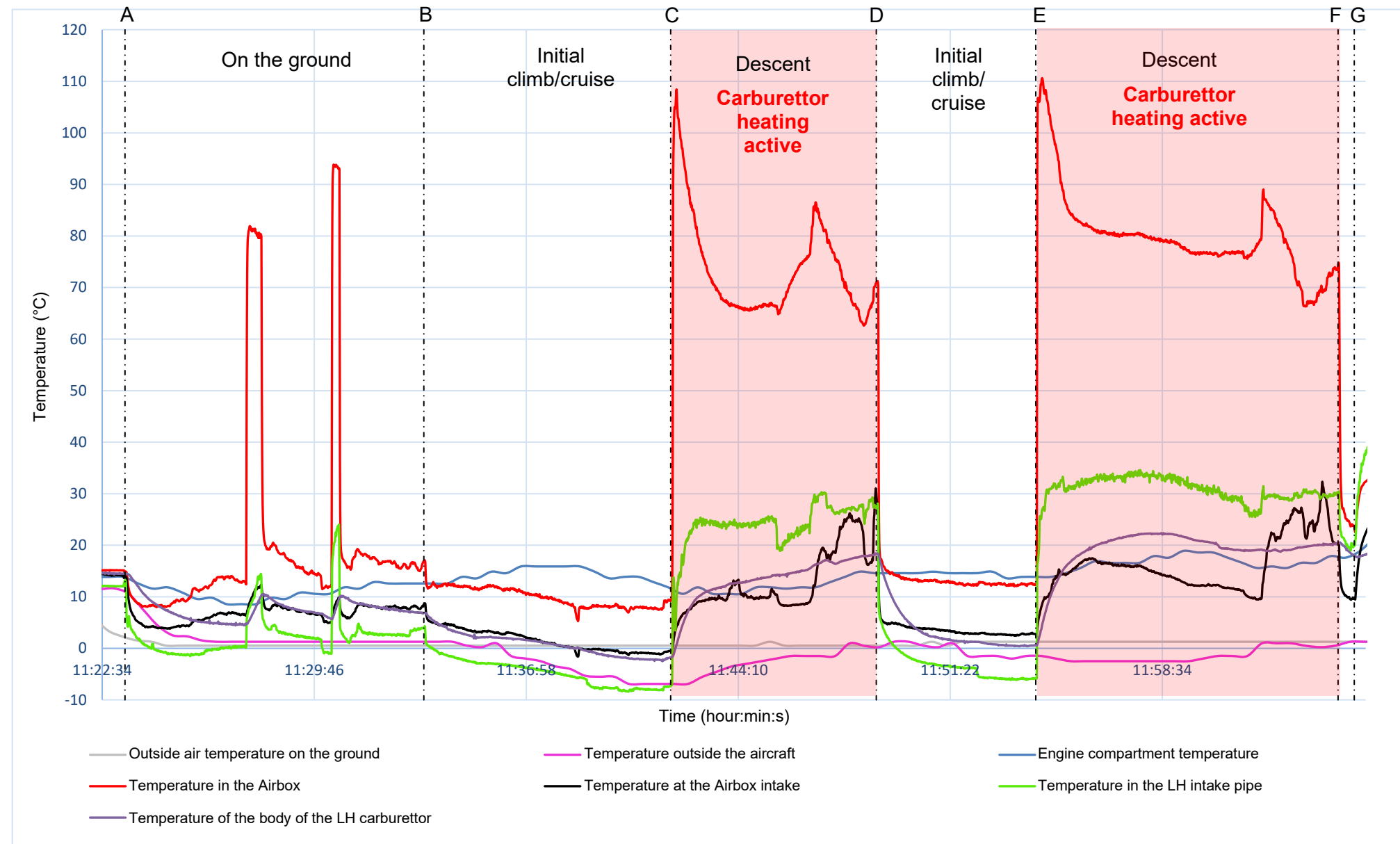


Figure 204: temperature measurements
Source: BEA

Key:

Reference line	Phase	Reference line	Phase
A	Engine start-up	B	Take-off / Power-up
C	Start of descent	D	Touch and go
E	Start of descent	F	Landing
G	Engine shut-down		

Comments:

During engine start-up, it was observed that:

- the temperature at the Airbox intake decreased by around 8°C for one minute, then increased by around 5°C;
- the temperature in the Airbox decreased by around 10°C for two minutes, then increased by around 3°C;
- the temperature of the carburettor body gradually decreased until it was around 10°C below the start-up temperature;
- the temperature in the intake duct suddenly decreased by around 14°C.

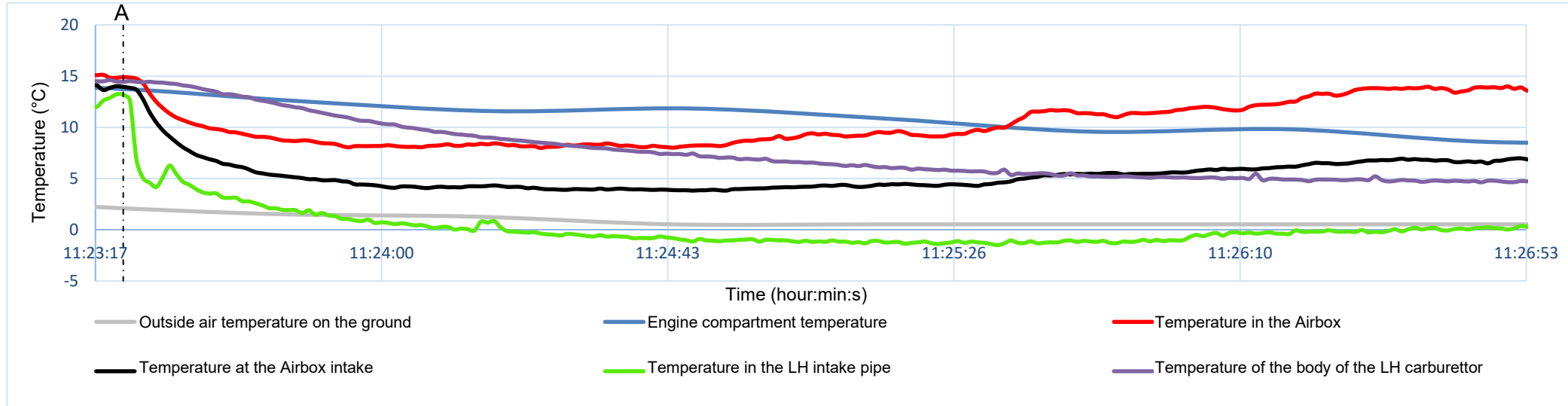


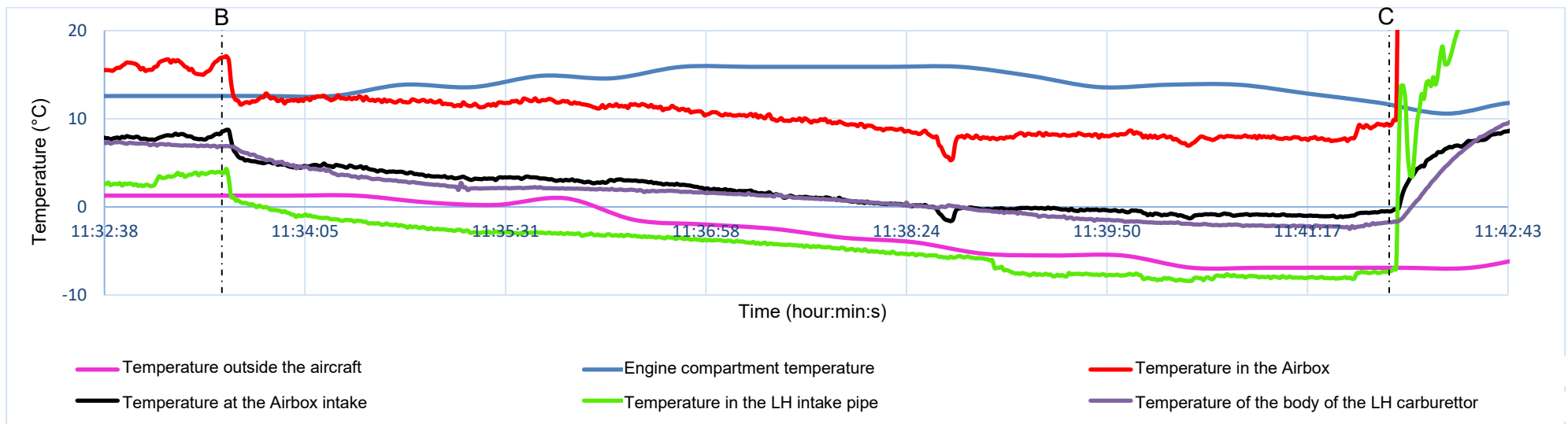
Figure 205: temperature measurements

Source: BEA

From start-up to take-off, the temperature under the cowlings decreased very slightly, 8 to 11°C higher than the outside air temperature.

In the first “climb/cruise” phase, we can observe that:

- the temperature under the cowlings was never lower than the temperature under the cowling during take-off, and it was higher by around 3°C during this phase;
- the temperature at the Airbox intake was around 2 to 6°C higher than the outside air temperature;
- the temperature in the Airbox was around 10 to 14°C higher than the outside air temperature and around 7 to 9°C higher than the temperature at the Airbox intake;
- the temperature in the intake duct was around 1 to 2°C lower than the outside air temperature;
- the temperature on the outer surface of the carburettor remained higher than the outside air temperature despite it falling to below 0°C during this flight phase.



In each descent phase, the carb heat system was activated. This activation instantly resulted in:

- a very marked increase in temperature of around 100°C in the air intake, followed by a decrease until it was around 60°C higher than that prior to activation of the heat system;
- an increase in the temperature of around 10°C at the Airbox intake;
- an increase in the temperature of around 24°C in the intake duct;
- an increase in the temperature of around 15°C of the outer surface of the carburettor.

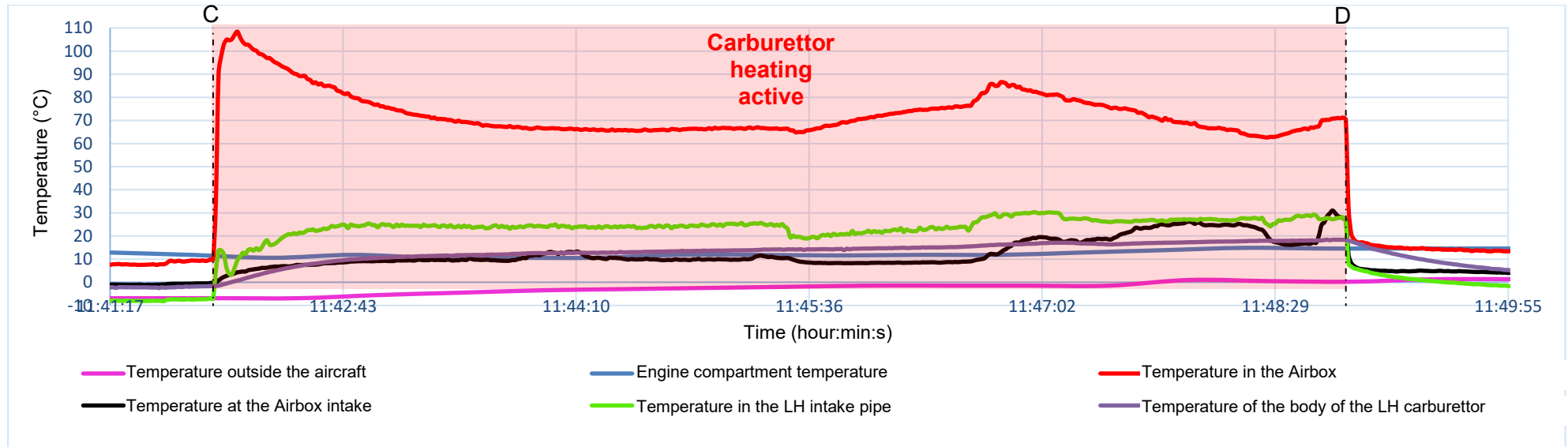


Figure 207: temperature measurements
Source: BEA

5.6.3.2.4 - TECNAM P2008 JC

The flight of this aircraft took place on 21 January 2022.

Information pertaining to the aircraft and its propulsion system:

Aircraft status*	Registered aeroplane Certification: CS-VLA
Engine installed on the aircraft	912 S2 delivering a maximum power of 100 hp (EASA Type Certificate No. EASA.E.121)
Powerplant type	Type 2 / carburettors associated with an Airbox

*: <https://www.easa.europa.eu/document-library/type-certificates/aircraft-cs-25-cs-22-cs-23-cs-vla-cs-lsa/easaa583-tecnam-p2008>



Figure 208: aeroplane on which the measurements were taken
Source : <http://tagazous.free.fr/affichage2.php?img=57907>



Figure 209: powerplant of the aeroplane used
Source: BEA

To conduct these tests, an approval was obtained from the EASA (EASA Approval Number: 60078213), then from the DGAC (No. 0652/21/NO/NAV).

1. Applicant		2. Applicant's Reference	
AVIALPES		AVIALPES_FRANCE-F_HCTF-Measures in flight	
3. Aircraft manufacturer/type		4. Serial number(s)	
TECNAM / P2008IC / Registration: F-HCTF		1036	
5. Purpose (i.a.w. 21.A.701(a))			
1	2	3	4
<input checked="" type="checkbox"/>	<input type="checkbox"/>	<input type="checkbox"/>	<input type="checkbox"/>
5	6	7	8
<input type="checkbox"/>	<input type="checkbox"/>	<input type="checkbox"/>	<input type="checkbox"/>
9	10	11	12
<input type="checkbox"/>	<input type="checkbox"/>	<input type="checkbox"/>	<input type="checkbox"/>
13	14	15	16
<input type="checkbox"/>	<input type="checkbox"/>	<input type="checkbox"/>	<input type="checkbox"/>
Initial duration for Permit to Fly: From: 1st April 2021 Until: 1st April 2022 Urgent - AOG <input type="checkbox"/>			
6. Aircraft configuration			
The above aircraft for which a flight permit is requested will only be fitted with six sensors. The installation of these sensors will not require any modification of the aircraft. (Detailed description of the installation in chapter 4.3)			
7. Substantiations			
All the sensors used will be electrically autonomous. Under these conditions, the electrical balance of the aircraft will remain unchanged and the operating conditions of the aircraft systems are not affected by the sensors used.			
8. Conditions/Restrictions			
This flight permit is required for one flight, lasting a total of approximately 0.5 to 1 hour. The test program is shown in the attachment.			
The flight conditions approval remains valid provided the declared configuration is applicable, the aircraft is maintained in accordance with defined instructions, and compliance with airworthiness directives is observed.			
9. Statement			
The flight conditions have been established and justified in accordance with 21.A.708.			
The aircraft as defined in Field 6 above has no features and characteristics making it unsafe for the intended operation under the identified conditions and restrictions.			
10. Approved under Organisation Approval Number (if applicable):			
11. Date of issue	12. Applicant name and signature		
14/04/2021	CHAINE JEREMIE		
Date	Name		Signature
Important Note: EASA cannot accept applications without signature. Please make sure that you sign the application and the Flight Conditions for a Permit to Fly – Approval Form			
13. EASA Approval - To be filled in only by the European Aviation Safety Agency			
EASA Approval Number	60078213		
Name	Ralph MENZES		
28 Apr 2021, Köln			
Date	Signature		
An agency of the European Union			

Completion Instructions F18B.dc
Please double-click on the icon to access the completion instructions

Figure 210: EASA approval
Source: BEA

LAISSEZ-PASSER PERMIT TO FLY	
DIRECTION GENERALE DE L'AVIATION CIVILE N°0652/21/NO/NAV	
<p>Ce laissez-passer est délivré conformément à l'article 5(4)(a) du règlement (CE) 216/2008 et certifie que l'aéronef est capable d'exécuter le(s) vol(s) prévu(s) en sécurité dans les conditions énumérées ci-dessous et est valide dans tous les Etats Membres.</p> <p>This permit to fly is issued pursuant to Regulation (EC) 216/2008, Article 5(4)(a) and certifies that the aircraft is capable of safe flight for the purpose and within the conditions listed below and is valid in all Member States.</p> <p>Cette autorisation de vol est également valable pour le vol vers et au-dessus des Etats non membres de l'UE sous réserve de l'obtention d'une approbation séparée des autorités compétentes de ces Etats.</p> <p>This permit is also valid for flight to and within non-Member States provided separate approval is obtained from the competent authorities of such States.</p>	
1. Marques de nationalité et d'immatriculation Nationality and registration marks F-HCTF	
2. Constructeur et type de l'aéronef Aircraft manufacturer and type COSTRUZIONI AERONAUTICHE TECNAM S.P.A P2008 JC	3. Numéro de série Serial number 1036
4. Ce laissez-passer couvre The permit to fly covers Vois de développement Development	
5. Détenteur Holder Avialpes 8 Route de Côte merle 74370 Epagny Metz-Tessy	
6. Conditions/Remarques Conditions/Remarks Les conditions de vols sont définies dans le document Avialpes_France-F_HCTF-Measures in flight du 14/04/2021, approuvé 60078213 le 28/04/2021, qui doit être en permanence associé au présent laissez-passer. The flight conditions are defined in the document Avialpes_France-F_HCTF-Measures in flight dated 14/04/2021, approved under/by 60078213 on 28/04/2021, which must be associated to this permit-to-fly. Remarques: a. Une autorisation de convoyage comprend un ou des vols de réception technique à l'aérodrome de départ et le convoyage proprement dit avec les escalas techniques indispensables b. Le détenteur indiqué au §5 est responsable du respect de toutes les conditions associées à ce laissez-passer c. L'utilisation de l'aéronef doit être faite conformément aux règles d'exploitation des aéronefs applicables et les pilotes doivent être détenteurs des licences et qualifications adéquates valides en France, même s'ils sont mentionnées sur le laissez-passer ou un document associé. d. Si des marques provisoires ont été délivrées à l'aéronef, elles ne sont utilisables que pendant la durée de validité du laissez-passer ; ces marques ne permettent pas l'inscription au registre français d'immatriculation des aéronefs.	
7. Période de validité du 19/11/2021 au 01/04/2022 inclus Validity period	
8. Lieu et date de délivrance Paris, le 19/11/2021 Place and date of issue	
9. Signature du représentant de l'autorité compétente Signature of the competent authority representative Benoît PINON Chef du pôle DSAC/NO/NAV 	
AESA Form 20a	

Figure 211: DGAC approval
Source: BEA

The content of the tests approved by these approvals is specified below:

- **Take-off and landing airport:**

LFLP ANNECY Mont-Blanc airport

GPS location:

- latitude: 45° 55' 46" N;
- longitude: 006° 05' 56" E;

Altitude: 1,522 ft (463.9 m).

- **Flight programme:**

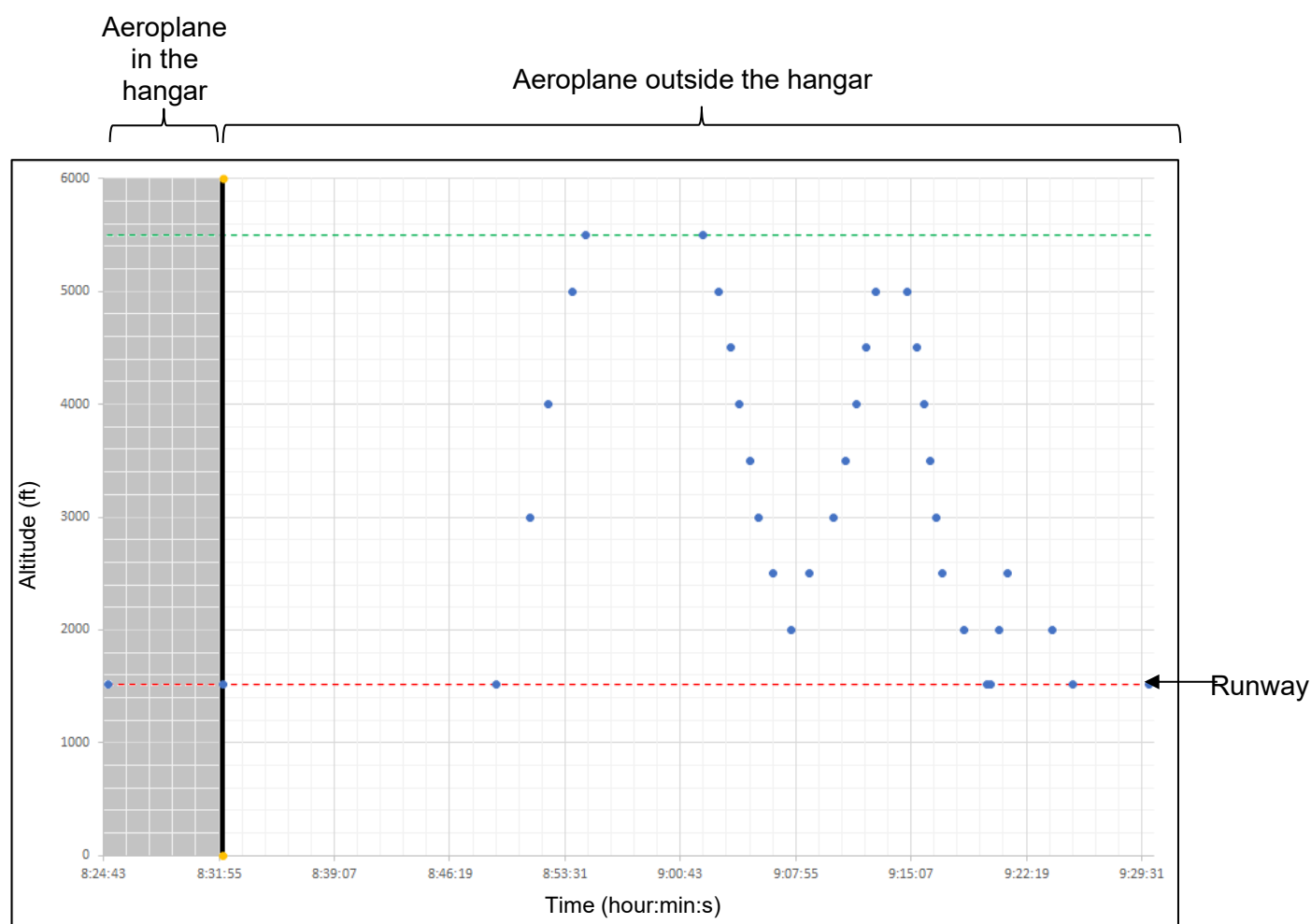


Figure 212: flight profile
Source: BEA

Position of the sensors on the aircraft

One thermocouple attached to the outer surface of the body of the RH carburettor (temperature measurement)

←
Front

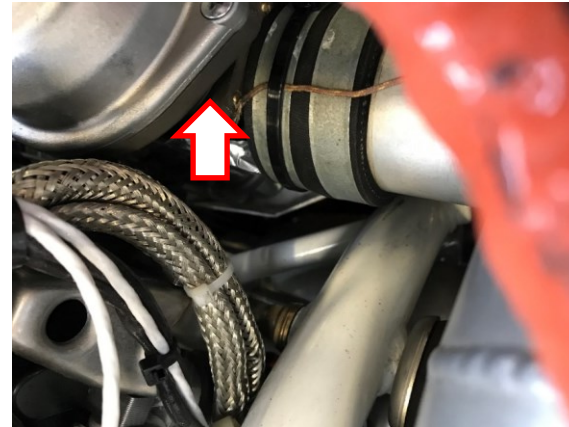


Figure 213: temperature measurement sensor
Source: BEA

One thermocouple attached in the Airbox (temperature measurement)

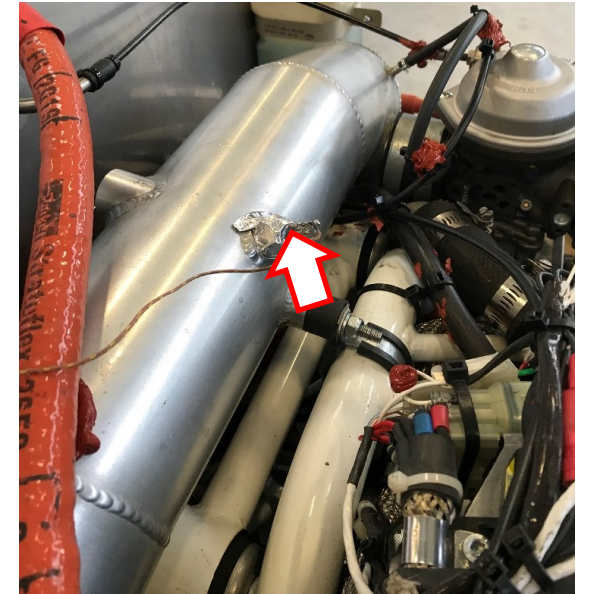


Figure 214: temperature measurement sensor
Source: BEA

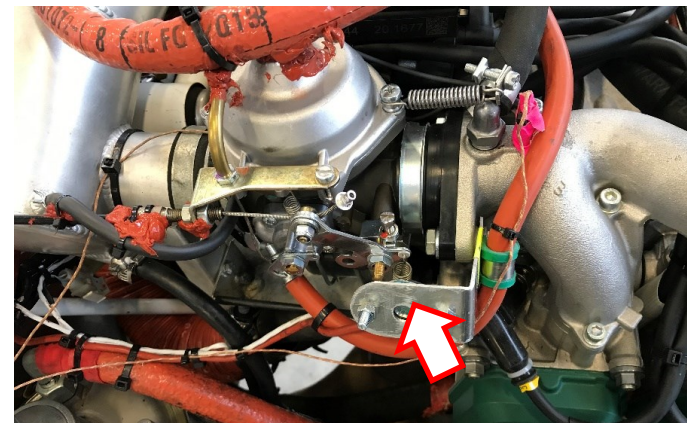
One iButton sensor positioned on the outside of the aircraft, attached to the lower surface/leading edge of the RH wing (temperature and relative humidity measurement)



Figure 215: position of the temperature and relative humidity measurement sensor
Source: BEA



One iButton sensor positioned under the engine cowlings, in the immediate vicinity of the LH carburettor (temperature and relative humidity measurement)



→
Front

Figure 217: temperature and relative humidity measurement sensor
Source: BEA

One thermocouple attached immediately downstream of the RH carburettor butterfly valve (temperature measurement)

The thermocouple is located in the air flow in line with the carburettor output section.

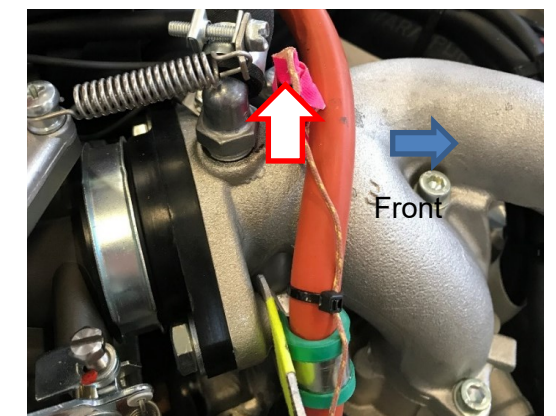


Figure 216: temperature measurement sensor
Source: BEA

Conditions during the flight:

Key:

- Weather conditions, on the ground, taken from the airport report
Start of tests: 0.7°C / 67% humidity / Dew point temperature -4.9°C
- Weather conditions, on the ground, logged by the sensor installed on the outside of the aircraft
Start of tests: 0.5°C / 65 % humidity / Dew point temperature -8.9°C
- Weather conditions at the start of the first descent
-6.5°C / 79 % humidity / Dew point temperature -5.6°C (similar conditions at the start of the second descent)
- Weather conditions during the first descent to 3,500 ft
-5.3°C / 86% humidity / Dew point temperature -7.2

If we reposition these conditions on the graph proposed by the EASA, these conditions were conducive to serious icing in descent.

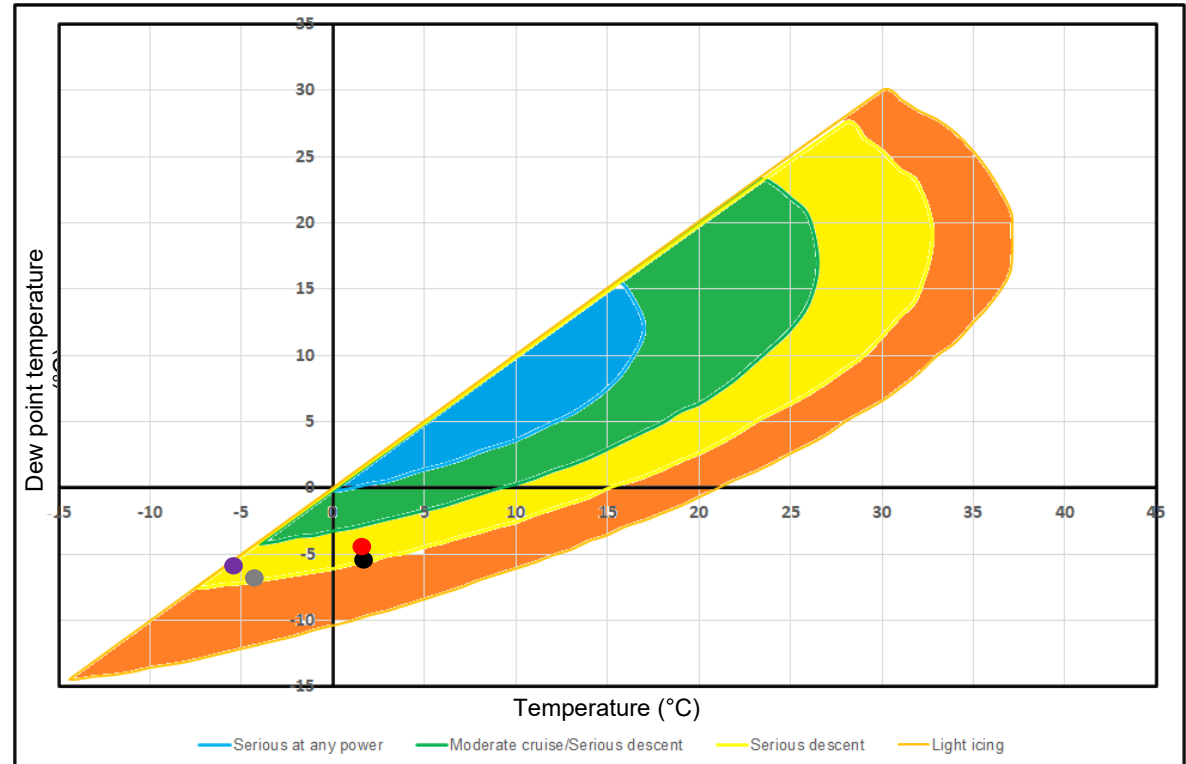


Figure 218: repositioning the test conditions on the EASA graph
Source: BEA

Temperature changes - Ground phase:

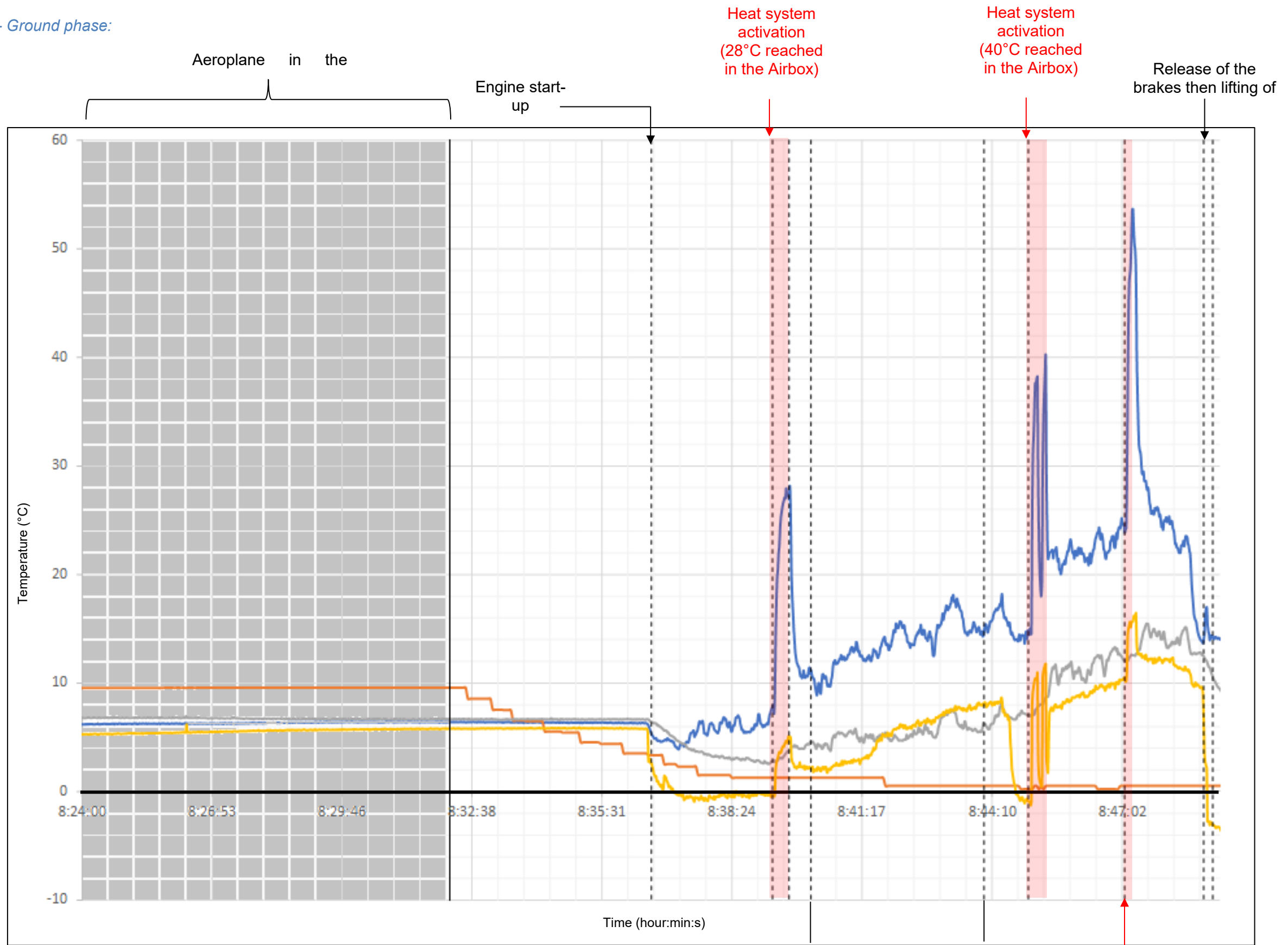
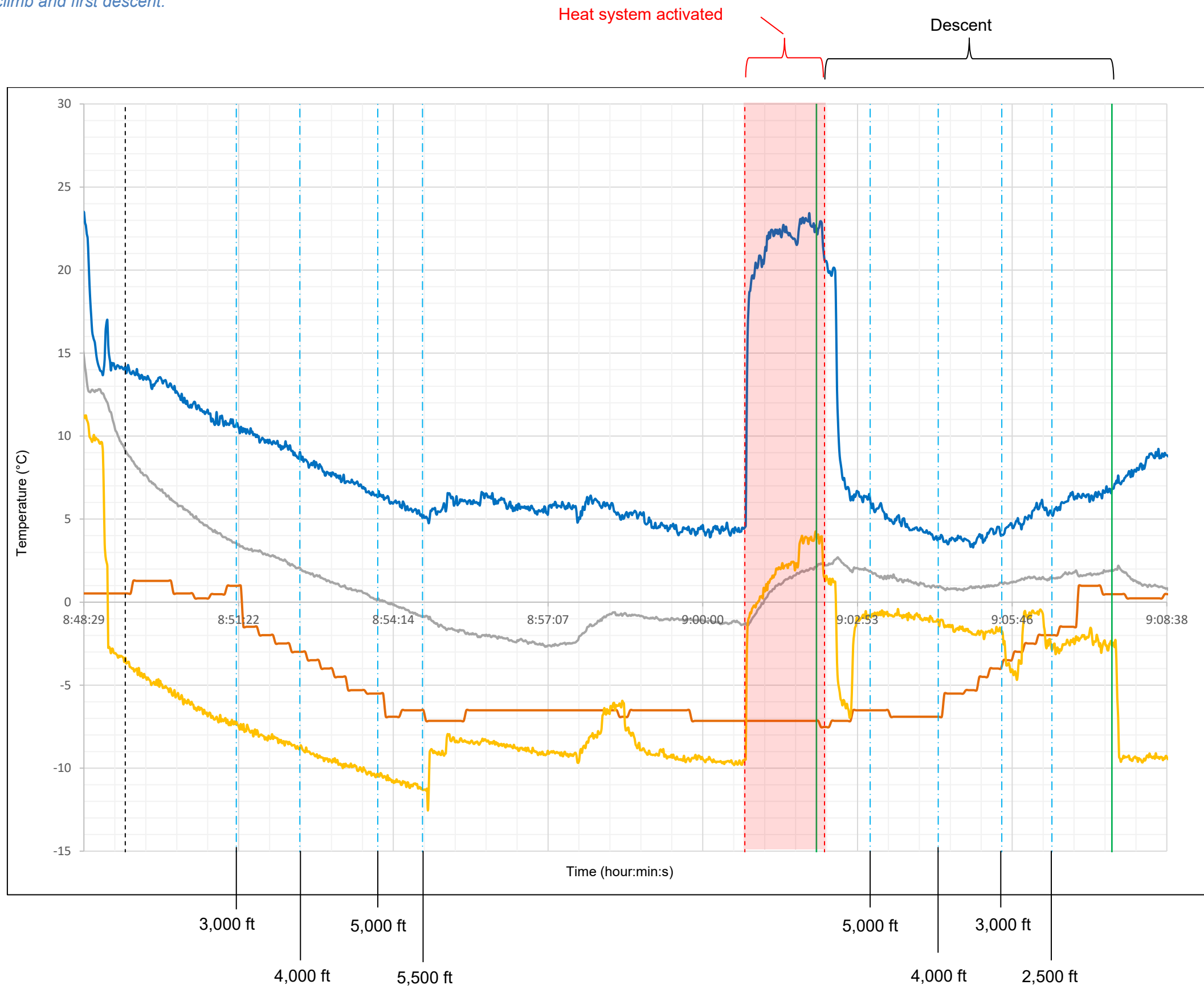


Figure 219: temperature changes on the ground
Source: BEA

	Temperature of the Airbox
	Temperature of the outer surface of the RH carburettor
	Temperature downstream of the RH carburettor butterfly valve
	Outside air temperature

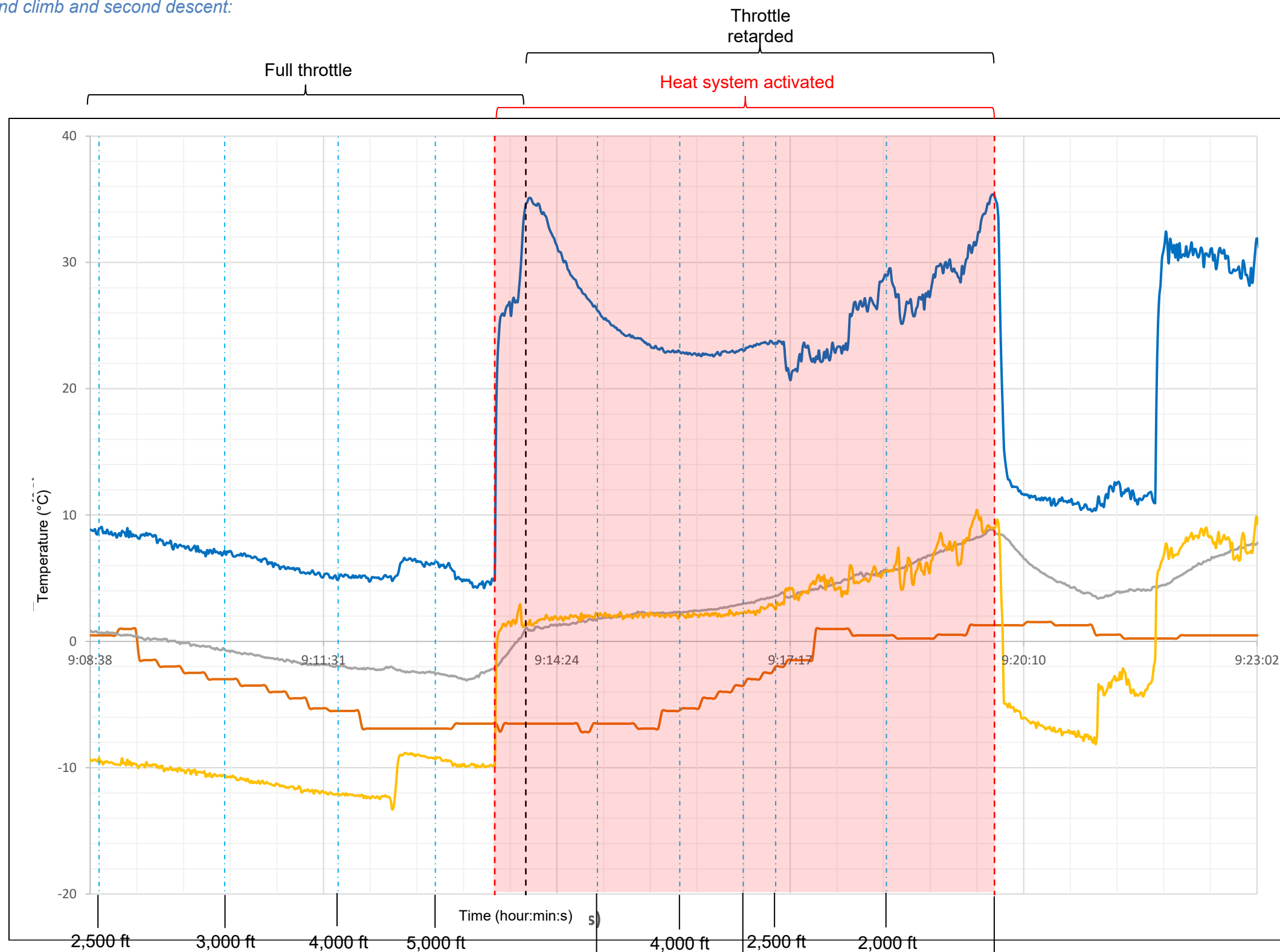
Running

Heat system activation (54°C reached in the Airbox)



	Temperature of the Airbox
	Temperature of the outer surface of the RH carburettor
	Temperature downstream of the RH carburettor butterfly valve
	Outside air temperature

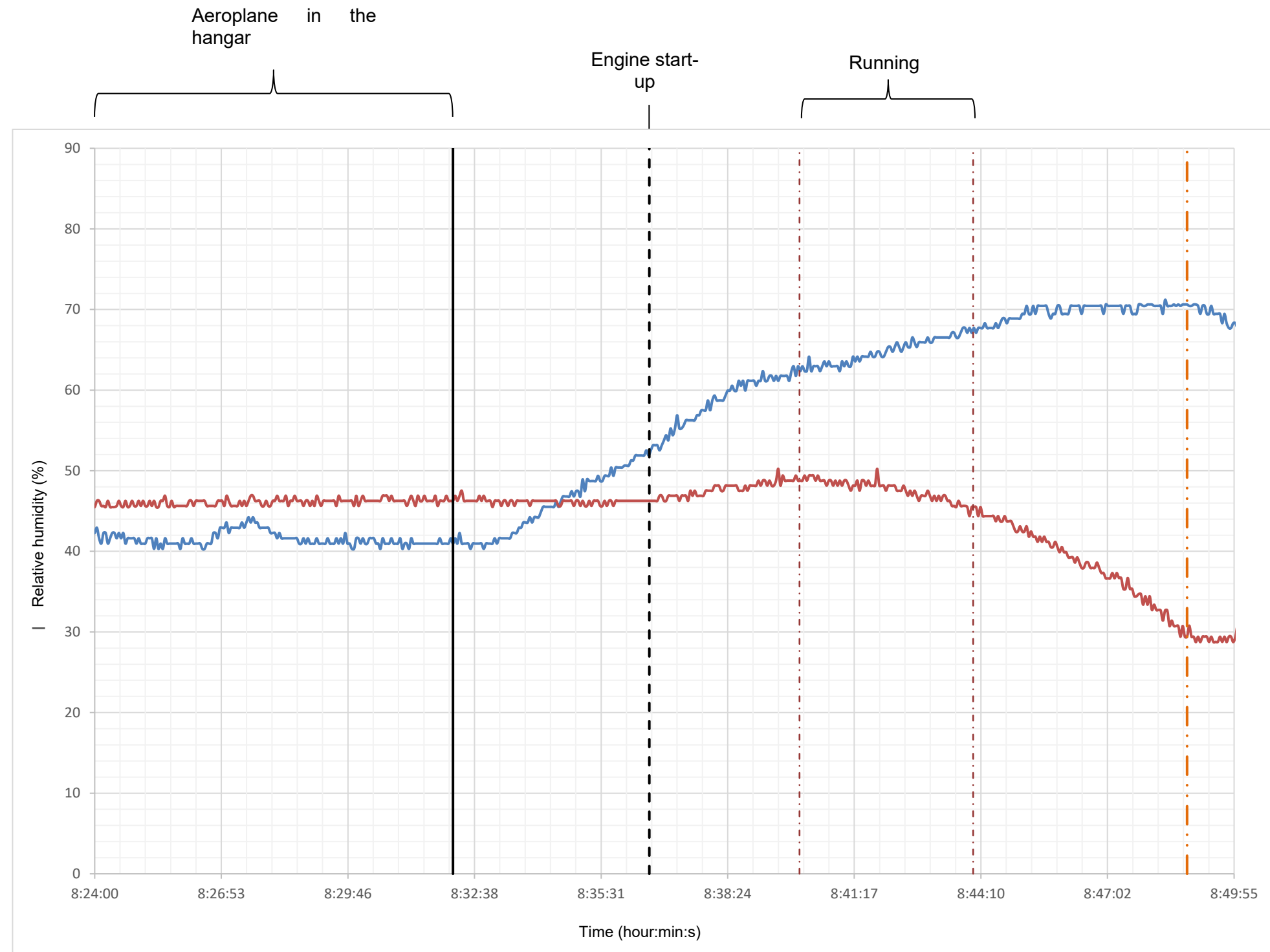
Figure 220: temperature changes in initial climb and first descent (without heating)
 Source: BEA



—	Temperature of the Airbox
—	Temperature of the outer surface of the RH carburettor
—	Temperature downstream of the RH carburettor butterfly valve
—	Outside air temperature

Figure 221: temperature change during the second climb and the second descent (with heating)
Source: BEA

Relative humidity change - Ground phase:





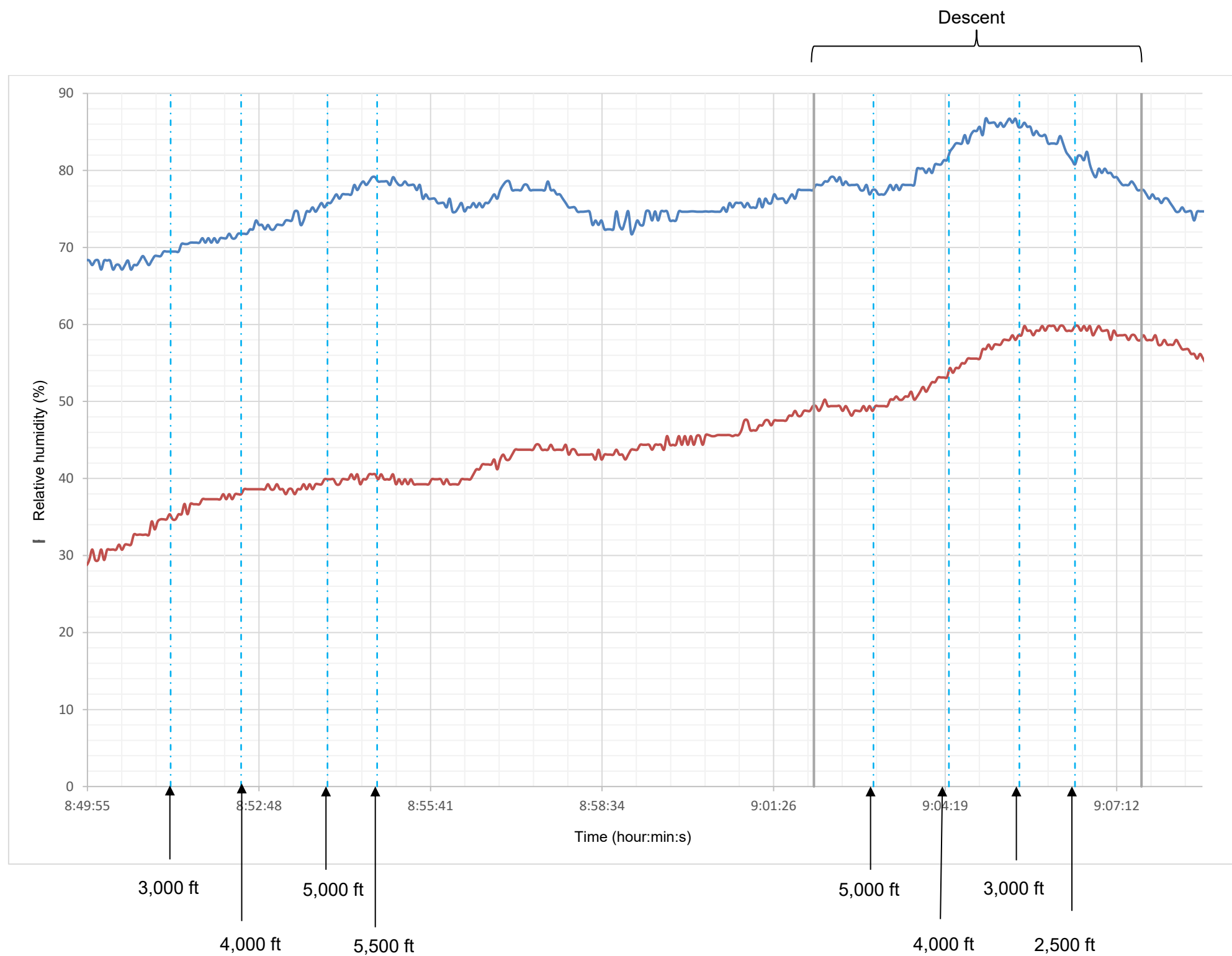
	Outside relative humidity
	Relative humidity under the engine cowlings

Figure 222: relative humidity change on the ground
Source: BEA

Relative humidity change - Initial climb and first descent:



—	Outside relative humidity
—	Relative humidity under the engine cowlings

Figure 223: relative humidity change in initial climb and first descent (without heating)
Source: BEA

5.6.4. Measurements at the test stand



Figure 224: Rotax 914 engine at the test stand

Source: BEA

The following sensors were installed:

- an iButton sensor in the test chamber, separate from the engine, to log the conditions of the day;
- an iButton sensor attached to the rear face of the reduction gearbox;
- a thermocouple in the RH intake pipe, immediately downstream of the carburettor;

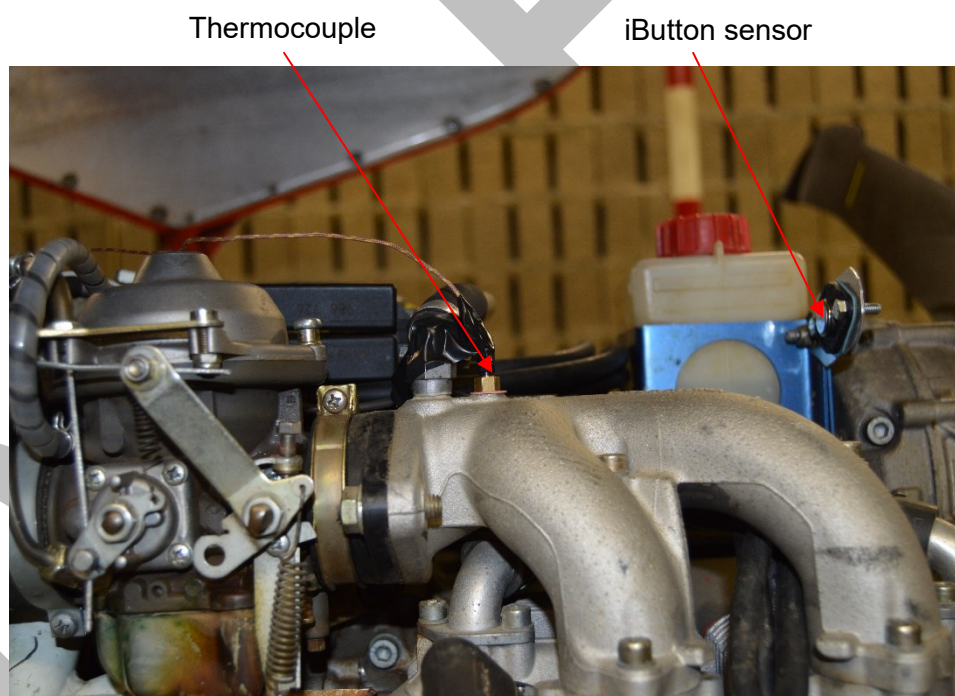


Figure 225: position of the sensors

Source: BEA

- a thermocouple in the Airbox;

Thermocouple

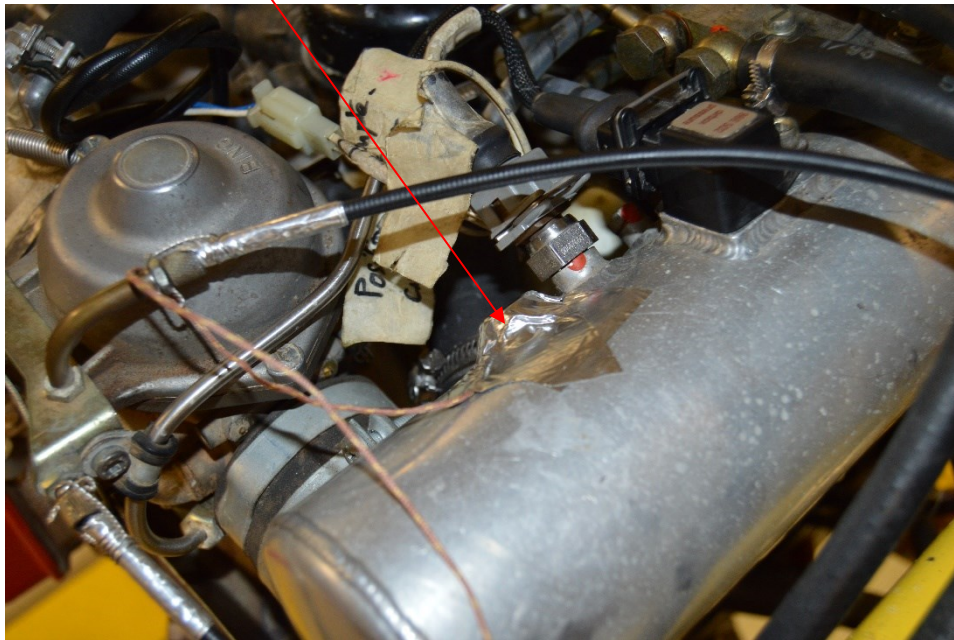


Figure 226: thermocouple in the Airbox.
Source: BEA

- a thermocouple in the hose connecting the turbocharger to the Airbox.

DRAFT

Thermocouple

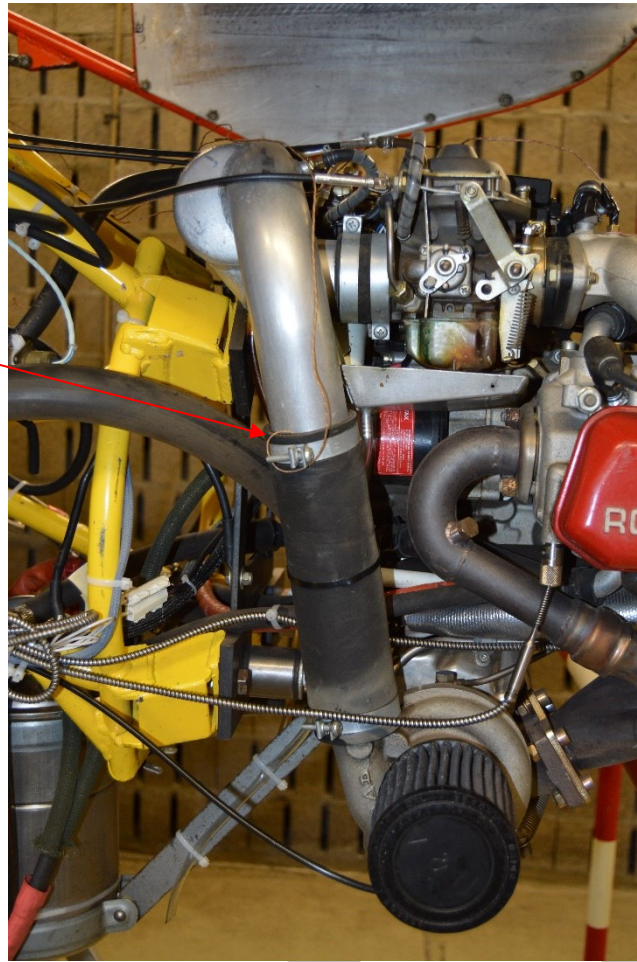


Figure 227: thermocouple between the turbocharger and the Airbox

Source: BEA

The results of these measurements are as follows:

DRAFT

Temperature

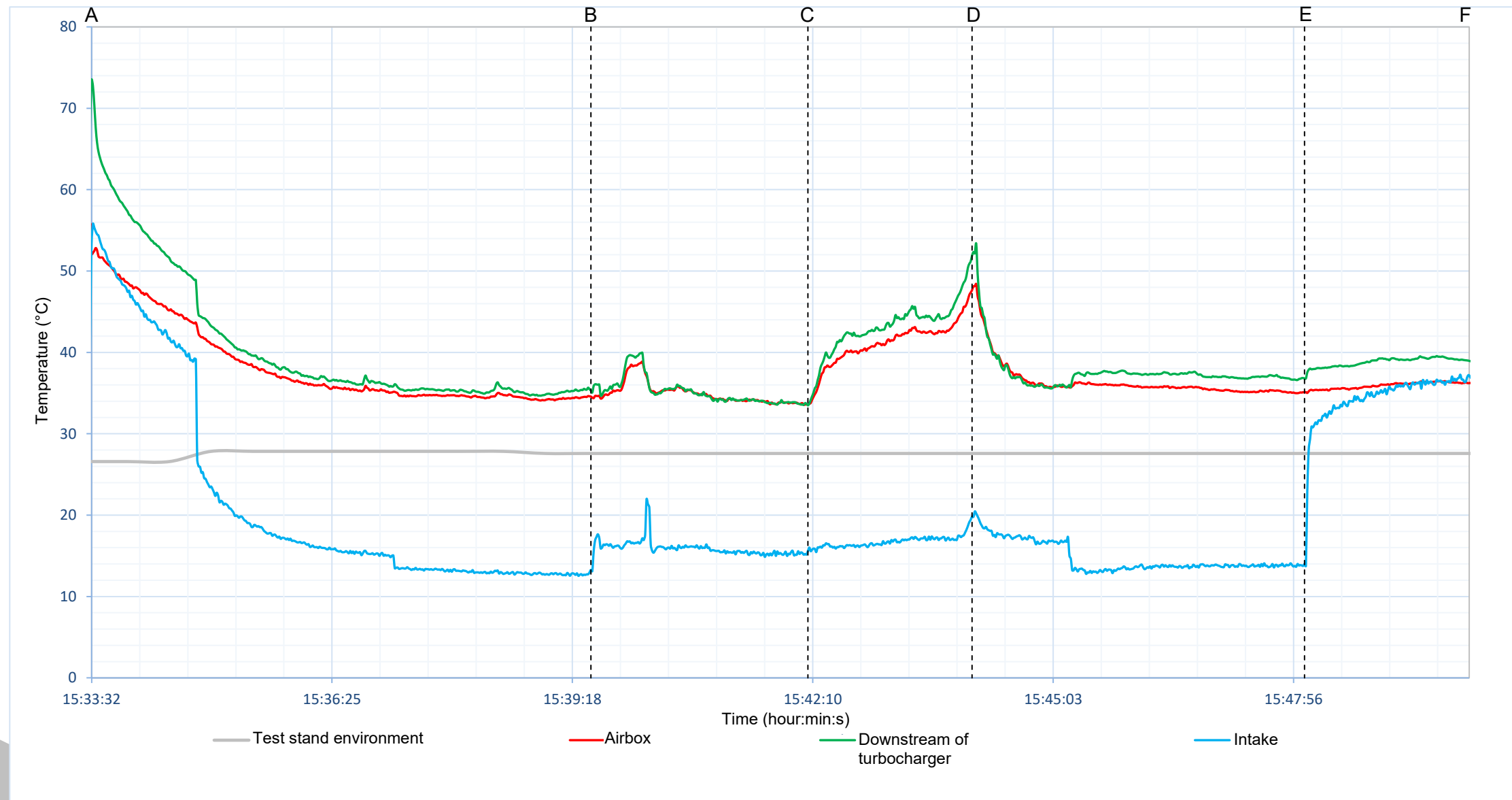


Figure 228: temperature measurements
Source: BEA

Key:

Reference line	Phase	Reference line	Phase
A	Start-up	D	Decrease to 4,000 rpm
B	Increase to 4,000 rpm	E	Idle
C	Increase to 5,300 rpm	F	Shut-down

Comments:

Relative humidity

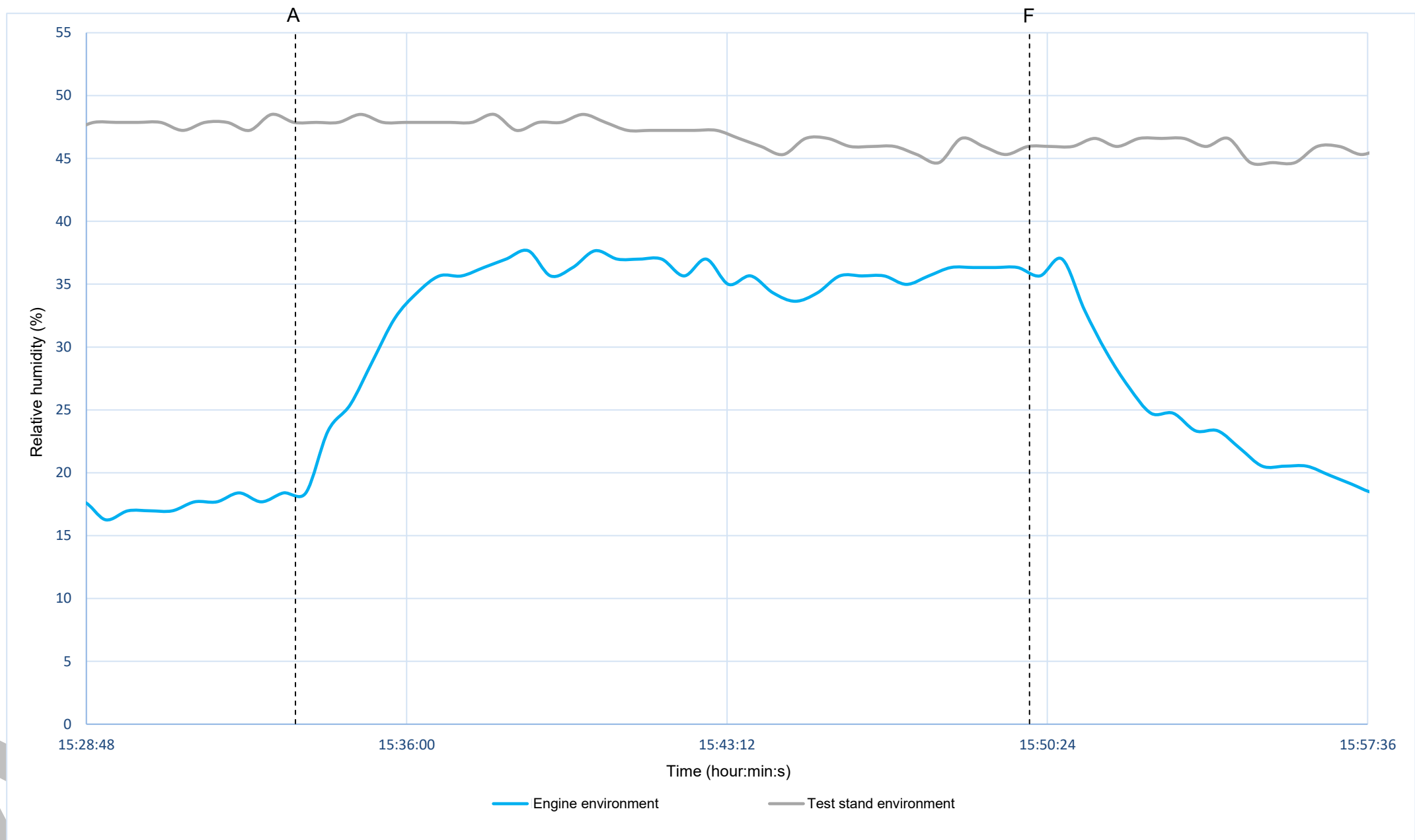


Figure 229: temperature measurements

Source: BEA

Key:

Reference line	Phase	Reference line	Phase
A	Start-up	F	Shut-down

Comments:

5.7. Summary and comments

The bibliographic research conducted by the BEA did not identify validated data likely to meet the requirements of a rigorous and objective investigation approach, in the event of suspected induction system icing on aircraft equipped with a Rotax engine.

Data provided in the manufacturer flight manuals varies. However, we noted that several manuals state that icing is more likely to occur when the temperature is below 10°C, independently of the dew point temperature.

No scientific article on Rotax 912/914 engines and icing was identified. The two articles identified focus on two-stroke engines. In these articles, the author focuses on the importance of the temperature of the outer surface of the carburettor, with icing not starting due to a temperature that was too high.

The tests conducted by the BEA on different aircraft showed that variations in temperature and relative humidity differ greatly depending on the aircraft and the powerplant.

- **Three-axis aircraft with a type 1 powerplant (para. 5.2):**

At engine start-up, an immediate decrease in the temperature downstream of the throttle butterfly valve was systematically recorded. This decrease in temperature was generated by the flow of air circulating in the venturi and at fuel injection.

If we compare the data logged on the Tecnam P92 (para. 5.6.3.2.2) and the Aeroprakt A-22L (para. 5.6.3.2.3), this decrease in temperature is different:

	Tecnam P92	Aeroprakt A-22L
Decrease in temperature downstream of the throttle butterfly valve	Around 10 to 12°C	Around 5°C

On the Tecnam, this decrease in temperature was associated with a decrease in temperature of around 6°C of the outer surface of the carburettor. On the Aeroprakt, this decrease in temperature was not observed.

On these two aircraft, the change in parameters also differed during **the period on the ground, between engine start-up and take-off**, with an outside air temperature that remained consistent:

	Tecnam P92	Aeroprakt A-22L
Temperature in the engine compartment	Almost consistent	Temperature increase of around 12°C
Temperature downstream of the throttle butterfly valve	Temperature increase of around 5°C	Temperature increase of around 6°C
Temperature of the outer surface of the carburettor	Temperature increase of around 1 to 2°C	Temperature increase of around 5°C
Relative humidity in the engine compartment	Almost consistent	Gradual decrease of around 40%

During this same period, if we compare the measurements logged on the two Aeroprakt A-22 (one with carburettor - para. 5.6.3.2.3 and the other with injection - para. 5.6.3.1), we observed practically identical temperature increases in the engine compartment. The decrease in relative humidity in the engine compartment was, however, lower on the injection aircraft (decrease of around 30%).

On the Tecnam P92 (para. 5.6.3.2.2) and the Aeroprakt A-22L (para. 5.6.3.2.3), the change in parameters also differed during **the period between take-off (power-up) and cruise flight**, with an outside air temperature that decreased by around 3°C for the Tecnam and around 5°C for the Aeroprakt):

	Tecnam P92	Aeroprakt A-22L
Temperature in the engine compartment	Temperature increase of around 7°C	Decrease in temperature of around 5°C, corresponding to the decrease in outside air temperature
Temperature downstream of the throttle butterfly valve	Almost consistent	Almost consistent
Temperature of the outer surface of the carburettor	Almost consistent	Decrease in temperature of around 5°C, corresponding to the decrease in outside air temperature
Relative humidity in the engine compartment	10 to 35% lower than the outside relative humidity	40 to 50% lower than the outside relative humidity

During the **descent phase**, the only parameter that changed was the temperature downstream of the throttle butterfly valve. In both cases, this temperature increased by around 5°C due to the decrease in engine speed.

Considering this data, the phase that appears to be the most critical is therefore the ground phase, prior to take-off. In the flights made, the factors that were most conducive to icing were measured on the Tecnam P92.

This observation seemed to corroborate the experience of operators of aircraft equipped with a Rotax engine, who reported phenomena that could be icing on the ground prior to take-off.

However, the data logged suggested that the temperature and relative humidity parameters did not seem conducive to icing during the descent phase. We noted in particular a relative humidity under the engine cowlings that was much lower than the outside relative humidity and a temperature of the outer surface of the carburettors that was much higher than the temperature measured downstream of the throttle butterfly valve.

The variations observed between the Tecnam P92 and the Aeroprakt A-22L show the importance of the specificities of powerplants.

- **Three-axis aircraft with a type 2 powerplant (para. 5.2):**

At engine start-up, an immediate decrease in the temperature downstream of the throttle butterfly valve was systematically recorded. This decrease in temperature was generated by the flow of air circulating in the venturi and at fuel injection.

If we compare the data logged on the Tecnam P2002 (para. 5.6.3.2.3) and the Tecnam P2008 (para. 5.6.3.2.4), these decreases in temperature are different:

	Tecnam P2002	Tecnam P2008
Decrease in temperature downstream of the throttle butterfly valve	Approximately 14°C	Approximately 6°C
Decrease in temperature in the Airbox	Approximately 7°C	Approximately 1 to 2°C

Following engine start-up, we also observed a decrease in the temperature of the outer surface of the carburettor. This decrease was more gradual and lasted several minutes.

	Tecnam P2002	Tecnam P2008
Decrease in temperature of the outer surface of the carburettor	Approximately 10°C	Approximately 2 to 3°C

After engine start-up, up to take-off, we observed the following temperature changes. For these changes, it is important to consider one-off increases in speed performed.

	Tecnam P2002	Tecnam P2008
Temperature downstream of the throttle butterfly valve	Temperature increase of around 4 to 5°C	Temperature increase of around 4 to 5°C
Temperature of the outer surface of the carburettor	Temperature increase of around 2 to 3°C	Temperature increase of around 6°C
Temperature in the Airbox	Temperature increase of around 4 to 5°C	Temperature increase of around 8°C

At take-off, at power-up, the following temperature changes were observed:

	Tecnam P2002	Tecnam P2008
Temperature downstream of the throttle butterfly valve	Temperature decrease of around 6 to 7°C	Temperature decrease of around 14°C
Temperature of the outer surface of the carburettor	Temperature decrease of around 4 to 5°C	Temperature decrease of around 10°C
Temperature in the Airbox	Temperature decrease of around 5 to 6°C	Temperature decrease of around 5°C

During activation of the heat system, the variations in temperature logged differed markedly between the Tecnam P2002 (para. 5.6.3.2.3) and the Tecnam P2008 (para. 5.6.3.2.4).

	Tecnam P2002	Tecnam P2008
Temperature downstream of the throttle butterfly valve	Temperature increase of around 30 to 35°C	Temperature increase of around 12 to 14°C
Temperature of the outer surface of the carburettor	Temperature increase of around 15°C	Temperature increase of around 4°C
Temperature in the Airbox	Temperature increase of around 50 to 100°C	Temperature increase of around 20 to 30°C

It is important to note that the increase in temperature of the outer surface of the carburettor occurred much more slowly than the other two temperatures.

DRAFT

- **Comparison of type 1 and type 2 powerplants:**

On the ground:

The temperature variation trends were similar. It is interesting to note that, in type 2 powerplants, the temperature in the Airbox decreased after engine start-up. This temperature then gradually increased again.

To illustrate these observations, values are presented in the table below:

Tecnam P92	Aeroprakt A-22	Tecnam P2002	Tecnam P2008
Outside air temperature = 15°C	Outside air temperature = 24°C	Outside air temperature = 1 - 1.5°C	Outside air temperature = -6.5°C
> Decrease in T downstream of the carburettor at start-up = -11°C	> Decrease in T downstream of the carburettor at start-up = -5°C	> Decrease in T downstream of the carburettor at start-up = -8°C	> Decrease in T downstream of the carburettor at start-up = -5°C
> Trend in T downstream of the carburettor on the ground = very little increase	> Trend in T downstream of the carburettor on the ground = very little increase	> Trend in T downstream of the carburettor on the ground = decrease of around 5 to 6°C	> Trend in T downstream of the carburettor on the ground = increase of around 4°C
> Decrease in T of the outer surface of the carburettor at start-up = -5°C	> Trend in T of the outer surface of the carburettor on the ground = +6°C	> Trend in T of the outer surface of the carburettor on the ground = decrease of around 6°C	> Trend in T of the outer surface of the carburettor on the ground = increase of around 7°C
> Trend in T in the engine compartment = consistent	> Trend in T in the engine compartment = increase of more than 10°C	> Trend in T of the Airbox = increase of around 2 to 3°C	> Trend in T of the Airbox = increase of around 10°C

During climb:

The temperature variation trends differed from aircraft to aircraft.

In type 2 powerplants, a critical parameter is the decrease in the temperature of the outer surface of the carburettors, of between 4 and 10°C.

To illustrate these observations, values are presented in the table below:

Tecnam P92	Aeroprakt A-22	Tecnam P2002	Tecnam P2008
> T downstream of carburettor = decrease of around 14°C	> T downstream of carburettor = decrease of around 13°C	> T downstream of carburettor = decrease of around 5 to 6°C	> T downstream of carburettor = decrease of around 15 to 17°C
> T of the outer surface of the carburettor = almost consistent	> T of the outer surface of carburettor = follows the decrease in outside air temperature	> T of the outer surface of carburettor = decrease of around 4°C	> T of the outer surface of carburettor = decrease of around 10 to 11°C
> T of the engine compartment = increase of around 7°C	> T in the engine compartment = follows the decrease in outside air temperature	> T in the Airbox = decrease of around 4 to 5°C	> T in the Airbox = decrease of around 10 to 12°C

In cruise:

Of the four aircraft presented in para. 5.6.3.2, the temperature changes downstream of the carburetors, in relation to the outside air temperature, were less marked for type 2 powerplants (equipped with an Airbox) than for type 1 powerplants.

We noted that the temperature changes of the outer surface of the carburetors, in relation to the outside air temperature, were similar.

We also noted that the temperature changes in the engine compartment (for type 1 powerplants) and temperature changes in the Airbox (for type 2 powerplants), in relation to the outside air temperature, were very similar.

To illustrate these observations, values are presented in the table below:

Tecnam P92	Aeroprakt A-22	Tecnam P2002	Tecnam P2008
Outside air temperature = 11.5°C	Outside air temperature = 18.8°C	Outside air temperature = -4°C	Outside air temperature = -6.5°C
> T downstream of carburettor - Outside air T = -6.5°C	> T downstream of carburettor - Outside air T = -8°C	> T downstream of carburettor - Outside air T = -1.5°C	> T downstream of carburettor - Outside air T = -2.5°C
> T of the outer surface of carburettor - Outside air T = +3.5°C	> T of the outer surface of carburettor - Outside air T = +6°C	> T of the outer surface of carburettor - Outside air T = +4°C	> T of the outer surface of carburettor - Outside air T = +4°C
> T in the engine compartment - Outside air T = +13 / +14°C	> T in the engine compartment - Outside air T = +14°C	> T in the Airbox - Outside air T = +11 / +12°C	> T in the Airbox - Outside air T = +11 / +12°C

The parameter missing for type 2 powerplants is relative humidity in the Airbox.

In descent:

Due to activation of the heat system on type 2 powerplants, the comparison is not relevant.

- **Gyroplanes:**

On the two aircraft tested by the BEA, the environment in the immediate vicinity of the carburettors varied in completely different ways:

- On the gyroplane with an unducted powerplant, on the ground and at the start of the flight, the temperature in the immediate vicinity of the carburettor was higher than the outside air temperature and the relative humidity was lower than the outside relative humidity. After several minutes, the temperature in the immediate vicinity of the carburettor decreased and balanced with the outside air temperature. The relative humidity followed the same trend. In this context, the conditions in the second half of the flight and during the descent seemed to be more conducive to icing than during the initial ground phase and the take-off.
- On the gyroplane with a ducted powerplant, the changes in temperature and relative humidity were the complete reverse. On the ground and at the start of the flight, the temperature and relative humidity in the immediate vicinity of the carburettors were practically identical to the environmental conditions. The temperature in the immediate vicinity of the carburettors then gradually increased and became markedly higher than the outside air temperature (around 15°C higher in the case of the flights made). The relative humidity then gradually decreased around the carburettors and became markedly lower than the outside relative humidity (around 30% lower in the case of the flights made). In this context, the conditions on the ground and at the very start of the flight seemed to be more conducive to icing than the conditions throughout the rest of the flight. Moreover, icing was felt by the pilot on the ground prior to a flight.

On the 914 engine family, the tests conducted at the test stand suggested that the addition of the turbocharger caused an increase in temperature in the Airbox of around 3 to 5°C.

DRAFT

6 - CONCLUSIONS

6.1. Established facts

- The most recent data identified in the American publications and those researched in the BEA's archives revealed that the percentage of events associated with piston engine induction system icing was low, between 1 and 2.5%.

Of these events, the percentage that resulted in the fatal injury of the aircraft's occupants was also low. However, it was higher for the data published by the BEA, with the taking into account of events involving microlights.

- There are three types of piston engine induction system icing:
 - impact icing (on filters, the edge of air intakes, protrusions, etc.);
 - carburettor or butterfly valve icing;
 - fuel icing due to the presence of water in the fuel.

All of the literature researched contains the same description of these phenomena. However, carburettor icing remains the form of icing that is referred to and discussed most often.

Impact icing was never referred to in the bibliographic research relating to safety investigations.

- The certification requirements published by the EASA and the FAA essentially focused on the heat system, defining minimal temperature increases for defined conditions.
- The aeronautical authorities propose four different graphs to define the probability of icing and its severity, as a function of the outside air temperature and the dew point temperature. Data enabling the construction of these diagrams was not identified.
- Older graphs, essentially taken from scientific studies conducted in the United States between 1945 and 1950, were identified and analysed.

This work was conducted on pressure carburettors that differ greatly from the float-type carburettors equipping modern engines.

These graphs are different from those proposed by the authorities.

This work was largely conducted in a laboratory, on carburettors separated from the propulsion system. The influence of the powerplant was not therefore taken into consideration.

- Piston engine induction system icing is dealt with in the same way in the reports published by the aeronautical investigation authorities.

In these reports, the analysis is essentially based on the weather conditions and their application in one of the graphs published by the aeronautical authorities. Powerplant specificities are not considered.

- The flight manuals published by aircraft manufacturers contain very little information about piston engine induction system icing:
 - the most common symptoms are specified: decrease in power and occurrence of vibrations;
 - the information provided essentially concerns use of the carb heat system, and in particular specifies that this system is an all-or-nothing type system and that the mixture needs to be adjusted when it is activated.

These manuals do not specify the probability of powerplant icing.

- No relevant information about induction system icing was identified in the carburettor manufacturer documentation.
- A series of tests were conducted at a test stand on the powerplant of a Socata TB10. These tests, albeit not easily, revealed carburettor icing. The conditions that enabled ice to form were:
 - low temperature of around 3 to 4°C;
 - relative humidity very close to 100%;
 - low established engine speed (between 1,500 and 1,900 rpm);
 - thermally insulated carburettor.

These icing conditions were similar to those identified in the publication “Carburetor Ice Test Methodology Evaluation Final Report / CRC Report No. AV-17-13 - J. M. Thom, Associate Professor, Purdue University B. Kozak, PhD., Purdue University T. Yother, Purdue University - December 2015”. This is the most recent publication identified on piston engine induction system icing.

The influence of each parameter was not studied.

- Powerplants equipped with Rotax 912 and 914 Series four-cylinder engines vary greatly.

For three-axis aircraft, two configurations are encountered:

- Type 1: Each carburettor is equipped with an air filter. The air that is then sucked in by the engine is the air present under the cowlings, renewed by the air intakes, that differ in size and position depending on the aircraft.

- Type 2: Each carburettor is connected to an Airbox located just behind the carburettors. This Airbox is connected via a flexible hose to an air intake.

No scientific publication on the icing of these powerplant was identified.

Temperature and relative humidity measurements were taken on seven aircraft, of microlight or VLA status. These measurements were taken in flight, in varying weather conditions.

No induction system icing was felt by the pilots in flight. In only one case, the symptoms of icing were identified by the pilot on the ground, after engine start-up.

For type 1 powerplants, it was noted that the conditions of the air sucked in by the carburettors were very different from those of the outside air.

The temperature in the engine compartment was higher than the outside temperature (10 to 14°C higher) and the relative humidity in the engine compartment was markedly lower than the outside humidity (40 to 50% lower). On the aircraft tested, temperature and relative humidity changes varied depending on the aircraft.

On this type of powerplant, considering this data, induction system icing could be possible but in extreme conditions (low temperature and very high relative humidity). In addition, the phase that seemed critical was the ground phase. The statements of several pilots support this theory.

For type 2 powerplants, the air in the Airbox was higher in temperature than the outside air temperature, slightly lower than the temperature prevailing in the engine compartment. The relative humidity was not measured in the Airbox.

The temperature changes were similar to those observed on type 1 powerplants.

In these conditions, the analysis was similar to that proposed for type 1 powerplants.

The conditions obtained after activation of the heat system differed depending on the powerplant.

For the two gyroplanes tested, the changes in temperature and relative humidity were completely different.

6.2. Analysis and comments

The four graphs proposed by the aeronautical authorities, defining the probability of icing and its severity, are not investigative tools. They must be considered as conservative envelopes that do not take into account the specificities of powerplants.

In the context of a safety investigation, the analysis of piston engine induction system icing, based solely on outside weather conditions and on one of the several graphs proposed by the authorities, is not appropriate.

It is essential to consider the specificities of the powerplant when analysing icing.

Due to certification requirements, every aircraft manufacturer (certified aeroplane) is expected to have an in-depth knowledge of the probability of icing.

BEA

Bureau d'Enquêtes et d'Analyses
pour la sécurité de l'aviation civile

DRAFT